The Identification and Pharmacological Characterisation of Novel Apelin Receptor Agonists *In Vitro* and *In Vivo*

by

Cai Read

Jesus College

Experimental Medicine and Immunotherapeutics

Research Supervisor: Dr Anthony P. Davenport

August 2018

This dissertation is submitted for the degree of

Doctor of Philosophy

UNIVERSITY OF CAMBRIDGE

This dissertation is the result of my own work and includes nothing which is the outcome of work done in collaboration except as declared in the Preface and specified in the text.

It is not substantially the same as any that I have submitted, or, is being concurrently submitted for a degree or diploma or other qualification at the University of Cambridge or any other University or similar institution except as declared in the Preface and specified in the text. I further state that no substantial part of my dissertation has already been submitted, or, is being concurrently submitted for any such degree, diploma or other qualification at the University of Cambridge or any other University or similar institution except as declared in the Preface and specified in the text

The length of this dissertation does not exceed 60,000 words.

Table of Contents

Acknowledgements

I would like to thank my supervisor Dr Anthony Davenport for all of his help and support during my PhD. His door has always been open and he has been more than happy to share his wealth of experience to provide advice and guidance to me. I am particularly grateful for his encouragement and enthusiasm for me to present my work throughout my PhD.

I am also extremely grateful to Dr Janet Maguire for all of her help in every aspect of the PhD. Her critical discussions and willingness to help have been greatly appreciated, while her help in organising aspects of the animal work have been invaluable.

I thank Mrs Rhoda Kuc and Dr Peiran (Brian) Yang for their patience in teaching me a range of laboratory techniques. I particularly thank Rhoda for her technical advice and for always knowing where things are, as well as for being the person in the lab I could talk to about all things cricket! I especially thank Brian for teaching me a range of *in vivo* techniques and his constant enthusiasm and company on long shifts.

I additionally thank Amanda Kennedy, Thomas Williams, Duamene Nyimanu, Petra Sulentic, and Nicola Owen, the other students in the Davenport laboratory, for their help at various points during the last four years.

The Royal Papworth Hospital Research Tissue Bank supported by National Institute for Health Research Cambridge Biomedical Research Centre is acknowledged for the supply of surgical samples of cardiovascular tissue for this work.

I am particularly grateful to the British Heart Foundation for funding my PhD and thank Suzanne Diston, the organiser, and Professor Martin Bennett, the head of the BHF programme in Cambridge. I would also like to thank my fellow students on the programme for their friendship.

I thank the British Pharmacological Society, The Physiological Society, the Italian Pharmacological Society and the Australasian Pharmaceutical Science Association for providing me with opportunities to present the work from my PhD. They have also provided travel funding along with the Cambridge Philosophical Society and the Jesus College Doctoral Research Fund.

I am extremely grateful to Jesus College which has largely been my home and made me feel incredibly welcome over the last seven years. I will cherish my time there and value the friendships made with people from all over the world. I am especially thankful for the Graduate Cricket Team which has been such an important part of my social life.

Lastly, but most importantly, I would like to thank my family for supporting me in all of my endeavours and for providing me with an outlet to escape the bubble. My parents have always been on hand to give good advice and I have always appreciated how they listen and take an interest in my work. I also thank my father for proof-reading this thesis.

Publications

Read C., Yang P., Kuc R.E., Nyimanu D., Williams T.L., Fitzpatrick C.M., Foster R., Glen R.C., Maguire J.J. and Davenport A.P. (2018). *The G Protein Biased Small Molecule Apelin Agonist CMF-019 is Disease Modifying in Endothelial Cell Apoptosis In vitro and Induces Vasodilatation without Desensitisation In Vivo.* **Biochem Pharmacol. *In Submission.***

Read C., Yang P., Kuc R.E., Nyimanu D., Williams T.L. Glen R.C., Holt L.J., Arulanantham H., Smart A., Davenport A.P. and Maguire J.J. (2018). *Apelin Peptides Linked to Anti-Serum Albumin Domain Antibodies (AlbudAb^{TM}) Retain Affinity In Vitro and are Efficacious Receptor Agonists In Vivo.* **Cardiovasc Res. *In Submission***

Yang P., **Read C.***, Kuc R.E., Nyimanu D., Williams T.L., Crosby A., Buonincontri G., Southwood M., Sawiak S.J., Morrell N.W., Davenport A.P. and Maguire J.J. (2018). *A Novel Cyclic Biased Agonist of the Apelin Receptor, MM07, is Disease Modifying in the Rat Monocrotaline Model of Pulmonary Arterial Hypertension.* **BJP. *In Revision.* *Joint First Author**

Garfield B.E., Crosby A., Shao D., Yang P., **Read C.**, Sawiak S., Moore S., Parfitt L., Harries C., Rice M., Paul R., Ormiston M.L., Morrell N.W., Polkey M.I., Wort S.J. and Kemp P. (2018). *Growth/Differentiation Factor 15 Causes TGFβ Activated Kinase 1 Dependent Muscle Atrophy in Pulmonary Arterial Hypertension.* **Thorax. *In Press.***

Yang P., **Read C**., Kuc R.E., Buonincontri G., Southwood M., Torella R., Upton P.D., Crosby A., Sawiak S.J., Carpenter T.A., Glen R.C., Morrell N.W., Maguire J.J., Davenport A.P. (2017). *Elabela/Toddler is an Endogenous Agonist of the Apelin APJ Receptor in the Adult Cardiovascular System, and Exogenous Administration of the Peptide Compensates for the Downregulation of its Expression in Pulmonary Arterial Hypertension.* **Circulation 135:1160-1173.**

Read C., Fitzpatrick C.M., Yang P., Kuc R.E., Maguire J.J., Glen R.C., Foster R.E. and Davenport A.P. (2016). *Cardiac Action of the First G protein Biased Small Molecule Apelin Agonist.* **Biochem Pharmacol. 166:63-72.**

Kennedy A.J., Yang P., **Read C.**, Kuc R.E., Yang L., Taylor E.J., Taylor C.W., Maguire J.J., Davenport A.P. (2016). *Chemerin Elicits Potent Constrictor Actions via Chemokine-Like Receptor 1 (CMKLR1), not G-Protein-Coupled Receptor 1 (GPR1), in Human and Rat Vasculature.* **J Am Heart Assoc. 14:5(10), e004421.**

Presentations

CMF-019, the First G Protein Biased Small Molecule Apelin Agonist, is a Vasodilator and Positive Inotrope *In Vivo*

Oral Communication, British Heart Foundation (BHF) Centre for Research Excellence Research Symposium (2018), *Cambridge, UK*

Oral Communication, Australasian Pharmaceutical Science Association – Australasian Society of Clinical and Experimental Pharmacologists and Toxicologists (APSA-ASCEPT) Joint Scientific Meeting (2017), *Brisbane, Australia*

Poster Presentation, British Pharmacological Society (BPS) 7th Focused Meeting on Cell Signalling (2018), *Nottingham, UK*

Poster Presentation, BHF Student Symposium (2018), *Edinburgh, UK*

BPS Representative at Voice of the Future, 2018

Parliamentary Event for Young Scientists to Ask Questions of Government Ministers and Scientific Advisers, *Westminster, UK*

Role of a New Endogenous Agonist for the Human Apelin Receptor, Elabela/Toddler, in Pulmonary Arterial Hypertension

Oral Communication, Medicine Research Day (2017), *Cambridge, UK*

Cardiac Action of the First G Protein Biased Small Molecule Apelin Agonist

Oral Communication, BPS Annual Meeting (2016), *London, UK*

Poster Presentation, BHF Student Symposium (2017), *London, UK*

Poster Presentation, Physiology 2016, *Dublin, Ireland*

Poster Presentation, Italian Pharmacological Society (SIF) (2016), *Rimini, Italy*
Chairperson Cardiovascular Oral Communications Session, SIF (2016), *Rimini, Italy*

Characterisation of Apelin Receptor Agonists in Clinically Relevant Human Tissue

Poster Presentation, BPS Focused Meeting on Exploiting New Pharmacology and Application to Drug Discovery (2015), *Edinburgh, UK*

Poster Presentation, Physiology 2015, *Cardiff, UK*

Abstract

The apelin system is an evolving transmitter system consisting of the G protein coupled apelin receptor and two endogenous peptide ligands, apelin and elabela. It is implicated as a potential therapeutic for a number of diseases; however, the endogenous peptides are limited by half-life and bioavailability. This study aims to identify and pharmacologically characterise apelin agonists *in vitro* and *in vivo* and to evaluate their therapeutic potential in pulmonary arterial hypertension as a model disease.

CMF-019 was identified as the first G protein biased apelin agonist. To date, suitable small molecule apelin agonists as experimental tool compounds have been limited and CMF-019 represents an important advance. CMF-019 was active *in vivo*, producing an increase in cardiac contractility and vasodilatation, similar to apelin. These effects were achieved without receptor desensitisation, supporting the remarkable G protein bias observed *in vitro*. Furthermore, it was disease-modifying *in vitro* in an endothelial cell apoptosis assay but despite this, did not prevent pulmonary arterial hypertension in a monocrotaline rat model of the disease.

An apelin mimetic peptide possessing an unnatural amino acid, MM202, conjugated chemically via a polyethylene glycol linker to an anti-serum domain antibody (AlbudAb™) was also characterised. The product MM202-AlbudAb™ represents the first time an AlbudAb™ has been conjugated chemically to an unnatural peptide mimetic, providing protection from proteolysis and glomerular filtration. Importantly, it retained binding to albumin and demonstrated *in vitro* and *in vivo* activity at the apelin receptor.

In conclusion, this thesis has identified and pharmacologically characterised two novel apelin agonists that possess significant advantages over the endogenous peptides. CMF-019 is suitable as an experimental tool compound and, as the first G protein biased small molecule, provides a starting point for more suitable therapeutics. In addition, MM202-AlbudAb™ proves that unnatural peptides can be conjugated to AlbudAb™, supporting use of this technology in other small-peptide ligand transmitter systems.

Abbreviations

ACE2, Angiotensin Converting Enzyme 2

AlbudAb™, Anti-Serum Albumin Domain Antibody

Apela, Apelin Receptor Early Endogenous Ligand

cAMP, 3',5'-Cyclic Adenosine Monophosphate

CHO, Chinese Hamster Ovary

CHX, Cycloheximide

CICR, Calcium Induced Calcium Release

DMSO, Dimethylsulphoxide

EBM-2, Endothelial Cell Basal Media 2

EGM-2, Endothelial Cell Growth Media 2

ELA, Elabela

ELISA, Enzyme-Linked Immunosorbent Assay

ERK1/2, Extracellular Signal Regulated Kinases 1/2

ESC, Embryonic Stem Cell

FBS, Foetal Bovine Serum

FDA, U.S Food and Drug Administration

GF, Growth Factor

GLP-1, Glucose-Dependent Insulinotropic Peptide 1

GPCR, G Protein Coupled Receptor

HF, Heart Failure

HGCN, HUGO Gene Nomenclature Committee

HIV, Human Immunodeficiency Virus

HSA, Human Serum Albumin

HUGO, Human Genome Organisation

IP, Intraperitoneal

IP_3, Inositol 1,4,5-Trisphosphate

IP_3R, Inositol 1,4,5-Trisphosphate Receptor

LV, Left Ventricle

LVSP, Left Ventricular Systolic Pressure

MAPK, Mitogen Activated Protein Kinase

MCT, Monocrotaline

MLCK, Myosin Light Chain Kinase

NCX, Na^+-Ca^{2+} Exchanger

NF-κB, Nuclear Factor Kappa-Light-Chain-Enhancer of Activated B Cells

NHE, Na^+-H^+ Exchanger

PAEC, Pulmonary Artery Endothelial Cell

PAH, Pulmonary Arterial Hypertension

PBS, Phosphate Buffered Saline

PEG, Polyethylene Glycol

PI, Propidium Iodide

PIC, Protease Inhibitor Cocktail

PI3K, Phosphoinositide 3-Kinase

PKC, Protein Kinase C

PLC, Phospholipase C

PV, Pressure-Volume

[Pyr^1]apelin-13, Pyroglutamated Apelin-13

rhVEGF, Recombinant Human Vascular Endothelial Growth Factor

RLC, Regulatory Light Chain

RLU, Relative Light Unit

RV, Right Ventricle

RVSP, Right Ventricular Systolic Pressure

RyR, Ryanodine Receptor

SIV, Simian Immunodeficiency Virus

TGFβ, Transforming Growth Factor β

TNFα, Tumour Necrosis Factor α

TNF-R1, Tumour Necrosis Factor Receptor 1

VEC, Vascular Endothelial Cell

VSMC, Vascular Smooth Muscle Cell

List of Figures and Tables

1. Introduction

2. Methods

3. Identification and Characterisation of CMF-019, the First G Protein Biased Apelin Agonist

4. *In Vivo* Cardiovascular Assessment of [Pyr^{1}]apelin-13 and CMF-019 Responses in Normotensive Male Sprague-Dawley Rats

5. CMF-019 and MM07 as Disease-Modifying Compounds for Pulmonary Arterial Hypertension *In Vitro* and *In Vivo*

6. An Apelin Mimetic Peptide, MM202, Linked to an Anti-Serum Albumin Domain Antibody (AlbudAb™) is Efficacious *In Vitro* and *In Vivo*

1. Introduction

1.1 Background

The apelin receptor is a class A G protein coupled receptor (GPCR) identified in 1993 (O'Dowd *et al*., 1993) and paired with its cognate ligand apelin in 1998 (Tatemoto *et al*., 1998). Since then, there has been a large body of work studying the relationship between the ligand and receptor, as well as their physiological and pathophysiological roles in a number of diseases. Only recently has an additional ligand at the apelin receptor been discovered. Elabela/Toddler is a 54 amino acid peptide which is cleaved to produce a 32 amino acid mature secreted protein (Chng *et al*., 2013, Pauli *et al*., 2014). Here the preferred nomenclature that will be used is elabela (ELA), following the precedence of discovery (Chng *et al*., 2013). ELA is an endogenous ligand and functional in the adult mammalian system (Yang *et al*., 2017b). Interestingly, although it shows little sequence homology to apelin with only about 25% conservation (Xie *et al*., 2014), there is some similarity in the location of hydrophobic residues.

The discovery of this new ligand opens up a number of exciting possibilities. It greatly enhances the spatiotemporal signalling potential through the apelin receptor and how it is modulated in disease, with evidence that ELA is downregulated in human pulmonary arterial hypertension and animal models of the disease already demonstrated (Yang *et al*., 2017b). Meanwhile, it also offers the possibility to explore a new class of ligand at the apelin receptor based on the structure of ELA. However, perhaps most of all, it suggests that, in addition to ELA, there may be other genes of pharmacological importance located in regions of the genome that have previously been overlooked.

This introduction will discuss the structure and signalling pathways of the apelin receptor and its endogenous ligands, apelin and ELA, before moving on to the developments that have occurred for the production of synthetic agonists and antagonists. It will discuss some of the roles that apelin and ELA have been shown to play in both physiological and pathophysiological conditions; therefore, highlighting the importance of the two ligands and the therapeutic potential of targeting the apelin system. Finally, it will explore concepts designed to improve the therapeutic targeting

of the apelin system, such as the development of biased agonists and peptide-antibody conjugates, as these have been the primary focus of this project.

1.2 Apelin Receptor Structure

The human apelin receptor has a seven transmembrane structure and consists of 380 amino acids. It was initially identified through homology with the angiotensin II type 1 receptor (AT1) with which it shares 54% sequence similarity. Despite this homology the apelin receptor does not bind angiotensin and, until the recent discovery of ELA, was thought to bind only its cognate ligand, apelin. There are no known apelin receptor subtypes in mammals and the receptor is well conserved with 91% and 89% homology with the 377 amino acid long mouse and rat receptors, respectively. In the zebrafish, there are two receptor subtypes, aplnra and aplnrb. Aplnrb shows greater homology with mammalian apelin receptors and it is in this receptor that the only known naturally occurring mutation occurs, the grinch^{s608} mutation. This mutation involves a Trp^{85} to Leu^{85} amino acid change in the second transmembrane domain and a loss of apelin binding which, in the most severely affected mutants, causes a failure of the heart to develop (Scott *et al*., 2007). It is unknown whether the second zebrafish apelin receptor is a result of duplication or whether mammalian systems have lost this as a vestigial receptor, perhaps offering an explanation for the limited homology between apelin and ELA.

Ma *et al.* (2017) have recently reported the 2.6-Ångstrom resolution crystal structure of the human apelin receptor in a complex with a synthetic 17-amino-acid apelin analogue agonist. The receptor shows the expected seven transmembrane helical structure with a short eighth helix also observed in other GPCRs. The structure is in reasonable agreement with studies using nuclear magnetic resonance (Langelaan *et al*., 2013) and molecular dynamics simulations (Macaluso and Glen, 2010, Yang *et al*., 2017b). However, a number of changes to the receptor and ligand were introduced to achieve crystallisation and it is worth noting some caveats that prompt a cautious interpretation of the data. Looking at the receptor, residues were removed from the N-terminus (residues 1–6) and C terminus (residues 331–380); meanwhile mutations V117A and W261K were introduced. These mutations force the intracellular portion into an inactive state and render the receptor unable to bind apelin-13. Looking at the ligand, a synthetic 17-amino-acid apelin analogue agonist was used, which is significantly different from apelin. In particular, a macrocycle and significant mutations have been introduced to it and these may alter the peptide conformation and its interactions. Finally, the crystal structure is unable to explain the importance of the

Arg2 and Leu5 residues of apelin 13, known key binding elements from mutation data (Fan *et al*., 2003, Medhurst *et al*., 2003).

Although the structure confirms the presence of two disulphide linkages present in a number of class A GPCRs (Cys19-Cys281 and Cys102-Cys181), it does not clarify the importance of post-translational modifications in the apelin receptor. The receptor is likely to be glycosylated (Medhurst *et al*., 2003) and contains two glycosylation motifs expected at residues in the N-terminal tail (Asn15) and ECL2 (Asn175), both of which appear to be involved in agonist binding. Glycosylation is known to be significant in GPCR function (Lanctot *et al*., 1999) and, in some cases, affects agonism and bias (Soto *et al*., 2015) but its importance in the case of the apelin receptor is not known. In addition, there are a number of potential palmitoylation sites in the intracellular C-terminal region of the receptor. Based on predictions from the SwissPalm protein S-palmitoylation database (Blanc *et al*., 2015) and CSS-Palm (Ren *et al*., 2008), residues Cys325 and Cys326 on the putative helix TM8 are expected to be palmitoylated. Palmitoylation is key in GPCR expression and function (Qanbar and Bouvier, 2003). Finally, the C-terminus appears to contain a “phosphorylation barcode” (Nobles *et al*., 2011) and Ser348 has been identified as a novel phosphor-regulatory site (Chen *et al*., 2014).

1.3 Apelin Receptor Signalling in the Cardiovascular System

Infusion of apelin leads to vasodilatation, in humans *in vitro* (Maguire *et al*., 2009) and *in vivo* (Brame *et al*., 2015) and in rodents *in vivo* (Tatemoto *et al*., 2001), as well as cardiac inotropy *in vitro* (Maguire *et al*., 2009, Perjes *et al*., 2014, Szokodi *et al*., 2002) and *in vivo* in rats (Atluri *et al*., 2007, Berry *et al*., 2004, Jia *et al*., 2006), mice (Ashley *et al*., 2005) and humans (Japp *et al*., 2008) without hypertrophy. Interestingly, in denuded vessels, apelin promotes vasoconstriction (Katugampola *et al*., 2001, Maguire *et al*., 2009) and it is only in intact tissues that the endothelium-dependent vasodilatation is observed. This endothelium-dependent vasodilatation has been suggested to be either nitric oxide-dependent (Tatemoto *et al*., 2001) or prostanoid-dependent (Maguire *et al*., 2009), perhaps reflecting species or whole organism versus isolated vessel differences.

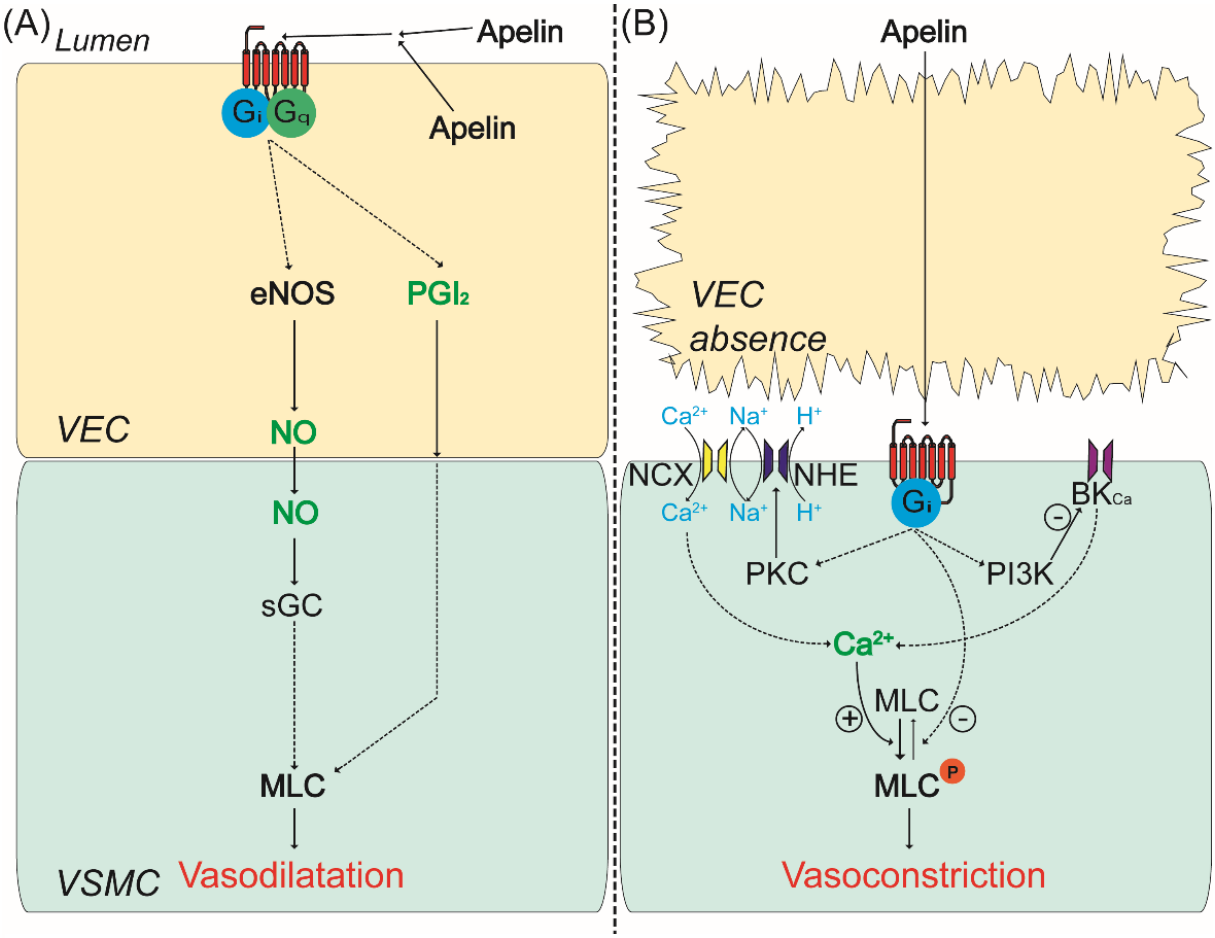

Figure 1.1: The key signalling pathways suspected to be activated in vascular endothelial cells (VEC) and smooth muscle cells (VSMC) by the apelin receptor. Apelin binding can promote $G_{\alpha i}$, $G_{\alpha q}$ and β-arrestin recruitment to the receptor. In the presence of the endothelium, both $G_{\alpha i}$ and $G_{\alpha q}$ promote relaxation of smooth muscle cells through nitric oxide and prostacyclin release. In the absence of the endothelium, apelin binds directly to the receptor on the smooth muscle cells and leads to constriction through undetermined intermediate steps but most likely involving PKC, phosphoinositide 3-kinase (PI3K) and myosin light chain phosphorylation. Figure taken from Yang *et al.,* (2015a).

Mechanistically, these processes are poorly understood, although the apelin receptor is thought to signal primarily through $G_{\alpha i}$, leading to decreased intracellular cyclic adenosine monophosphate (cAMP) by inhibition of adenylyl cyclase, as evidenced by inhibition of forskolin-stimulated cAMP production (Habata *et al*., 1999) and pertussis sensitivity (Hosoya *et al*., 2000, Masri *et al*., 2002). Figure 1.1 shows a summary of the possible downstream pathways activated following $G_{\alpha i}$ activation by the apelin receptor as suggested by (Yang *et al*., 2015a).

As well as activating $G_{\alpha i}$, there is also significant evidence that the apelin receptor may couple $G_{\alpha q}$, particularly in cardiomyocytes (Szokodi *et al*., 2002), promoting phospholipase C (PLC) and, in turn, inositol triphosphate (IP_3) and protein kinase Cε (PKCε, but not PKCα; Perjes *et al*., 2014). IP_3 activates IP_3 receptors (IP_3R) and Ca^{2+} release, which can feed-back to ryanodine receptors (RyR); leading to calcium induced calcium release (CICR). PKCε might enhance Na^+-H^+ exchange (NHE) on the sarcolemma; thus, increasing intracellular Na^+ and consequently, enabling the Na^+-

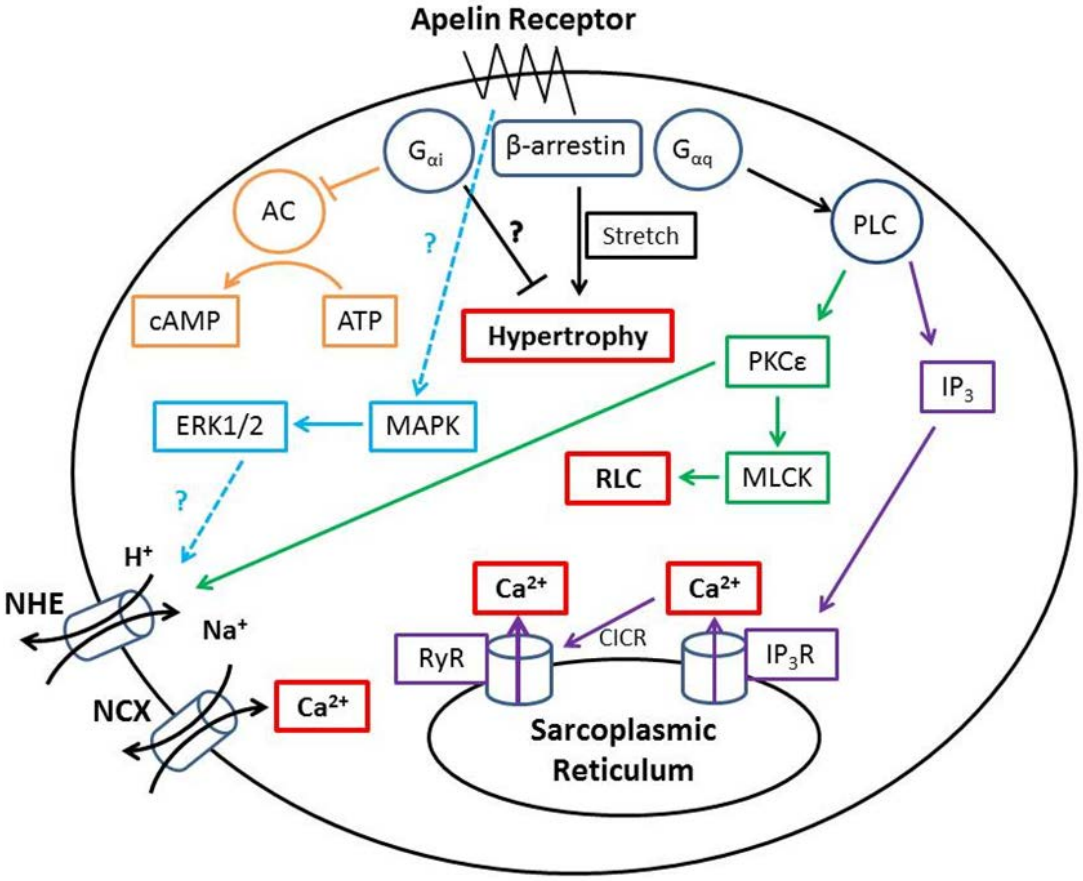

Figure 1.2: The key signalling pathways suspected to be activated in cardiomyocytes by the apelin receptor. Apelin binding can promote $G_{\alpha i}$, $G_{\alpha q}$ and β-arrestin recruitment to the receptor, these pathways are thought to ultimately lead to cardiac inotropy without hypertrophy. However, in the absence of apelin, β-arrestin recruitment may lead to stretch-mediated hypertrophy.

Ca^{2+} exchanger (NCX) to raise intracellular Ca^{2+} concentrations (Chandrasekaran *et al*., 2008). It has also been suggested that mitogen activated protein kinase (MAPK) and extracellular signal regulated kinases 1/2 (ERK1/2) can regulate cardiac contractility through an independent mechanism (Perjes *et al*., 2014), though how this pathway is activated or increases contractility is not clear. Finally, it has also been suggested that apelin can activate myosin light chain kinase (MLCK), which can phosphorylate the regulatory light chain (RLC) of myosin II resulting in greater Ca^{2+} sensitivity of the force generating machinery (Perjes *et al*., 2014). These pathways are summarised in Figure 1.2.

Ligand	Action	Binding Affinity	Units	Bias	References
[Pyr^{1}]Apelin-13 (E)	Full Agonist	7.0-8.8	pIC_{50}	n/a	Kawamata *et al.*, 2001 Medhurst *et al.*, 2003
Apelin-13 (E)	Full Agonist	8.8-9.5	pIC_{50}		Fan *et al.*, 2003 Hosoya *et al.*, 2000 Medhurst *et al.*, 2003
Apelin-17 (E)	Full Agonist	7.9-9.0	pIC_{50}	β-arrestin	El Messari *et al.*, 2004 Medhurst *et al.*, 2003
Apelin-36 (E)	Full Agonist	8.2-8.6	pIC_{50}		Fan *et al.*, 2003 Hosoya *et al.*, 2000 Kawamata *et al.*, 2001 Medhurst *et al.*, 2003
Elabela/Toddler-11 (E)	Full Agonist	7.2	pIC_{50}		Yang *et al.*, 2017b
Elabela/Toddler-21 (E)	Full Agonist	8.7	pIC_{50}	β-arrestin	Yang *et al.*, 2017b
Elabela/Toddler-32 (E)	Full Agonist	8.7	pIC_{50}	β-arrestin	Yang *et al.*, 2017b
MM07	Full Agonist	9.5	pEC_{50}	G protein	Brame *et al.*, 2015
CMF-019	Full Agonist	8.6	pIC_{50}	G protein	Read *et al.*, 2016
ML233	Full Agonist	-	-		Khan *et al.*, 2011
E339-3D6	Full Agonist	6.4	pK_i		Iturrioz *et al.*, 2010

Table 1.1: Some of the key agonists at the apelin receptor, their binding affinities and whether they demonstrate bias compared to [Pyr^{1}]apelin-13 (the most abundant apelin isoform in the cardiovascular system) . Endogenous agonists are denoted by '(E)'.

1.4 Endogenous Agonists

To date, two endogenous peptide agonists have been identified at the apelin receptor, apelin and ELA. Though they show limited sequence homology, they have similarity in the location of hydrophobic residues and can be docked into the same binding pocket in a molecular dynamics simulation of the receptor (Figure 1.3). Apelin was discovered in bovine stomach extracts by Tatemoto *et al*. in 1998, since then there has been significant advance in our understanding of the isoforms of apelin and their binding to the apelin receptor. ELA, however, has only been discovered relatively recently by two groups working independently (Chng *et al*., 2013, Pauli *et al*., 2014) and as such, there is still much to be learnt about its endogenous isoforms and interactions at the apelin receptor. The important question of why there are two endogenous ligands for the apelin receptor and their relationship remains to be addressed.

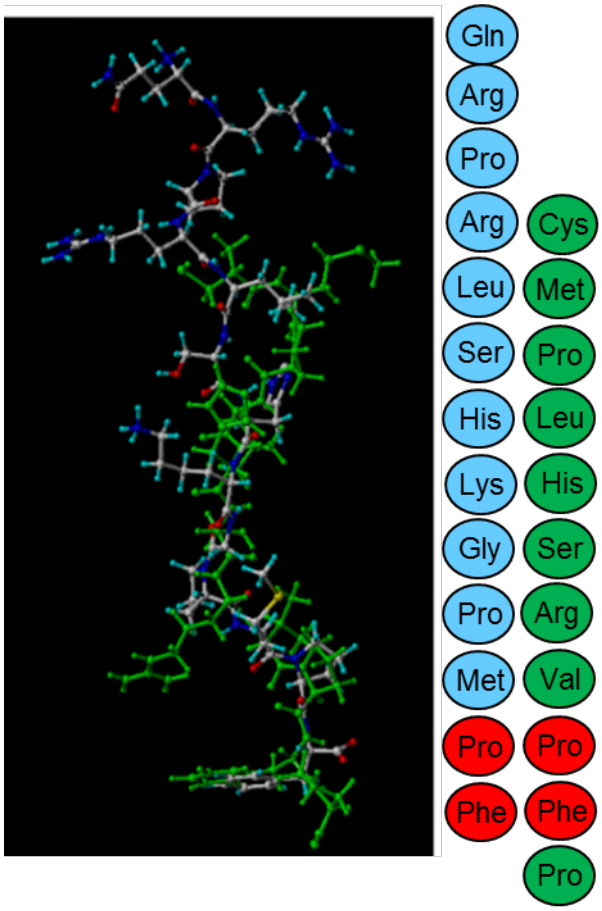

Figure 1.3: An overlay of ELA-11 (green) and apelin-13 (blue) docked in the apelin receptor binding pocket. The peptide sequences are shown alongside with the same colour scheme. The red amino acids show where identical residues line up. Overlay taken from Yang *et al.* (2017b).

1.4.1 Apelin

Apelin is expressed as a 77-amino acid pre-protein, pre-pro-apelin, consisting of the 55-amino acid pro-apelin fragment and an N-terminal secretory sequence. Following secretion, pro-apelin is cleaved to produce three main apelin fragments; apelin-36, apelin-17 and apelin-13, the last of which can undergo cyclisation of the glutamine at its N-terminus to produce pyroglutamated apelin-13 ([Pyr^{1}]apelin-13; Figure 1.4) (Pitkin *et al*., 2010). It was originally hypothesised that cleavage occurred sequentially with pro-apelin first cleaved to apelin-36 and then in turn to the smaller apelin-17 and apelin-13 fragments, always retaining the bioactive C-terminus. These cleavages were predicted due to expected basic cleavage sites in the peptide sequence and the identification of apelin-36, -17 and -13 as active sequences found in biological samples (Kleinz and Davenport, 2005). However, because of this, the enzymes involved are not well characterised and warrant further investigation. This is especially true for the production of apelin-36 and -17. Recently, Shin *et al*. (2013) proposed that furin can directly cleave pro-apelin to apelin-13 *in vitro* without producing these longer isoforms. Apelin-36 is also cleaved by angiotensin converting enzyme 2 (ACE2) with high catalytic efficiency to remove the C-terminal phenylalanine. Similarly, apelin-13 can be cleaved by ACE2 to produce apelin-13$_{(1\text{-}12)}$ (Vickers *et al*., 2002). Interestingly, apelin-13$_{(1\text{-}12)}$ retains activity as demonstrated by recruitment of β-arrestin to the apelin receptor *in vitro*, constriction of saphenous vein *ex vivo* and positive inotropy and blood pressure decrease *in vivo*. However, most critically it was also able to induce an increase in forearm blood-flow in human volunteers (Yang *et al*., 2017a). Additional support for this is evidenced by the retention of activity when the terminal phenylalanine of apelin-13 is mutated to alanine (Fan *et al*., 2003, Medhurst *et al*., 2003, Yang *et al*., 2017a) and furthermore C-terminal truncation studies have suggested activity is retained even as far as apelin-13$_{(1\text{-}11)}$ (Zhang *et al*., 2014). This last study also reported that the N-terminal glutamine in position 1 is not essential for binding either, suggesting that the 10-amino acid apelin-13$_{(2\text{-}11)}$ fragment is the smallest active fragment (Zhang *et al*., 2014). Although the N-terminal glutamine residue is not essential to binding, the cyclisation to pyroglutamate is widely observed *in vivo* and enhances the stability of the peptide fragment (Habata *et al*., 1999, Van Coillie *et al*., 1998). Interestingly, while the C-terminal amino acids of apelin-36 make the smallest active fragment for binding

to the apelin receptor, it has been suggested that N-terminal portions may aid the molecule in interacting with the receptor (Hosoya *et al*., 2000).

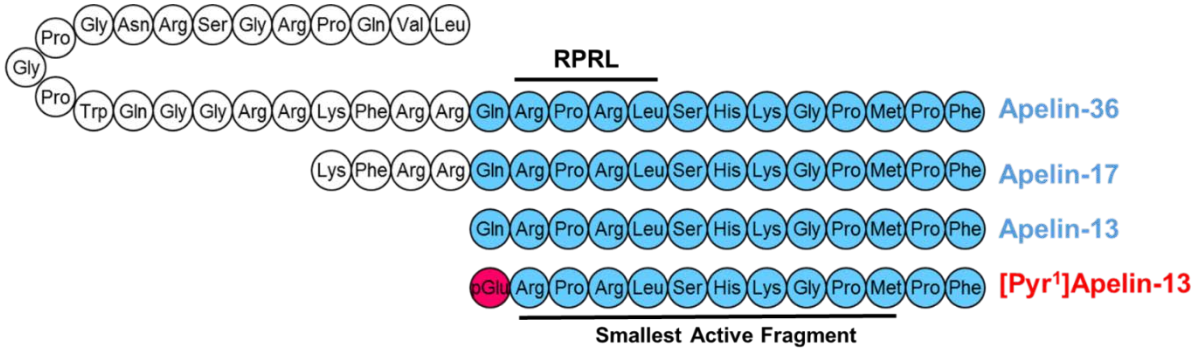

Figure 1.4: The amino acid sequences of cleaved apelin fragments. [Pyr[1]]apelin-13 is the most abundant form in the cardiovascular system and is shown in red with the pyroglutamate residue in pink. The smallest active fragment is highlighted, as well as the RPRL motif which has been thought critical to binding.

Having considered the smallest active fragments of apelin, it is important to discuss how the different fragments bind to the receptor and maintain activity to inform the development of synthetic molecules. Deductions of apelin binding have been largely achieved through alanine scanning mutagenesis and receptor modelling approaches; a crystal structure has only very recently been reported (Ma *et al.*, 2017). It was initially found that mutating the arginine residues in positions 2 and 4 of the apelin peptide greatly reduced the ability of the fragment to bind to the receptor (Fan *et al*., 2003, Medhurst *et al*., 2003). This, alongside the detrimental effect of mutating the lysine in position 8, suggested the importance of positive charge on the apelin peptide for interacting with the receptor (Fan *et al*., 2003). Indeed, concurrent studies utilising the receptor identified that the second ten N-terminal residues of the apelin receptor are essential to interact with the ligand. These residues are largely negatively charged, with the N-terminus of the apelin receptor possessing a net charge of -7, supporting the hypothesis that ionic interactions play a critical role in apelin binding to its receptor (Zhou *et al*., 2003a). Meanwhile, Medhurst and colleagues reported that the largest loss of binding observed in their alanine mutagenesis studies occurred with loss of leucine in position 5 and postulated that the 'RPRL' motif from positions 2-5 plays a critical role in apelin binding. Macaluso and Glen (2010) confirmed the importance of the RPRL motif through elegant cyclisation experiments. They showed that the RPRL sequence produces a favourable β-turn motif which is essential in interaction with the apelin receptor, indeed, when they locked the peptide in an unfavourable turn at the

RLSH sequence, these cyclised peptides were unable to bind the receptor efficiently despite higher sequence homology to the endogenous agonist.

Recent studies have found support for both ionic and RPRL sequence interactions and propose a two-step binding process for apelin peptides to the receptor. First initial ionic interactions occurring between the N-terminal tail of the receptor and the ligand promote binding of the ligand to the receptor. Following this, the ligand moves deeper into the binding pocket where it is able to find more stable interactions and promote receptor activation (Gerbier *et al*., 2015, Langelaan *et al*., 2013, Iturrioz *et al*., 2010b). This greater understanding of how apelin peptides bind to the receptor has informed the design of a number of synthetic agonists based on the apelin sequence and these will be discussed in Section 1.5.

As well as binding the receptor differentially, the different length fragments may activate different pathways at the receptor, leading to different signalling bias. It is important to understand this as any differences could be exploited physiologically by enhanced production of one isoform in a given tissue or at a given time. Additionally, the endogenous bias observed could also be utilised to inform the development of synthetic biased molecules. One area which has been explored is the rate of internalisation and recycling of receptor-ligand complexes, which appear to be highly ligand dependent (Lee *et al*., 2010, Zhou *et al*., 2003a). Lee *et al*. (2010) demonstrated that apelin-13 mediated internalisation could be rapidly reversed when washed out; however, apelin-36 resulted in more prolonged receptor internalisation. El Messari *et al*. (2004) have also reported that apelin-17 is better able to recruit β-arrestin and internalise the receptor than apelin-13. Meanwhile, it has been shown that loss of the C-terminal phenylalanine can induce bias towards G protein signalling (Ceraudo *et al*., 2014). These studies, therefore, suggest that longer length peptides are able to reach a binding pocket that is not accessible to the shorter apelin-13 isoform to induce β-arrestin recruitment and internalisation. This is further supported by longer length ELA peptides also possessing β-arrestin bias (Yang *et al*., 2017b). Accessing this deeper pocket in the receptor likely leads to the ultimate phosphorylation of the C-terminal Ser^{348} residue which when mutated, showed abolition the G protein receptor kinase/ β-arrestin pathway signalling, whilst preserving signalling through the G protein pathway (Chen *et al*., 2014). It is interesting that β-arrestin recruitment and internalisation of the apelin receptor appear to be mediated by only one

phosphorylation site and not by a more complex ‘phosphorylation barcode’ as suggested with other GPCRs (Tobin *et al*., 2008, Butcher *et al*., 2011). Furthermore, it has been suggested that the β-arrestins are not internalised with the ligand-receptor complex, unlike for some other GPCRs (Evans *et al*., 2001).

1.4.2 Elabela

The endogenous agonist, ELA, was named following its discovery (Chng *et al*., 2013). It was independently given the name ‘toddler’ following its discovery as a motogen during gastrulation (Pauli *et al*., 2014). Previously, it had been designated *Ende* when studied as a novel transcript involved in the development of mouse endoderm (Hassan *et al*., 2010). Since then the gene encoding the peptide has been renamed apela (apelin receptor early endogenous ligand) by the HUGO (human genome organisation) gene nomenclature committee (HGCN).

Interestingly, ELA was identified in a previously designated non-coding region of the genome and had already been predicted due to discrepancies between apelin and apelin receptor mutations (Charo *et al*., 2009). Notably, knock-outs of the apelin receptor in mice caused pre-natal mortality (Ishida *et al*., 2004, Roberts *et al*., 2009, Charo *et al*., 2009, Scimia *et al*., 2012, Kang *et al*., 2013) due to disrupted cardiac development with rudimentary or no heart (Kang *et al*., 2013). In contrast, apelin knock-outs had normal heart development (Kidoya *et al*., 2008, Charo *et al*., 2009), though they were at greater risk from age-related and induced disease (Kuba *et al*., 2007). Studies exploring ELA knock-outs in zebrafish found that these phenocopied the apelin receptor mutations (Chng *et al*., 2013, Pauli *et al*., 2014). Furthermore, it has been shown that during development, the apelin receptor was expressed during gastrulation, at the same time as ELA whereas, apelin was not expressed until the end of gastrulation (Pauli *et al*., 2014, Scott *et al*., 2007). While this ligand was first discovered in zebrafish embryos as a factor involved in cardiac development, it has since been shown to have activity in adult mammalian systems (Murza *et al*., 2016, Perjes *et al*., 2016, Yang *et al*., 2017b) and its expression is altered in disease (Yang *et al*., 2017b).During its discovery in zebrafish development, ELA was found to be a 54 amino acid peptide which was cleaved to produce a 32 amino acid mature secreted protein. This mature protein was in turn predicted to undergo cleavage by furin to produce two more fragments of length 21 and 11 amino acids (Chng *et al*., 2013, Pauli *et al*., 2014), all of which have been pharmacologically characterised by Yang *et al.* (2017b; Figure

1.5). Murza *et al*. (2016) have also suggested fragments of 22 and 14 amino acids with a potential 23 amino acid variant. It is notable that the 11 amino acid fragment is invariant between species suggesting strong evolutionary conservation. Interestingly, ELA is more strongly positively charged than apelin and also displays higher binding affinities to the receptor at corresponding fragment sizes (Table 1.1), lending support to an ionic interaction as critical to binding.

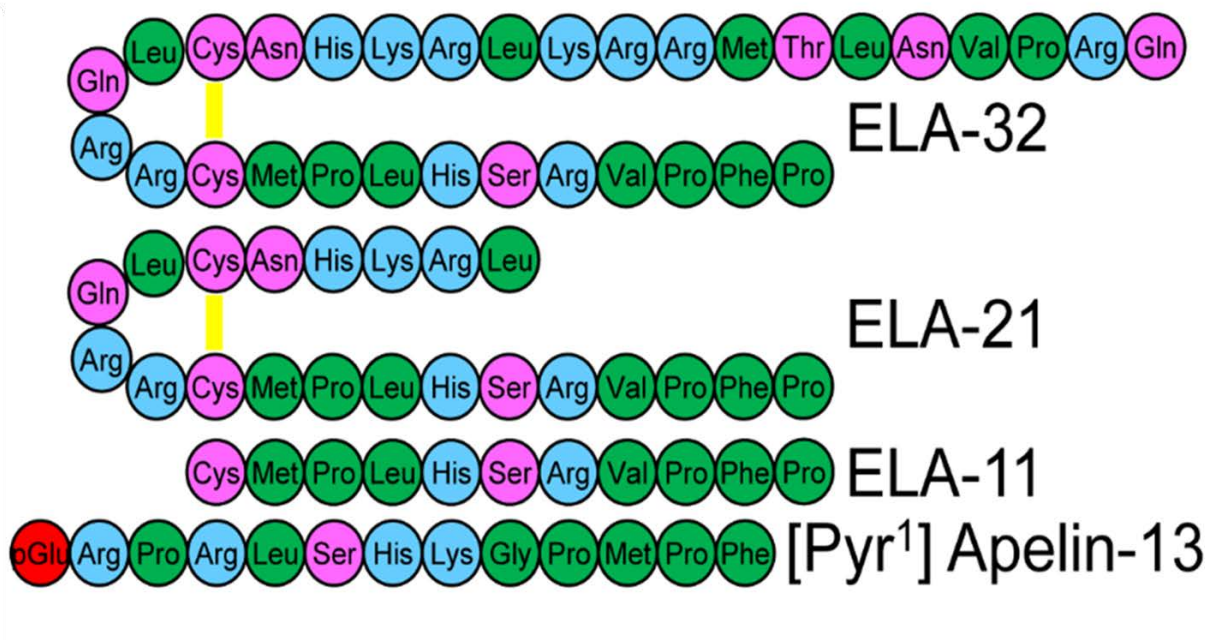

Figure 1.5: The amino acid sequences of the predicted cleaved ELA fragments compared to [Pyr[1]]apelin-13, the most abundant apelin isoform in the cardiovascular system. There is little sequence homology between ELA and apelin fragments; however, there are some similarities in the positioning of charged residues. Disulphide bridges are yellow lines, hydrophobic amino acids are shown in green, uncharged polar amino acids in pink, basic amino acids in blue and pyroglutamate in red. Figure taken from Yang *et al.* (2017b).

1.5 Synthetic Agonists

Given the evidence that apelin treatment can be beneficial in a number of models of disease (discussed below), it is unsurprising that there have been many attempts to produce synthetic apelin agonists with improved characteristics. Such improvements have largely focused on increasing half-life due to the potential limitations of apelin therapeutically as a short-lived peptide. Many of these efforts have produced modified peptides based on the smallest active fragments of apelin, employing techniques such as polyethylene glycol (PEG-)ylation, the addition of unnatural amino acids and cyclisation. One anticipates that soon modified peptides based on the structure of the ELA will be identified and characterised. Finally, while small molecule synthetic agonists would prove to be most useful, only a few small molecule agonists have been reported and these have generally proven unsuitable for experimental or therapeutic use.

1.5.1 Peptide Modifications

PEGylation of certain drugs has previously been shown to improve their pharmaceutical properties and has led to 12 drugs in the clinic since 1990 (Turecek *et al*., 2016). For peptides these benefits for the most part consist of an improvement in half-life through shielding from proteolytic enzymes. Attempts to PEGylate apelin have met with reasonable success. Jia *et al.* (2012) demonstrated that PEGylation of apelin-12 resulted in a 400-fold loss in binding affinity but that N-terminal PEGylation of apelin-36 with a 40kDa PEG conjugate was tolerated. Moreover, *in vivo* assessment of ventricular ejection fraction following 20 minute infusion showed maintained potency. These inotropic effects could still be observed 100 minutes following cessation of infusion, whereas the response was already lost after 30 minutes using the endogenous peptide. In another study, Murza *et al.* (2012) illustrated that modification of C-terminal and central amino acids by addition of $(PEG)_4$, $(PEG)_6$ and $(Ala)_4$ linkers to apelin-13 was able to extend plasma stability. These studies support PEGylation as a means to improve the plasma stability of apelin peptides without compromising functionality if the modifications are made appropriately.

The addition of unnatural amino acids can help to improve stability and potency. For apelin-13 the key modifications have generally been made at the C-terminus as this is where cleavage by ACE2 occurs to remove phenylalanine. Wang. *et al.* (2013b) reported two apelin analogues which were resistant to cleavage of this phenylalanine

residue and identified that one was effective as an apelin mimetic being able to protect against ischaemia-reperfusion injury both *in vivo* and *ex vivo*. Similarly, Murza *et al.* (2015) focussed on replacing the terminal phenylalanine with unnatural amino acids and identified several peptides with improved affinity. In particular, the use of large aromatic groups significantly improved binding with F13Tyr(OBn) displaying a 60-fold improvement over the native peptide and remarkably, the alpha methylated D-analogue, F13(αMe)DTyr(OBn), displaying picomolar affinity. Interestingly, they reported that these molecules were more effective than apelin-13 in preventing cAMP accumulation but were equipotent in β-arrestin recruitment, suggesting that modifications at the C-terminus of the apelin peptide may be important for imparting biased signalling properties. Recently, a group has reported that through a combination of using unnatural amino acids and lipidation of apelin-13, they were able to produce an apelin agonist with a greatly enhanced *in vitro* half-life of 29 hours in rat plasma (Juhl *et al*., 2016). Such a finding is remarkable, particularly since they report that the molecule maintains a high potency at the receptor.

Cyclisation of peptides results in conformational restriction and can improve stability by preventing peptidase action, especially in small peptides, such as apelin, where there is ordinarily a large amount of free movement. Initial experiments showed that apelin-12 peptides when cyclised could retain potency in recombinant human apelin receptor expressing cell lines (Hamada *et al*., 2008). Experiments by Macaluso and Glen (2010), as discussed earlier, demonstrated the importance of the RPRL motif and some following attempts focussed on cyclisation around the RPRL motif. From this approach, MM07 (Figure 1.6) was identified by Brame *et al.* (2015) and showed greater stability over [Pyr^{1}]apelin-13 with a half-life of 17 minutes compared to 2 minutes in rat plasma. Interestingly, this peptide also displayed bias at the receptor, an effect that was maintained in humans when tested using both Aellig hand-vein and forearm venous occlusion plethysmography techniques.

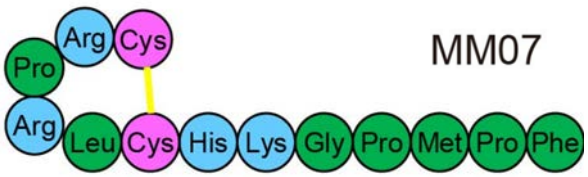

Figure 1.6: The amino acid sequence of MM07. The disulphide bridge is shown as a yellow line, hydrophobic amino acids in green, uncharged polar amino acids in pink and basic amino acids in blue.

Murza *et al.* (2017) have also reported on biased cyclised apelin-like peptides. Instead of cyclising around the RPRL motif they replaced His-7 and Met-11 with allylglycine and cyclised between these residues. They further replaced the C-terminal phenylalanine residue with Tyr(OBn) and produced various modifications upon this scaffold structure. They were able to display that replacement of the Tyr(OBn) residue with non-aromatic residues or transfer into the ring structure markedly reduced the ability to recruit β-arrestins. Such bias towards G protein signalling was similar to MM07; however, unlike MM07 which produced clear decreases in blood pressure in human volunteers, Murza *et al*. (2017) reported that their G-protein biased compounds had a reduced ability to induce hypotensive effects in rats. Such an observation is supported by the report of modified apelin-17 peptide fragments biased towards the β-arrestin pathway which were more able to induce decreases in blood pressure in rats (El Messari *et al*., 2004). Of the compounds described by Murza *et al*. (2017), compound 18 is notable, despite its low micromolar affinity. This is due to its lack of the RPRL motif, a motif previously thought critical to binding. Additional studies that have looked at cyclisation away from the RPRL motif include a patent by Novartis (Golosov *et al*., 2013) producing peptides based on [Pyr^{1}]apelin-13 with a range of bridging linkers including, esters, disulfides, amides, and short polyether bridges. Of these, some showed improved half-lives and a few were reported to possess similar potency to Pyr^{1}]apelin-13.

While many studies have focussed on unnatural amino acid addition, cyclisation and PEGylation as a means to improve the pharmacological properties of peptides, one very interesting study has looked at the use of pepducins. These are lipidated peptide sequences usually 8-16 amino acids in length and based on the structure of the intracellular loops of G-protein coupled receptors. McKeown *et al.* (2014) produced a complete array of N-lipidated 12-mer peptide sequences for the apelin receptor and 7 demonstrated agonism at 1μM or 10μM and were resynthesized. One compound, designated compound 1, displayed activity and was found to be selective for the apelin receptor. This result was not unexpected given the sequence from which it was based is a poorly conserved region of the GPCR. Furthermore, to confirm selectivity they produced the peptide with D-amino acids as well as without the N-terminal palmitate lipidation and demonstrated a complete loss of activity. Such a unique approach is very interesting and could be widely applicable to drug discovery at orphan GPCRs.

1.5.2 Small Molecules

While the above studies have produced a number of improved apelin peptide molecules, particularly with regards to enhanced plasma half-life, they still possess the limitations that all peptide therapies inevitably have, most notably poor oral bioavailability. Sufficient improvements in plasma half-life could reduce the impact of this and, as evidenced by diabetic therapy, daily injections are tolerable if necessary. However, the production of a small molecule apelin agonist would nevertheless have much greater potential therapeutically and could be used much more widely and easily as a pharmacological tool compound than a peptide. For these reasons there have been a number of attempts to produce a small molecule apelin agonist. Only relatively recently have suitable molecules started to emerge.

One of the first reports of a peptidomimetic small molecule was E339-3D6 (Iturrioz *et al*., 2010a) which showed a reasonable affinity for the apelin receptor (K_i~400nM in radioligand binding experiments) and selectivity over other related GPCRs. However, with a molecular weight of 1400Da it is debatable whether it would qualify as a small molecule; moreover, it was later shown to be a mixture of polymethylated species (Margathe *et al*., 2014). The constituents of this mixture were separated and some were found to bind to the apelin receptor with improved affinity compared to the parent mixture, however, these affinities were still relatively low and the molecules too big.

Another attempt to identify a small molecule agonists utilised a high-throughput screen of ~330,600 molecules and found ML233 (Khan *et al*., 2010). This molecule conformed to the traditional definition of a small molecule with a molecular weight of 359Da under the usual 500Da cut-off defined by Lipinski's rules. Unfortunately, it showed poor solubility in saline at room temperature and its structure indicated it would likely be toxic through being both a Michael acceptor and possessing a reactive activated quinone group (Lagorce *et al*., 2015). Indeed observations in animal studies have supported this suspected toxicity (*Pers. Comm.* Yang, Maguire and Davenport).

Recently, several studies and patents have reported the development of more suitable drug-like small molecules. Narayanan *et al.,* (2016) used a drug library of approximately 100 compounds screened in a high-throughput Ca^{2+} mobilisation assay and identified four compounds based on the same structural scaffold which they designated compound 1. By experimenting with three key side chain sites, they explored the changes that were tolerated by the scaffold and suggested that this could

act as a starting point for the production of more suitable drug-like small molecules. While these molecules were small (molecular weight ~500Da), they possessed relatively low potencies in the micromolar range. The important question will be whether potency can be improved by side-chain experimentation or if it is a limit of the scaffold itself.

1.5.3 Summary

There have been significant advances in the development of synthetic agonists at the apelin receptor. Studies utilising peptide modification have been able to improve plasma stability and affinity through a variety of methods, including PEGylation, cyclisation and the addition of unnatural amino acids. Initial studies to identify small molecules have had significant issues and newer more suitable small molecules are required. Such molecules would be very useful as tool compounds and in the development of small molecule therapeutics.

Ligand	*Action*	*Binding Affinity*	*Units*	*References*
MM54	Antagonist	8.2	pK_i	Macaluso *et al*., 2011
ALX40-4C	Antagonist	5.5	pIC_{50}	Zhou *et al*., 2003b
ML221	Antagonist	-	-	Maloney *et al.,* 2012
Protamine	Antagonist	6.4	pK_i	Le Gonidec *et al.,* 2017

Table 1.2: Some of the key antagonists at the apelin receptor and their binding affinities. MM54, a designed antagonist, consists of a cyclised peptide based around the RPRL motif. ALX40-4C and protamine both consist of a series of positively charged amino acids and display low binding affinities and likely low selectivity for the apelin receptor.

1.6 Synthetic Antagonists

Just as there has been much interest in the development of agonists at the apelin receptor, antagonists at the receptor have also been sought. So far, though a number have been described, there is still a need to find more suitable molecules for use both in *in vitro* and *in vivo* studies. Apelin antagonists might also possess therapeutic potential themselves and recently there has been interest in their use for the treatment of cancer due to their anti-angiogenic effects.

One of the first antagonists described was F13A, an apelin analogue in which the C-terminal phenylalanine was mutated to an alanine residue. Initially, De Mota *et al.* (2000) described alterations in the apelin peptide K17F (a 17 amino acid chain stretching from lysine (1) to phenylalanine (17) of the apelin sequence) and identified that the first four amino acids were not required for activity, thus, describing apelin-13. They further suggested that substitution of the terminal phenylalanine for alanine completely abolished activity. Lee *et al.* (2005) later described the antagonist activity of F13A in spontaneous hypertensive rats through the blockade of hypotensive responses induced by apelin. Despite these two studies suggesting F13A does not possess agonist activity and the latter describing it as an antagonist, other studies dispute this. Both Fan *et al.* (2003) and Medhurst *et al.* (2003) describe it in alanine mutagenesis studies as an agonist as discussed in Section 1.4.1. Fan *et al.* (2003) reported that F13A possessed equal potency to apelin-13 in inducing receptor internalisation, meanwhile, Medhurst *et al.* (2003) reported a decrease in both binding affinity to the apelin receptor (2-14-fold) and in potency in a FLIPR assay (8-fold). In a recent study, Yang *et al*. (2017a) also reported on the activity of F13A, demonstrating that it possessed similar activity to [Pyr^{1}]apelin-$13_{(1-12)}$ in an *in vitro* β-arrestin recruitment assay and that it was also able to contract saphenous vein *ex vivo* with sub-nanomolar potency. These studies suggest, therefore, that F13A retains agonistic activity and is not in fact an antagonist. Perhaps, the best explanation is that it acts as a partial agonist - this would explain its ability to antagonise hypotensive responses to apelin (Lee *et al*., 2005) and its agonist activity when tested on its own (Medhurst *et al*., 2003, Yang *et al*., 2017a).

Another reported peptide antagonist is ALX40-4C (Zhou *et al*., 2003b). It was originally identified at the CXCR4 chemokine receptor in the context of HIV infection (it was through this that Zhou and colleagues identified its activity at the apelin receptor which

acts as a co-receptor for HIV infection; Section 1.7.6). They demonstrated direct binding to the receptor with an IC_{50} of 2.9μM and inhibition of internalisation induced by apelin. Despite antagonistic effects, there is little evidence that it could be used as a selective apelin antagonist. Indeed, it was identified initially as a CXCR4 antagonist and although its sequence of a string of highly charged amino acids might make it effectual in blocking the apelin receptor, it is unlikely to aid selectivity over other GPCRs. Without selectivity it is unlikely to find use either as a pharmacological tool compound or in therapy.

A peptide agonist, MM54, designed based on known functionality of apelin sequences at the apelin receptor would be expected to show more promising selectivity (Macaluso *et al*., 2011). Macaluso and colleagues started with the RPRL motif to produce two cyclic 'anchors' with a dipeptide linker in between. They hypothesised that the linker could be altered to act as a 'switch', thus, alternating receptor stabilisation between agonist and antagonist states. MM54, bound to the human apelin receptor in left ventricular (LV) heart homogenates with micromolar affinity (K_D = 3.42μM) and was able to competitively antagonise [Pyr^1]apelin-13 in cAMP accumulation assays in Chinese hamster ovary (CHO)-K1 cells giving a similar affinity in Schild analysis (K_D = 1.32μM). While the affinity of MM54 is not especially high, the fact that it is a designed apelin antagonist should aid in the development of new antagonists based on the same structure. Recently Harford-Wright *et al.* (2017) have reported on the use of MM54 to treat glioblastoma. In this study, they tested MM54 for selectivity for the apelin receptor by screening it in radioligand binding assays against a panel of 55 other GPCRs or ion channels. They found that MM54 at 10μM inhibited 50% of agonist binding in apelin and only 6 other potential off-target receptors.

A small molecule, ML221, displayed antagonistic action in the micromolar range to both cAMP and β-arrestin signalling through the apelin receptor (Maloney *et al*., 2012). However, it showed a poor pharmacokinetic profile with very limited solubility in aqueous media at pH7.4 and poor stability. Despite these drawbacks, it could still be useful for *in vitro* studies and has good selectivity for the apelin receptor, only showing significant activity at the benzodiazepinone and κ-opioid receptors. Its use is not recommended for *in vivo* studies as it has been observed to possess high toxicity (*Pers. Comm.* Yang, Maguire and Davenport).

Most recently, the U.S Food and Drug Administration (FDA)-approved compound, protamine, has been identified as an antagonist at the apelin receptor (Le Gonidec *et al*., 2017). This compound is usually used after cardiac surgery as it binds to heparin and therefore, reverses anticlotting activity. The study demonstrates a binding affinity of 390nM at the apelin receptor and full antagonistic activities against both G protein and β-arrestin signalling, as well as against *in vivo* dilatation in mice. Screening against several other homologous GPCRs, such as, the AT1 receptor suggests some degree of selectivity. However, caution is advised as the structure of protamine is based on a series of highly positively charged arginine residues and is reminiscent of ALX40-4C.

There is still a need for a selective antagonist at the apelin receptor as currently available molecules possess limitations. Future studies will hopefully lead to selective, high affinity antagonists for use in pharmacological study as well as in therapy.

1.7 Apelin Physiology and Pathophysiology

1.7.1 Development

ELA appears to be the principal developmental peptide at the apelin receptor. It was in part due to discrepancies in apelin receptor and apelin peptide knock-out zebrafish, as well as the fact that apelin is not expressed until much later in development than its receptor, that prompted the discovery of ELA (Pauli *et al*., 2014). Nevertheless, apelin has been shown to have some developmental roles. Kidoya *et al.* (2015) found that apelin through its receptor was important for arterial-venous alignment in the skin. They demonstrated that knock-out mice of both the receptor and peptide were less able to deal with hot or cold heat stress, suggesting an important role in thermoregulation.

1.7.2 Cancer

Apelin expression is elevated in a number of cancers, such as, lung non-small cell carcinomas, gastroesophageal, colon, hepatocellular, prostate, endometrial and oral squamous cell carcinoma. It induces endothelial cell migration and proliferation, supporting a role in tumour neoangiogensis; for a detailed review on the subject see Yang *et al*. (2016). The high expression of apelin in cancerous tissues raises the possibility of using it as a biomarker and clinical trials are underway to determine if a reduction in serum apelin levels can be used to assess the efficacy of bevacizumab treatment as a measure of tumour vasculature normalisation following similar observations in a mouse model (Zhang *et al*., 2016).

Directly targeting the apelin receptor with antagonists could prove a useful therapy if used in appropriate combination with current market drugs. In a recent study, Harford-Wright *et al.* (2017) reported on MM54 treatment of glioblastoma. They demonstrated that glioblastoma stem-like cells expressing higher apelin levels were better able to initiate tumour development. Furthermore, knocking down apelin with shRNA could reduce the number of progressing tumours in an *in vivo* implant model. They went on to look at pharmacological inhibition with MM54 and showed that it impaired the expansion of glioblastoma stem-like cells that were resistant to standard therapy *in vitro*. This translated to the *in vivo* tumour xenograft model with MM54 reducing tumour growth and promoting survival of transplanted mice. Interestingly, targeting the apelin receptor in this model proved beneficial by reducing vascularisation and proliferation in the tumour, however, another recent study has identified loss-of-function mutations

in the apelin receptor in patients refractory to immunotherapy (Patel *et al.,* 2017). They showed a role for the apelin receptor in modifying T-cell responses through the JAK-STAT pathway, leading to an augmentation of the interferon-γ response. This response appeared to be independent of canonical G protein signalling through the apelin receptor and whereas the authors demonstrated that knocking-down the apelin receptor in mouse melanoma models reduced the efficacy of T-cell-based therapies, they did not show whether an antagonist would do the same. This question should be addressed as, if the JAK-STAT response is ligand-independent, this could avoid the potential complication of apelin receptor blockade reducing host immune responses in cancer.

1.7.3 Fibrosis

Apelin is involved in fibrotic mechanisms in a number of tissues, including kidney, liver, heart and lung; for a detailed review see Huang S. *et al*. (2016). Intriguingly, apelin displays conflicting roles in these different tissues, protecting against renal, myocardial and pulmonary fibrosis, whilst potentially promoting liver fibrosis.

In the kidney, plasma apelin levels are significantly lower in patients with autosomal dominant polycystic kidney disease compared to controls and apelin levels correlated with estimated glomerular filtration rate (Kocer *et al*., 2016). The mechanism by which apelin is protective has been suggested to involve transforming growth factor β (TGFβ) signalling with demonstrations that apelin is able to reduce renal interstitial fibrosis through suppressing tubular epithelial to mesenchymal transition via a smad-dependent mechanism (Wang *et al*., 2014). Moreover, in a renal ischaemia/reperfusion model in rats, apelin was down-regulated and infusion of apelin-13 could reduce acute injury through suppressing of TGF- β1 (Chen *et al*., 2015).

In addition to its involvement in renal fibrosis, TGFβ is known to have roles in numerous fibrotic mechanisms (Leask and Abraham, 2004) including in the myocardium (Koitabashi *et al*., 2011). A downstream miRNA of TGF- β, miR-125b, has been shown to be upregulated in cardiac fibrosis and to inhibit apelin (Nagpal *et al*., 2016). This supports a role for apelin down-regulation in fibrosis and provides a mechanism through which it may occur. It also suggests that apelin replacement could be beneficial. Indeed, it has been shown that infusion of various apelin isoforms is beneficial in several models of myocardial damage, for example, in mice with ligated

coronary arteries to induce infarction and subsequent cardiac hypertrophy and fibrosis, apelin-13 was protective (Li *et al*., 2012). Furthermore, apelin recruited bone marrow cells and adenovirally-mediated overexpression of apelin in these cells enhanced cardiac repair (Li *et al*., 2013). In isolated perfused rat hearts, infusion of apelin-12 analogues were beneficial in reducing myocardial infarct size, cell membrane damage and cardiac dysfunction. This protection was associated with activation of various cellular kinases, leading to activation of numerous downstream targets including, nitric oxide synthase, mitochondrial K_{ATP} channels and the sarcolemmal Na^+/H^+ and Na^+/Ca^{2+} exchangers (Pisarenko *et al*., 2015a). Additionally, these apelin-12 analogues reduced reactive oxygen species, resulting in a reduction in cellular membrane damage (Pisarenko *et al*., 2015b). Other reports have suggested that apelin-13 can protect against *in vivo* myocardial ischaemia-reperfusion by inactivation glycogen synthase kinase 3β, preventing the opening of the mitochondrial permeability transition pore involved in the reperfusion injury salvage kinase pathway (Yang *et al*., 2015b). In apoE-KO mice infused with angiotensin II to induce atherosclerosis of the coronary arteries, co-infusion of apelin-13 could activate nitric oxide and thereby, attenuate atherosclerosis of these vessels, as well as preventing vascular remodelling in a vein graft model (Chun *et al*., 2008).

Pulmonary fibrosis occurs in many lung pathologies and there is evidence that apelin can help to prevent this from occurring. In a rat model of bronchopulmonary dysplasia (a chronic disease which normally occurs in premature infants treated with oxygen and positive pulmonary pressure) treated with apelin-13, pulmonary fibrin deposition and inflammation were reduced (Visser *et al*., 2010). Meanwhile, in a rat model of acute respiratory distress syndrome induced by oleic acid, apelin-13 treatment could reduce inflammation and lung injury. F13A also reduced oleic acid induced histopathological changes, although the authors erroneously refer to F13A as an antagonist (Fan *et al*., 2015a).

Unlike in kidney, myocardial and lung fibrosis where apelin is beneficial, in hepatic fibrosis the role of apelin is less clear. In cirrhotic rat liver, both the apelin receptor and peptide are increased, meanwhile in cirrhotic patients, circulating apelin levels are increased (Principe *et al*., 2008). However, treatment of cirrhotic rats with F13A led to an alleviation of liver fibrosis (Principe *et al*., 2008, Reichenbach *et al*., 2012). This might suggest that the lower activity of F13A is sufficient to partially antagonise the

elevated endogenous apelin, supporting a role as a partial agonist. Alternatively, it is possible that the elevation of apelin is a protective mechanism and hence, F13A is protective as an agonist. Further studies are required to clarify the role of apelin in liver fibrosis.

Overall, apelin is beneficial in a number of different disease models of tissue fibrosis in kidney, heart and lung tissues; however, it may accentuate liver fibrosis. Such a role in myocardial and pulmonary fibrosis could be particularly useful in treating heart failure and PAH where substantial fibrosis is known to occur in both organs (Murtha *et al*., 2017, Thenappan *et al*., 2018) and where apelin has already been identified as a potential therapeutic strategy.

1.7.4 Pulmonary Arterial Hypertension (PAH) and Heart Failure (HF)

The vasodilatory and inotropic effects of apelin signalling have made it of particular interest as a potential therapeutic for diseases, such as, PAH and heart failure (HF) (Yang *et al*., 2015a). Interestingly, there is significant evidence that the apelin peptide is downregulated in both diseases. In PAH this has been found in human patient plasma (Goetze *et al*., 2006), sugen-hypoxia and monocrotaline (MCT) models in rats (Kim *et al*., 2013, Falcao-Pires *et al*., 2009) and a mouse model with an endothelial cell specific PPARγ (peroxisome proliferator-activated receptor gamma) deletion (Alastalo *et al*., 2011). In HF it has been shown in several studies that apelin levels are decreased in human patient plasma (Chong *et al*., 2006, Foldes *et al*., 2003, Francia *et al*., 2007), in tissues from a number of rat models (Iwanaga *et al*., 2006, Koguchi *et al*., 2012), in mouse doxorubicin-induced cardiotoxicity and in a dog model (Wang *et al*., 2013a). Another study in human patients has suggested that apelin plasma levels are only decreased in late stage HF and are in fact increased in early stage disease (Chen *et al*., 2003). Such an effect would be unsurprising, given what is known about HF progression, with an often compensatory early stage followed by maladaptation later. However, these results were not corroborated in a study on Dahl-salt sensitive rats in which there was no change in apelin levels in the early stage of the disease but the levels did decrease as expected in later disease (Iwanaga *et al*., 2006). Overall, these studies support plasma apelin levels as a useful biomarker of disease progression. Importantly, apelin levels can also be modulated in disease and it has been shown that patients fitted with LV assist devices display higher apelin levels in addition to improved disease parameters (Chen *et al*., 2003, Francia *et al*., 2007).

Even though apelin is highly downregulated, expression of the apelin receptor appears to be less strongly suppressed in these diseases and crucially, remains responsive to apelin. In rats induced to develop PAH by hypobaric hypoxia, apelin receptor levels were unchanged (Andersen *et al*., 2009), whereas in an MCT model, the apelin receptor was downregulated in concert with apelin (Falcao-Pires *et al*., 2009). In rat models of HF, apelin receptor expression has mostly been found to decrease. This was the case in LV myocytes from hypertensive animals, where infusion of [Pyr^{1}]apelin-13 restored some receptor expression (Pang *et al*., 2014), as well as in the myocardium of an isoproterenol-induced injury model (Jia *et al*., 2006). Studies using Dahl salt-sensitive hypertensive rats have demonstrated a decrease in apelin receptor expression in the same pattern as observed for the apelin peptide (Koguchi *et al*., 2012, Iwanaga *et al*., 2006) while one also found no change in the early stage of the disease (Iwanaga *et al*., 2006), perhaps suggesting that earlier intervention could be more beneficial. Mice induced to exhibit cardiotoxicity with doxorubicin also displayed reductions in apelin receptor expression (Hamada *et al*., 2015). A study using microembolisation-induced HF in dogs, showed that the apelin receptor was not decreased compared to controls, even though apelin was (Wang *et al*., 2013a). However, most crucially human subjects with HF were still able to respond to infused [Pyr^{1}]apelin-13 and this was more efficacious in patients receiving PDE5 inhibitor treatment (Barnes *et al*., 2013, Brash *et al*., 2018) . Additionally, it has been shown in patients fitted with LV assist devices that the apelin receptor is the most upregulated gene, in concert with improved disease parameters (Chen *et al*., 2003). Together these studies demonstrate that while the apelin receptor may undergo some downregulation in disease, this is susceptible to modulation and its expression is seen to increase alongside positive changes in cardiac parameters.

Given the downregulation of apelin but maintenance of signalling through the receptor, replacement of the downregulated endogenous agonist could be useful therapeutically. One concern with this strategy is that in the diseased state, one would anticipate the endothelium becoming damaged and therefore, less responsive to apelin, limiting therapeutic efficacy. However, previous work has shown that infusion of apelin is beneficial in a number of disease models. [Pyr^{1}]apelin-13 given intraperitoneally (IP) was able to alleviate right ventricle (RV) hypertrophy and diastolic dysfunction in the MCT rat model of PAH (Falcao-Pires *et al*., 2009). It has also been shown that ELA is

able to replace the missing endogenous apelin peptide and prevent PAH in an MCT model (Yang *et al*., 2017b). In several rat models of HF, including isoproterenol-induced (Jia *et al*., 2006), Dahl salt-sensitive hypertensive (Koguchi *et al*., 2012), two-kidney, one clip hypertensive (Pang *et al*., 2014) and in left anterior descending coronary artery ligation (Atluri *et al*., 2007, Berry *et al*., 2004), apelin induced beneficial changes in the disease state. In mice subjected to transverse aortic constriction to induce a pressure-overload model of HF, [Pyr^{1}]apelin-13 administered IP in liposomal nanocarriers displayed a longer duration of action and a reduction in LV size and fibrosis compared to controls or even mice administered [Pyr^{1}]apelin-13 (Serpooshan *et al*., 2015). Such a result is promising in suggesting that simply by extending the duration of action, rather than the dose of [Pyr^{1}]apelin-13 administered, it would be possible to extend the benefits observed in disease. The improvements in rodent models were recapitulated in the microembolism-induced dog model given apelin-13 discussed earlier, with an improvement in ejection fraction and LV systolic parameters observed acutely (Wang *et al*., 2013a). As well as demonstrating that apelin can be beneficial when infused, studies have also shown that deletion of the apelin receptor and ligand exacerbate disease. In a doxorubicin-induced mouse model of cardiotoxicity, deletion of the apelin receptor led to a more severe reduction in cardiac contractility and accelerated myocardial damage compared to control animals (Hamada *et al*., 2015). At the same time, apelin knock-out mice developed impaired cardiac contractility when aged, or chronic HF when subjected to pressure-overload (Kuba *et al*., 2007). An interesting study in patients has also hinted at beneficial effects of apelin in humans (Boal *et al*., 2015). This study discussed the idea that patients with higher body mass indices and decompensated HF displayed lower in-hospital mortality, while apelin is also increased in these obese patients. Using an obese mouse model subjected to ischaemia-reperfusion to test this hypothesis, they suggest a mechanism whereby apelin prevents the nuclear translocation of a transcription factor critical to mitochondrial regulation, FoxO3, thus, promoting cell survival pathways and consequent cardioprotection.

In conclusion, there is strong evidence that the apelin-apelin receptor signalling axis is perturbed in both PAH and HF and that modulation of this system by reintroduction of the downregulated apelin ligand or of ELA could be beneficial.

1.7.5 Obesity and Diabetes

Apelin is increased in the morbidly obese (Soriguer *et al*., 2009) and patients with Type 2 diabetes mellitus (Li *et al*., 2006). Interestingly, apelin has been suggested to have beneficial effects in metabolic disease and diabetes in a number of studies. It is reviewed in detail in Castan-Laurell *et al*. (2012).

[Pyr^{1}]apelin-13 is beneficial in promoting brown adipose tissue differentiation, in addition to promoting brown adipose tissue basal activity, as shown by the enhanced expression of uncoupling protein 1, increased mitochondrial biogenesis and increased oxygen consumption. Furthermore, it has been suggested from *in vitro* and *in vivo* experiments that it can even promote brown-like adipose tissue characteristics in white adipose tissue (Than *et al*., 2015).

Apelin has been shown to be expressed in beta and alpha cells of the pancreas, while the receptor is found on INS-1 clonal beta cells in mice and humans (Ringstrom *et al*., 2010). Selective deletion of the apelin receptor in pancreatic islet β-cells of mice resulted in a reduction of islet size, density and cell mass. These cells showed a decreased insulin secretion *in vitro* and the mice displayed decreased glucose tolerance (Han *et al*., 2015). Furthermore, apelin administration reduced insulin resistance during a hyperinsulinemic-euglycemic clamp in mice, by stimulating glucose uptake in soleus muscle (Dray *et al*., 2008). Further studies in mice have shown that chronic apelin treatment decreases insulin resistance by increasing fatty acid oxidation and mitochondrial biogenesis (Attane *et al*., 2012). Finally, in a study to assess whether apelin could be beneficial when administered in a diabetic rat model, it was found that [Pyr^{1}]apelin-13 could induce a reduction in plasma insulin and glucose levels with a concurrent reduction in blood pressure (Akcilar *et al*., 2015). These studies, therefore, indicate an important role for the apelin system in the regulation of glucose in diabetes and suggest it could potentially be used as a therapeutic intervention.

Observational human studies have confirmed the presence of increased apelin concentrations in type 2 diabetes mellitus and obesity (Castan-Laurell *et al*., 2011) and they have raised the possibility of its use as a biomarker (Ma *et al*., 2014). Studies in patients receiving either metformin alone or in combination with vildagliptin demonstrated that apelin levels were enhanced when compared to controls for those receiving the monotherapy and even more greatly increased when on combinatorial

therapy (Fan *et al*., 2015b). These increases in apelin were seen alongside an improvement in fasting glucose and glycosylated haemoglobin levels, supporting the use of apelin as a marker of improved diabetic control in patients.

Only one published study has measured the metabolic effects of intravenously infused apelin in humans. Gourdy *et al.* (2018) demonstrated that apelin infused over a 2-hour period during hyperinsulinemic-euglycemic clamping improves insulin sensitivity in overweight men. Meanwhile, unpublished data from our group demonstrated a decrease in blood glucose in non-diabetic volunteers following a 6 minute apelin intravenous infusion (100 nmol/min) (*Pers. Comm.* Brame and Davenport, 2013).

1.7.6 HIV/SIV Co-Receptor

Human immunodeficiency viruses (HIV) and Simian immunodeficiency viruses (SIV) generally use the CD4 receptor and a co-receptor, usually one of the chemokine receptors CCR5 or CXCR4, to infect host cells. However, the apelin receptor (which displays some structural similarities to CXCR) can also perform this function for a number of HIV-1 and SIV strains (Choe *et al*., 1998, Edinger *et al*., 1998, Zhang *et al*., 1998, Puffer *et al*., 2000) and this can be blocked by apelin (Puffer *et al*., 2000, Cayabyab *et al*., 2000, Zou *et al*., 2000). Zhou *et al*., (2003a) demonstrated that the key interactions occur through the first 20 N-terminal amino acids of the apelin receptor and the gp120 HIV-1 viral protein and that apelin blocked this by interacting with the second ten residues of the N-terminus. Since these early studies, there have been few follow-up studies and the relevance and implications of apelin receptor involvement in HIV-1/SIV infection have not been addressed.

1.7.7 Fluid Homeostasis

Apelin has been shown to have roles in the uptake and retention of fluid as reviewed by Flahault *et al*. (2017). These responses were modest and appear mostly to be through interactions with regions of the central nervous system associated with arginine-vasopressin. Apelin receptor knock-out mice drank less than wild-type mice though the volume and osmolality of urine excreted did not differ. Furthermore, although wild-type mice showed reduced urine volume and increased osmolality following 24 hour water deprivation, apelin receptor knock-out mice did not (Roberts *et al*., 2009). In rats injected intracerebroventricularly with [Pyr^{1}]apelin-13, a dose-dependent increase in drinking behaviour and water uptake was observed (Taheri *et*

al., 2002). It has also been shown more recently that apelin-17 can directly affect the collecting ducts in the kidney to counteract the anti-diuretic effects of vasopressin, thus, enhancing the diuretic effects of apelin and the complexity of apelin-vasopressin interactions (Hus-Citharel *et al*., 2014).

1.8 ELA Physiology and Pathophysiology

1.8.1 Developmental Roles

ELA was first discovered as a critical developmental peptide in zebrafish cardiogenesis (Chng *et al*., 2013, Pauli *et al*., 2014), an important role which is supported by the high degree of conservation at the functional C-terminal end of the peptide. This effect is mediated through the apelin receptor and may occur through an enhancement of nodal/TGFβ signalling. In fact, nodal elevation in aplnra/b double knock-out zebrafish embryos is sufficient to rescue them from the resulting cardiac differentiation defects (Deshwar *et al*., 2016). Following its identification, it was not initially clear whether ELA was involved in other developmental mechanisms and consequently, a number of studies set out to investigate this.

In experiments also studying zebrafish embryos Helker *et al.*, (2015) demonstrated that ELA was important for angioblast migration during the formation of large axial vessels, dorsal aorta and cardinal vein. Crucially, this was through the apelin receptor with knock-out embryos unable to form the vessels correctly. Additionally, WT angiobalsts injected into a knock-out background embryo were able to restore function, showing that these cells were responding to secreted ELA.

In mammalian development, ELA has been studied in human embryonic stem cells (ECSs; Ho *et al*., 2015) and mouse ESCs (Li *et al*., 2015). Both of these studies reported that neither human nor mouse ESCs express the apelin receptor; however, in both cases they do demonstrate ELA expression. Ho *et al.*, (2015) reported that a loss of ELA by shRNA knock-down leads to a loss of morphology and an inability to form teratomas, a characteristic trait of stem cells. This could be rescued by exogenously applied ELA, perhaps suggesting an alternative receptor in this cell type. Li *et al.* (2015), meanwhile, found that ELA was a downstream target of p53 whose knock-down could prevent DNA damage-induced apoptosis in mouse ESCs. They performed a BLAST search to identify potential additional targets of ELA with similar sequences to the apelin receptor but claim not to have identified any. They instead suggested that ELA RNA is involved in a feedback loop with p53 in mouse ESCs to regulate DNA damage-induced apoptosis and demonstrated that the coding region of ELA is dispensable to function in support of this. Recently, it has been shown that the ELA-apelin receptor axis plays an important role in coronary artery development in the

mouse heart (Sharma *et al*., 2017), supporting zebrafish studies and the vasculature defects observed in knock-out organisms. In this study, Sharma *et al.* (2017) genetically labelled apelin receptor expressing cells and found that these cells were found in sinus venosus and not endocardial coronary progenitors. In both homo- and heterozygous apelin receptor mutants, the sinus venosus coronary progenitors failed to migrate properly to form vasculature structures in the heart but this failure could be compensated by enhanced endocardial progenitor proliferation. ELA mutant hearts phenocopied the receptor mutants but apelin mutants did not, supporting ELA as the important signalling peptide in this pathway.

1.8.2 Adult Cardiovascular Roles

In addition to being present in various mammalian cell types including human pluripotent stem cells, Wang. *et al*., (2015) showed that ELA was able to perform functions in adult cell types and tissues. They demonstrated that ELA could induce angiogenesis of human umbilical vein endothelial cells *in vitro* in Geltrex coated wells and that this was abolished if apelin receptor was knocked-down. They also reported that ELA could induce relaxation in mouse aortic blood vessels. Since then further studies have identified ELA as a positive inotrope and vasodilatory agent *ex vivo* (Perjes *et al*., 2016) and *in vivo* in rats (Murza *et al*., 2016, Yang *et al*., 2017b). The study by Yang *et al*. (2017b) also looked at the ability of ELA peptides to bind to the apelin receptor in homogenates of human LV and to activate signalling pathways in cell-based assays expressing the human receptor. This study went on to demonstrate that ELA is present in both large and small diameter human blood vessels, as well as in human plasma.

1.8.3 Disease and the Possibility of a Second Receptor for ELA

Perhaps most interestingly, the study by Yang *et al*. (2017b) showed that ELA was down-regulated in plasma serum, pulmonary arterial endothelial cells and pulmonary microvascular endothelial cells from patients with PAH, raising the possibility that ELA is not only functional in the adult human but also altered in the diseased state. They went on to demonstrate that ELA was able to attenuate the onset of PAH in a MCT rat model. A number of other studies have also looked at the ability of ELA to modify disease in animal models. Chen. *et al.* (2017a) demonstrated that both ELA-32 and ELA-11 could protect against renal ischaemia-reperfusion injury, while Schreiber *et al.*

(2016) showed that adenovirally-delivered ELA could protect against kidney damage in a Dahl-salt sensitive rat model. However, what is still unclear is whether ELA mediates these protective effects through the apelin receptor or through a distinct receptor. Several studies have produced contradictory evidence regarding this.

Chen *et al.* (2017a) used siRNA knock-down of the apelin receptor in NRK-52E cells and did not observe any changes in cell viability either in normoxic or hypoxic conditions. Meanwhile, Ho *et al.* (2017) looked at ELA and apelin knock-out in pregnant mice. They showed that ELA and not apelin knock-outs displayed preeclampsia-like symptoms and that infusion of ELA could alleviate them. They also demonstrated that ELA knock-out mice placentas were not rescued by apelin but were by ELA infusion, again suggesting differences in signalling pathways. They conclude that the preeclampsia alleviation is likely achieved through apelin receptor signalling in endothelial cells. They also do not rule out a possible contribution from additional unidentified ELA receptors. On the contrary, Sato *et al.* (2017) suggested that administration of ELA peptide could protect against cardiac dysfunction, hypertrophy and fibrosis in pressure overload mice. Importantly, apelin receptor knock-out mice did not respond to ELA administration, demonstrating that the protection was mediated by the ELA-apelin receptor axis. These studies raise important questions about whether such a second receptor for ELA exists, since if this receptor was another GPCR, it would be remarkable that it should be selective between apelin and ELA. It is likely that, as many ligands do, apelin and ELA have different signalling profiles in different tissues/organs (as well as between cell and animal models) and this could explain discrepancies in ELA and apelin knock-outs; however, it would not be able to explain the differences in outcomes observed when the receptor is knocked-out. There has been some evidence, as mentioned previously, of ELA RNA having a role in development before the apelin receptor is expressed (Li *et al*., 2015) and it could be that such mechanisms are maintained to adulthood. The interactions of apelin, ELA and the apelin receptor in such conditions, therefore, warrants further investigation.

1.9 Knock-out Mouse Models

As discussed earlier, the second peptide at the apelin receptor, now identified as ELA, was predicted due to the discrepancies observed between embryonic knock-outs of apelin and its receptor (Charo *et al*., 2009). Knock-outs of the receptor in mice caused pre-natal mortality (Ishida *et al*., 2004, Charo *et al*., 2009, Roberts *et al*., 2009, Scimia *et al*., 2012, Kang *et al*., 2013) with a failure in cardiac development as the cause (Kang *et al*., 2013). Furthermore, neonates that survived to later embryonic stages displayed incomplete vascular maturation, in part due to a deficiency in vascular smooth muscle cells, as well as incomplete ventricular wall development (Kang *et al*., 2013). Those surviving to adulthood have been shown to display decreased contractile function in the heart which translates to a reduced exercise capacity (Charo *et al*., 2009). Interestingly, they also displayed a reduced propensity to develop HF in response to pressure overload (Scimia *et al*., 2012). In contrast, apelin peptide knock-outs had normal heart development (Kidoya *et al*., 2008, Charo *et al*., 2009) and were born in Mendelian ratio. They also displayed defects in contractility and exercise tolerance (Charo *et al*., 2009) but were at a greater risk from age-related and pressure overload-induced HF (Kuba *et al*., 2007).

In zebrafish, ELA knock-outs phenocopied apelin receptor mutations (Chng *et al*., 2013, Pauli *et al*., 2014) and it was this, among other observations, which aided in its identification as an endogenous apelin receptor ligand. It is only very recently that mouse ELA mutants have been produced (Freyer *et al*., 2017, Ho *et al*., 2017). The knock-out was embryonically lethal, in agreement with its role as a critical developmental signalling molecule. The likely cause of death was misregulation of haematopoietic progenitors at late gatrulation stages, leading to cardiac and vascular defects, thus, mimicking some of the observations of Kang *et al* (2013). Apelin and ELA double knock-outs did not further increase embryonic lethality, supporting the hypothesis that in mammalian systems it is ELA, and not apelin, that plays the crucial developmental role (Freyer *et al*., 2017). However, the authors suggest that some discrepancies, particularly with regards to survival rates between ELA and apelin receptor knock-outs, are suggestive of independent actions of the apelin receptor either though alternative ligands or potential stretch-mediated responses.

Therefore, while it seems evident that ELA plays a critical role in the early development of the cardiovascular system through the apelin receptor, it remains to be seen whether

the apelin receptor may have additional developmental roles. Furthermore, generation of an inducible ELA knock-out would be interesting by allowing further exploration of its roles in the adult mammalian system. Recent studies have illustrated activity in the adult cardiovascular system, as well as changes in ELA expression in the diseased state (Yang *et al*., 2017b). Given that the apelin peptide mutant shares some similarities with the adult apelin receptor mutants (Kuba *et al*., 2007), it is tempting to propose a dichotomous situation with ELA as the key developmental ligand through the apelin receptor and apelin as the key adult signalling peptide. Such a reductionist view is likely too simplistic and further exploration of the roles of ELA in the adult system will help to shed light on the possible interplay between the two endogenous apelin receptor agonists in health and disease.

Apelin Knock-out Mice	Apelin Receptor Knock-out Mice	Apela Mutant Mice
Mendelian Birth Ratio (Kidoya *et al.*, 2008; Charo *et al.*, 2009)	**Loss of Homozygous Mice** (Ishida *et al.*, 2004; Charo *et al.*, 2009; Roberts *et al.*, 2009; Scimia *et al.,* 2012; Kang *et al.*, 2013)	**Loss of Homozygous Mice** (Freyer *et al.,* 2017; Ho *et al.,* 2017)
Normal Heart Morphology (Kuba *et al.*, 2007; Kidoya *et al.*, 2008; Charo *et al.*, 2009)	**Severe Cardiac and Vascular Developmental Defects** (Kang *et al.*, 2013)	**Severe Cardiac and Vascular Developmental Defects** (Freyer *et al.,* 2017; Ho *et al.,* 2017)
Normal Blood Pressure (Charo *et al.*, 2009)	**Normal Blood Pressure** (Ishida *et al.*, 2004; Charo *et al.*, 2009)	**Pre-eclampsia** (Ho *et al.,* 2017)
Modest Decrease in Basal Cardiac Contractility (Charo *et al.*, 2009)	**Modest Decrease in Basal Cardiac Contractility** (Charo *et al.*, 2009)	**?**
Marked Decrease in Exercise Capacity (Charo *et al.*, 2009)	**Marked Decrease in Exercise Capacity** (Charo *et al.*, 2009)	**?**
Severe Heart Failure in Response to Pressure Overload (Kuba *et al.*, 2007)	**Markedly Reduced Heart Failure in Response to Pressure Overload** (Scimia *et al.,* 2012)	**?**

Table 1.3: Phenotypes observed in apelin, apelin receptor and apela knock-out mouse models. The lack of similarity between apelin and apelin receptor knock-out mice prompted the suggestion that there might be another ligand at the receptor. Apela knock-outs largely phenocopy the receptor knock-outs, supporting the idea that ELA is the missing endogenous ligand.

1.10 Biased Small Molecule Agonists as a Therapeutic Strategy at the Apelin Receptor

It is remarkable that a peptide with a half-life of two minutes (Brame *et al*., 2015) is able to induce the vast number of changes observed and to promote such a beneficial response in a multitude of deleterious circumstances. It is also promising that by something as simple as extending the release time of the peptide, through encapsulation in nanoparticles, these effects can be further improved (Serpooshan *et al*., 2015). The logical next step in advancing apelin as a treatment is to produce either longer-lasting peptide mimetics or to produce small molecules which will not be broken-down, thus, further extending the therapeutic benefits. Small molecules could also have the added benefit of being orally bioavailable, greatly increasing their ease of administration. This might improve patient compliance by making regular dosing an easier task, especially for those suffering from chronic diseases who will likely require treatment for the remainder of their lives, for example, those with diabetes, metabolic disease, HF and PAH.

A potential issue of using apelin as a therapy is that, upon activation of the receptor, bound apelin is rapidly internalised with the receptor through the β-arrestin pathway, potentially limiting clinical efficacy. Furthermore, there is evidence that activation of the β-arrestin pathway in the absence of ligand can lead to stretch-mediated hypertrophy (Scimia *et al*., 2012), an effect that would be accentuated in disease where the endogenous ligands are downregulated. One may envisage a situation where a biased molecule is utilised which does not activate the deleterious internalisation pathway but only activates the beneficial G protein signalling pathways to provide a therapeutic effect (Figure 1.7).

Biased agonism (or agonist trafficking among other names) is an emerging concept for GPCRs (Kenakin, 1995, Urban *et al*., 2007, Galandrin *et al*., 2007, Smith *et al*., 2011) and it is only now that its therapeutic potential is being realised. The concept relies on the idea that in order to activate downstream signalling pathways, GPCRs must alter their conformation upon binding of agonists. Originally, this was thought to be an ‘on-off’ switch mechanism, whereby when unbound the receptor was ‘off’ and when bound to an agonist it was ‘on’. It is now evident that, as complex proteins consisting of seven transmembrane domains, GPCRs can exist in a multitude of conformations determined by their energy state and that these states can fluctuate; an excellent discussion of this

is provided by Vaidehi and Kenakin (2010). In short, certain agonists can stabilise these conformations to different degrees. For example, if a GPCR spends more time in a G protein signalling energy state over a β-arrestin signalling energy state, it would display bias towards G protein signalling and vice versa. A biased molecule must, in that case, bind in certain regions of the endogenous agonist binding pocket at the exclusion of others.

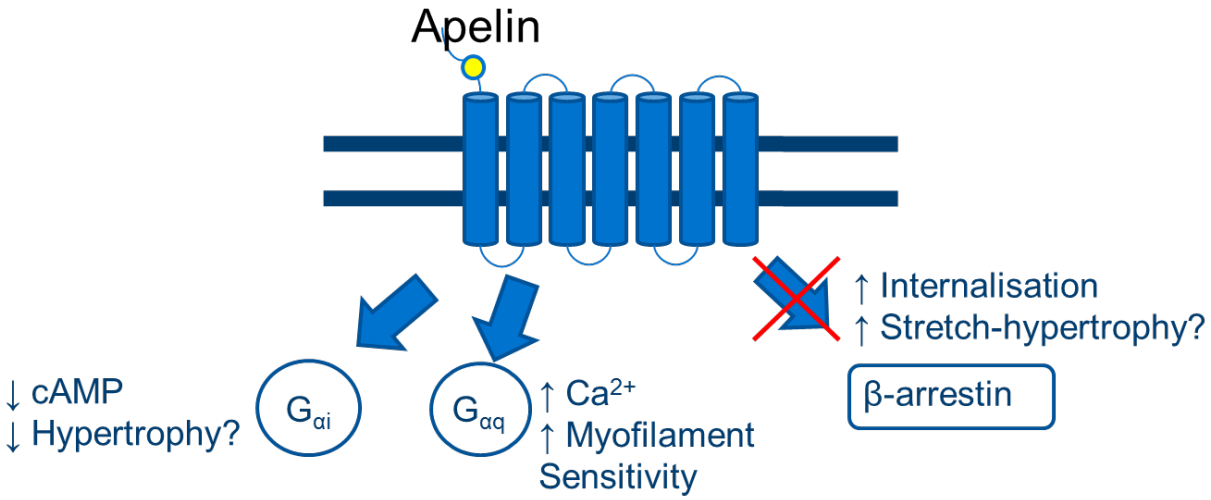

Figure 1.7: A schematic illustrating the proposed beneficial biased signalling profile at the apelin receptor. Apelin the endogenous agonist can activate $G_{\alpha i}$, $G_{\alpha q}$ and β-arrestin. A biased agonist would aim to only activate the G protein signalling pathways at the expense of the β-arrestin pathway. Such an effect would reduce receptor internalisation and potential stretch mediated hypertrophy.

It is important to note that although biased agonism is a novel idea, all current non-endogenous clinical therapies will be biased ligands in some way, even if the nature of that bias is poorly understood. The question, therefore, becomes not whether clinical drugs possess bias but rather, is this bias clinically relevant? A good example of this is illustrated by studies conducted on β-adrenoceptor antagonists (or β-blockers) and their role in chronic HF treatment. Although originally contraindicated in HF due to their negative chronotropic and inotropic effects potentially leading to excessive cardiac suppression in an already failing heart, β-blockers have since become a key treatment in chronic HF. The argument stems from the idea that in chronic HF compensatory mechanisms lead to a 'catecholamine storm', excessive β_1 stimulation, receptor downregulation and an altered receptor profile which promotes further catecholamine release in a positive feedback loop. Ultimately, this leads to cardiomyocyte apoptosis through catecholamine-induced toxicity. β-blockers can interrupt this positive feedback and exert beneficial effects, as can partial agonists, such as Pindolol. However, there

is now evidence that the 3rd generation of β-blockers, such as Carvedilol, possess ligand bias and may exert some of their beneficial effects through such mechanisms. Wisler *et al.* (2007) argue that carvedilol while antagonising the canonical $G_{\alpha s}$ pathway as expected, also promotes β-arrestin recruitment, receptor internalisation and ERK1/2 phosphorylation in the β_2 adrenergic receptor and that such effects were maintained in a G protein uncoupled mutant. Therefore, these 3rd generation β-blockers provide an example where, although the ligands were not designed with bias in mind, bias may nonetheless be critical to their mechanism of action.

Currently, there are a small number of molecules that have been designed to possess bias in a therapeutic setting. As yet none are approved for clinical use and only three have progressed to clinical trials. Two of these are Oliceridine (TRV-130) and TRV734 (Phase I), μ-opioid agonists that display bias towards G protein signalling over β-arrestin, thereby promoting beneficial analgesic effects with a similar potency to the classical analgesic morphine, without inducing gastrointestinal side-effects (Viscusi *et al*., 2016), www.trevena.com). It has been reported that these compounds still evoke respiratory depression as seen with morphine, though this is generally only problematic in cases of overdose. Oliceridine has been granted breakthrough status by the FDA and it was recently announced that it will be reviewed for approval later this year (www.trevena.com). Another new biased opioid ligand, PZM21, identified through computational docking experiments, displayed remarkably high bias towards G protein signalling over β-arrestin and, in contrast to Oliceridine, did not cause respiratory depression in mice *in vivo*, though it should be noted that these are recent and pre-clinical data (Manglik *et al*., 2016). Another compound that entered clinical trials was also from Trevena. TRV027 is an angiotensin type II receptor agonist biased towards β-arrestin signalling. It aims to reduce afterload while increasing cardiac performance and maintaining stroke volume, allowing it to be used for acute HF (Felker *et al*., 2015); however, no benefits were observed through a 30-day follow-up in a phase IIB clinical trial (Pang *et al*., 2017).

At the apelin receptor, it is hoped that biased agonism could be exploited such that it would not detract from the therapeutic signalling benefits of apelin but would ensure a longer duration of action and a consequent improvement in efficacy. Indeed, internalisation of the apelin receptor is rapid and 50% of receptors have been shown to be internalised after ten minutes in stably transfected CHO cells (Evans *et al*., 2001).

Furthermore, it is interesting that the rate of recycling of the apelin receptor back to the plasma membrane is highly dependent on the ligand (Lee *et al*., 2010, Zhou *et al*., 2003a). Thus, by altering the properties of the agonist, one might not only be able to reduce the propensity of receptor internalisation but also to increase the recycling rate back to the membrane of the receptors that are internalised.

A previously designed cyclised apelin peptide analogue, MM07, displayed G protein bias (Brame *et al*., 2015). This strategy resulted in an improved duration of action in a forearm blood flow study in human subjects with no decrease in response observed upon repeated dosing following a saline flush. An increase in efficacy over [Pyr^{1}]apelin-13 was observed both in vasodilatation in the human forearm study and in cardiac output in rat heart. Finally, it was demonstrated that MM07 can attenuate RV hypertrophy in the MCT model of PAH (Yang *et al*. In Revision). These data support the idea that the apelin receptor is tractable to biased signalling. Additional evidence is provided by a study in which alteration of a specific serine residue (Ser^{348}) in the apelin receptor showed abolition the G protein receptor kinase/ β-arrestin pathway signalling, whilst preserving signalling through the G protein pathway (Chen *et al*., 2014). Meanwhile, it has been reported that removal of the C-terminal phenylalanine of apelin-17 can induce bias towards G protein signalling (Ceraudo *et al*., 2014).

Having observed that the apelin receptor is tractable to bias and the previously demonstrated success of this approach with MM07, one of the aims of this study was to identify small molecules that can bind to the human apelin receptor with high affinity and exert biased signalling through the G protein pathway. Such small molecules should allow for a further improvement over peptides, such as MM07, by allowing for oral delivery and improved half-life.

1.11 Albudab™ Platform and Antibodies as a Therapeutic Delivery Strategy

Antibodies are increasingly being used in a therapeutic setting as they display some major advantages over other treatment strategies; however, they can also show serious limitations. Their key advantage stems from the high affinity of protein-protein interactions meaning they can be targeted to a specific pathway with a high degree of selectivity, limiting off-target effects. Moreover, if properly designed to avoid immune targeting, these molecules can have very long half-lives. For example, Alemtuzumab (Campath) is given as a treatment for multiple sclerosis in a series of 4 hour infusions for 5 days spaced 12 months apart (Multiple Sclerosis Society UK). Despite these advantages, antibodies must be given intravenously (though this issue is largely negated by their long half-life) and due to their high selectivity, resistance can develop; often it is required that they are given in combination with pre-existing treatments.

An example of an antibody combinative therapy is infliximab (an anti-tumour necrosis factor α (TNFα) antibody) given in combination with the anti-proliferative methotrexate for the treatment of rheumatoid arthritis. However, resistance to TNFα blockade, especially etanercept monotherapy, often occurs and more second line therapies are required (Anecchino *et al*., 2015). One such antibody, toclizumab (an anti-IL-6 antibody), has been approved, despite reports of serious adverse events, because benefits were observed in patients refractive to infliximab treatment, (this was not the case for patients switching from etanercept monotherapy; Wakabayashi *et al*., 2013). One of the issues highlighted by this example of antibody therapy is that, due to their high selectivity, direct antibody therapies provide relief only in situations where patients are known to possess a reported defect.

One of the best examples of a successful designed antibody therapeutic is imatinib which was designed to target the BCR-ABL fusion protein. A translocation between chromosome 9 and 22 occurs in all cases of chronic myeloid leukaemia (CML) leading to the production of this gene which encodes a permanently activated tyrosin kinase receptor (Nowell, 1962, Rowley, 1973). By targeting this aberrant growth receptor with imatinib, the progression of CML could be slowed (Savage and Antman, 2002). This is an excellent, albeit limited, example of a situation where a direct antibody therapy to target a known defect is successful. Perhaps with better and cheaper genome sequencing technologies, it will become easier to identify which antibodies or antibody

combinations will provide the best benefit in individual patients and antibodies will become increasingly the treatment of choice in an era of personalised medicine.

Although antibodies may be used to directly engage targets in disease, they are increasingly being explored as a potential mechanism for drug delivery. To do this linker motifs must be carefully chosen to link the antibody to the drug as these must be sufficiently stable so that the complex remains intact *in vivo* but breaks apart upon antibody-target engagement, allowing for optimal drug delivery. Novel approaches, such as, cyclisation, the use of unnatural amino acids and PEG spacers may be used to reduce proteolysis and retain antibody-drug complexes.

Antibody-drug combinations have gained particular interest in cancer treatments where targeted drug 'payload' delivery could reduce the chemotherapeutic doses required and thereby reduce debilitating side-effects. Two FDA approved antibody-drug combinations are Adcetris (brentuximab vedotin) and Kadcyla (trastuzumab emtansine) for refractory Hodgkin lymphoma and HER2 positive breast cancer, respectively. Adcetris consists of brentuximab an anti-CD30 antibody which binds and internalises on CD30 expressing cells to release the payload, monomethyl auristatin E, a powerful antimitotic through preventing tubulin polymerisation. Meanwhile, Kadcyla consists of trastuzumab, an anti-HER2 antibody, and emantisine, another tubulin-binding antimitotic. Since the approval of these antibody-drug combinations in 2011 and 2013, respectively, there has been a surge in investment and there are now more than 50 in various stages of clinical trials for a number of different cancers (Dan *et al*., 2018).

Rather than using antibodies to target specific cells, an alternative approach is to utilise them to extend the half-life and stability of other compounds. One platform to do this is conjugation to a human anti-serum albumin domain antibody (AlbudAb™). The AlbudAb^{TM} construct consists of a single variable domain of immunoglobulin G (IgG) and is approximately 1/10th the size of a conventional antibody. *In vivo* it binds rapidly with human serum albumin (HSA) to form a complex of approximately 81kDa, thus avoiding the size cut-off for glomerular filtration of around 50kDa and enhancing plasma half-life. By combining short peptides, which are susceptible to clearance through the kidneys, with an AlbudAb™ construct, the molecule can be protected and the transit time in the blood can be greatly increased.

Such an approach has been demonstrated previously with endogenous molecules conjugated genetically to AlbudAb™, such as soluble IL-1Rα (interleukin-1 receptor type 1; Holt *et al*., 2008), GLP-1 (glucose-dependent insulinotropic peptide 1; O'Connor-Semmes *et al*., 2014, Bao *et al*., 2013, Lin *et al*., 2015), tumour necrosis factor receptor 1 (TNF-R1; Goodall *et al*., 2015) and interferon-α2b (Walker *et al*., 2010), all of which demonstrated half-life extension with retained activity. A similar approach might be taken with apelin or apelin mimetic peptides. Importantly, in order to conjugate mimetic peptides that contain unnatural amino acids that cannot be genetically coded, the AlbudAb™ construct has also been modified such that it contains only one cysteine residue, Cys^{108}. This cysteine is distant from the albumin binding site, enabling it to be linked using maleimide chemistry to target molecules. Such an approach would use a linker, such as PEG, as well as unnatural amino acids to protect the molecule from peptidase degradation. Meanwhile, the AlbudAb™ would prevent renal clearance, thus, enhancing half-life and reducing the frequency of dosing required.

1.12 Hypothesis and Aims

The apelin system is clearly an important regulatory system and is perturbed in a number of diseases, particularly those affecting the cardiovascular system. In PAH both of the endogenous ligands apelin and ELA are downregulated but the apelin receptor expression levels are not decreased. This supports the hypothesis that targeting the apelin receptor in the disease could be beneficial. Prevention studies in the MCT rat model of PAH have confirmed this, with exogenous administration of [Pyr^{1}]apelin-13 and ELA-32 significantly improving outcome. This suggests that other apelin agonists may also show benefit in PAH and it is particularly noteworthy that there are no suitable small molecule agonists at the apelin receptor. Such molecules while having potential for the generation of novel therapeutics, would also crucially be able to progress the field of apelin research by providing suitable tool compounds for experimental study.

Therefore, the primary aim of this study was to identify a novel G protein biased small molecule agonist at the apelin receptor. Such a molecule would follow-up previous work in the laboratory which identified MM07 as a cyclic G protein biased peptide agonist of the apelin receptor and confirm that G protein bias can be retained in small molecules at the apelin receptor. Importantly, such a discovery would provide a much needed experimental tool compound for research and could provide a platform for the development of additional biased small molecule agonists that might be suitable for use as therapeutics in disease. This study discovered CMF-019 as such a molecule and then aimed to characterise its *in vitro* and *in vivo* pharmacology, as well as its potential as a disease-modifying therapeutic in PAH.

A secondary aim of the study built upon work already performed in the laboratory that generated an apelin peptide mimetic-AlbudAb™ conjugate. This conjugate utilised an apelin mimetic containing unnatural amino acids, MM202, linked to a $(PEG)_4$ spacer to reduce proteolysis. MM202-$(PEG)_4$ was then conjugated to AlbudAb™ using maleimide chemistry to enhance transit time of the molecule. The purpose here was to pharmacologically characterise MM202-AlbudAb^{TM} by assessing its *in vitro* and *in vivo* activity, as well as to see if it possessed therapeutic efficacy in the MCT model of PAH.

2. Methods

2.1 Materials

Chemicals were obtained from Sigma Aldrich Co. Ltd (Poole, UK) unless otherwise stated. [Pyr^{1}]apelin-13 (Glp-RPRLSHKGPMPF), Apelin-17, MM07, MM202, and MM202-AlbudAb^{TM} were manufactured and tested for greater than 95% purity using mass spectrometry by Severn Biotech (Kidderminster, UK). [Glp^{65},Nle^{75},Tyr^{77}][^{125}I]apelin-13 was from Perkin Elmer (MA, USA) and had a specific activity of 81.4MBq/nmol. CMF compounds (Figure 3.1) were synthesised in the School of Chemistry, University of Leeds. For *in vivo* studies the potassium salt of CMF-019 (Figure 4.2) dissolved in saline at pH9 was used as it showed better solubility than the parent compound. This was initially also synthesised in the School of Chemistry, University of Leeds, however, for later *in vivo* studies a large batch was synthesised by Tocris, (Bristol, UK). Human tissues were obtained with informed consent from the Papworth Hospital Research Tissue Bank (08/H0304/56) and ethical approval (05/Q104/142) and conformed to the principles outlined in the declaration of Helsinki. Animal experiments were performed in accordance with guidelines from the local ethics committee (University of Cambridge) and the Home Office (UK) under the Scientific Procedures Act (1986).

2.2 Preparation of Tissue Homogenates

Human LV tissue, whole rat and whole mouse hearts were first cut into small pieces and stored on ice. Homogenisation buffer (50mmol/L Tris-HCl, 5mmol/L $MgCl_2$, 5mmol/L EDTA, 1mmol/L EGTA, 1:500 protease inhibitor cocktail (PIC), pH 7.4 at 4°C) was added (10mL/g of tissue). The tissue was then homogenised in three twenty second bursts with cooling in between. The homogenate produced was centrifuged at a slow speed for a short time (1000g, 2min, 4°C) to produce a soft pellet. The supernatant was removed and then subjected to prolonged high speed centrifugation (40,000g, 30min, 4°C). Following this, the supernatant was discarded and the pellet resuspended in homogenisation buffer (2.5mL/g of tissue) before undergoing high speed centrifugation. This process was repeated once more. After the final high speed centrifugation, the pellet was resuspended in HEPES buffer (50mmol/L HEPES, pH7.4) and stored at -70°C until required. Samples were taken and assessed for protein concentration using a bicinchoninic acid (BCA) assay (BioRad, Hercules, CA, USA).

2.3 Competitive Radioligand Binding Assays

Homogenised human LV (1.5mg/mL) was used to determine binding affinities in native human receptors. Whereas, to determine binding affinities to rat and mouse receptors, whole heart homogenates (1.5mg/mL) were used. Compounds were incubated with the homogenate for 90min in assay buffer (Tris 50mmol/L, $MgCl_2$ 5mmol/L, pH7.4, 22ºC) and 0.1nmol/L [Glp^{65},Nle^{75},Tyr^{77}][^{125}I]apelin-13. Sigmacote® was used to siliconise apparatus and prevent label loss. Binding in the presence of 2µmol/L [Pyr^{1}]apelin-13 was deemed non-specific. Following incubation, the solutions were spun (20,000g, 10min, 4ºC), washed (50mmol/L Tris-HCl, pH7.4, 4˚C), spun again (20,000g, 10min, 4˚C) and the pellet counted using a gamma counter (Cobra 5003, Packard). Measurements were made in triplicate and data analysed using GraphPad Prism™. The binding affinities were calculated by the Cheng-Prusoff methodology using measured IC_{50} vales (Cheng and Prusoff, 1973). The K_i of [Glp^{65},Nle^{75},Tyr^{77}][^{125}I]apelin-13 was taken as 0.076nmol/L.

2.4 Cell Signalling Assays

2.4.1 β-Arrestin Assay

PathHunter® eXpress β-Arrestin GPCR assays were purchased from DiscoveRx (Fremont, CA, USA), this assay utilises CHO cells expressing the apelin receptor (AGTRL1). The assay provides a chemiluminescent read-out of β-arrestin (isoform 2) recruitment to the receptor through the use of ProLink™ technology (Figure 2.1). Upon activation of the receptor and recruitment of β-arrestin, the ProLink™ (a β-galactosidase fragment) attached to the β-arrestin complements its partner on the receptor, leading to production of a functional enzyme. This enzyme then cleaves the substrate located in the detection reagent and produces the chemiluminescent read-out.

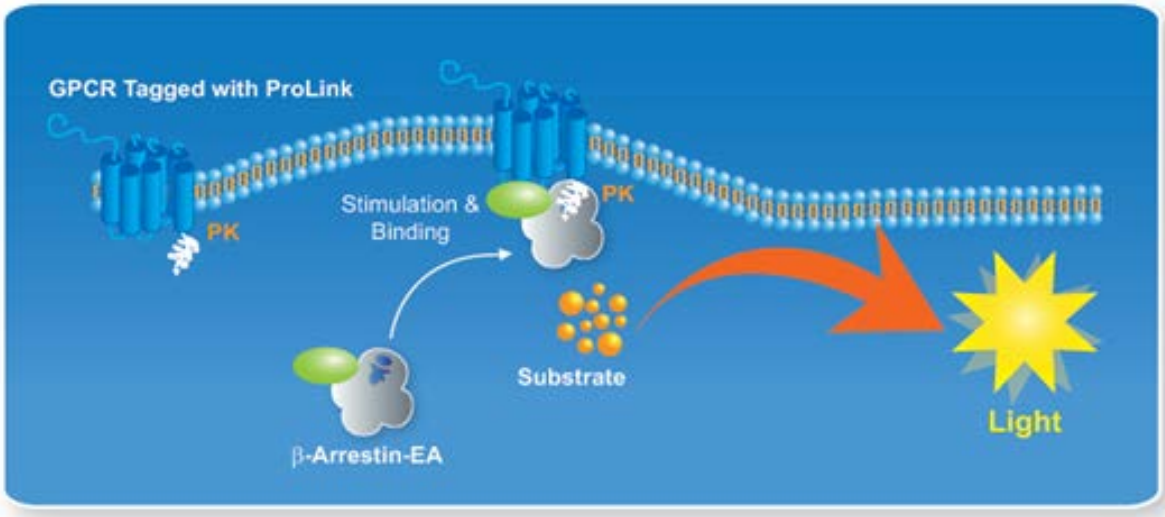

Figure 2.1: The mechanism of action of the β-arrestin cell signalling assay. Kits were purchased from DiscovRx™ and performed as described in the text. Figure taken from http://www.discoverx.com.

To perform the assay, the CHO cells were first thawed and resuspended in cell plating media (F12 HAM media containing 10% serum penicillin/streptomycin/glutamine) before being plated in 96-well plates and incubated for 48h (37˚C, 5% CO_2). Following this period, serial dilutions of stock compounds in cell plating media were performed to obtain a concentration range upon addition of 5µL of each dilution per well, with the final concentration of dimethylsulphoxide (DMSO) not exceeding 1%. DMSO controls were used at a concentration of 1%. Where possible, measurements were made in triplicate. After incubation for 90min with the agonist at 37°C, cell detection reagent

was added and left for a further 120min protected from light at room temperature. Luminescence was detected using a LumiLITE™ Microplate 4 Reader (DiscoveRx) and measured as relative light units (RLUs). Agonist responses were normalised to the mean maximal response detected for the endogenous agonist [Pyr^{1}]apelin-13 in that experiment. The data were then fitted to a four-parameter model using GraphPad Prism™ and the pD_2 ($-\log_{10}$ of the EC_{50}) and E_{Max} values calculated and compared.

Validation

This screening assay was purchased from DiscovRx and performed according to their instructions. They have reported that there are no differences in pH across the assay plating media and that there is no background expression of the apelin receptor in CHO cells.

Additional experiments have been performed in our laboratory to further validate the assay. Using [Glp^{65},Nle^{75},Tyr^{77}][^{125}I]apelin-13, receptor affinity and density were compared to human LV homogenate (experiments performed by Mrs Rhoda Kuc and data provided by Dr Janet Maguire). The radioligand bound to the receptor in CHO cells (K_D=0.16±0.04nM) and this was of the same order of magnitude to the binding in human LV homogenates (K_D=0.08±0.01nM). Crucially, the density of receptors measured were 45.3±8.2fmol/mg and 13.8±1.8fmol/mg, respectively, a 3-fold difference and within the same order of magnitude. This is important as often in cell expression systems, receptors can be greatly overexpressed, resulting in dramatic differences in receptor-G protein stoichiometry to those observed in clinically relevant human tissues. This can lead to the appearance of new signalling states and give a false interpretation of bias (Luttrell *et al*., 2015, Kenakin, 1995, Zhu *et al*., 1994, Cordeaux *et al*., 2000, Nasman *et al*., 2001).

Another factor that can lead to errors is the timing of the end-point reading as drug-receptor kinetics may vary in the assays. The biased calculations used to quantify bias rely upon adaptation of the Black and Leff operational model of agonism, one of the fundamental assumptions of which is that the reaction has reached equilibrium (Kenakin *et al*., 2012, Rajagopal *et al*., 2011, Black and Leff, 1983). Studies have shown that there is a kinetic variable to quantification of bias (Lane *et al*., 2017, Klein Herenbrink *et al*., 2016). To isolate the kinetics of the assay as a variable, concentration-response curves to both [Pyr^{1}]apelin-13 and MM07 have been

performed at different time-courses (experiments performed by Mrs Rhoda Kuc). It was found that the pD_2 to both compounds did not vary when readings were taken at 20, 30, 45 and 90 minutes, suggesting the potencies of the agonists are not dependent on incubation time.

2.4.2 cAMP Assay

cAMP Hunter™ eXpress GPCR assays were purchased from DiscovRx, this assay utilises CHO cells expressing the apelin receptor (AGTRL1). The assay provides a chemiluminescent read-out of cAMP activity **(**Figure 2.2). At low basal levels of cAMP activity, anti-cAMP antibodies bind to the endogenous cAMP, as well as cAMP molecules which have been modified with the addition of a β-galactosidase fragment. At high levels, the antibodies become saturated with endogenous cAMP allowing the β-galactosidase fragment-modified cAMP molecules to bind to their complementary partner fragment in solution. This leads to a functional enzyme that hydrolyses its substrate in the detection reagent and produces a chemiluminescent read-out.

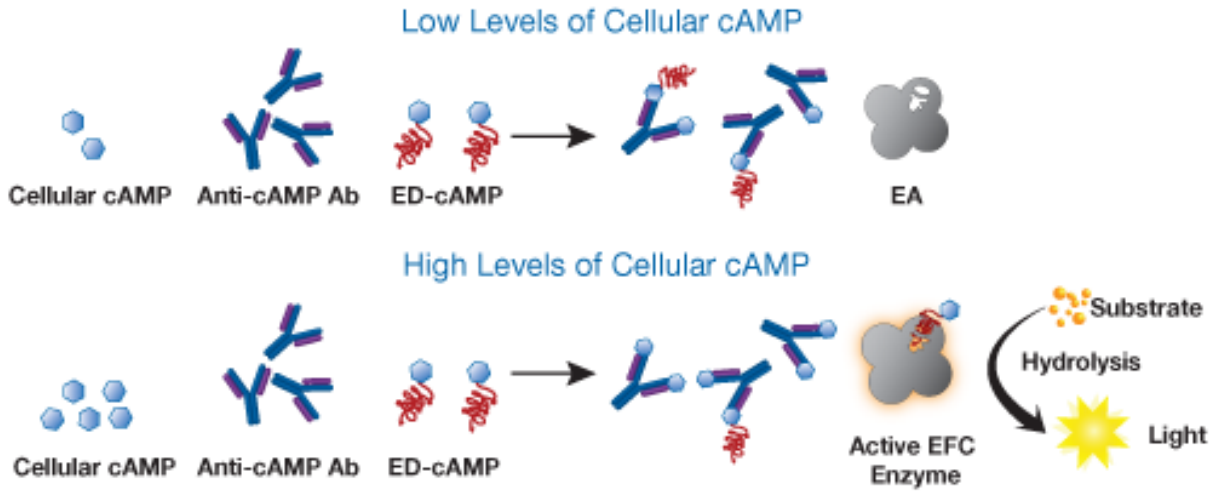

Figure 2.2: The mechanism of action of the cAMP cell signalling assay. Kits were purchased from DiscovRx™ and performed as described in the text. Figure taken from http://www.discoverx.com.

To perform the assay, the CHO cells were first thawed and resuspended in cell plating media (F12 HAM media containing 10% serum/penicillin/streptomycin/glutamine) before being plated in 96-well plates and incubated for 48h (37˚C, 5% CO_2). Following this period, the cell plating media was substituted with 45µL of a solution containing the cAMP antibody reagent and forskolin made up in cell assay buffer (Hanks' balanced salt solution modified with 10mM HEPES). Forskolin (15nmol/L) was required

as the apelin receptor couples to $G_{\alpha i}$ in this system. Serial dilutions of stock compounds were then made in cell assay buffer to obtain a concentration range upon addition of 15µL of each dilution per well, with the final concentration of DMSO not exceeding 1%. DMSO controls were used at a concentration of 1%. Where possible, measurements were made in triplicate. After incubation for 30min with the agonist at 37°C, cAMP working detection reagent consisting of cAMP lysis buffer (containing IBMX), substrate reagent 1, substrate reagent 2 and cAMP solution D (enzyme donor) was added and left for a further 60min, protected from light at room temperature. cAMP solution A (enzyme acceptor) was then added and the plates incubated for 180min protected from light at room temperature. Luminescence was detected as for the β-arrestin assay. Agonist responses were normalised to the maximal forskolin response at the lowest concentration of a given agonist. The data were fitted to a four-parameter model using GraphPad Prism™ and the pD_2 ($-\log_{10}$ of the EC_{50}) and E_{Max} values calculated and compared.

Validation

This screening assay was purchased from DiscovRx and performed according to their instructions. They have reported that there are no differences in pH across the assay plating media and that there is no background expression of apelin receptor in CHO cells.

Optimisation experiments performed in the laboratory (experiment performed by Mr Thomas L. Williams and data provided by Dr Janet Maguire) showed that the EC_{80} for forskolin stimulation occurred at 45µmol/L (Figure 2.3). The value recommended and expected by the manufacturer (DiscoveRx) was 15µmol/L forskolin. 15µmol/L forskolin was used in subsequent experiments so that the DMSO concentration was not too high, although this was closer to the EC_{50} as measured in our controls. As this meant the forskolin concentration was closer to the linear portion of the concentration-response curve, the baseline activation by forskolin controls was more variable than expected. To reduce this variability in the baseline, the data in subsequent analyses have been normalised to the maximal forskolin response of the given concentration-response curve. The inhibition of the forskolin response by the compounds can thus be more accurately compared.

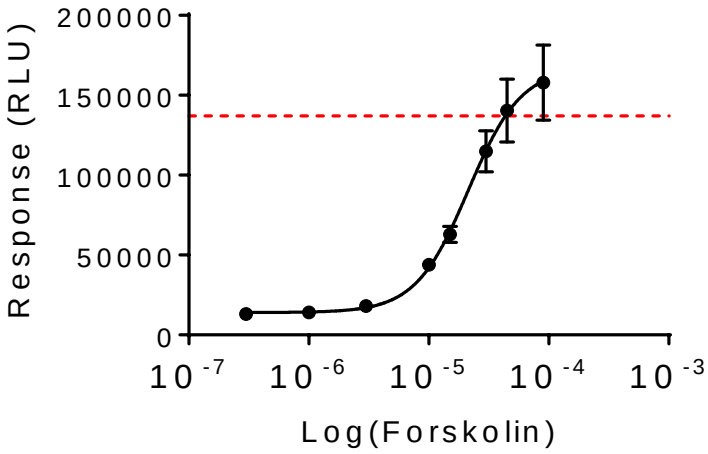

Figure 2.3: A forskolin control curve performed prior to experiments to establish the optimal forskolin concentration for use in the cAMP assay (experiment performed by Mr Thomas L. Williams and data provided by Dr Janet Maguire). The data show that the EC_{80} of forskolin stimulation occurred at about 45µmol/L as indicated by the dotted red line. The 15µmol/L concentration recommended by the manufacturer was closer to an EC_{50}.

cAMP standard curves were performed to ensure the amounts of cAMP detected for apelin compounds in the assay measured in RLUs were within the detection range of the assay. The cAMP standard curve elicited a maximal response of just over 200,000RLUs and the response to forskolin at 15µmol/L (Figure 2.4) was approximately 100,000RLUs. This was similar to the maximal responses measured for the tested compounds as expected, thus, indicating that even the maximal cAMP levels measured for the experimental compounds were easily within the detectable range of the assay.

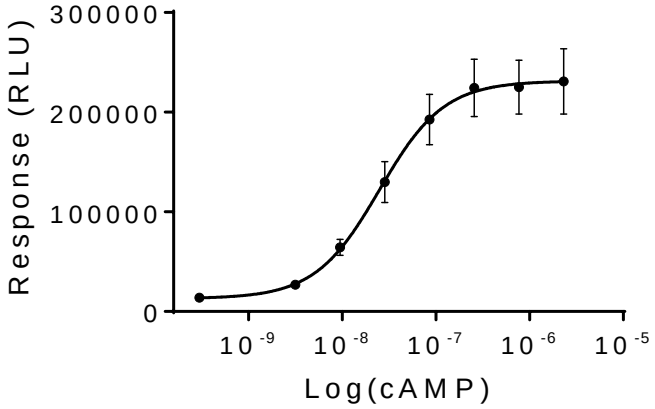

Figure 2.4: A cAMP standard control curve performed prior to experiments to establish that the cAMP levels detected in the assay were within the assay range (experiment performed by Mr Thomas L. Williams and data provided by Dr Janet Maguire). The data show that the range of RLUs detected were between 0 and 200,000RLUs putting the 15µmol/L forskolin concentration used in the assay well within the detectable range.

2.4.3 Internalisation Assay

PathHunter® eXpress Activated GPCR Internalisation assays were purchased from DiscoveRx, this assay utilises U20S cells expressing the apelin receptor (AGTRL1). The assay provides a chemiluminescent read-out of receptor internalisation through the use of ProLink™ technology (Figure 2.5). Upon receptor internalisation following binding of β-arrestin (isoform 2), the ProLink™ (a β-galactosidase fragment) attached to the β-arrestin complements its partner on the endosome, leading to a functional enzyme. This enzyme then cleaves the substrate located in the detection reagent and produces a chemiluminescent read-out.

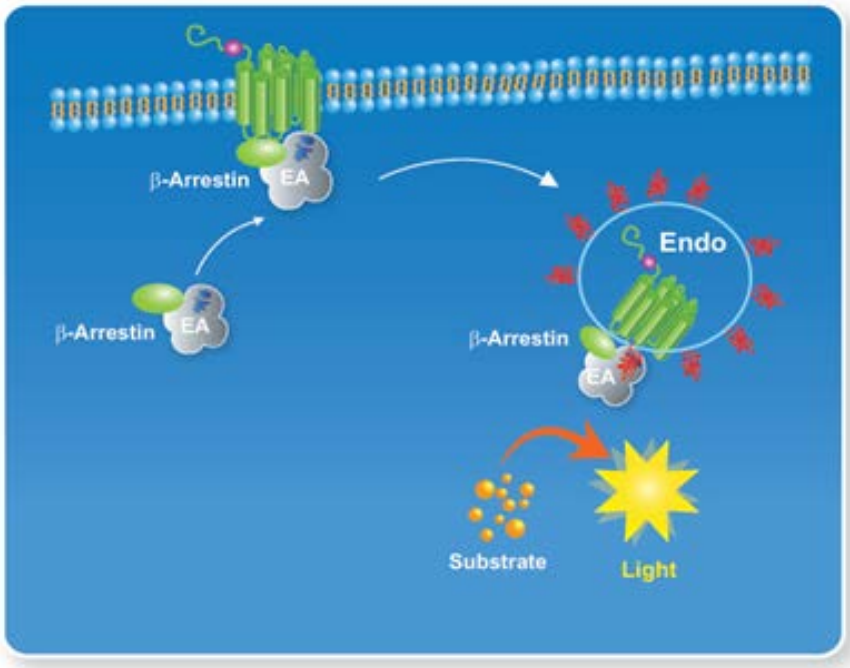

Figure 2.5: The mechanism of action of the receptor internalisation cell signalling assay. Kits were purchased from DiscovRx™ and performed as described in the text. Figure taken from http://www.discoverx.com.

To perform the assay, the U20S cells were first thawed and resuspended in cell plating media before being plated in 96-well plates and incubated for 48h (37˚C, 5% CO_2). Following this period, serial dilutions of stock compounds in cell plating media were performed to obtain a concentration range upon addition of 5µL of each dilution per well, with the final concentration of DMSO not exceeding 1%. DMSO controls were used at a concentration of 1%. Where possible, measurements were made in triplicate. After incubation for 120min with the agonist at 37°C, working detection reagent was added and left for a further 120min protected from light at room temperature. Luminescence was detected and analysis performed as for the β-arrestin assay.

Validation

This screening assay was purchased from DiscovRx and performed according to their instructions. Since the assay was in a different cell line to the other cell-based assays, it was largely used as a screening tool to check for consistency with the β-arrestin assay and no additional validation other than that by the manufacturer has been performed.

2.5 Apoptosis Assay Using Human PAECs

Human pulmonary artery endothelial cells (human PAECs) were purchased from Lonza (Cambridge, UK; n=5 donors: 1(lot#0000479486), 2(lot#4F3041), 3(lot#4F3034), 4(lot#000657513) and 5(lot#0000662151) passages 4-6). The human PAECs were maintained in endothelial cell growth media 2 (EGM-2 containing basal media, EBM-2, with added human epidermal growth factor (hEGF), hydrocortisone, GA-1000 (Gentamicin, Amphotericin-B), vascular endothelial growth factor (VEGF), human fibroblast growth factor-B (hFGF-B), R3-IGF-1 (an analogue of human insulin-like growth factor 1), ascorbic acid and heparin (Lonza, UK) supplemented with 10% heat inactivated foetal bovine serum (FBS; Gibco, NY, USA). In later experiments owing to an inability to supply further media by Lonza, Promocell (UK) EGM-2 was used. Again this was supplemented with 10% heat inactivated FBS; however, it did not contain antibiotics (GA-1000) and, though it was chosen for its similarity to the Lonza media, most likely had slightly different concentrations of the same growth factors (GFs).

Assays were performed largely as described by Long *et al.* (2015) although optimisation of the protocol was performed. The assay relies on the fact that, although tumour necrosis factor α (TNFα) usually prevents apoptosis of endothelial cells through activation of the NF-κB (nuclear factor kappa-light-chain-enhancer of activated B cells) pathway, in conditions of global protein synthesis suppression, such as, concurrent application of cycloheximide (CHX), apoptosis is induced through TNF-R1 leading to JNK and p-38 MAPK phosphorylation.

Briefly, at 80-90% confluency, human PAECs were seeded in three six-well tissue culture plates at 200,000cells/well in EGM-2 with 10% FBS and allowed to attach. On the next day, wells were washed with phosphate buffered saline (PBS) and the media changed to either EBM-2 with 2% FBS to serum and growth factor (GF) starve the cells or to EGM-2 10% FBS 'healthy' controls. [Pyr^{1}]apelin-13 (10 µM), MM07 (10µM), CMF-019 (1-10µM) or recombinant human vascular endothelial growth factor (rhVEGF) (10ng/mL; R&D Systems; Minneapolis, MN, USA) were added to the wells and incubated for 18 hours. Apoptosis was induced by incubating the cells with TNFα (R&D Systems) and CHX for 5 hours in the experimental wells. A plate map for the control plate is shown in Table 2.1; this was used to compensate between fluorescent channels for the flow cytometry data analysis.

Unstained Control EGM-2 10% FBS No TNF-α/CHX Unstained	**Annexin Only** EBM-2 2% FBS TNF-α/CHX Annexin	**Serum and GF Starved** EBM-2 2% FBS No TNF-α/CHX Annexin/PI
'Healthy' Cell Control EGM-2 10% FBS No TNF-α/CHX Annexin/PI	**PI only** EBM-2 2% FBS TNF-α/CHX PI	**TNFα/CHX Treated** EBM-2 2% FBS TNF-α/CHX Annexin/PI

Table 2.1: The control plate set-up for the human PAEC apoptosis assay. Each quadrant represents one well of a six well plate and the treatments administered to that well are listed. The control plate provided controls for both compensation of the flow cytometry data and the controls for the experiment. In addition to this plate there were two experimental plates in which the two rightmost well conditions were repeated but with different concentrations of the compounds incubated for 18 hours.

In addition to the control plate there were two experimental plates in each experiment. These plates featured one well of the serum and GF starved and one well of the TNFα/CHX treated conditions per compound at a given concentration. All compounds were added to the cells 18 hours prior to the TNFα/CHX treatment regardless of whether they were in the control or experimental group.

Cells were then washed in PBS, trypsinised (Lonza), transferred into 1x binding buffer for the apoptosis assay (Thermoscientific; Waltham, MA, USA) and stained with anti-annexin-V FITC-conjugated antibody and propidium iodide (PI, 20µg/mL) for 15 minutes at room temperature. Cells were filtered through 50µM filters (Sysmex/Partec; Görlitz, Germany) and kept on ice before flow cytometry (Canto II, BD Biosciences; San Jose, CA, USA). 10,000 events were recorded for each condition. Human PAECs were selected based on forward and side scatter areas and single cells selected by comparing forward scatter width vs area. Data analysis was performed on FlowJo v10 (FlowJo LLC; Ashland, OR, USA) and each experiment compensated between channels using the internal unstained, annexin-only and PI-only controls. $Annexin^+/PI^+$ cells were classified as 'dead', $Annexin^+/PI^-$ cells 'apoptotic' and $Annexin^-/PI^-$ as 'healthy'. Gates were adjusted such that approximately equal numbers of 'healthy' and 'apoptotic' cells occurred in the TNFα/CHX treated group as this provided a large window for either further induction or rescue of apoptosis; this is illustrated in Figure 2.6. These gates were applied to the rest of the experimental conditions for that experiment.

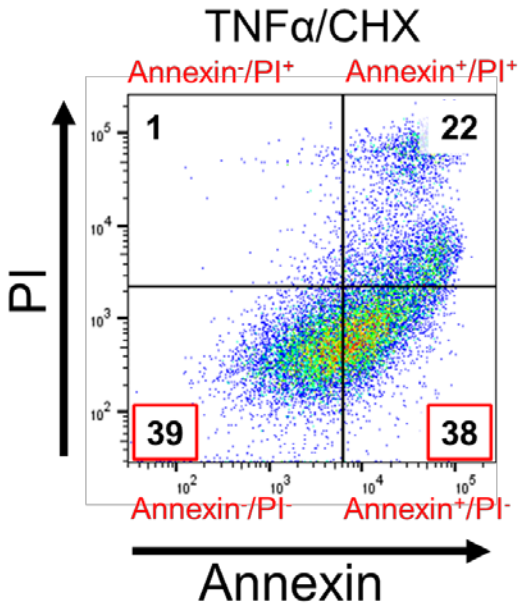

Figure 2.6: An example of a scatter plot collected by flow cytometry of human PAECs treated with TNFα/CHX and stained with annexin-FITC and PI. The quadrants clockwise from bottom left show the annexin$^-$/PI$^-$ 'healthy', annexin$^-$/PI$^+$, annexin$^+$/PI$^+$ 'dead' and annexin$^+$/PI$^-$ 'apoptotic' populations. The gates were adjusted such that approximately equal numbers of 'apoptotic' and 'healthy' cells (highlighted in the red boxes) occurred under this condition before being applied to the rest of the experimental conditions tested for that experiment.

2.5.1 Use of Low Passage Number Human PAECs

Low passage numbers (passages 4-6) were used in experiments to ensure human PAECs were healthy prior to the start of experimentation as it was observed that later passage numbers (>7) were less susceptible to apoptosis induced by TNFα/CHX. This may reflect the fact that later passages are more susceptible to serum and GF starvation induced apoptosis (Varani *et al*., 1995) and so less able to respond to further apoptotic stimuli. Endothelial cells are known to start endothelial-to-mesenchymal transition and elongate in culture if exposed to fibroblast-derived soluble factors (Kuzuya and Kinsella, 1994). Similar observations have been seen if endothelial cells are cultured for long periods of time or too sparsely. Cells were tested by Lonza prior to purchase for α-actin staining and cell morphology was carefully monitored throughout culture. Endothelial cells should maintain a classical rounded 'cobblestone' morphology in culture and not form cell projections or elongate.

2.5.2 Annexin Concentration Optimisation

In order to obtain the maximum apoptotic window induced in the TNFα/CHX treatment compared to the EBM-2 2% FBS control, the concentration of annexin used was adjusted from that suggested in the protocol by Thermoscientific. These experiments were performed in donors 2 and 3. Using the stock concentration (Figure 2.7, top panel), there was a large amount of annexin staining in the serum and GF starved (EBM-2 2% FBS) control which would narrow the window for apoptotic induction by TNFα/CHX treatment. Therefore, a 1:10 dilution of the stock (Figure 2.7, middle panel) was tested but this resulted in minimal staining compared to the unstained control. Finally, a 1:2 dilution (Figure 2.7, bottom panel) was tested. This concentration of annexin resulted in moderate staining in the EBM-2 2% control, such that the peak of the population was central and clearly distinguishable from the unstained population but there was also potential for a rightward shift upon TNFα/CHX treatment. Using a lower concentration of annexin was also advantageous as this was the limiting substrate in the assay kit, allowing more experiments to be performed per kit.

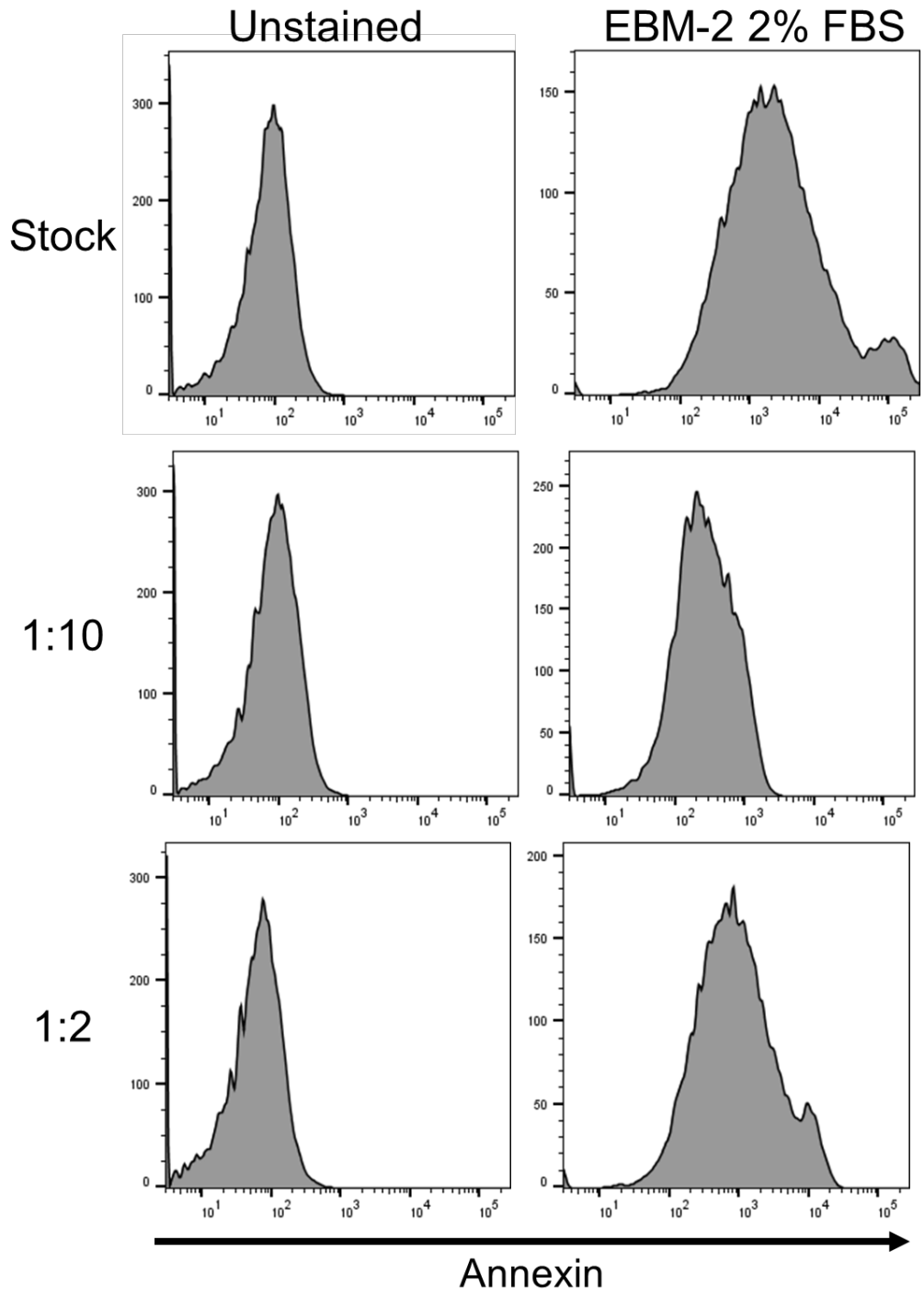

Figure 2.7: Histogram plots of annexin staining collected by flow cytometry in unstained and serum and GF starved (EBM-2 2% FBS) treated human PAECs. Each panel horizontally illustrates differing concentrations of annexin diluted from the stock concentration provide by Thermoscientific. The optimal condition was a 1:2 dilution (bottom panel) as this demonstrated a clear rightward shift in annexin staining with serum and GF starvation but was not so great that it would restrict further shifts being observed following apoptotic induction with TNFα/CHX treatment. This also conserved the annexin solution which was the limiting substrate in the assay.

2.5.3 TNFα and CHX Concentration Optimisation

The initial concentrations of TNFα/CHX used were 3ng/mL and 50µg/mL, respectively, after discussion with the authors of the Long *et al.* (2015) paper. However, these concentrations were found to be too severe in the cell lines used and different concentrations of TNFα/CHX were tested both with and without the positive control, rhVEGF, in donor 2 to find the optimal concentrations to use. The highest concentrations used were 3ng/mL TNFα and 20µg/mL CHX. However, due to the six-well format limiting assay space, rescue with rhVEGF could not be tested at this concentration. This had previously been tested in other experiments using donor 2 with little success, suggesting that the TNFα/CHX treatment was still too harsh to allow for rescue of the induced apoptosis. The concentrations of TNFα/CHX were reduced to test at 1.5ng/mL and 20µg/mL, 1.5ng/mL and 10µg/mL and 0.5ng/mL and 10µg/mL, respectively; the results are shown in Figure 2.8. There was little difference in apoptotic induction between the 3ng/mL and 1.5ng/mL concentrations of TNFα with a fixed concentration of 20µg/mL CHX. With the lower 10µg/mL CHX concentration there were approximately 10% fewer annexin stained cells and this dropped by a further 5% when the TNFα concentration was reduced to 0.5ng/mL. Since the rescue from rhVEGF was fairly consistent at all concentrations in restoring annexin staining to the basal level observed in the EBM-2 2% control but 1.5ng/mL TNFα and 20µg/mL CHX induced the most apoptosis; this concentration provided the largest window for potential rescue from apoptosis and was chosen as the optimal concentration tested.

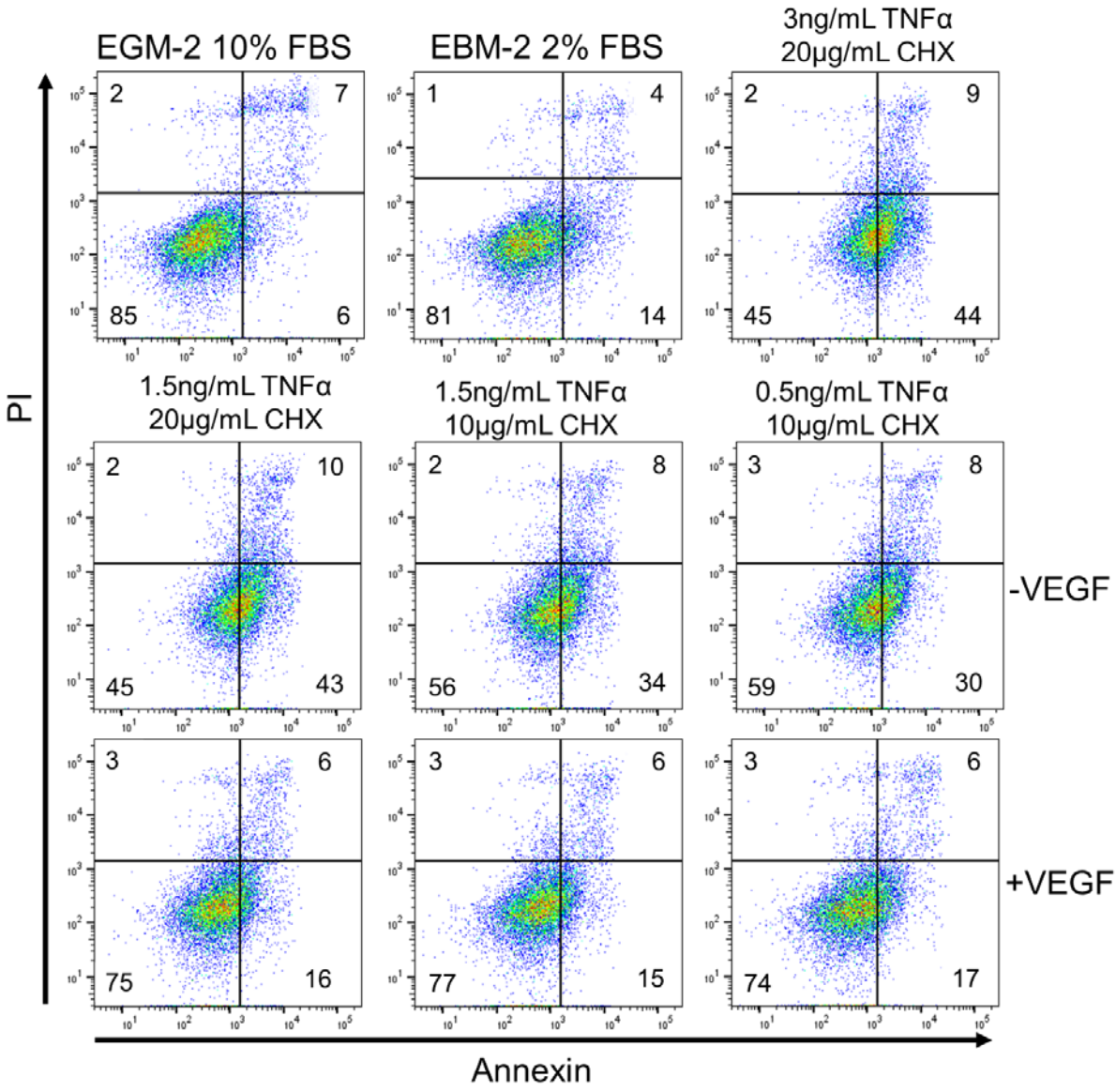

Figure 2.8: Scatter plots of annexin staining vs PI staining detected by flow cytometry in human PAECs treated with either EGM-2 10% FBS ('healthy' controls), EBM-2 2% FBS (serum and GF starved) or different concentrations of TNFα/CHX with or without rhVEGF. The numbers in each corner give the percentage of cells located in that quadrant. TNFα/CHX resulted in a rightward shift of the population leading to a greater number of cells in the annexin^{+}/PI^{-} 'apoptotic' quadrant which was reduced by rhVEGF treatment in each condition. The condition that provided the largest window of apoptotic rescue was 1.5ng/mL TNFα and 20µg/mL CHX.

2.5.4 Data Analysis

Experiments were performed at least in triplicate in the five donor human PAEC lines using passages 4-6. Optimisation experiments were performed in lines 1-3. It was found that, at the optimal concentrations chosen of 1.5ng/mL TNFα and 20μg/mL CHX, there was no significant induction of apoptosis in lines 4 and 5 (2.80±1.60%, ns). Moreover, although there was no induction of apoptosis over the EBM-2 2% FBS control, rhVEGF still reduced $Annexin^{+}/PI^{-}$ staining. This suggests that the response to rhVEGF was a rescue of GF and serum starvation. GF and serum starvation is something that has been widely observed in various endothelial cell lines (Gama Sosa *et al*., 2016, Gerber *et al*., 1998b, Karsan *et al*., 1997, Ueda *et al*., 2005, Date *et al*., 2005, Raymond *et al*., 2004) and the mechanisms for rescue with rhVEGF are thought to occur by both upregulation of the MAPK/ERK pathway alongside downregulation of JNK pathway (Gupta *et al*., 1999), leading to enhanced bcl-2 and decreased bax signalling (Gerber *et al*., 1998a, Ueda *et al*., 2005, Karsan *et al*., 1997). In contrast, TNFα/CHX stimulates apoptosis primarily through the TNF-R1 leading to induction of the JNK and p-38 MAPK pathways.

Data where there was insufficient apoptotic induction by TNFα/CHX were excluded because the mechanisms of induction were not comparable to those in donors 1-3. Similarly, experiments that showed less than 5% induction of apoptosis were excluded from the analysis as these provided insufficient window and again suggest different mechanisms involved in apoptotic induction. The average induction of apoptosis of the analysed experiments using donors 1-3 was 19.53±1.76% (****$p<0.0001$).

Since raw percentages of annexin staining were compared in this assay, variability in the basal amount of apoptotic induction between the replicates was observed. This likely reflects differences in the cell line and their susceptibility to TNFα/CHX induced apoptosis, as well as passage number. It has been reported that older passages are more susceptible to serum and GF starvation (Varani *et al*., 1995) and this may render them less able to respond to further apoptotic stimuli, thus restricting the window of observation in the experiment. To remove this variability and compare the data trends which can be observed in the raw data between experiments (Figure 2.9), a matched ANOVA was utilised.

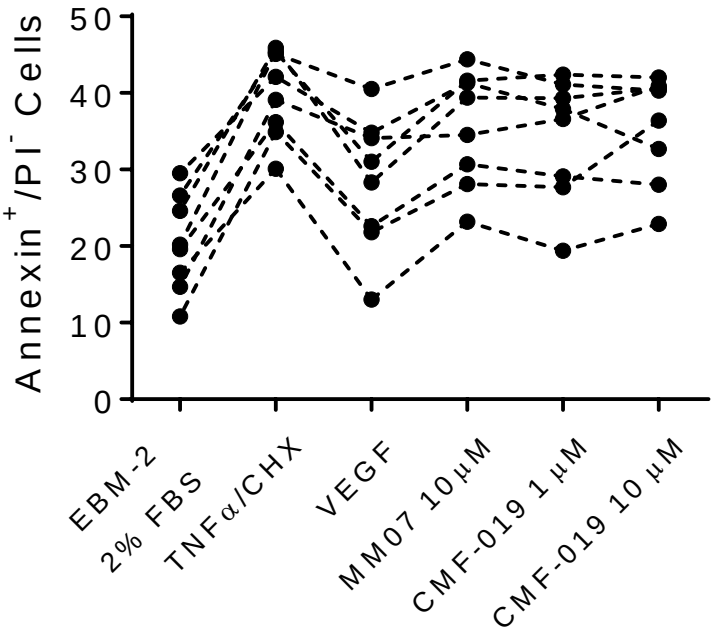

Figure 2.9: Dot and line plot of the percentage of annexin$^+$/PI$^-$ human PAECs detected by flow cytometry for each experimental condition. Each line represents one experimental replicate (8 replicates over 3 cell lines) such that trends in the data can be observed. It can be seen that the relative amounts of initial annexin$^+$/PI$^-$ staining were variable but the staining across each experiment was consistent as demonstrated by the limited cross-over between experiments.

2.5.5 Evaluation

In this assay it was very difficult to compare across cell lines and passage numbers due to the variability in apoptotic induction. Furthermore, the assay had to be thoroughly optimised from a previously published protocol (Long *et al.* 2015). The number of controls that were required and the small six-well plate format meant that it was very limited in throughput and the concentrations that could be tested; hence, concentration-response data could not be collected. Overall this suggests that the assay is not sufficiently robust and alternative assays with greater throughput and requiring less substantial optimisation should be used in preference.

2.6 Surgical Techniques

Surgical techniques were developed based on the heart catheterisation protocols described previously by Pacher *et al*., 2008. In later experiments, a technique for femoral artery catheterisation was also devised and incorporated into the protocol. These techniques enabled the assessment of acute cardiovascular responses to bolus intravenous drug administration *in vivo*, as well as RV and LV catheterisation to assess RVSP and LVSP following a MCT PAH prevention study.

2.6.1 Surgical Procedures to Assess Acute Cardiovascular Responses

The equipment used for surgery is shown in Figures 2.10 and 2.11. Preparation of the animal for surgery is shown in Figure 2.12. In brief, normotensive Male Sprague-Dawley rats (Charles River Laboratories, Margate, UK) were induced to anaesthesia with inhalation of 5% isoflurane in an induction box (reduced to 3% once unconscious) and then maintained under 1.5-2% isoflurane via a face mask. Temperature was monitored throughout the surgical procedure using a rectal probe. Prior to the start of surgery, it was ensured that pain reflexes had ceased by use of a hind-paw pinch test. The breathing rate and, once catheterised, the heart rate were monitored to determine and maintain a suitable depth of anaesthesia. The catheters (SPR-869, Millar Inc.; Houston, TX, USA) were electronically calibrated using the MPVS Ultra system (ADIstruments; Dunedin, NZ) prior to the start of surgery.

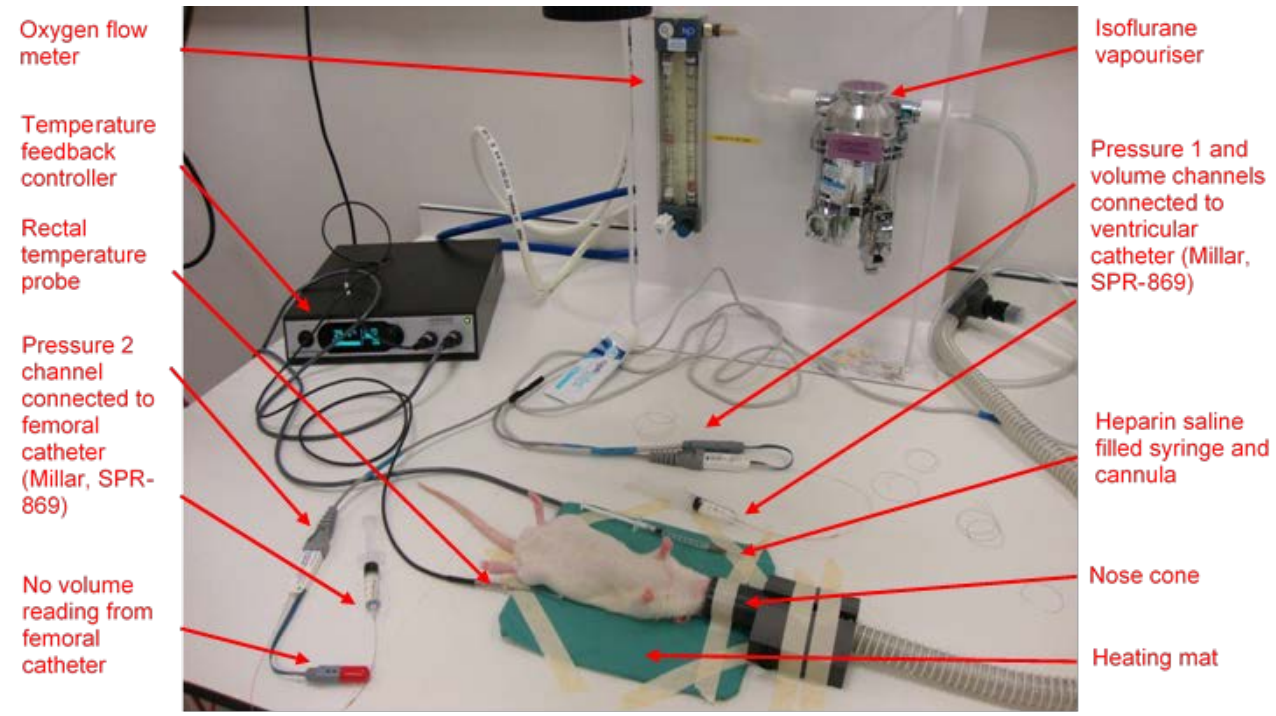

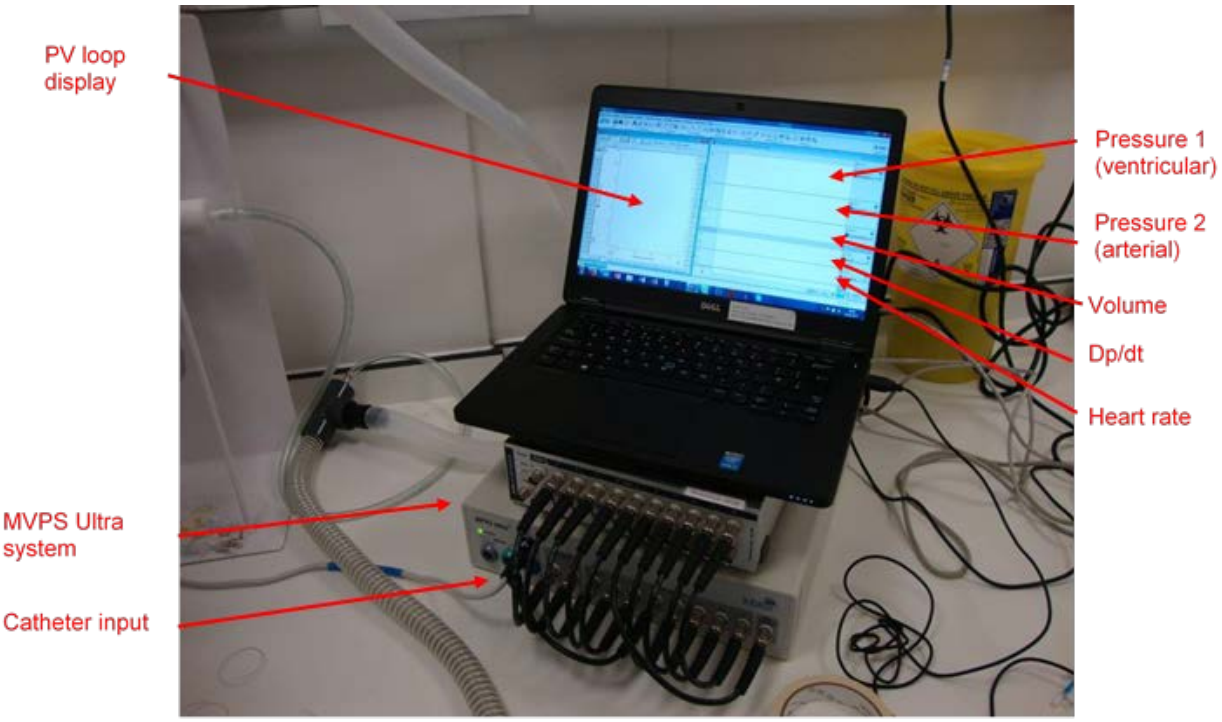

Experimental set-up for surgery.

Top panel, Figure 2.10: The equipment required for maintenance of anaesthesia, temperature and performing surgery.

Bottom panel, Figure 2.11: The computational equipment and display used for recording the data acquired following completion of surgery.

Induction to anaesthesia

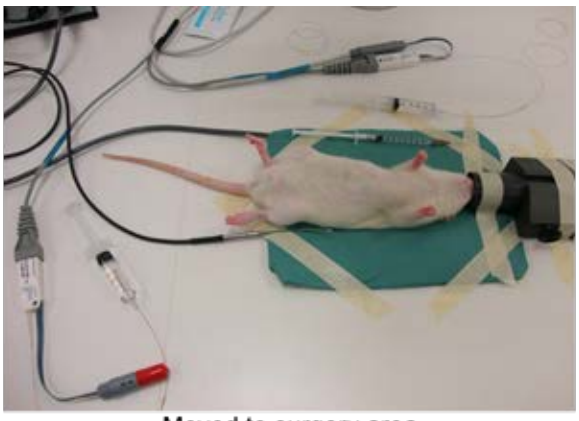

Moved to surgery area

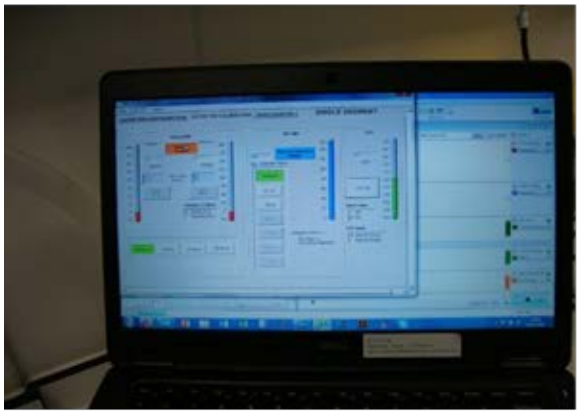

Catheters electronically calibrated using MPVS Ultra system

Hind-paw pinch test

Positive response to pinch

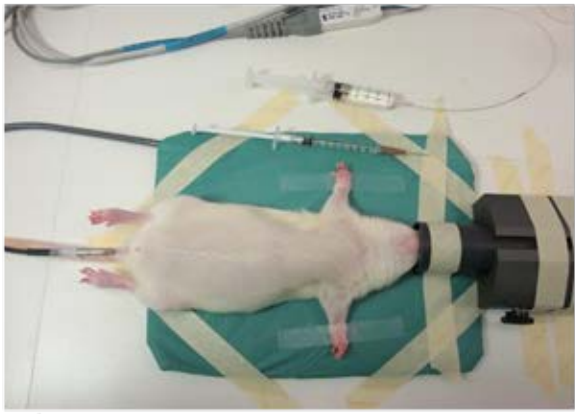

Once unresponsive, arms tapped down to aid access for surgery

Figure 2.12: Procedures for the preparation of the rat for surgery. The animal was anaesthetised and tested for responsivity. The catheters were calibrated prior to the start of surgery.

The surgical procedures are shown in Figures 2.13, 2.14 and 2.15. In brief, the right external jugular vein was exposed, cannulated (Figure 2.13) and flushed with heparin solution (2%, 0.9% saline, pH5, Macopharma; Tourcoing, FR). The right common carotid artery was then located and a catheter inserted and advanced to the LV (Figure 2.14). Once a stable pressure-volume (PV) loop could be observed, the femoral artery was exposed and a second catheter inserted to record arterial pressure responses simultaneously to ventricular responses (Figure 2.15). Drugs or saline controls were then administered intravenously via the jugular vein catheter, followed by a saline flush (0.9%, 0.1mL, pH5) at a minimum of ten minute intervals or when a stable baseline was reached before the next injection. Data were acquired using the MPVS Ultra system (ADInstruments) and analysed using LabChart 8 (ADInstruments). Values for the maximal change in arterial pressure, left ventricular systolic pressure (LVSP), stroke volume, cardiac output, heart rate, contractility (dP/dt_{MAX}) and lusitropy (dP/dt_{MIN}) from baseline were calculated from the raw data and compared. Following completion of the measurements the animal was euthanised by exsanguination under high flow isoflurane (5%).

Arms taped down and neck exposed

Neck opened

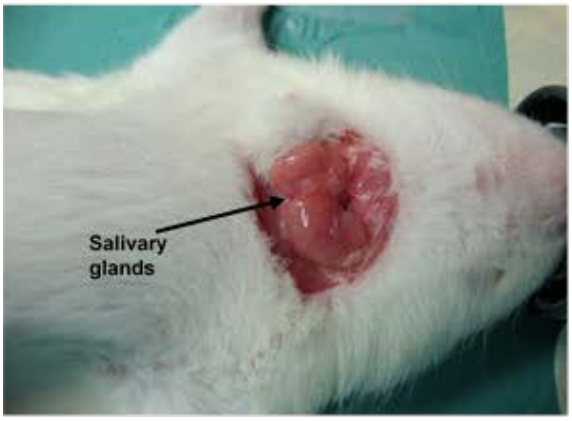

Salivary glands located

Salivary glands pulled upwards and clamped in place

Jugular vein located

Jugular vein pulled upwards and tied with suture

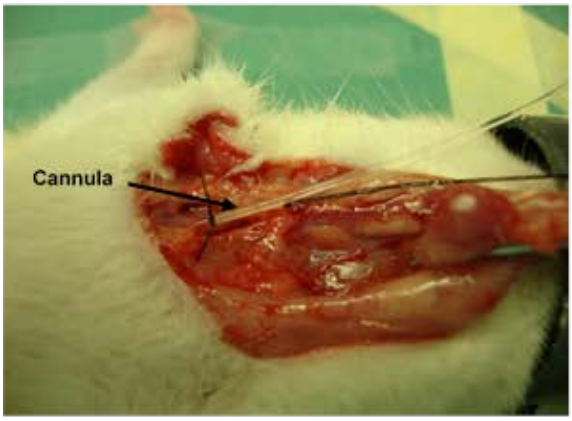

Cannula inserted and tied in place

Figure 2.13: Surgical procedures for cannulation of the right external jugular vein.

On next page, Figure 2.14: Surgical procedures for catheterisation of the LV via the right common carotid artery.

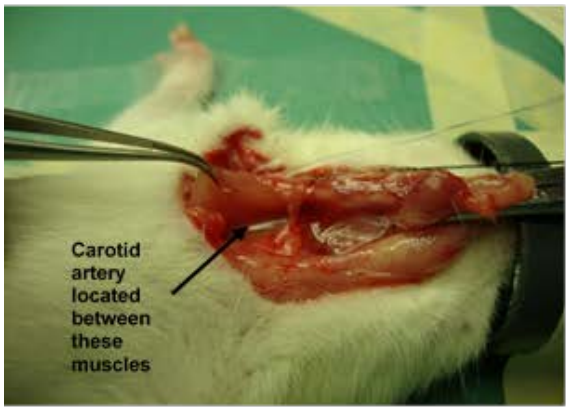

Carotid artery located

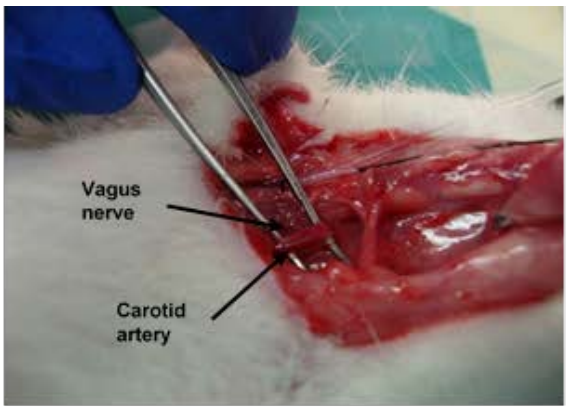

Carotid artery and vagus nerve isolated

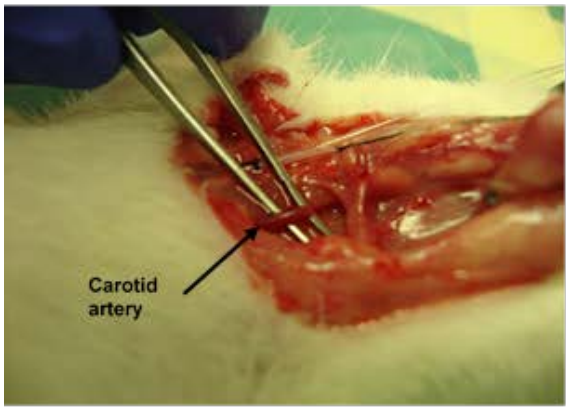

Vagus nerve carefully removed

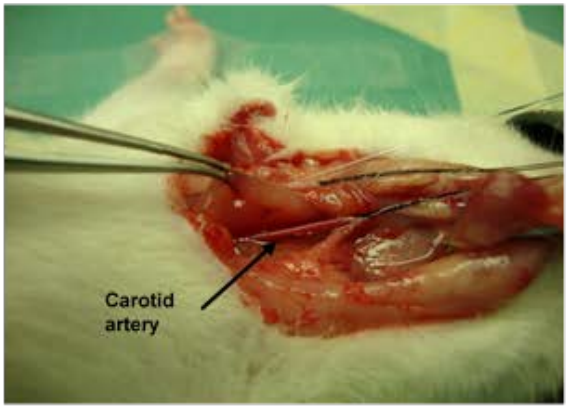

Carotid artery pulled upwards and tied with suture

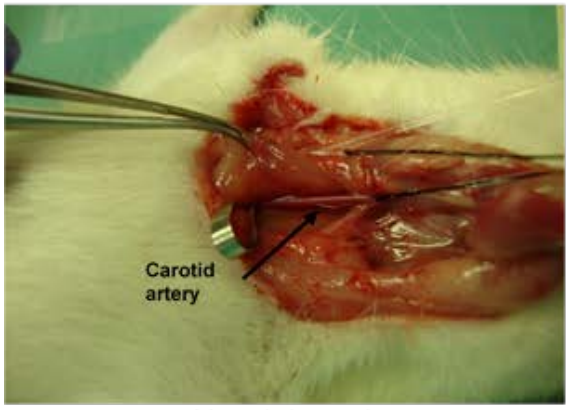

Vessel clamped

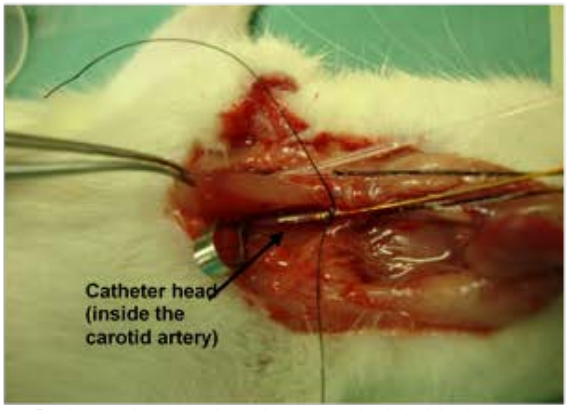

Catheter inserted and suture tied behind the head

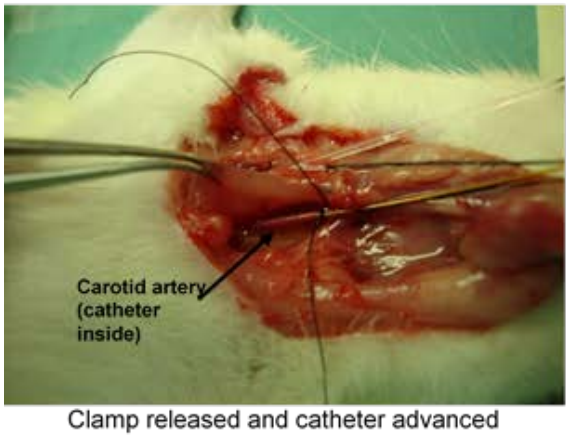

Clamp released and catheter advanced

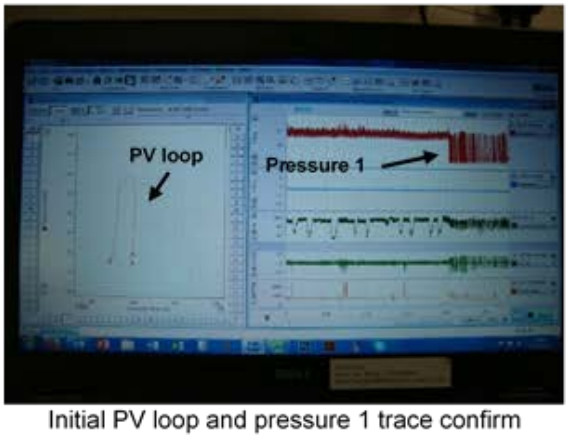

Initial PV loop and pressure 1 trace confirm catheter in the ventricle

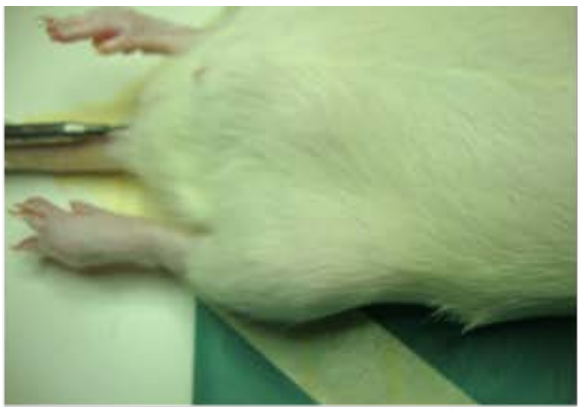

Microscope adjusted to focus on left leg

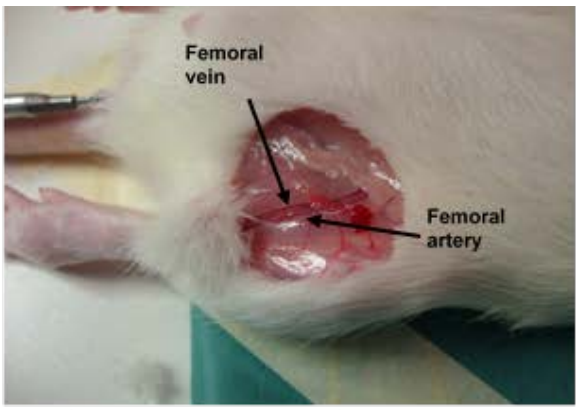

Left leg opened to expose femoral artery and vein

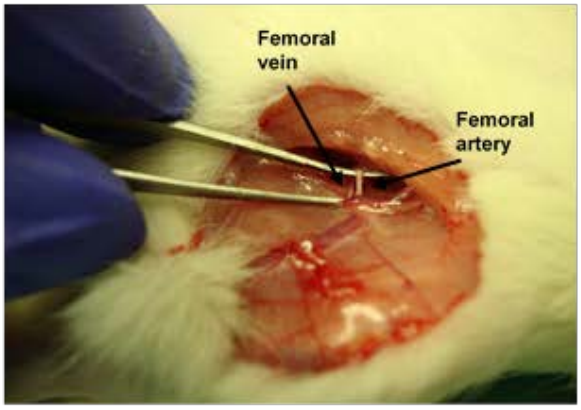

Section of artery exposed and separated from vein

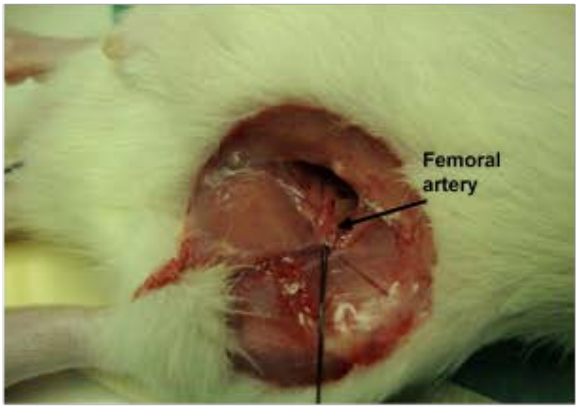

Femoral artery pulled downwards and tied with suture

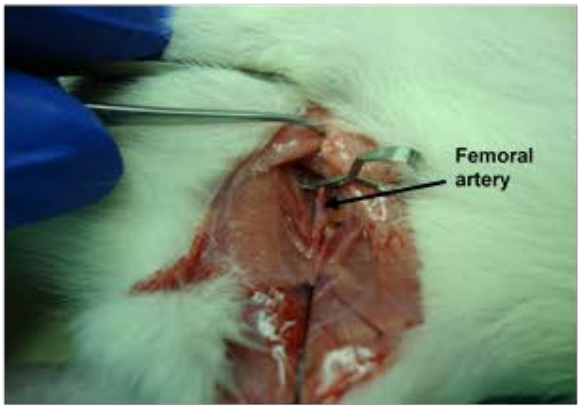

Vessel exposed further up and clamped

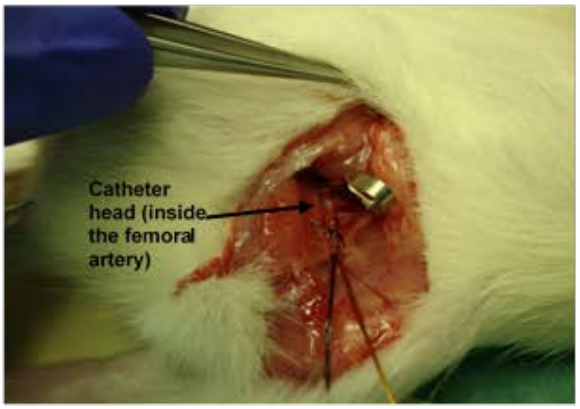

Catheter inserted and suture tied behind the head

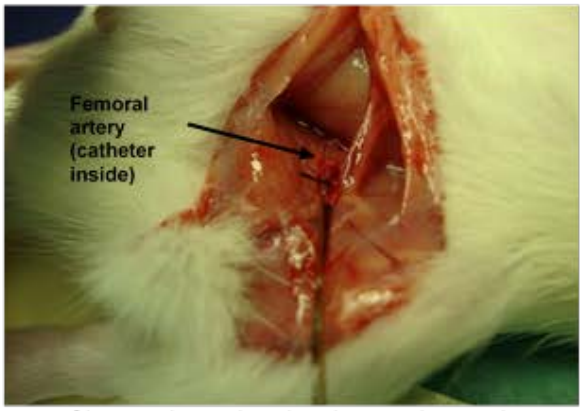

Clamp released and catheter advanced

Figure 2.15: Surgical procedures for catheterisation of the femoral artery.

2.6.2 Surgical Procedures to Measure LVSP and RVSP Following a MCT Prevention Study of PAH

The MCT prevention study of PAH was performed as previously described (Falcao-Pires *et al*., 2009, Yang *et al*., 2017b). Briefly, male Sprague-Dawley rats (Charles River Laboratories, Margate, UK) received a single subcutaneous injection of MCT (60mg/kg) or a saline control. Thereafter, they received IP injections of either the treatment or saline (equivalent volume by weight) for 21 days. On the final injection date, the LV and RV were catheterised using broadly the same surgical techniques described above to measure LVSPs and right ventricular systolic pressures (RVSPs). The Fulton index recorded as a measure of hypertrophy (Fulton *et al*., 1952). The experimental timeline is shown below (Figure 2.16).

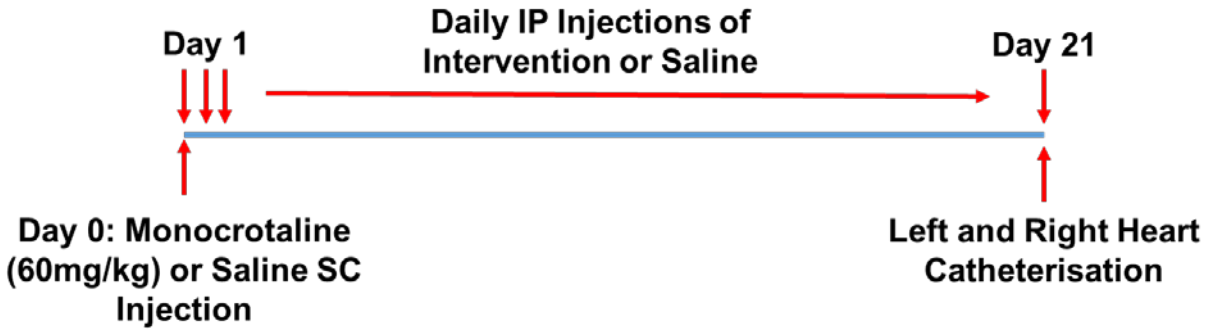

Figure 2.16: Timeline of events for a MCT prevention study of PAH. Male Sprague-Dawley rats received a single SC injection of either MCT or saline to induce PAH. Thereafter, they received daily IP injections of either the intervention or saline control up to and including day 21 at which point their LV and RV were catheterised and the Fulton index recorded.

Preparation for surgery was largely the same as shown in Figures 2.12, however, in this case only one catheter (Millar Inc., SPR-869) was required. Especially careful monitoring throughout anaesthesia was required with MCT-treated animals due to their impaired lung function increasing the chance of asphyxiation from isoflurane inhalation. No cannula was inserted for the surgery as described previously, and instead a PV catheter was inserted into the RV through the right external jugular vein by the same methodology (Figure 2.13). When this was complete, it was sealed off with a single tight suture and the LV then catheterised as described in Figure 2.14 via the right common carotid artery with the same catheter. The femoral artery was not catheterised. Following termination by exsanguination under high flow isoflurane (5%), the heart was excised and dissected carefully to remove the atria. The Fulton index, a

measure of hypertrophy calculated as the RV wet weight divided by the LV and interstitial septum wet weight, was recorded.

2.7 Apelin Enzyme-Linked Immunosorbent Assay

Apelin-12 enzyme-linked immunosorbent assays (ELISA; EK-057-23) were purchased from Phoenix Pharmaceuticals Inc. (Burlingame, CA, USA) and performed according to the manufacturer's instructions with the exception of using [Pyr^{1}]apelin-13 as a standard. In brief, samples, primary antibody and the biotinylated peptide were incubated on an orbital shaker (300-400rpm) for two hours at room temperature in a secondary antibody pre-coated 96-well plate. All wells were then washed four times with assay buffer, thoroughly dried and incubated with streptavidin-horseradish peroxidase for one hour at room temperature (300-400rpm). Next, the wells were washed and dried again before the enzyme substrate added for a further hour at room temperature and protected from light (300-400rpm). Finally, the plate was treated with 2N hydrochloric acid to stop the reaction and the plate read on a microtiter plate reader at 450nm absorbance. Since the apelin-like immunoreactivity in the sample competes against the biotinylated peptide for binding to the primary antibody in this assay, the greater the concentration of peptide in the sample then the less streptavidin-horseradish peroxidase is available to react with the substrate and the lower the absorbance detected. Samples were performed in duplicate and concentrations interpolated from the [Pyr^{1}]apelin-13 standard curve.

2.8 Statistical Analysis

All data are expressed as mean±SEM values and statistical analyses were performed with GraphPad Prism 6 (La Jolla, CA, USA) unless otherwise stated. Binding and cell-based DiscovRx experiments were performed in triplicate. For DiscovRx assays, n-values are given as the number of replicates/number of experiments.

For flow cytometry, experiments were performed at least in triplicate. Donors 4 and 5 were excluded from the analysis as they showed a particularly small window of apoptotic cell induction using TNF-α and CHX (2.80±1.60%), this was not significantly different to the EBM-2 2% FBS control (Matched ANOVA). Of the remaining donors, technical replicates were excluded if the apoptotic induction was less than 5%. The average induction of apoptosis of the analysed experiments was 19.53±1.76%. Data were normally distributed using the D'Agostino-Pearson omnibus K^2 test and trends were compared using a matched ANOVA to account for variability observed in the basal amount of apoptotic induction observed between replicates.

For the acute *in vivo* studies, values for the cardiovascular parameters measured in saline and treated animals were compared using a two-tailed Student's t-test. For the cross study analysis of [Pyr^1]apelin-13 responses *in vivo*, the doses compared were not always given at the corresponding dose schedule so that while the dose administered is always the same, it may have been given as the first or second dose the animal received. Data have not been included where the preceding dose was not either a saline dose or a lower dose of [Pyr^1]apelin-13. A number of saline controls from different dose schedules have been included to attempt to control for this. Data were tested for normality using the D'Agostino-Pearson omnibus K^2 test and analysed using a two-tailed Student's t-test. Statistical significance was taken as 5%.

For the chronic MCT study, parameters were compared to their corresponding controls using a two-tailed Student's t-test. N values were too small to use the recommended D'Agostino-Pearson omnibus K^2 test to test for normality; however, data were normally distributed using a Shapiro-Wilks test. Statistical significance was taken as 5%.

3. Identification and Characterisation of CMF-019, the First G Protein Biased Apelin Agonist

3.1 Introduction

One of the primary aims of this study was to identify small molecule agonists at the apelin receptor. To date, very few small molecule agonists have been identified at this receptor and those that have possess significant limitations in their use, this was discussed at length in Section 1.4. The identification of small molecule ligands that bind to the receptor with high affinity could greatly progress the apelin research field by providing cheaper and more easily manufactured molecules for experimental study. Additionally, such molecules might be suitable either as therapeutics themselves in disease, for example in PAH, as discussed in Section 1.6, or they might provide a starting point for the development of a newer generation of agonists for treatment.

To identify small molecules that bind to the apelin receptor, a patent search was performed, revealing two series of structures, one from Sanford-Burnham (Pinkerton and Smith, 2015) and one from Sanofi (Hachtel *et al*., 2014). Compounds from both series have previously been screened in the laboratory and the Sanford-Burnham series deemed unsuitable due to a lack of solubility. However, the Sanofi series based upon the benzimidazole scaffold was taken forwards and of the 20 assessed, four compounds, CMF-013, CMF-015, CMF-019 and CMF-021 (Figure 3.1), were selected for further screening. CMF-019 was chosen as the lead compound and modifications of the structure were made. In the first instance, the structural scaffold of CMF-019 was altered to introduce an additional nitrogen atom into the benzimidazole ring, producing a molecule designated CMF-087. CMF-087 then underwent side-chain modifications to produce two further molecules for study, MM239 and MM240. In a later series, an attempt was made to amalgamate the structure of CMF-087 with the structures of the Sanford-Burnham triazole series (Pinkerton and Smith, 2015) and the recently identified RTI International pyrazole series (Narayanan *et al*., 2016); the resulting compound was designated CMF-167.

This chapter details the screening of the four original CMF compounds -013, 015, -019 and -021, before going on to compare the CMF-019 derivatives to the parent molecule.

Ultimately, CMF-019 was selected as the most promising compound and was taken forward for further study as described in subsequent chapters.

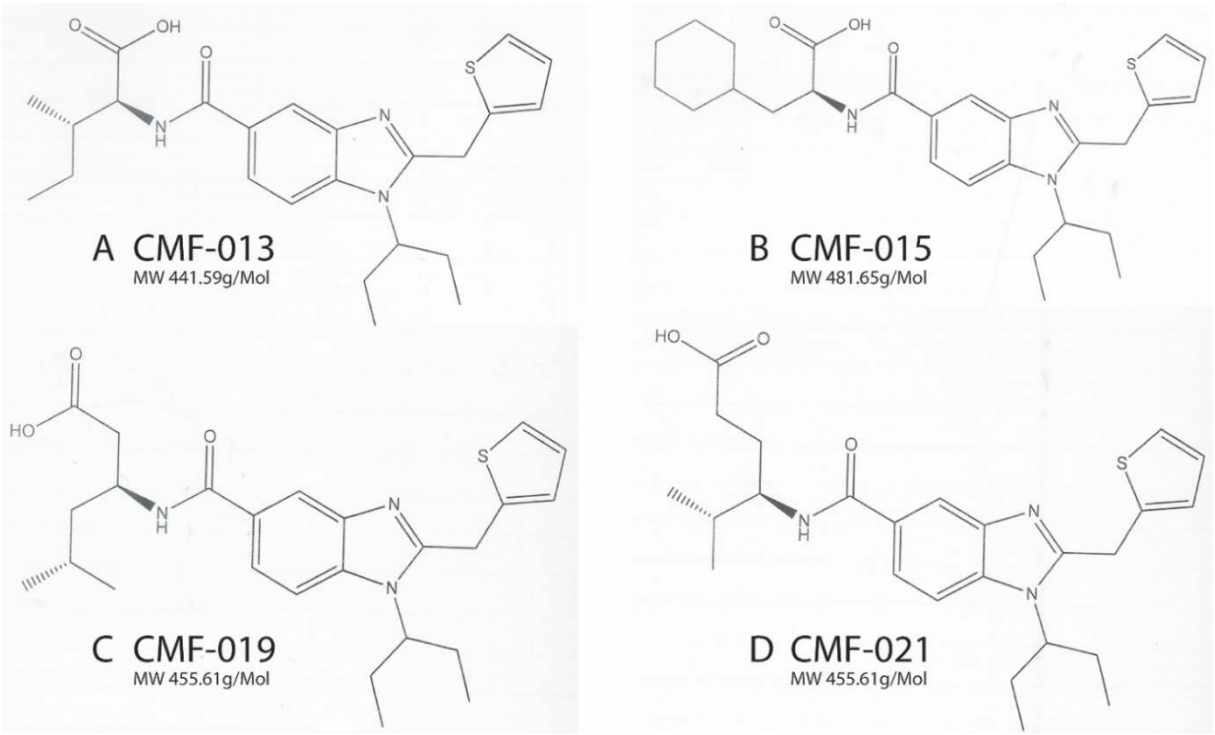

Figure 3.1: The chemical structures of the four original CMF compounds based on the benzimidazole scaffold, CMF-013, -015, -019 and -021. The molecular weights of each compound are displayed below.

3.2 Methods

3.2.1 Materials

All CMF compounds and synthetic modifications to previous structures were designed and synthesised by Christopher Fitzpatrick, Dr Richard Foster (University of Leeds) and Professor Robert Glen (University of Cambridge).

3.2.2 Competitive Radioligand Binding Assays

Human LV homogenate, whole rat and whole mouse hearts were homogenised as described in Section 2.2. [Pyr^{1}]apelin-13 (5µmol/L-1pmol/L), CMF-013, -015, -021, MM239 and MM240 (0.1mmol/L-50pmol/L), CMF-019 (5µmol/L-1pmol/L) and CMF-087 (50µmol/L-10pmol/L) were competed against 0.1nmol/L [Glp^{65},Nle^{75},Tyr^{77}][^{125}I]apelin-13 as described in Section 2.3. In one experiment competing [Pyr^{1}]apelin-13 in whole mouse heart homogenate, the concentration of protein used was 1mg/mL rather than 1.5mg/mL as used in all other experiments.

3.2.3 Cell Signalling Assays

3.2.3.1 β-Arrestin Assay

[Pyr^{1}]apelin-13 (n=9/33) (1µmol/L-10pmol/L), CMF-013 (n=3/8), -015 (n=3/8), -019 (n=4/13), -021 (n=4/11), -087 (n=4/12), MM239 (n=4/12) and MM240 (n=4/11) (0.1mmol/L-1nmol/L) were assessed for their ability to recruit β-arrestin to the apelin receptor in a CHO based cell assay as described in Section 2.4.1.

3.2.3.2 cAMP Assay

[Pyr^{1}]apelin-13 (n=12/36) (30nmol/L-1pmol/L), CMF-013 (n=4/11), -015 (n=3/9), -021 (n=4/9) (10µmol/L-1pmol/L), CMF-019 (n=5/14) (30nmol/L-0.1pmol/L), CMF-087 (3/9) (1µmol/L-1pmol/L), MM239 (n=4/12) and MM240 (n=4/10) (1µmol/L-10pmol/L) were assessed for their ability to reduce cAMP expression following forskolin stimulation in a CHO based cell assay as described in Section 2.4.2.

3.2.3.3 Internalisation Assay

[Pyr^{1}]apelin-13 (n=3/8) (1µmol/L-10pmol/L), CMF-013 (n=1/3), -015 (n=1/3), -021 (n=1/3) (0.1mmol/L-1nmol/L) and CMF-019 (n=3/9) (0.1mmol/L-0.1nmol/L) were assessed for their ability to internalise the apelin receptor in a U20S based cell assay as described in Section 2.4.3.

3.2.4 Statistical Analysis

Binding experiments were performed in triplicate and K_i values calculated using the Cheng-Prusoff methodology (Cheng and Prusoff, 1973). Binding data are displayed graphically over the same concentration range for ease of comparison. Data are listed as pK_i±SEM; however the K_i values without error have been included in summary tables for ease of comparison.

Cell signalling assays were performed in triplicate where possible and are listed as n=biological replicates/technical replicates and analysis was performed as means of means. Data are listed as pD_2±SEM but EC_{50} values calculated as geomeans have been listed without error in summary tables for ease of comparison. Where sufficient biological replicates are available, bias calculations have been performed (van der Westhuizen *et al*., 2014) to obtain values for relative effectiveness compared to [Pyr^1]apelin-13 within each cell-based assay and bias factors to compare the relative activities of the agonists between the different pathways.

Linear regression analysis was performed on pK_i±SEM, pD_2±SEM and ΔΔlogR±SEM values and presented as the line of best fit calculated and the goodness of the fit as the r^2 value.

3.3 Results

3.3.1 Competitive Radioligand Binding Studies

3.3.1.1 [Pyr[1]]apelin-13 Bound to Apelin Receptors

The endogenous agonist [Pyr[1]]apelin-13 bound to native apelin receptors in human LV (8.82±0.05), rat whole heart (9.50±0.06) and whole mouse heart (8.73±0.06) homogenates with similar nanomolar affinity (Figure 3.2).

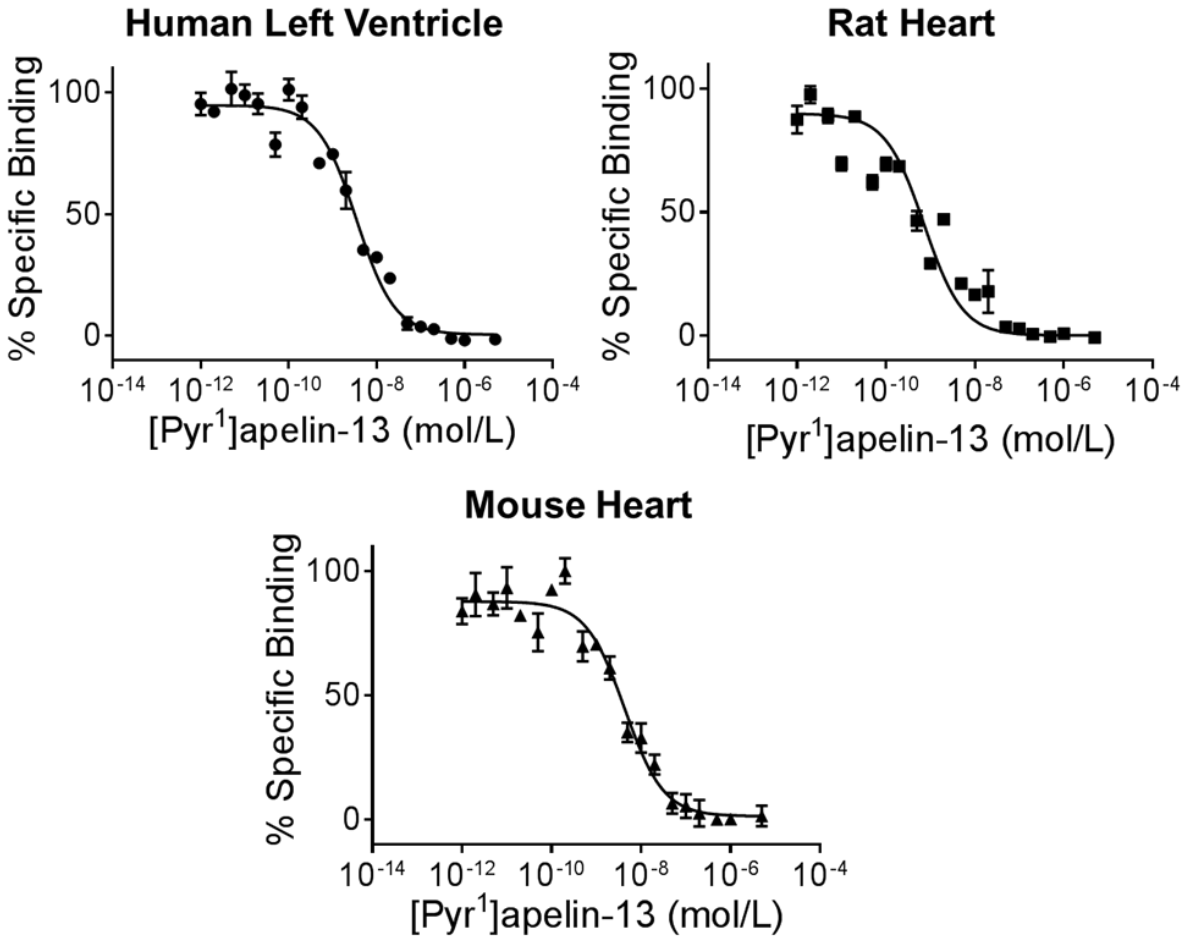

Figure 3.2: Specific binding of 0.1nM [Glp[65],Nle[75],Tyr[77]][[125]I]apelin-13 to human LV (●), rat whole heart (■) and mouse whole heart (▲) homogenates with increasing concentrations of [Pyr[1]]apelin-13. K_i values were calculated from IC_{50} values using the Cheng-Prusoff methodology (K_i[Glp65,Nle75,Tyr77][[125]I]apelin-13=0.076nmol/L). In whole mouse heart homogenate the concentration of protein used was 1mg/mL rather than 1.5mg/mL as in all other experiments. Data displayed over the same concentration range for ease of comparison.

3.3.1.2 CMF-013, -015, -019 and -021 Bound to the Human Apelin Receptor

In human LV homogenates, CMF-013, -015, -019 and -021 bound competitively with nanomolar affinity to the native apelin receptor (7.89±0.06, 7.59±0.07, 8.58±0.04, 7.67±0.05, respectively; Figure 3.3).

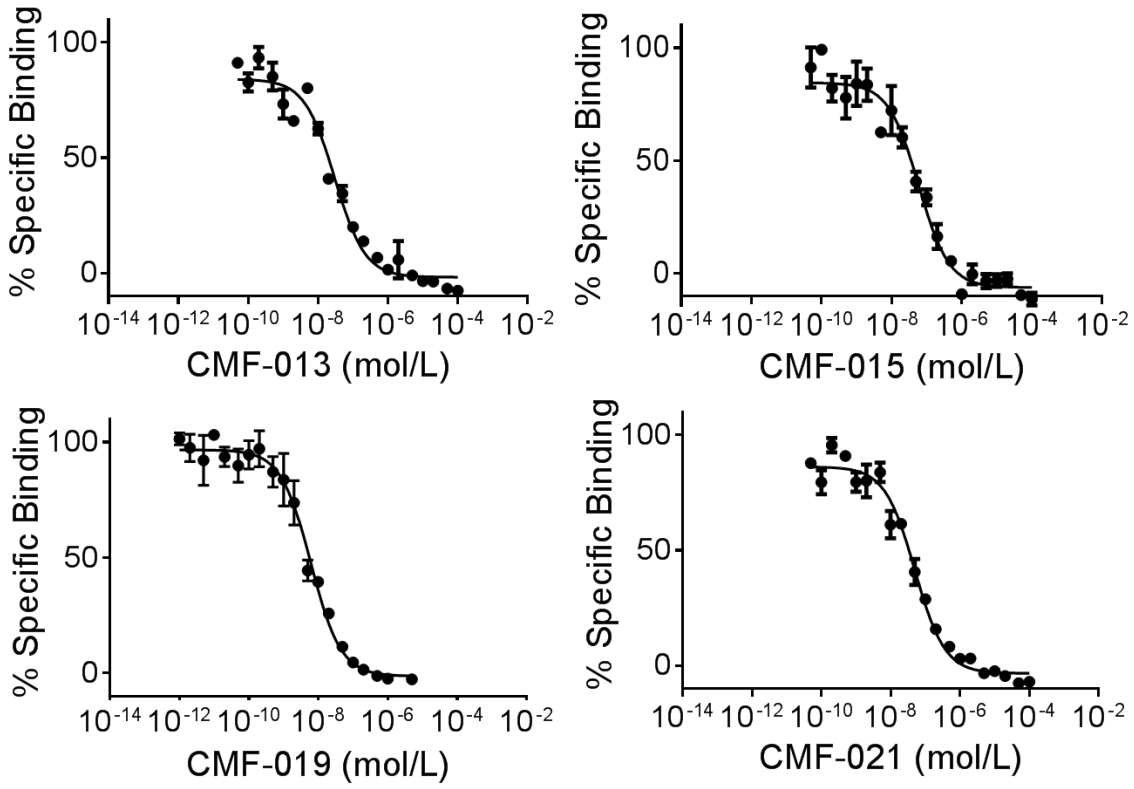

Figure 3.3: Specific binding of 0.1nM [Glp^{65},Nle^{75},Tyr^{77}][^{125}I]apelin-13 to human LV homogenates with increasing concentrations of either CMF-013, -015, -019 or -021. K_i values were calculated from IC_{50} values using the Cheng-Prusoff methodology (K_i[Glp65,Nle75,Tyr77][^{125}I]apelin-13=0.076nmol/L). Data displayed over the same concentration range for ease of comparison.

3.3.1.3 CMF-019 Bound to Rat and Mouse Apelin Receptors

Similar binding was observed in rat and mouse whole heart homogenates for CMF-019 compared to in human LV homogenates (8.49±0.04 and 8.71±0.06, respectively; Figure 3.4).

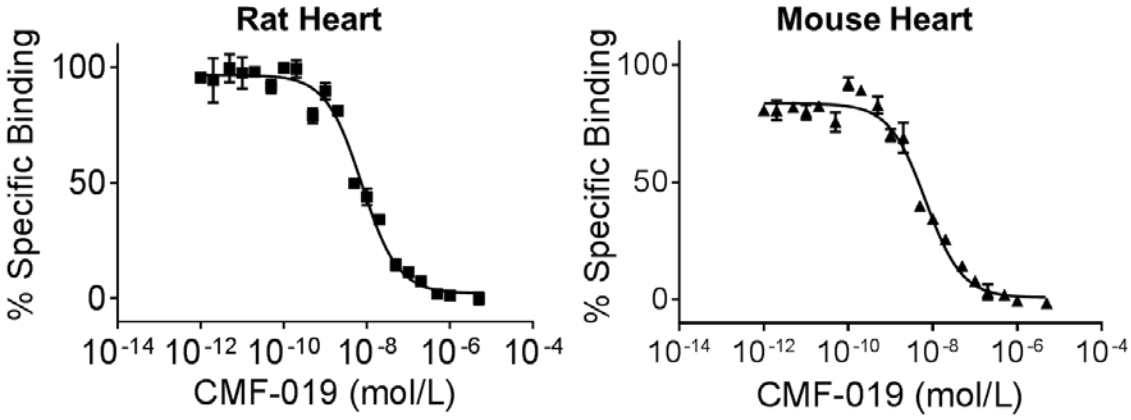

Figure 3.4: Specific binding of 0.1nM [Glp^{65},Nle^{75},Tyr^{77}][^{125}I]apelin-13 to rat whole heart (■) and mouse whole heart (▲) homogenates with increasing concentrations of CMF-019. K_i values were calculated from IC_{50} values using the Cheng-Prusoff methodology (K_i[Glp65,Nle75,Tyr77][^{125}I]apelin-13=0.076nmol/L). Data displayed over the same concentration range for ease of comparison.

3.3.1.4 CMF-087 Bound to the Human Apelin Receptor

The CMF-019 analogue, CMF-087, bound to the native apelin receptor in human LV homogenates with 20-fold lower nanomolar affinity than CMF-019 (7.28±0.05; Figure 3.5).

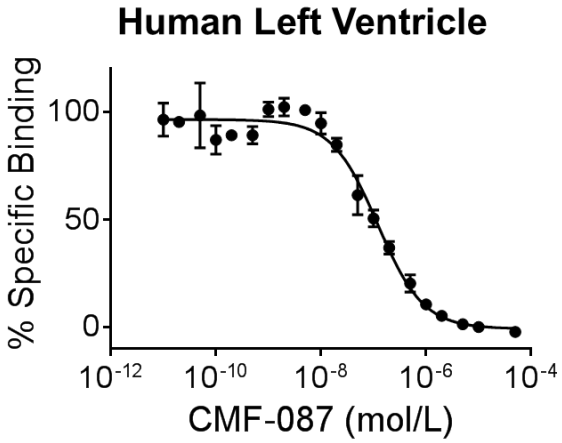

Figure 3.5: Specific binding of 0.1nM [Glp^{65},Nle^{75},Tyr^{77}][^{125}I]apelin-13 to human LV homogenates with increasing concentrations of CMF-087. The K_i value was calculated from IC_{50} values using the Cheng-Prusoff methodology (K_i[Glp65,Nle75,Tyr77][^{125}I]apelin-13=0.076nmol/L).

3.3.1.5 MM239 and MM240 Bound to Native Human and Rat Apelin Receptors

The CMF-087 analogues, MM239 and MM240, bound to the native human apelin receptor in LV homogenates with higher affinities than CMF-087 (8.67±0.05 and 7.64±0.07, respectively; Figure 3.6). They also both bound to the native rat apelin receptor in whole rat heart homogenates with lower affinities than to the human receptor (7.92±0.05 and 7.12±0.04, respectively; Figure 3.6).

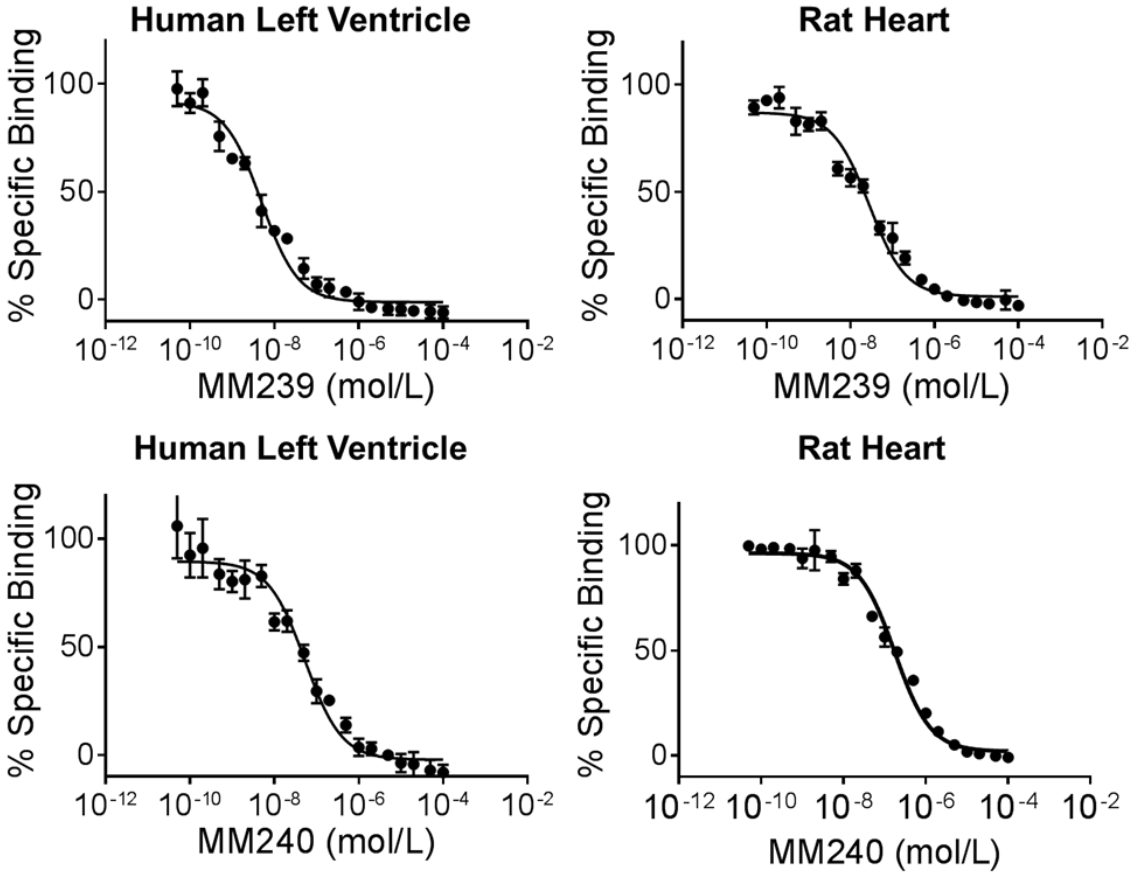

Figure 3.6: Specific binding of 0.1nM [Glp^{65},Nle^{75},Tyr^{77}][^{125}I]apelin-13 to human LV (●) and rat whole heart (■) homogenates with increasing concentrations of MM239 or MM240. K_i values were calculated from IC_{50} values using the Cheng-Prusoff methodology (K_i[Glp65,Nle75,Tyr77][^{125}I]apelin-13=0.076nmol/L). Data displayed over the same concentration range for ease of comparison.

3.3.2 Cell Signalling Assays

3.3.2.1 CMF-013, -015, -019 and -021 Displayed G Protein Signalling Bias

CMF-013, -015, -019 and -021 were assessed for their ability to reduce cAMP levels following forskolin stimulation via the $G_{\alpha i}$ pathway and their ability to recruit β-arrestin (Figure 3.7). They were also tested for the ability to induce receptor internalisation (Figure 3.8). All four compounds were biased towards the G protein pathway (Summary Table 3.4).

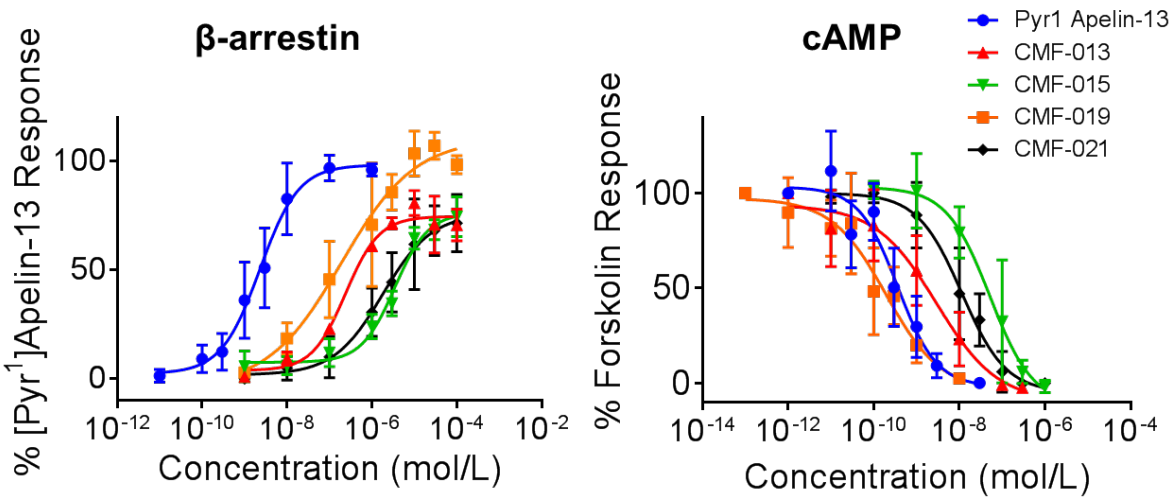

Figure 3.7: Pathway selectivity of ▲ CMF-013, ▼ -015, ■ -019 and ♦ -021 in CHO cell-based assays measuring β-arrestin recruitment and cAMP inhibition compared to the endogenous agonist ● [Pyr^1]Apelin-13.

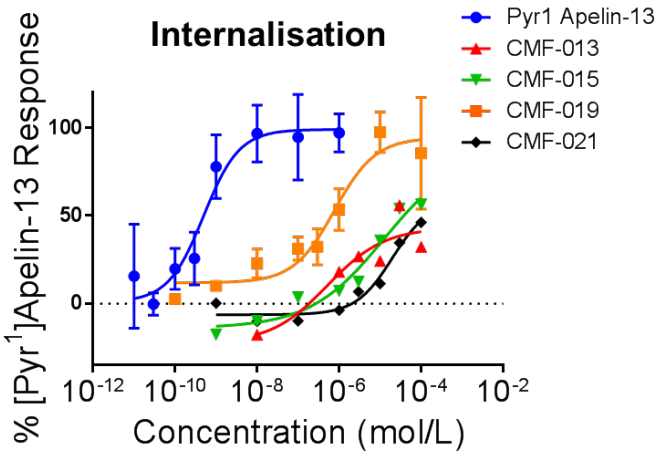

Figure 3.8: ▲ CMF-013, ▼ -015, ■ -019 and ♦ -021 in a U20S cell-based internalisation assay compared to the endogenous agonist ● [Pyr^1]Apelin-13. No SEM values are shown for ▲ CMF-013, ▼ -015 or ♦ -021 as only one biological replicate was performed.

3.3.2.2 CMF-087, MM239 and MM240 Displayed Reduced G Protein Signalling Bias Compared to the Parent Molecule, CMF-019

CMF-087, MM239 and MM240 were assessed for their ability to reduce cAMP levels following forskolin stimulation via the $G_{\alpha i}$ pathway and their ability to recruit β-arrestin (Figure 3.9). The compounds also displayed G protein bias but this was markedly reduced compared to the parent molecule, CMF-019 (Summary Table 3.4).

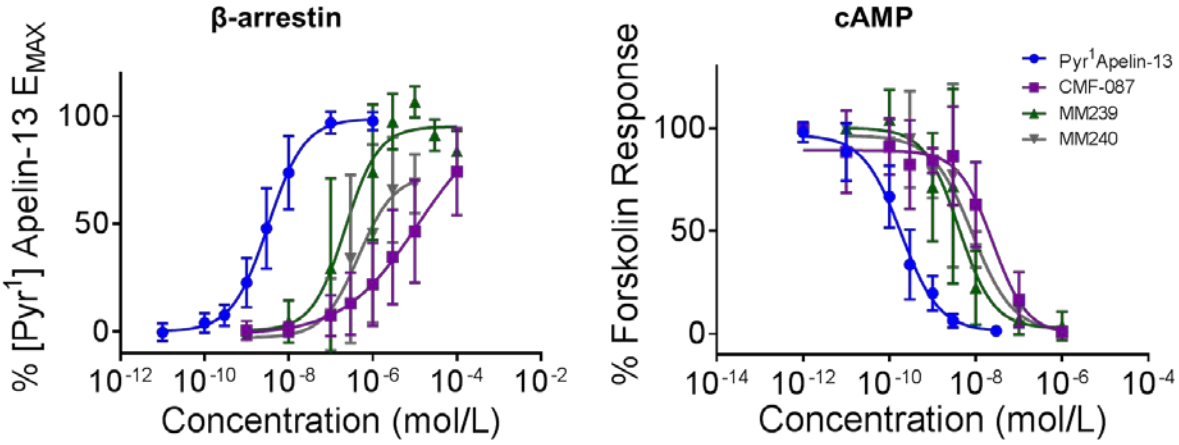

Figure 3.9: ■ CMF-087, ▲ MM239 and ▼ MM240 in CHO cell-based assays measuring β-arrestin recruitment and cAMP inhibition compared to the endogenous agonist ● [Pyr^1]Apelin-13.

3.3.2.3 Bias Calculations

For the most promising compound, CMF-019, bias calculations were performed for cAMP, β-arrestin and internalisation pathways. The data for CMF-019 from Figures 3.7 and 3.8 above are displayed in Figure 3.10 below for clarity and ease of comparison to the corresponding [Pyr^1]apelin-13 controls. CMF-019 induced β-arrestin recruitment to the apelin receptor (6.65±0.29) and subsequent receptor internalisation **(**6.23±0.25) but was less potent than [Pyr^1]apelin-13 (8.50±0.10; 9.30±0.13, respectively). In contrast, CMF-019 potently inhibited $G_{\alpha i}$-mediated cAMP production (9.95±0.17), comparable to [Pyr^1]apelin-13 (9.75±0.11).

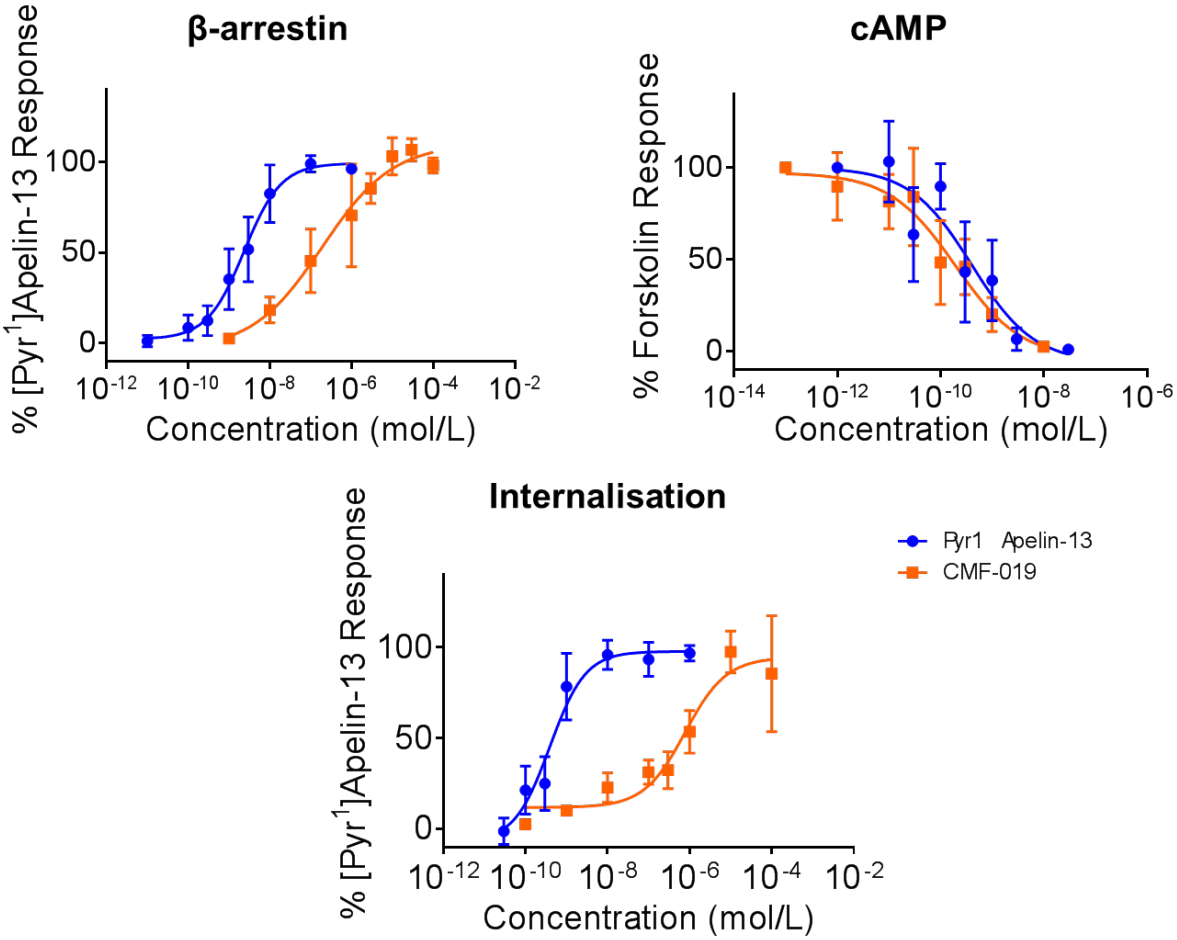

Figure 3.10: Pathway selectivity of CMF-019 determined from cell-signalling assays. Bias was calculated as described previously by van der Westhuizen *et al*., 2014; relative effectiveness and bias factors are shown in Tables 3.1 and 3.2, respectively.

In order to quantify the degree to which CMF-019 displayed bias towards the G protein signalling pathway compared to the reference agonist [Pyr^1]apelin-13, relative effectiveness and bias factors were calculated as described previously by van der Westhuizen *et al.* (2014) and are shown in Tables 3.1 and 3.2, respectively. Similar bias calculations were performed between β-arrestin and cAMP signalling assays for CMF-013, -015, -021, -087, MM239 and MM240. None of these compounds were as biased as CMF-019 with some displaying limited to no bias at all. The bias factors calculated were 82, 21, 104, 23, 4 and 11, respectively, and are shown in Summary Table 3.4.

	ΔLogR	Relative Effectiveness
β-arrestin	-1.91±0.35	0.012
Internalisation	-3.04±0.22	$9.13x10^{-4}$
cAMP	0.51±0.24	3.24

Table 3.1: Values of ΔLogR and Relative effectiveness for CMF-019 compared to [Pyr[1]]apelin-13 in β-arrestin, internalisation and cAMP assays. ΔLogR is $Log_{10}(\tau/K_A)$ where τ is a measure of agonist efficacy and K_A a measure of functional affinity as described by van der Westhuizen *et al.* (2014).

ΔΔLogR **Bias Factor**	β-arrestin	Internalisation
β-arrestin	n/a	1.13±0.41 **13**
cAMP	2.42±0.42 **264**	3.55±0.32 **3553**

Table 3.2: ΔΔLogR and **bias factors** for CMF-019 compared [Pyr[1]]apelin-13 in β-arrestin, internalisation and cAMP assays. ΔΔLogR is the difference between ΔLogR values in the different pathways and the **bias factor** is 10^ΔΔLogR as described by van der Westhuizen *et al.* (2014).

3.3.3 Summary Tables

3.3.3.1 Binding Affinities

The binding affinities of [Pyr^{1}]apelin-13, CMF-013, -015, -019, -021, -087, MM239 and MM240 in CHO-K1 cells expressing the human apelin receptor (experiments performed by Cerep; Celle L'Evescault, France) and human LV, whole rat and whole mouse heart homogenates are shown in Table 3.3 below as K_i and pK_i±SEM values. Not all compounds have been performed in each assay and only the most promising compounds were tested in rodent heart homogenates to inform potential *in vivo* study. A dash indicates where no data have been collected for this condition.

3.3.3.2 Bias Factors

The EC_{50}, pD_2±SEM and n-values in cAMP inhibition and β-arrestin recruitment assays, as well as the ΔΔlogR±SEM and bias factors for CMF-013, -015, -019, -021, -087, MM239 and MM240 compared to [Pyr^{1}]apelin-13 are summarised in Table 3.4.

	Cerep	Human Left Ventricle		Rat Heart		Mouse Heart	
	K_i	K_i	pK_i	K_i	pK_i	K_i	pK_i
[Pyr[1]]Apelin-13	-	**1.52nM**	8.82±0.05	0.31nM	9.50±0.06	1.87nM	8.73±0.06
CMF-013	-	**13.0nM**	7.89±0.06	-	-	-	-
CMF-015	-	**25.5nM**	7.59±0.07	-	-	-	-
CMF-019	32.4nM	**2.64nM**	8.58±0.04	3.26nM	8.49±0.04	1.96nM	8.71±0.06
CMF-021	-	**21.6nM**	7.67±0.05	-	-	-	-
CMF-087	47.9µM	**52.0nM**	7.28±0.05	-	-	-	-
MM239	24.0µM	**2.14nM**	8.67±0.05	12.0nM	7.92±0.05	-	-
MM240	38.9µM	**23.1nM**	7.64±0.07	76.3nM	7.12±0.04	-	-

Table 3.3: K_i and pK_i values for all apelin agonists compared to [Pyr[1]]apelin-13 in radioligand competition binding assays performed either in cells expressing the human apelin receptor (Cerep) or in homogenates of heart tissue from humans, rats or mice. Only the most promising compounds were tested in rodent heart homogenates to inform potential *in vivo* study.

	cAMP		β-arrestin		cAMP vs β-arrestin	
	EC_{50}	pD_2	EC_{50}	pD_2	ΔΔlogR	**Bias Factor**
[Pyr[1]]Apelin-13 (●)	0.18nM	9.75±0.11 (n=12/36)	3.13nM	8.50±0.10 (n=9/33)	n/a	n/a
CMF-013 (▲)	1.10nM	8.96±0.09 (n=4/11)	0.29μM	6.51±0.11 (n=3/8)	1.92±0.33	**82**
CMF-015 (▼)	48.3nM	7.32±0.13 (n=3/9)	3.18μM	5.50±0.13 (n=3/8)	1.32±0.30	**21**
CMF-019 (■)	0.11nM	9.95±0.17 (n=5/14)	0.22μM	6.65±0.29 (n=4/13)	2.42±0.42	**264**
CMF-021 (♦)	2.18nM	8.66±0.75 (n=4/9)	1.79μM	5.75±0.19 (n=4/11)	2.02±0.41	**104**
CMF-087 (■)	13.6nM	7.87±0.25 (n=3/9)	12.0μM	4.92±0.57 (n=4/12)	1.37±0.53	**23**
MM239 (▲)	3.02nM	8.52±0.27 (n=4/12)	0.29μM	6.53±0.37 (n=4/12)	0.55±0.46	**4**
MM240 (▼)	12.2nM	7.91±0.23 (n=4/10)	0.61μM	6.22±0.27 (n=4/11)	1.03±0.40	**11**

Table 3.4: EC_{50}, pD_2, ΔΔLogR and bias factors for all apelin agonists compared to [Pyr[1]]apelin-13 in β-arrestin and cAMP assays. ΔΔLogR is the difference between ΔLogR values in the different pathways and the bias factor is 10^ΔΔLogR as described by van der Westhuizen *et al.* (2014).

3.4 Discussion

3.4.1 CMF-019 is a G protein Biased Small Molecule with High Nanomolar Affinity to the Apelin Receptor

Two screening methods were employed to pharmacologically characterise the small molecule apelin receptor agonists described. First, the compounds were tested for binding to the native apelin receptor in homogenates of human LV tissue using a competitive radioligand binding assay. Crucially, this assay utilised clinically relevant human tissue. Second, the compounds were tested for their cell signalling capabilities in human apelin receptor expressing cells. These assays focussed on β-arrestin recruitment to the receptor and cAMP inhibition through the $G_{\alpha i}$ pathway. By comparing the differences in signalling through these pathways to the endogenous agonist, [Pyr^{1}]apelin-13, it was possible to establish the degree to which the compound displayed signalling bias. We have previously hypothesised that a G protein biased molecule would be beneficial by preventing receptor downregulation and thus, would be a desirable trait for a small molecule apelin agonist, as discussed in Section 1.9.

Starting with CMF-013, -015, -019 and -021 identified from a patent and based upon the benzimidazole scaffold (Hachtel *et al*., 2014), it was found that they all bound to the native apelin receptor in human LV homogenates with high nanomolar affinity. CMF-019 bound with the highest affinity of 2.64nM which was very similar to the endogenous peptide, [Pyr^{1}]apelin-13, at 1.52nM. The higher affinity of CMF-019 translated into functional efficacy, with it demonstrating the highest potencies in cAMP inhibition, β-arrestin recruitment and receptor internalisation. When assessed for bias between the $G_{\alpha i}$ and β-arrestin pathways, it was found that the much higher efficacy through the $G_{\alpha i}$ pathway translated into a greater bias factor of 264 for CMF-019 than observed for -013 (82), -015 (21) or -021 (104). CMF-019 also demonstrated a bias factor of 3553 between the $G_{\alpha i}$ and receptor internalisation assays, however, this result must be interpreted cautiously. The internalisation assay was performed in U20S cells rather than CHO cells and there could be system bias that might confound the data. It was decided to not continue further study in this system and fewer than 3 biological replicates were obtained for CMF-013, -015 and -021. The data for this assay have been presented separately, do not include SEMs and bias calculations have not been performed. Nevertheless, the rank order of potency between the β-arrestin assay and internalisation assay are consistent, supporting the data obtained.

Since CMF-019 demonstrated the highest binding affinity and greatest degree of bias at the apelin receptor, it was chosen as the most suitable compound to take forward from the four compounds involved in this initial screen. To assess its suitability for future *in vivo* experiments, the binding affinity at both mouse and rat apelin receptors was performed by the same methodology as for the human receptor. These experiments were very important for assessing the usefulness of the apelin system for the development of future therapeutics. Although the primary binding screen in the study used clinically relevant human tissue to establish the compound's usefulness in man, without similar binding affinity at rodent receptors, compound development can be significantly hampered. An example of such a case is with Palosuran, a non-peptide urotensin-II antagonist, which demonstrated more than a thousand-fold lower affinity at rat urotensin-II receptors compared to human (IUPHAR Guide to Pharmacology, Ligand ID: 3516; Lawson *et al*., 2009; Kim *et al*., 2010), complicating the interpretation of subsequent *in vivo* experiments. Importantly, CMF-019 bound with nanomolar affinities to all three mammalian apelin receptors, similarly to [Pyr^{1}]apelin-13, supporting its future use in animal studies.

Modification of the benzimidazole scaffold to introduce a nitrogen atom into the ring was performed to try to develop suitable CMF-019 derivatives with improved characteristics. The resulting compound, CMF-087, was found to have markedly reduced (100-fold) binding to the apelin receptor compared to the parent compound in I^{125} binding assays performed in CHO-K1 cells expressing the human apelin receptor (Cerep; Celle L'Evescault, France). In human LV homogenates, although the binding to the native receptor was reduced, it was not as severe as predicted with only a 20-fold loss of affinity. Side chain modification of CMF-087 to produce molecules MM239 and MM240 was able to rescue some of this binding affinity and was most pronounced for MM239, which demonstrated similar affinity to CMF-019 at the native human receptor. For potential future *in vivo* study, the binding in rat heart homogenates was also assessed and interestingly both compounds displayed slightly reduced binding affinities compared to at the human receptor; nonetheless, they bound strongly with nanomolar affinities.

Assessing the functional activities of the molecules, revealed that the scaffold modification in CMF-087 reduced efficacy in both the β-arrestin and cAMP assays and largely abolished bias towards the $G_{\alpha i}$ pathway. This may in part be a reflection of the

20-fold decrease in binding affinity but this is unlikely to be the only cause, since the relative decreases in efficacy were greater than 20-fold in both assays. This suggests that the way the molecule engages the receptor helices within the binding pocket has likely been perturbed. Notably, a greater loss of efficacy was observed for the cAMP assay than the β-arrestin assay, leading to the loss of bias. Both MM239 and MM240 displayed improved binding and improved efficacy in β-arrestin signalling compared to CMF-087 but showed very little improvement in cAMP inhibition, resulting in an almost complete abolition of biased signalling for these molecules. Overall, this suggests that the new scaffold structure based on CMF-087 has less inherent bias than the original benzimidazole scaffold, and while side-chain extension can improve binding, it also leads to a reduction in bias. This is not unexpected as longer peptides have previously been thought to reach deeper within the binding pocket of the receptor to better engage β-arrestin signalling motifs, as previously discussed in Section 1.3. It is possible that the side-chain extensions are capable of performing a similar role with these compounds.

Following exploration of this series of compounds, an attempt was made to amalgamate the structure of CMF-087 with the structures of two other recently identified small molecule apelin agonists from the Sanford-Burnham triazole series (Pinkerton and Smith, 2015) and the RTI International pyrazole series (Narayanan *et al*., 2016). It was hoped that the resulting compound, designated CMF-167, would combine three series of diverse agonists, providing a molecule with strong activity at the apelin receptor. However, the molecule displayed no binding in the I^{125} Cerep screening assay or activity in a β-arrestin assay, suggesting that the molecule lacked any engagement with the receptor.

After screening the compounds based on CMF-019, none of them demonstrated an improvement on the parent molecule. Although MM239 and MM240 rescued binding affinity compared to CMF-087, they showed a loss of bias and it was decided that CMF-019 as a biased molecule with high affinity should be taken forwards as the lead compound.

3.4.2 CMF-019 is a Full Agonist at the Apelin Receptor

Potencies between compounds have been compared and bias factors calculated. This did not take into account E_{MAX} values and whether they function as full or partial agonists. Looking at the β-arrestin and internalisation assays for CMF-013, -015 and -021 it can be seen that the E_{Max} values do not reach 100% of the [Pyr^1]apelin-13 maximal response. However, it is difficult to assess whether this is a demonstration of genuine partial agonism in these compounds because concentrations higher than 0.1mmol/L could not be achieved without increasing the DMSO concentration (in which the compounds were dissolved) above 1% in the assay. It is not recommended that the DMSO concentration exceeds this level as it causes depression in responses close to or above this threshold. Indeed, the lower E_{MAX} values with these compounds may be a result of the signal beginning to drop at the maximal 1% DMSO concentration used. A similar effect was also seen in the β-arrestin assay with CMF-087 and was particularly pronounced with MM240. The highest concentration of 0.1mmol/L for MM240 was excluded from the data (Figure 3.9) as a substantial drop in signal was observed at this concentration, perhaps suggesting some cell toxicity at high concentrations with this compound. Therefore, without higher concentrations of CMF-013, -015, -021, -087 and MM240 being attainable in these assays, it is difficult to establish full or partial agonism. Nevertheless, one can be confident that both CMF-019 and MM239 displayed full agonism as they achieved stimulation of the apelin receptor to a level that was the same as the endogenous agonist, [Pyr^1]apelin-13.

3.4.3 Regression Analyses

A series of regression analyses were performed (Figure 3.11) to try to further understand the relationship between functional signalling, bias and binding affinity for the small molecules tested in this chapter.

Binding in human LV correlated to some extent with both β-arrestin signalling ($y=1.5x-6.0$; $r^2=0.71$) and $G_{\alpha i}$ signalling ($y=1.2x-1.1$; $r^2=0.60$). This is as expected and demonstrates some correlation between efficacy and affinity through both pathways. The basal level of signalling through the $G_{\alpha i}$ pathway seemed greater than for β-arrestin for these small molecules. This is an interesting observation as it has been suggested that longer apelin peptides, such as, apelin-17, have greater binding affinity and also greater β-arrestin bias than the shorter forms, such as, apelin-13 (El Messari *et al*.,

2004, Ceraudo *et al*., 2014, Iturrioz *et al*., 2010b). The hypothesis is that these longer peptides can reach deeper into the apelin binding pocket and stabilise the β-arrestin signalling confirmation better than shorter molecules. Perhaps the higher intrinsic basal signalling through the $G_{\alpha i}$ pathway compared to the β-arrestin for these small molecules is indicative of the fact that they are less able to reach these deeper regions of the receptor binding pocket.

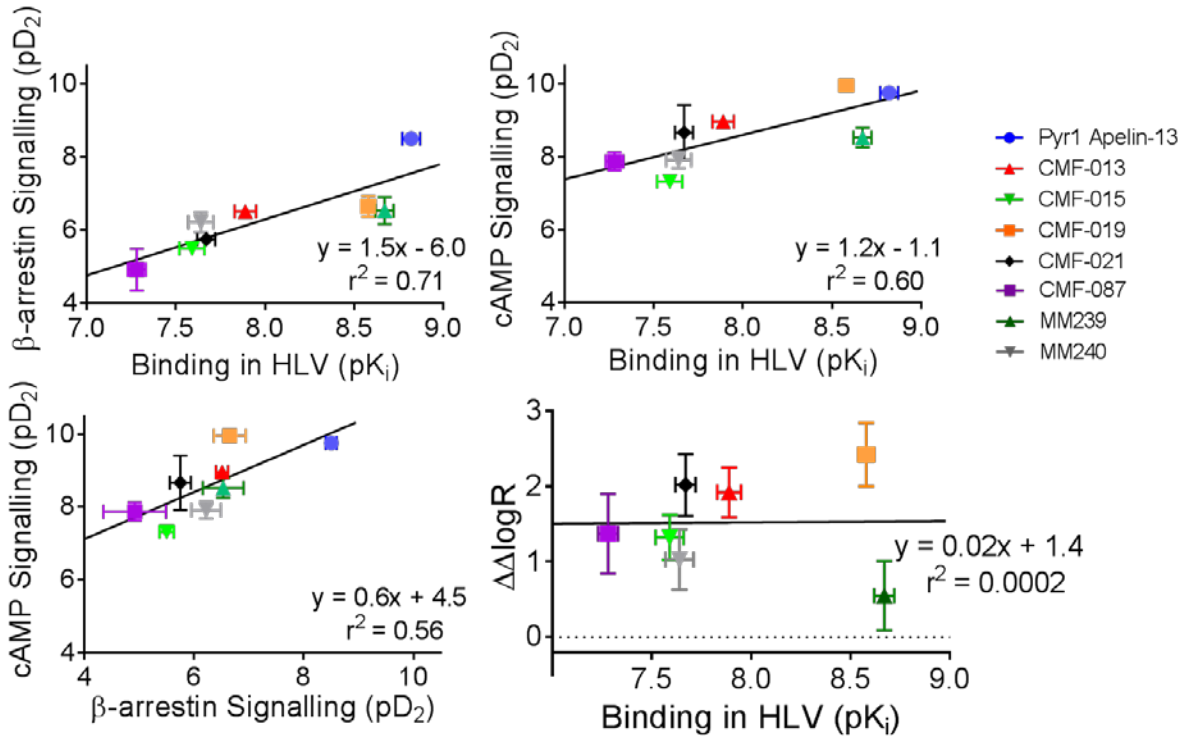

Figure 3.11: A series of regression analyses between functional signalling assays, ΔΔLogR values and binding affinities to the native human apelin receptor in human LV homogenates. The line of best fit is shown and the goodness of fit given as the r^2 value. All correlations significantly differed from zero except for the correlation between ΔΔlogR and human LV binding. The key indicates the location of each compound, [Pyr[1]]apelin-13 is not included in the ΔΔlogR vs human LV binding correlation as by definition it possess a ΔΔlogR of 0.

Although β-arrestin and $G_{\alpha i}$ signalling correlate to some extent with binding affinity, the fact that the correlation is not perfect is unsurprising and indicates how the efficacy in either β-arrestin or $G_{\alpha i}$ signalling will depend greatly upon the contacts made by the compound's functional groups with the receptor helices within the binding pocket once bound. This is reinforced by the fairly poor correlation between the two signalling pathways themselves ($y=0.6x+4.5$; $r^2=0.56$) and is clearly illustrated by the fact that ΔΔLogR values (measuring bias) did not correlate with binding affinity at all

(y=0.02x+1.4; r^2=0.0002). Interestingly, this last result suggests that, while longer peptides may show higher binding affinities, which correlates with greater β-arrestin signalling, such a hypothesis does not seem to hold for these small molecules where any extensions of the molecule will be much shorter. Ultimately, the bias for these small molecules depends on where and not how well the molecule binds to the receptor, something that can only be assessed by measuring the individual signalling pathways involved.

3.4.4 CMF-019 is the First Evaluated Biased Small Molecule Agonist at the Apelin Receptor

The work presented in this chapter has focussed on the investigation of small molecule apelin agonists with the aim of identifying molecules with high binding affinities to the native human apelin receptor and with a desirable biased pharmacological profile. To our knowledge, CMF-019 is the first report of a biased small molecule apelin agonist.

Previous synthetic apelin agonists have lacked the desirable characteristics required of drug-like molecules. E339-3D6, a reported peptidomimetic agonist exhibited vasoactivity in rat aorta preconstricted with noradrenaline and *in vivo* prevented vasopressin release when injected intracerebroventricularly in water-deprived mice (Iturrioz *et al*., 2010a); however, the high molecular weight (1400Da) suggests it would be an unsuitable drug molecule, particularly for oral dosing. Moreover, it was later shown to be a mixture of polymethylated species from which a number of analogues were subsequently purified (Margathe *et al*., 2014). These molecules, displayed low micromolar binding affinities for the apelin receptor compared to CMF-019 which binds in the nanomolar range. ML233, a small molecule of molecular weight of 359Da, was limited by low solubility in saline at room temperature (Khan *et al*., 2010). Moreover, the structure suggests that it would likely have toxicity, including being a Michael acceptor and having an activated quinone (Lagorce *et al*., 2015). This is supported by unpublished observations from our laboratory which have suggested the compound displays significant *in vivo* toxicity when given to male Sprague-Dawley rats (*Pers. Comm.* Yang, Maguire and Davenport). Finally, the RTI International series (Narayanan *et al*., 2016) (which was reported at a similar time to the publication of CMF-019 (Read *et al*., 2016)), although containing the most suitable small molecules (~500Da) identified up to that point, showed much weaker activity than CMF-019 with potencies in the micromolar range. Therefore, CMF-019 represents a first-in-class small molecule apelin agonist and has the potential to greatly progress the apelin field

as an experimental tool compound and in the development of small molecule therapeutic agonists.

3.4.5 CMF-019 Displays Bias in a Therapeutically Relevant Range

One important consideration when assessing compound bias is how much bias is necessary to achieve a therapeutically desirable effect? Indeed it is becoming increasingly clear that different studies are seeing dramatically different observations of bias. Whereas some observe only a few fold changes in activity over the endogenous molecule, some see a complete abolition of signalling through a given pathway. Since there are currently no designed biased ligands in therapeutic use and only a few in clinical trials, it is not easy to answer which of these situations is desirable. Logically, one would think that a complete abolition of signalling could be a dangerous prospect. This would particularly be the case for compounds biased to limit β-arrestin mediated internalisation, such as CMF-019, since without any ability to internalise the receptor, one could see a situation where overstimulation of the receptor could potentially lead to toxicity and on-target side effects. Considering the Trevena compound oliceridine (TRV130), which has been granted breakthrough status by the FDA and will be reviewed for approval later this year (www.trevena.com), the bias of the compound is only 3-fold over the endogenous agonist morphine (DeWire *et al*., 2013). Therefore, even a bias factor of 3-fold seems enough to have a clinically useful outcome. CMF-019 displayed a bias factor of 264 between cAMP and β-arrestin signalling which should, therefore, be sufficient to observe a measurable and real therapeutic effect over the endogenous molecule.

A potential limitation of any assay designed to measure bias is whether assay-specific factors could have an impact on the interpretation of bias. Although in these experiments some validation of receptor expression levels and kinetics have been performed previously (Section 2.4), there were additional factors that could have impacted the bias measured. The kinetics of the assay have been considered for both [Pyr^{1}]apelin-13 and MM07 and equilibrium was found to be reached. Nevertheless, it is possible that if CMF-019 possessed remarkably different kinetics to these other apelin agonists, then this could have had an impact on the bias measured. Additionally, differences in some of the reagents between assays could have potentially impacted the interpretation of bias. Most notably, the phosphodiesterase inhibitor, IBMX, was present in the cAMP lysis buffer in the cAMP assay but there was no equivalent in the

β-arrestin assay. In future experiments, if the proprietary information could be obtained, an equivalent concentration of IBMX could be added to the β-arrestin assay as an additional control.

A more notable limitation of this study is whether the G protein bias observed from the $G_{\alpha i}$ signalling pathway is able to predict similar $G_{\alpha q}$ bias that would be in a therapeutically useful range. It is arguable that an assay measuring $G_{\alpha q}$ signalling would be more useful as a predictive tool for therapeutic use of apelin agonists given its importance in promoting cardiac inotropy in the heart, as well as vasodilatation in the vasculature, as discussed in Section 1.2. Previous studies in the laboratory were unable to identify a suitable $G_{\alpha q}$ signalling assay using the DiscovRx platform, something that was considered desirable to reduce system bias, as previously discussed. The development of a novel and suitable assay for measuring $G_{\alpha q}$ signalling in the apelin system was beyond the scope of this project due to limitations of time. Hopefully, future studies will be able to identify robust Ca^{2+} signalling assays to measure $G_{\alpha q}$ signalling for use in further screening of biased apelin agonists.

3.4.6 CMF-019 Binds in a Critical Region of the Apelin Receptor

The experiments in this chapter identified CMF-019 as the lead candidate for further study based upon its binding affinity and biased signalling profile. Although from competitive radioligand binding experiments it was known that the molecule bound into an orthosteric site on the receptor, the contacts made with the receptor were unknown. Therefore, to determine the nature of CMF-019 binding into the receptor, molecular dynamics simulation studies were performed by our collaborators, Christopher Fitzpatrick and Dr Richard Foster in the University of Leeds and Professor Robert Glen in the University of Cambridge (Read *et al*., 2016). They utilised a homology model constructed from the 2.5Å resolution crystal structure of the human CXCR4 chemokine receptor (Brame *et al*., 2015) and docking was performed in the absence of water and ions using the programme GOLD (CCDC 2015; Jones *et al*., 1995, Jones *et al*., 1997). It was found that CMF-019 bound into a mainly hydrophobic cavity on the apelin receptor near the SHK region of bound apelin-13. The carboxylic acid of CMF-019 was predicted to form a strong hydrogen bond (2.3Å) with the side-chain of Arg^{168}. The thiophene, which is important for maintenance of good potency, formed a π-stacking interaction with residue Tyr^{88}. A ligand/protein plot of these close interactions between CMF-019 and the apelin receptor was generated (Figure 3.12A), as well as a close up

view of the ligand receptor interactions (Figure 3.12B). CMF-019 and the predicted apelin-13 docked structure are overlaid in Figure 3.12C to compare the similarity in the expected binding regions.

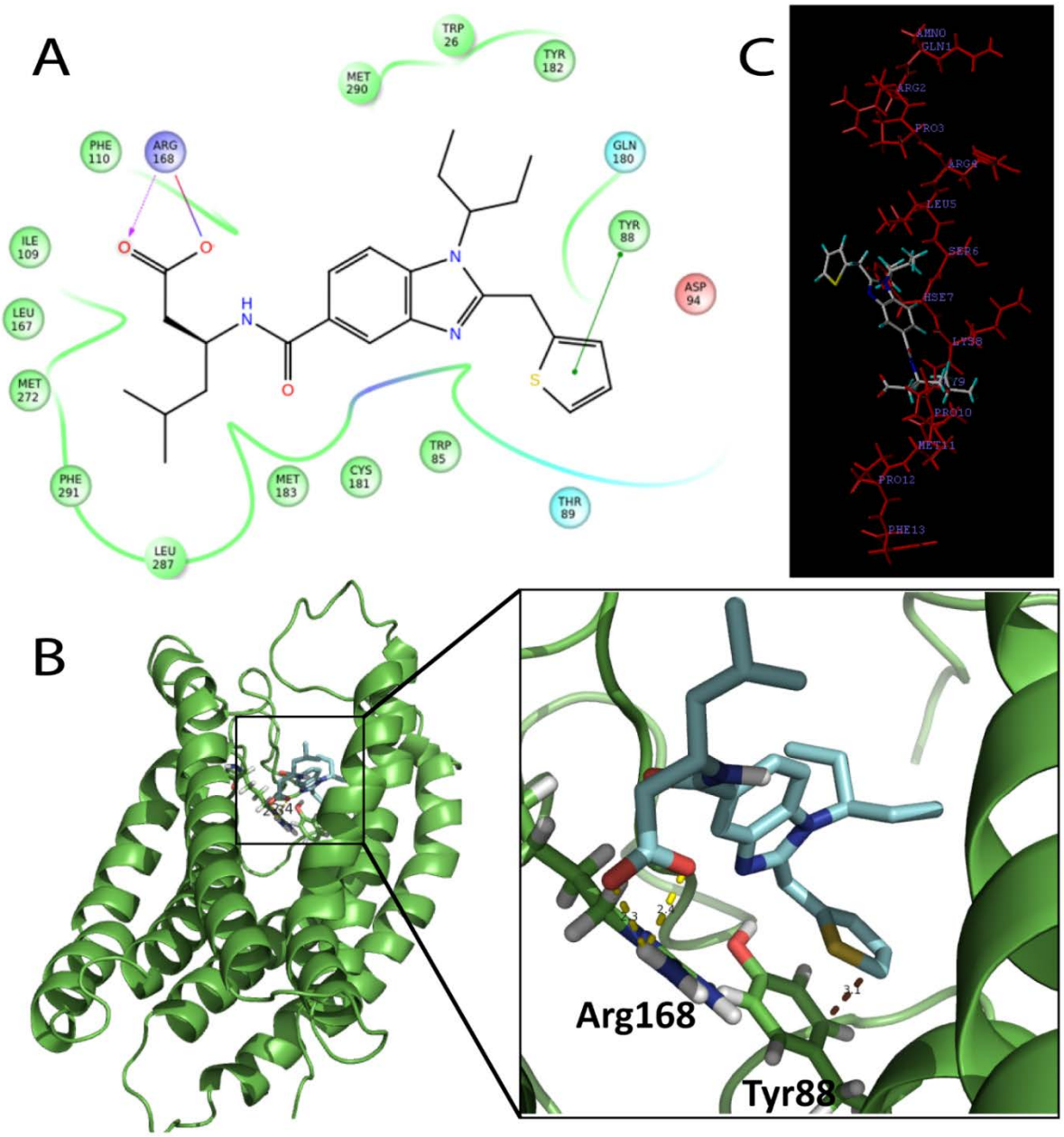

Figure 3.12: Computational docking of CMF-019 into a homology model of the apelin receptor.
(A) A 2D interaction map showing the binding site and interactions between CMF-019 and the apelin receptor. The key interactions are π-stacking (thiophene to Tyr88, green line) and ionic (carboxylate to Arg168, purple lines) bonds.
(B) CMF-019 (pale blue sticks) docked via GOLD into the apelin receptor (green). The key binding interactions between the ligand and apelin receptor (at Arg168 and Tyr88) are highlighted (dotted yellow lines) with intermolecular distances shown.
(C) The favoured overlay of apelin 13 (red lines) with CMF-019 (grey lines) places CMF-019 at the SHK region, suggesting that the SHK sequence of apelin-13 is the most promising region for binding of CMF-019 to the APJ receptor. Figure taken from Read *et al.* 2016.

Interestingly, analysis of the predicted binding region of CMF-019 within this hydrophobic cavity near the SHK region of bound apelin-13 revealed close proximity to the only reported naturally occurring mutation in the apelin receptor to date. In the zebrafish, *Danio rerio*, a single allele of a recessive mutation, grinch^{s608}, leads to a Trp^{85} to Leu^{85} amino acid change in the second transmembrane domain and results in a complete loss of apelin binding. As a consequence of this loss of function, in the most severely affected mutants the heart fails to develop (Scott *et al*., 2007). In our model the almost adjacent Tyr^{88} residue is located within the SHK region of the bound apelin-13 molecule. Both of these residues have been conserved in humans and all species where apelin receptor sequences have been reported, suggesting CMF-019 binds in a critical region of the receptor. This is a highly desirable characteristic and means that CMF-019 is likely to be able to bind to apelin receptors in different experimental models and settings, making it very useful as an experimental tool compound. Moreover, the receptor is extremely unlikely to be mutated in the CMF-019 binding region in humans, giving it greater therapeutic potential.

3.4.7 Newly Identified Small Molecule Apelin Agonists Possess Structural Similarities to CMF-019

In support of our findings, several series of small molecule apelin agonists that share some structural similarity to CMF-019 have recently been reported by Amgen (Chen *et al*., 2017b), Bristol-Myers Squibb (Myers *et al*., 2017), RTI International (Narayanan *et al*., 2016) and Sanford-Burnham (Pinkerton and Smith, 2015). They all possess two hydrophobic substituents extending from a heterocyclic core, reminiscent of the Sanofi series of compounds from which CMF-019 is derived (Hachtel *et al*., 2014; Figure 3.13).

The compound CMF-167, described earlier, attempted to combine some of the characteristics of the Sanofi (CMF-019), Sanford-Burnham and RTI International series but was unsuccessful.

The structural similarities between these compounds suggests that they may bind within the same site in the apelin receptor and computational docking experiments performed by Dr David Huggins support this (Figure 3.14). The identification of five series of small molecule apelin agonists that bind in the same region of the receptor seems a remarkable case of convergent evolution in drug discovery. Furthermore, the fact that all of these compounds have been identified from patents likely indicates good selectivity of these structures for the apelin receptor as non-selective compounds are usually removed from such screens. It will be fascinating to see if the compounds display G protein bias similarly to CMF-019. To our knowledge, these experiments have not yet been performed. Hopefully, following our observations with CMF-019, this will become an area of interest.

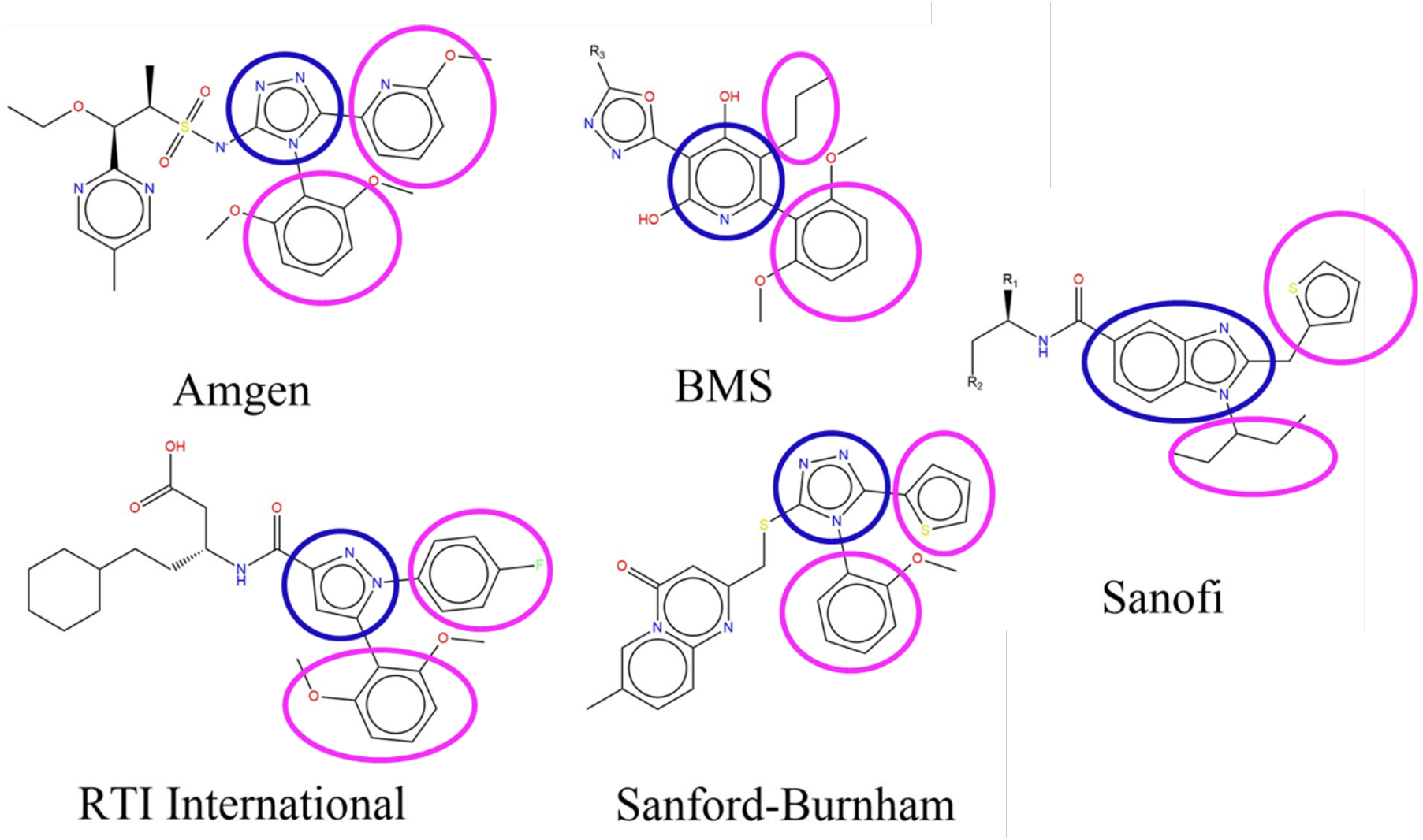

Figure 3.13: The scaffold structures of five reported series of small molecule apelin agonists from Amgen, Bristol-Myers Squibb, RTI International, Sanford-Burnham and Sanofi. CMF-019 is derived from the Sanofi series. All of these molecules possess a broadly similar structure, consisting of two hydrophobic groups (circled in pink) extending from a heterocyclic core group (in blue).

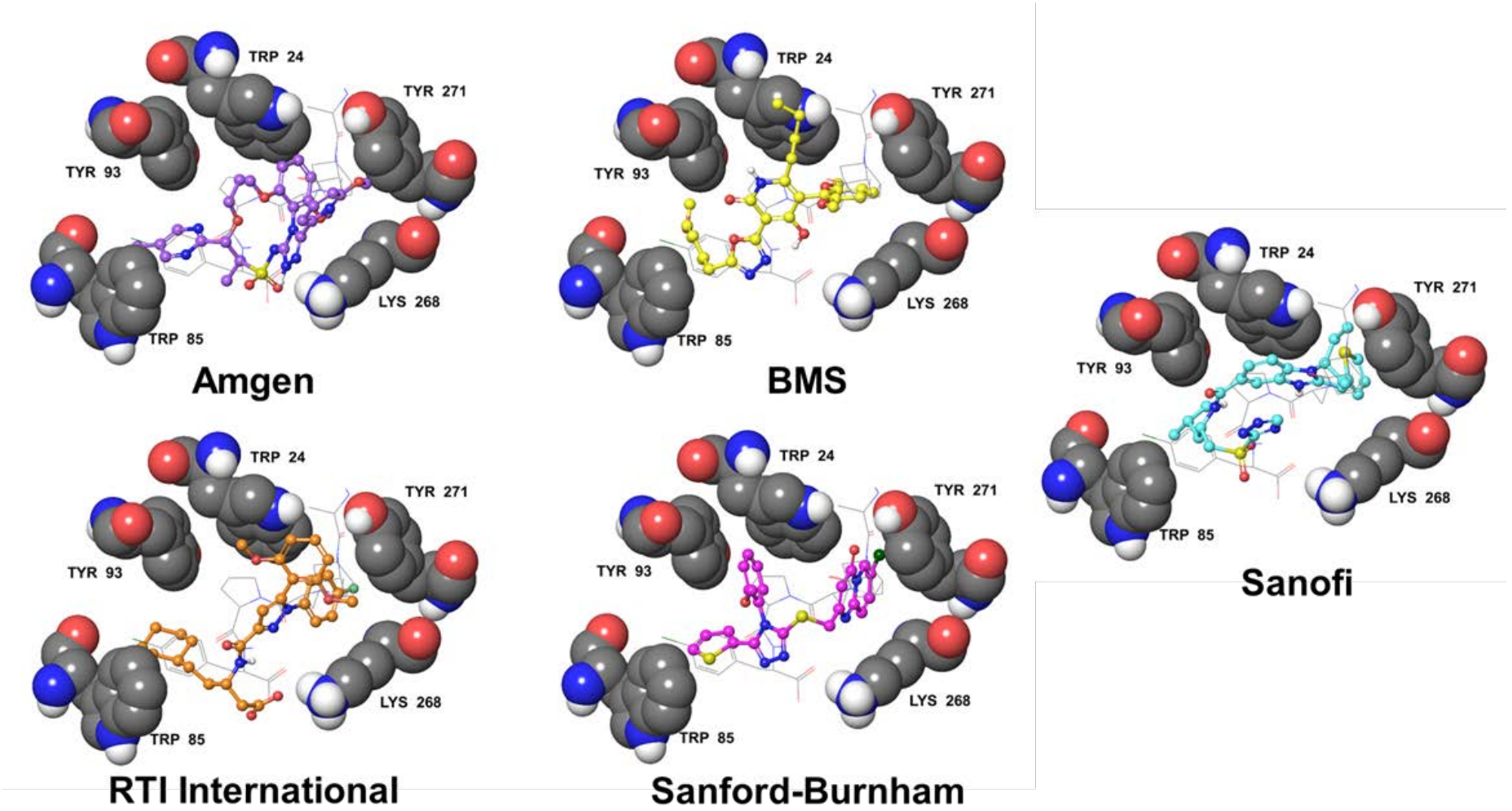

Figure 3.14: The apelin receptor structure from PDBID 5VBL (Ma *et al.* 2017) with docked poses of five series of apelin agonists. The apelin receptor residues, W^{24}, W^{85}, Y^{93}, K^{268}, and Y^{271} are labelled and displayed as grey space filling. The structure of the four C-terminal residues of the apelin analogue from PDBID 5VBL are displayed as grey sticks. The receptor and peptide are overlaid with docked poses of an Amgen (violet balls and sticks), a Bristol-Myers Squibb (yellow balls and sticks), an RTI International (orange balls and sticks), a Sanford-Burnham (magenta balls and sticks) and a Sanofi (cyan balls and sticks) small molecule apelin agonist. Only polar hydrogens are shown. Figures provided by Dr David Huggins, University of Cambridge.

3.5 Conclusions

The primary aim of this study was to identify a small molecule apelin agonist for use as an experimental tool compound. Biased agonism towards the G protein over the β-arrestin pathway was considered a desirable trait for a potential therapeutic as this could prevent receptor internalisation while maintaining beneficial signalling and such an approach has previously been demonstrated with a cyclised peptide, MM07.

This chapter has shown that CMF-019 is a small molecule that possesses very high nanomolar affinity for the apelin receptor. It is remarkable that such a small molecule is able to bind with such high affinity and that this is close to the affinity with which the endogenous molecule binds. This study has demonstrated that biased agonism can be maintained in a small molecule and further confirms that the apelin receptor is tractable to biased signalling.

A number of new apelin agonist series have recently been identified with structural similarity to CMF-019. It is thought that these molecules are likely to bind in the same binding pocket, a highly conserved region within the receptor. It will be very interesting to establish whether these molecules also possess bias, similarly to CMF-019, and future studies should be performed. Following their identification, it should not be long until these new apelin agonists are characterised; hopefully providing new avenues for therapeutic targeting of the receptor.

4. *In Vivo* Cardiovascular Assessment of [Pyr^{1}]apelin-13 and CMF-019 Responses in Normotensive Male Sprague-Dawley Rats

4.1 Introduction

Apelin has been shown to induce vasodilatation in rodents *in vivo* (Tatemoto *et al*., 2001), as well as cardiac inotropy *in vivo* in rats (Atluri *et al*., 2007, Berry *et al*., 2004, Jia *et al*., 2006) and mice (Ashley *et al*., 2005). Importantly, similar observations have been made in humans (Japp *et al*., 2008, Brame *et al*., 2015, Brash *et al*., 2018). To test the activity of apelin compounds in animals *in vivo*, an assay was developed based on the surgical techniques originally described by Pacher *et al.* (2008) with several additions and modifications. These methods are described in Section 2.7. An example of the read-out for a baseline PV loop is shown in Figure 4.1. Initially, the catheter was adjusted to obtain a stable and symmetrical PV loop from which accurate baseline parameters could be derived, for example, the contractility (Dp/Dt$_{MAX}$) as shown.

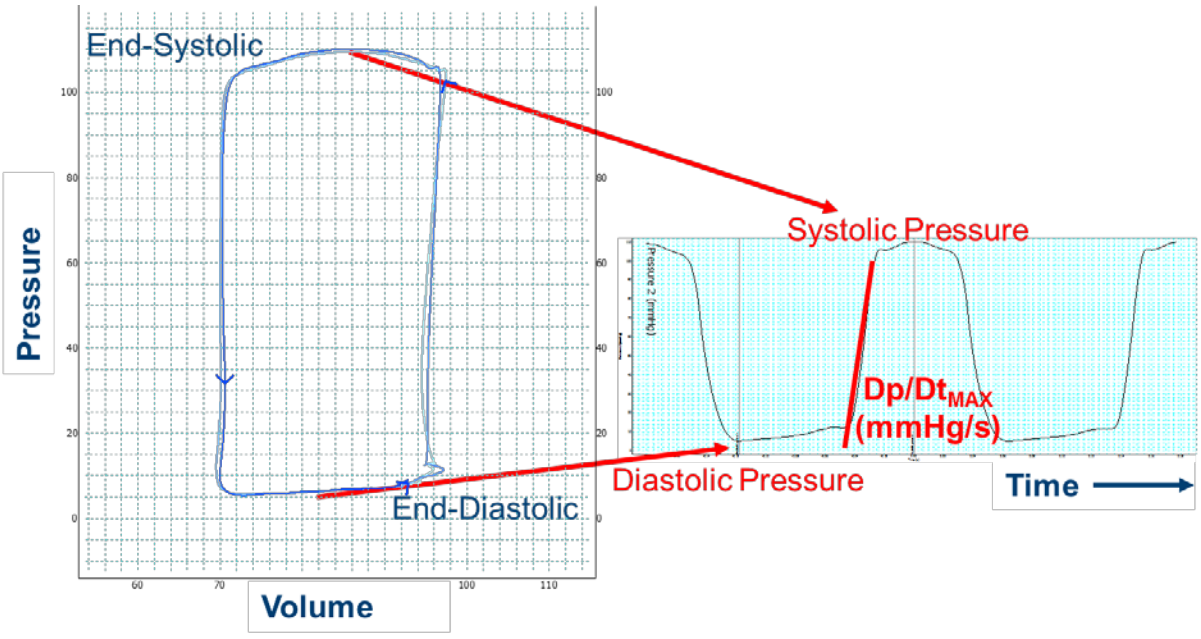

Figure 4.1: An example baseline PV loop. A number of cardiovascular parameters can be derived from this trace, including the cardiac contractility which is calculated as the maximal change in pressure against time. For this reason artefacts that lead to elevated end-systolic pressures can give overestimates of contractile function for positive inotropes (see Figure 4.12)

Using these techniques, the *in vivo* responses to [Pyr^{1}]apelin-13 have been robustly measured in normotensive male Sprague-Dawley rats over a number of different studies. A recent study has used an invasive method of catheterisation to measure responses to [Pyr^{1}]apelin-13 in patients with PAH (Brash *et al*., 2018) and as such our study provides a very useful means of establishing the relevance of responses in normotensive naïve rats to responses in humans with disease. In initial studies, the method of femoral catheterisation had not been developed and activity was primarily measured as an increase in cardiac contractility, cardiac output and stroke volume. In later studies, the femoral artery was also catheterised and arterial pressure decreases measured.

The lead compound, CMF-019, was studied in two separate *in vivo* experiments. The first study again did not utilise a femoral catheter and aimed to primarily assess *in vivo* activity through cardiac contractility, cardiac output and stroke volume. As arterial pressure could not be measured accurately in this experiment, it was not evident whether CMF-019 was capable of inducing vasodilatation. This is an important question to answer as previous studies have suggested that β-arrestin signalling and subsequent receptor internalisation are required for vasodilatation through the apelin receptor (El Messari *et al*., 2004, Ceraudo *et al*., 2014, Iturrioz *et al*., 2010b, Besserer-Offroy *et al*., 2018). This would suggest that G protein biased molecules, such as CMF-019, would be less able to induce vasodilatation and could limit their clinical efficacy. However, previous experiments in our laboratory have not supported this hypothesis and MM07, a cyclised G protein biased peptide, was capable of producing robust vasodilatation in humans *in vivo* (Brame *et al*., 2015). In order to answer this question, a second *in vivo* study was performed following development of the femoral catheterisation technique. Additionally, a fourth dose of [Pyr^{1}]apelin-13 at 50nmol was given to all of the animals in this study. This was to assess the relative desensitisation of the apelin receptor *in vivo* by either saline, [Pyr^{1}]apelin-13 or CMF-019 and establish if the *in vitro* bias observed in Chapter 3 for CMF-019 translated.

4.2 Methods

4.2.1 [Pyr[1]]apelin-13: Cross-study Cardiovascular Responses *In Vivo*

[Pyr[1]]apelin-13 (50nmol n=32, 400nmol n=10, 0.5mL, 0.9% saline, pH5) and saline (n=17 and 10, respectively, 0.9%, 0.1mL, pH9) responses were taken from six different studies (colour coded) conducted over a period of two and a half years and compared. N values for the arterial pressures were lower [Pyr[1]]apelin-13 (50nmol n=24, 400nmol n=2) and saline (n=7 and n=4, respectively) since this technique was developed later. In so far as it was possible, the [Pyr[1]]apelin-13 doses were compared to their corresponding saline control doses. All data were tested for normality using the D'Agostino-Pearson omnibus K^2 test. This was the recommended test and takes into account both skewness and kurtosis, as well as how much each individual value differs from that expected in a Gaussian distribution. However, the test requires n values of 8 or more and so the arterial pressure for saline controls (n=7, n=4) and the 400nmol dose of [Pyr[1]]apelin-13 (n=2) could not be computed as the n-values were too low. Data were compared using a two-tailed Student's t-test (GraphPad Prism 6). Statistical significance was taken as 5%.

4.2.2 *In Vivo* LV Catheterisation for Measurement of Acute Cardiovascular Changes Upon Administration of CMF-019: Study 1

Male Sprague-Dawley rats (273±6g, n=18) underwent jugular vein cannulation and LV catheterisation as described in Section 2.7. Owing to solubility issues in saline with the original CMF-019 compound (Figure 3.1C), the chemical structure was modified to include the incorporation of a potassium salt on the carboxylic acid group (Figure 4.2). Saline was adjusted to pH9 from pH5 to help dissolve the acid.

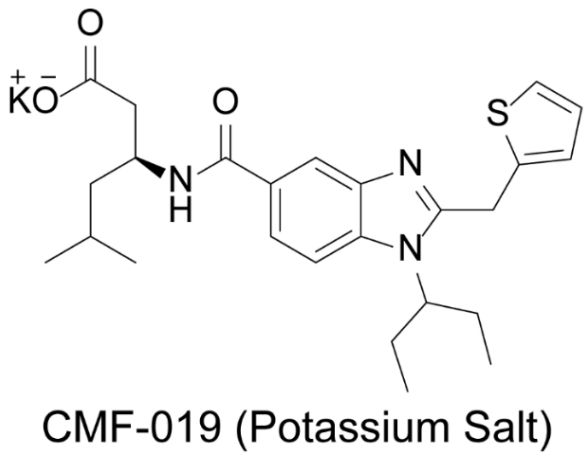

CMF-019 (Potassium Salt)

Figure 4.2: Chemical structure of the potassium salt of CMF-019. Figure taken from Read *et al*. (2016).

Three cumulative bolus doses of CMF-019 (50-5000nmol, 0.5mL, 0.9% saline, pH9), saline (0.9%, 0.1mL, pH9) or [Pyr^1]apelin-13 (50, 400nmol, 0.5mL, 0.9% saline, pH5) were then administered intravenously, followed by a saline flush (0.9%, 0.1mL, pH5) via the cannula at a minimum of ten minute intervals or when a stable baseline was reached before the next injection. Animals were randomly chosen to receive CMF-019, saline or [Pyr^1]apelin-13.

4.2.2.1 Analysis of Plasma Samples by Mass Spectrometry

Analysis of plasma samples was performed by Peakdale Molecular (Chapel-en-la-Frith, UK). End-point blood samples were taken from rats (n=6) following completion of three cumulative doses of CMF-019 in the first *in vivo* study, approximately 10 minutes after the last intravenous administration. The blood was collected in heparin-coated vials and spun at low speed (2000g, 5min), the plasma supernatant was removed and frozen. Quantitative analysis was performed using LC-MS/MS with metaprolol as an internal standard and CMF-019 to quantify CMF-019 in the samples.

4.2.3 *In Vivo* LV and Femoral Artery Catheterisation for Measurement of Acute Cardiovascular Changes Upon Administration of CMF-019: Study 2

The methodology for this study was very similar to the first study; however, in this case male Sprague-Dawley rats (271±3g, n=17) also underwent femoral artery catheterisation as described in Section 2.7. The [Pyr^1]apelin-13 doses were adjusted to 10, 50 and 150nmol (0.5mL, 0.9% saline, pH5) and all animals received a 50nmol dose of [Pyr^1]apelin-13 as a fourth dose after they had received their first three doses whether they be saline, CMF-019 or [Pyr^1]apelin-13 (Figure 4.3).

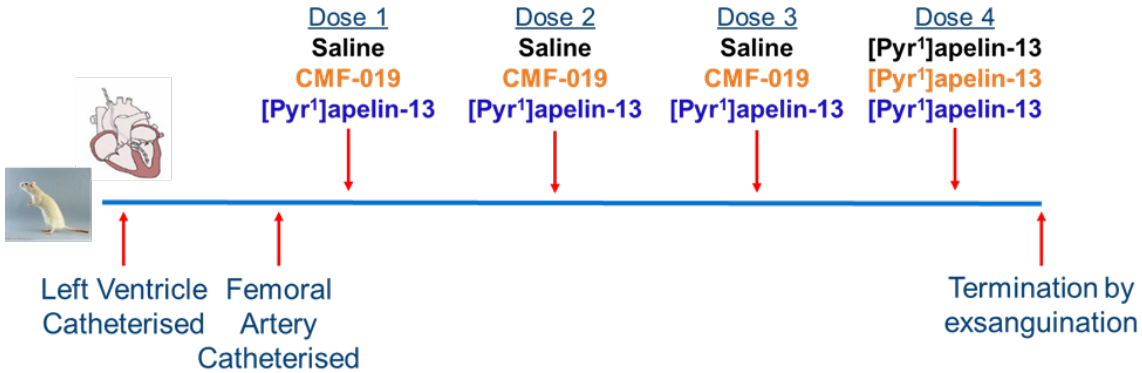

Figure 4.3: Dosing schedule for the second acute *in vivo* study of CMF-019. The LV and femoral artery were catheterised in normotensive male Sprague-Dawley rats. The animals were randomly chosen to receive either three doses of saline, CMF-019 or [Pyr^1]apelin-13, before a fourth dose of 50nmol [Pyr^1]apelin-13 was administered regardless of the previous doses administered. Doses were administered at ten minute intervals, or when a stable baseline was reached, after which the animal was terminated by exsanguination under high flow isoflurane.

4.3 Results

4.3.1 [Pyr[1]]apelin-13 Produced Robust Observable Responses *In Vivo* in Real-Time

Looking at an example trace following a dose of 50nmol [Pyr[1]]apelin-13 compared to saline (Figure 4.4) in the same animal, it is clear that [Pyr[1]]apelin-13 induced robust observable vasodilatation (LVSP and arterial pressure) and cardiac inotropy (dp/dt_{MAX}). Stroke volume and heart rate may also have slightly increased, leading to an increase in cardiac output; however, it is harder to observe clear responses in these parameters in real-time.

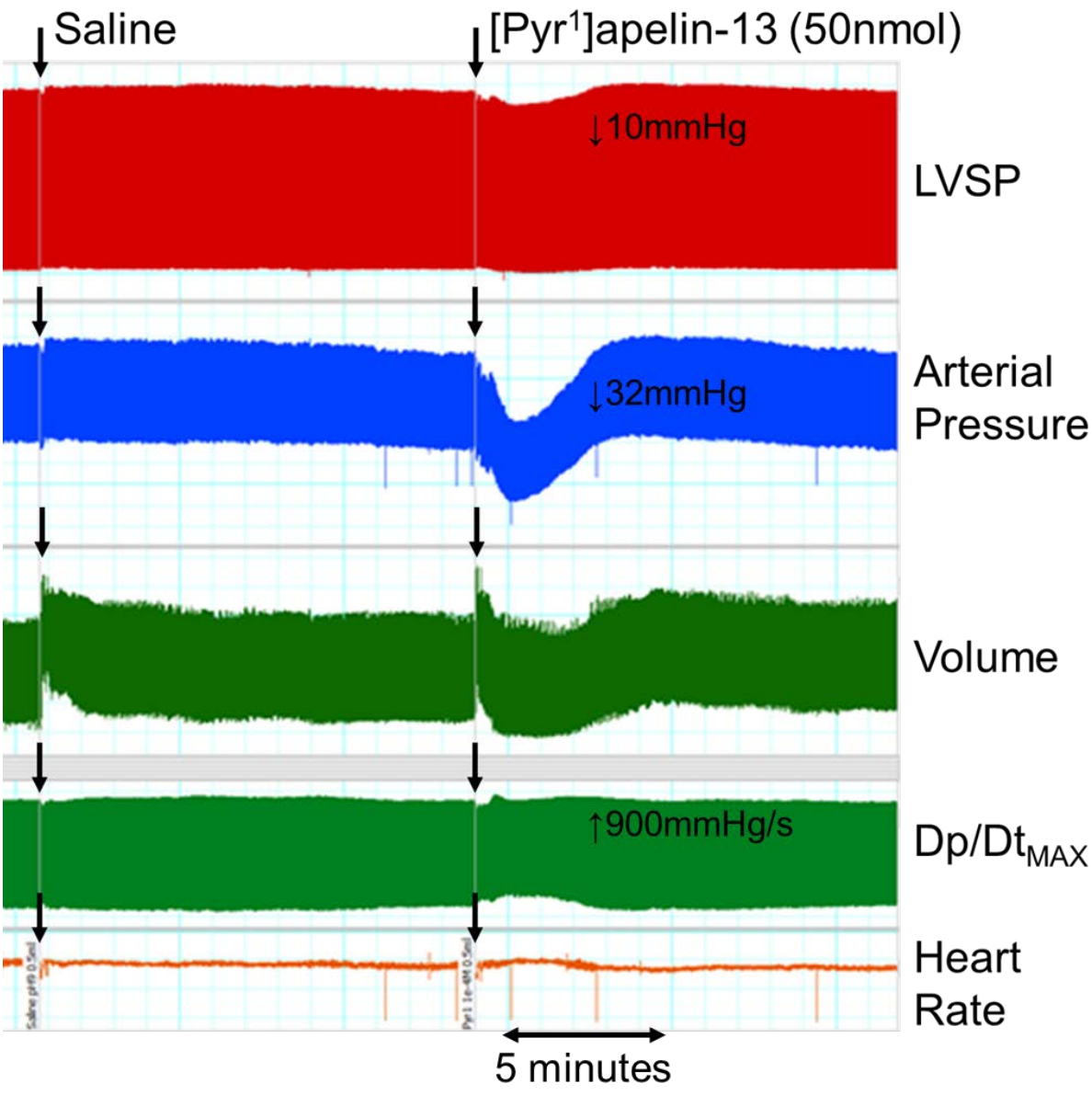

Figure 4.4: An example trace showing cardiovascular responses to saline and [Pyr[1]]apelin-13 (50nmol) *in vivo* in one male Sprague-Dawley rat. The read-outs show changes in LVSP, arterial pressure, volume, contractility (dp/dt_{MAX}) and heart rate. Real-time observable changes are evident in the LVSP (10mmHg decrease), arterial pressure (32mmHg) and contractility (900mmHgs).

4.3.2 Cross-study Analysis Comparing Consistency of *In Vivo* Cardiovascular Responses to [Pyr^{1}]apelin-13

In order to establish the consistency of [Pyr^{1}]apelin-13 responses and to validate the statistical tests used for the *in vivo* analysis, cumulative cross-study data of [Pyr^{1}]apelin-13 are presented (Figure 4.5). All responses that could be tested for normality using a D'Agostino-Pearson omnibus K^2 test were normally distributed. [Pyr^{1}]apelin-13 consistently decreased both LVSP (Figure 4.5A) and arterial pressure (Figure 4.5B) at both doses administered with changes of 9.43±0.95mmHg (****p<0.0001) and 30.62±3.47mmHg (****p<0.0001) at 50nmol and 11.65±2.21mmHg (****p<0.0001) and 40.13±4.71mmHg (****p<0.01) at 400nmol, respectively. For contractility (Figure 4.5C), the 50nmol dose of [Pyr^{1}]apelin-13 produced a small increase of 550±209mmHg/s (*p<0.05), however, at the higher 400nmol dose there was a much larger increase of 3100±566mmHg/s (****p<0.0001). There was a propensity for [Pyr^{1}]apelin-13 to act as a negative lusitrope at the 50nmol dose causing a consistent reduction in the relaxation rate of 819±231mmHg/s (***p<0.001). This effect was not observed at the higher 400nmol dose (Figure 4.5D). Increases in cardiac output (Figure 4.5E) of 2334±323RVU/min (****p<0.0001) and 3601±518RVU/min (****p<0.0001) at 50nmol and 400nmol doses, respectively, were mirrored by increases in stroke volume (Figure 4.5F) of 6.37±0.94RVU (****p<0.0001) and 8.28±1.02RVU (****p<0.0001) but not by heart rate (Figure 4.5G), which only showed a significant increase at the 400nmol dose of 16.75±6.37BPM (*p<0.05). The rats that are presented in Figure 4.5 had all received [Pyr^{1}]apelin-13 as a first dose or following only saline administration and 100% responded by observation. Qualitatively assessing responses in all 72 animals that received the 50nmol dose of Pyr^{1}]apelin-13 at any stage of their dose schedule, 67 demonstrated an observable response, giving an overall response rate of 93%. Looking at the 5 'non-responders', all had previously received a dose of another compound which may have perturbed their baseline parameters. In one case no response was detected to [Pyr^{1}]apelin-13 in two consecutive rats and a different batch was used subsequently to the first dose in the second rat. A robust response was observed suggesting the first batch as the reason for the lack of response and it was not used in further experiments. Therefore, in actuality a response rate of 93% to [Pyr^{1}]apelin-13 is likely an underestimate and considering only naïve rats, the response rate was 100%.

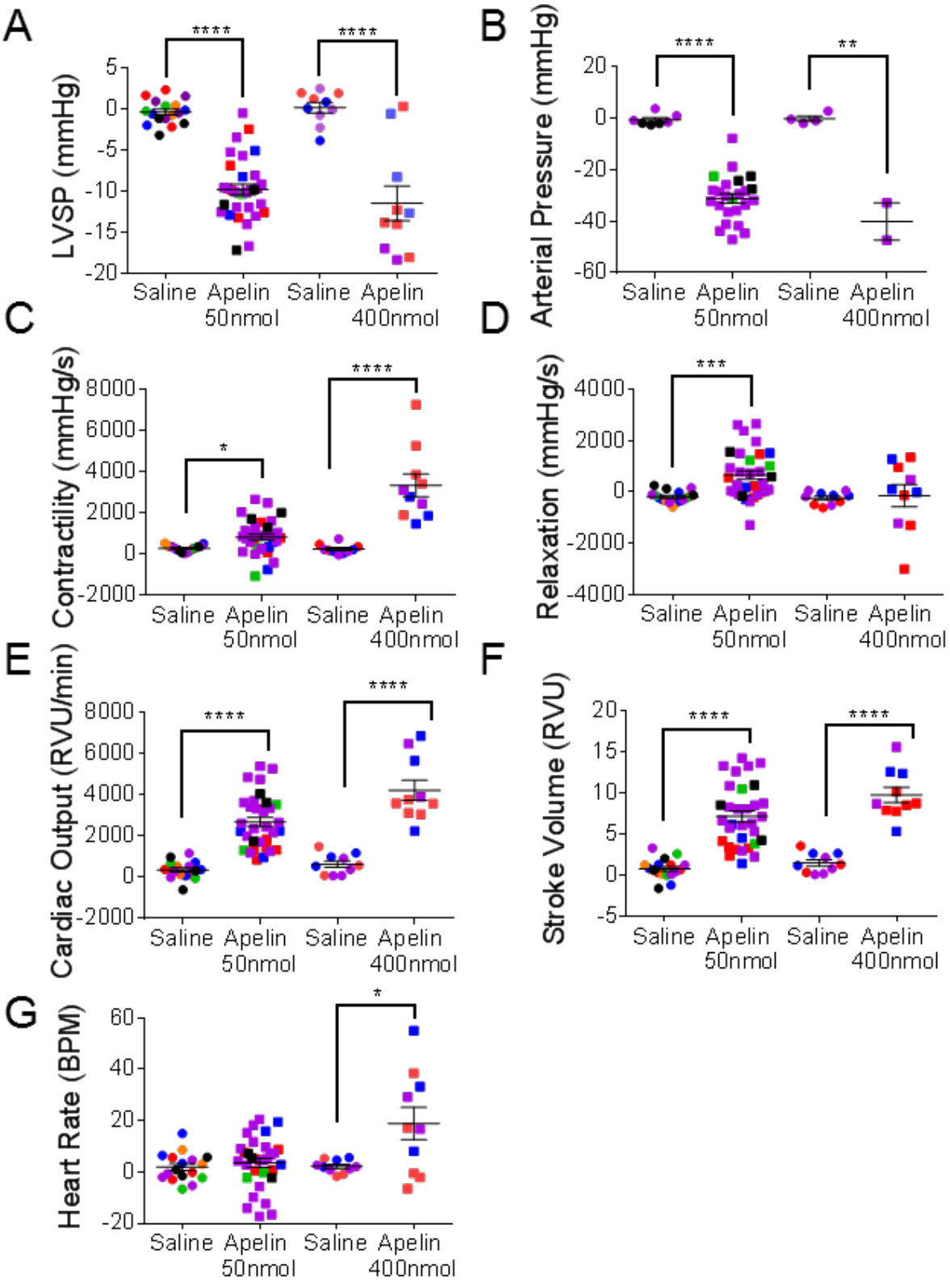

Figure 4.5: Cardiovascular responses to [Pyr[1]]apelin-13 (50nmol n=32, 400nmol n=10) or saline (n=17 and 10, respectively) administration *in vivo*. Graphs show changes in LVSP (A), arterial pressure (B), contractility (dp/dt_{MAX}; C), relaxation (dp/dt_{MIN}; D), cardiac output (E), stroke volume (F), and heart rate (G). The different colours represent different studies in which the data were acquired. Each [Pyr[1]]apelin-13 dose was compared by a Student's t-test to the corresponding saline control and statistical significance was taken as 5%. *p<0.05, **p<0.01, ***p<0.001, ****p<0.0001

4.3.3 CMF-019 Produced Acute Cardiac Responses *In Vivo* in Normotensive Male Sprague Dawley Rats: Study 1

4.3.3.1 CMF-019 is a Positive Inotrope In Vivo

Injection of CMF-019 caused a dose dependent increase in the $dP/dt_{MAX,}$ a measure of cardiac contractility, with significance at 500nmol of 703±148mmHg/s (***p<0.001) and at 5000nmol of 903±260mmHg/s (**p<0.01) (Figure 4.6A). [Pyr^{1}]apelin-13 also caused a dose dependent increase with a significant response at 400nmol of 3119±753mmHg/second (**p<0.01) (Figure 4.6B).

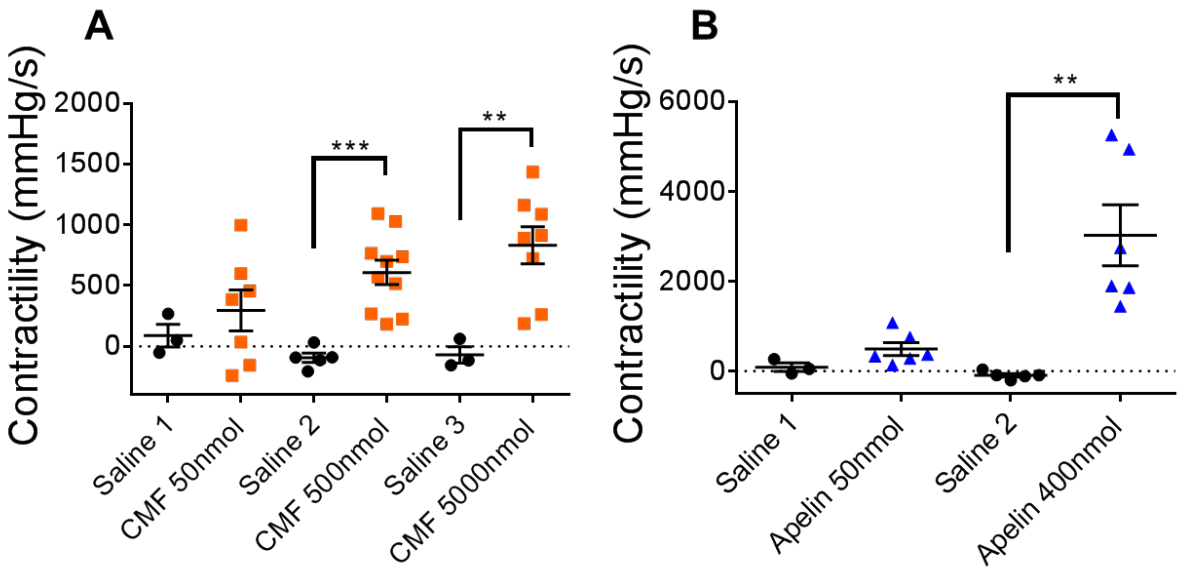

Figure 4.6: The cardiac contractile responses to CMF-019 and [Pyr^{1}]apelin-13 *in vivo* in the first acute study. Dose dependent increases in LV contractility in anaesthetised rats to (A) intravenous CMF-019 potassium salt (■, n=7-9) and (B) [Pyr^{1}]apelin-13 (apelin, ▲, n=8) compared to saline (●, n=3-5) control. Each dose was compared by a Student's t-test to its corresponding saline control as doses were administered cumulatively and statistical significance was taken as 5%. *p<0.05, **p<0.01, ***p<0.001, ****p<0.0001

[Pyr^{1}]apelin-13 dose dependently caused a significant increase in stroke volume and cardiac output of 3.00±0.88RVU (**p<0.01) and 1237±326RVU/min (**p<0.01) at 50nmol and 8.38±1.23RVU (****p<0.0001) and 3761±721RVU/min (***p<0.001), respectively (Figure 4.7D,F). CMF-019 similarly increased these parameters with smaller responses of 1.82±0.64RVU (*p<0.05) and 982±302RVU/min (**p<0.01) at 500nmol, respectively (Figure 4.7C,E). At 500nmol, CMF-019 also resulted in a small but significant elevation in the heart rate of 9.18±2.40BPM (**p<0.01, Figure 4.7G). For [Pyr^{1}]apelin-13, although there was a trend towards increased heart rate, especially at 400nmol, the response was more variable and the increase was not significant in this

study (Figure 4.7H). Neither [Pyr[1]]apelin-13 nor CMF-019 altered the dP/dt_{MIN}, a measure of lusitropy (Figure 4.7I-J).

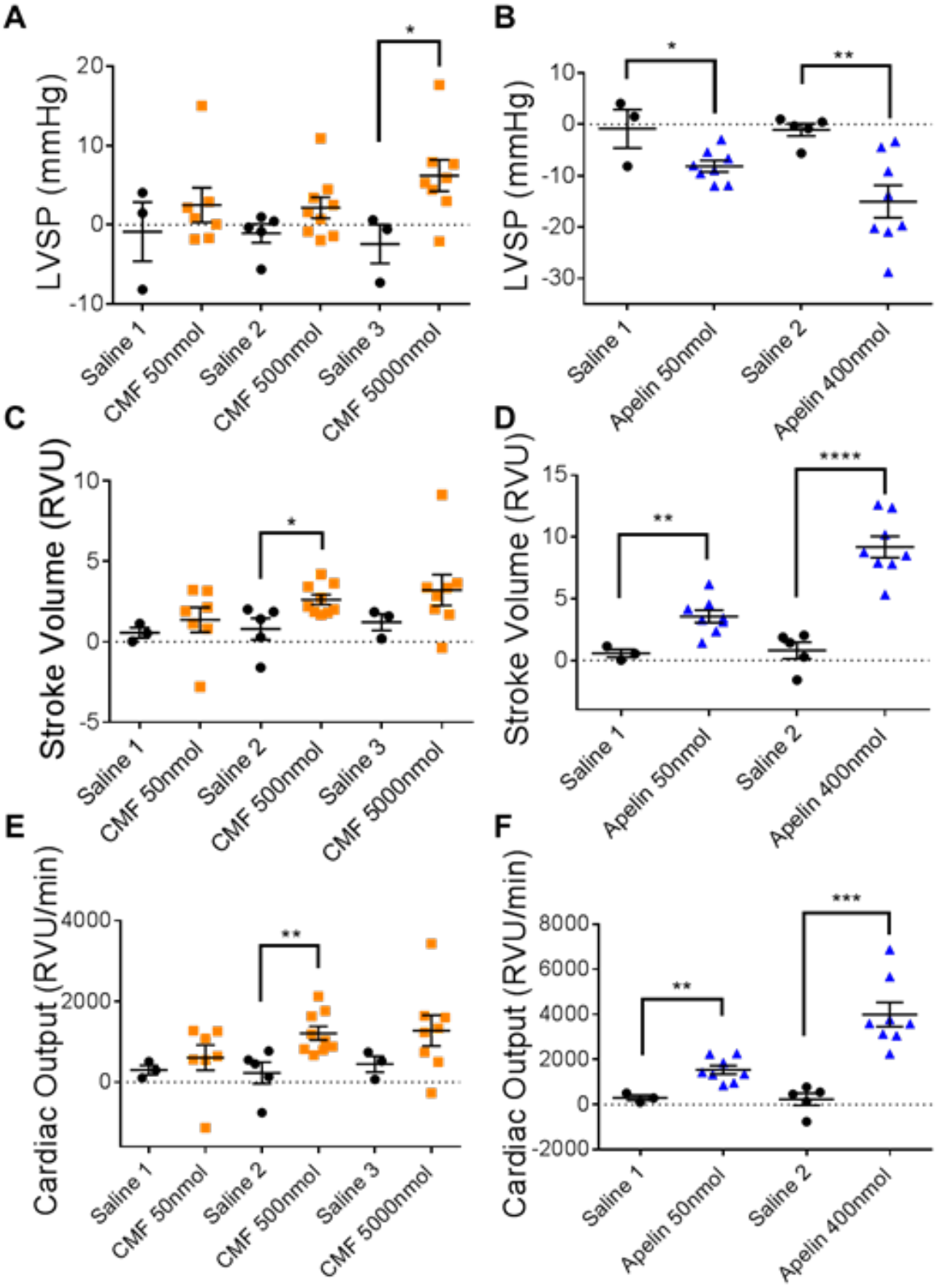

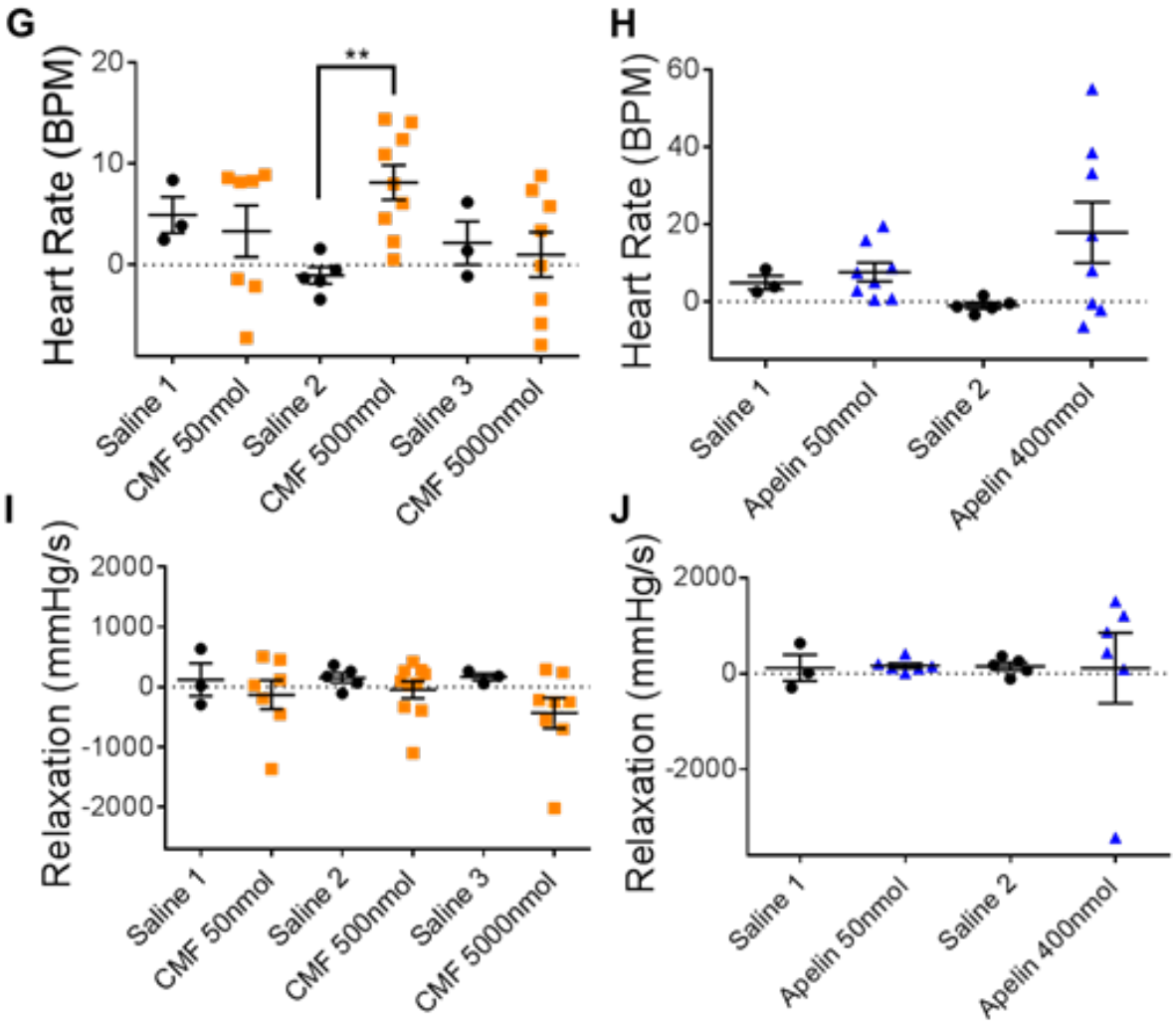

Figure 4.7: Cardiovascular responses to CMF-019 and [Pyr[1]]apelin-13 *in vivo*. Graphs showing changes in LVSP (A-B), stroke volume (C-D), cardiac output (E-F), heart rate (G-H) and relaxation (dp/dt_{MIN}) (I-J) for CMF-019 potassium salt (■, n=7-9, A,C,E,G) and [Pyr[1]]apelin-13 (apelin, ▲, n=8, B,D,F,H) compared to saline (●, n=3-5, A-H) when injected intravenously into anaesthetised male Sprague-Dawley rats. Each dose was compared by a Student's t-test to its corresponding saline control as doses were administered cumulatively and statistical significance was taken as 5%. *p<0.05, **p<0.01, ***p<0.001, ****p<0.0001

[Pyr[1]]apelin-13 caused a significant dose dependent drop in the LVSP with a drop of 7.29±2.77mmHg at 50nmol (*p<0.05) and a maximal drop of 13.97±4.16mmHg detected at 400nmol (**p<0.01) (Figure 4.7B). In contrast, CMF-019 resulted in an increase in pressure of 8.64±3.61mmHg at 5000nmol (*p<0.05) (Figure 4.7A). No adverse effects were observed at any of the concentrations administered.

4.3.3.2 CMF-019 is Present in Rat Plasma Samples

Analysis of the plasma samples taken from rats treated with CMF-019 demonstrated a mean plasma concentration of 25.4±2.5µM (heparinised samples, n=6).

4.3.4 CMF-019 Produced Acute Cardiac and Vascular Responses *In Vivo* in Normotensive Male Sprague Dawley Rats: Study 2

4.3.4.1 CMF-019 is a Vasodilator In Vivo

A further study was conducted whereby in addition to a ventricular catheter, a femoral artery catheter was inserted to measure arterial blood pressure changes. To study the consistency of responses between the two studies, all of the cardiac parameters from the previous study have been analysed. CMF-019 again caused an increase in cardiac contractility with a change of 251±89mmHg/s (*p<0.05) observed at 500nmol (Figure 4.8A). At the higher 5000nmol dose the response was not significant. The response to [Pyr[1]]apelin-13 was also consistent and an increase of 1038±464mmHg/s (***p<0.001) was observed at a lower maximal concentration of 150nmol (Figure 4.8B).

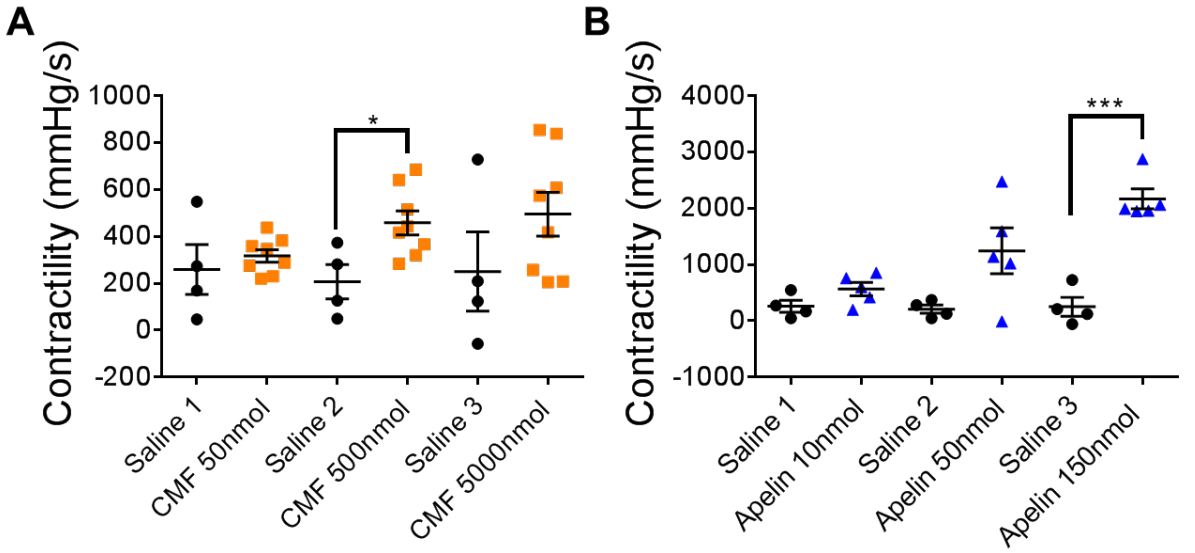

Figure 4.8: The cardiac contractile response to CMF-019 and [Pyr[1]]apelin-13 *in vivo* in the second acute study. Increases in LV contractility in anaesthetised male Sprague-Dawley rats to (A) intravenous CMF-019 potassium salt (■, n=8) and (B) [Pyr[1]]apelin-13 (apelin, ▲, n=5) compared to saline (●, n=4) control. Each dose was compared by a Student's t-test to its corresponding saline control as doses were administered cumulatively and statistical significance was taken as 5%. *p<0.05, **p<0.01, ***p<0.001, ****p<0.0001

For the arterial pressure, CMF-019 caused a dose-dependent decrease at 50nmol and 500nmol of 4.16±1.18mmHg (**p<0.01) and 6.62±1.85mmHg (**p<0.01), respectively (Figure 4.9A). At the highest dose the response was not significant. [Pyr[1]]apelin-13

caused a dose dependent and larger decrease in blood pressure at all doses administered; 10nmol 12.06±3.51mmHg (*p<0.05), 50nmol 31.24±8.70mmHg (**p<0.01) and 150nmol 31.75±9.53mmHg (*p<0.05) (Figure 4.9B).

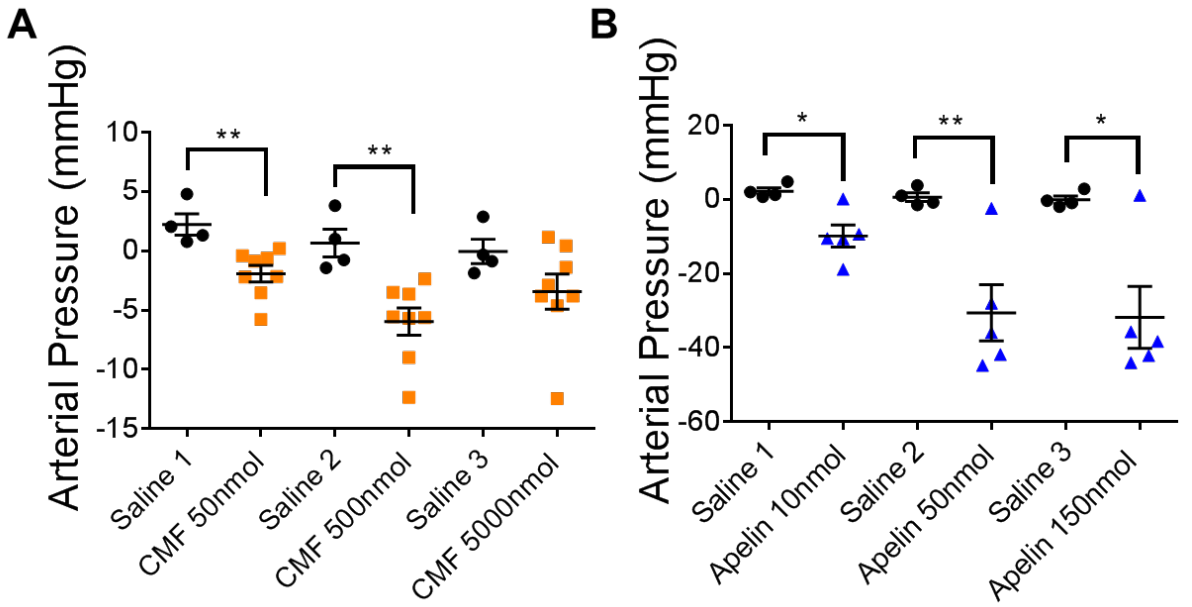

Figure 4.9: The arterial pressure change in response to CMF-019 and [Pyr[1]]apelin-13 *in vivo* in the second study. Decreases in arterial pressure in anaesthetised male Sprague-Dawley rats to (A) intravenous CMF-019 potassium salt (■, n=8) and (B) [Pyr[1]]apelin-13 (apelin, ▲, n=5) compared to saline (●, n=4) control. Each dose was compared by a Student's t-test to its corresponding saline control as doses were administered cumulatively and statistical significance was taken as 5%. *p<0.05, **p<0.01, ***p<0.001, ****p<0.0001).

The responses in the other cardiovascular parameters measured in response to CMF-019 and [Pyr[1]]apelin-13 were largely consistent. Both CMF-019 and [Pyr[1]]apelin-13 caused dose-dependent increases in stroke volume and cardiac output (Figure 4.10C-F). CMF-019 resulted in increases of 2.63±0.82RVU (**p<0.01) and 1097±284RVU/min (**p<0.01) at 50nmol and 2.48±0.87RVU (*p<0.05) and 1012±340RVU/min (*p<0.05) at 500nmol, respectively. At the highest dose of 5000nmol neither of these parameters were significant. Meanwhile, [Pyr[1]]apelin-13 induced increases of 4.72±0.98RVU (**p<0.01) and 2008±464RVU/min (**p<0.01) at 10nmol, 9.70±1.93RVU (**p<0.01) and 3618±818RVU/min (**p<0.01) at 50nmol and 9.84±3.02RVU (*p<0.05) and 3961±1154RVU/min (*p<0.05) at 150nmol, respectively.

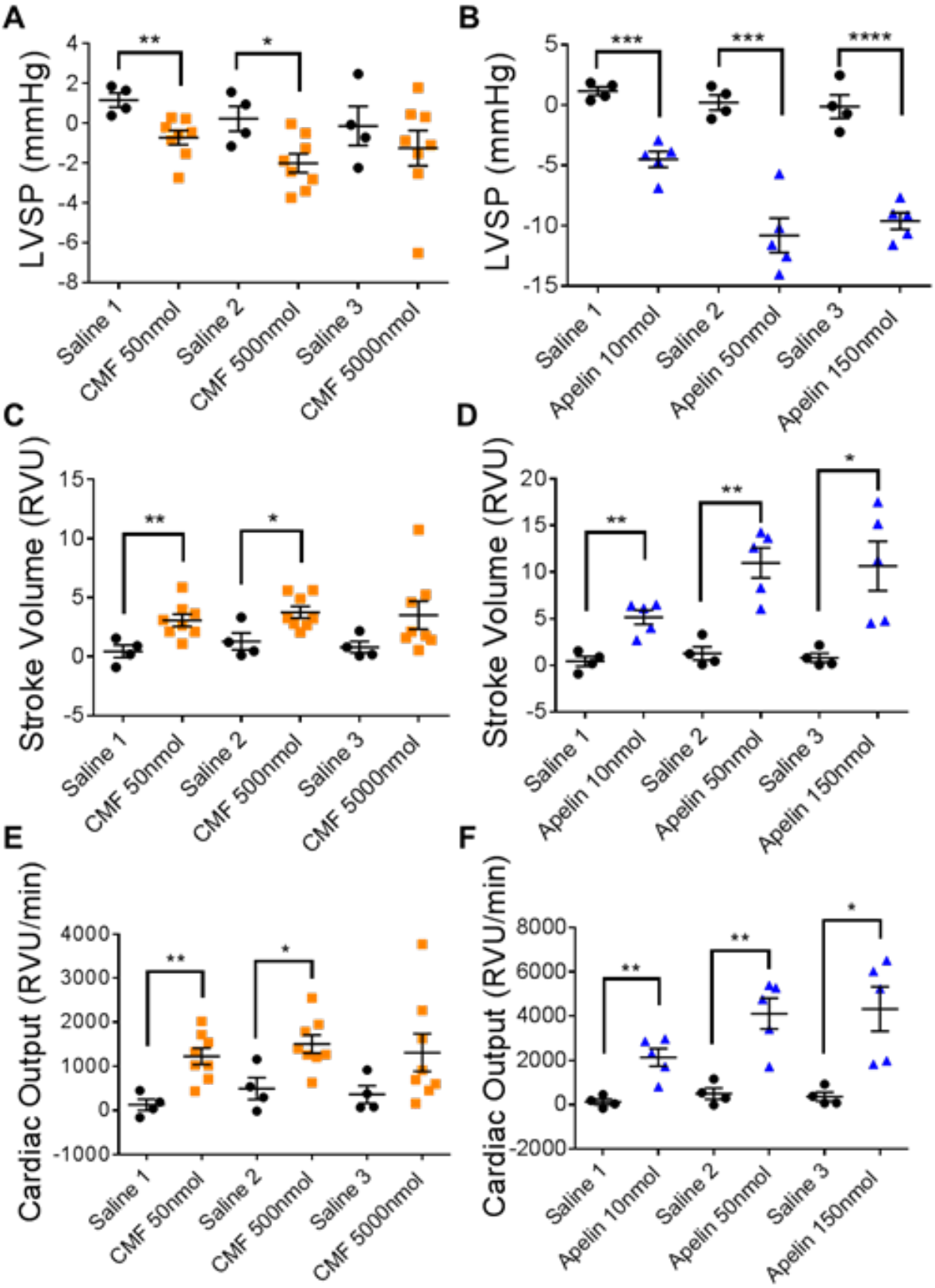
A
LVSP (mmHg)
4
2
0
-2
-4
-6
-8
**
*
Saline 1
CMF 50nmol
Saline 2
CMF 500nmol
Saline 3
CMF 5000nmol
B
LVSP (mmHg)
5
0
-5
-10
-15
***
***
****
Saline 1
Apelin 10nmol
Saline 2
Apelin 50nmol
Saline 3
Apelin 150nmol
C
Stroke Volume (RVU)
15
10
5
0
-5
**
*
Saline 1
CMF 50nmol
Saline 2
CMF 500nmol
Saline 3
CMF 5000nmol
D
Stroke Volume (RVU)
20
15
10
5
0
-5
**
**
*
Saline 1
Apelin 10nmol
Saline 2
Apelin 50nmol
Saline 3
Apelin 150nmol
E
Cardiac Output (RVU/min)
4000
3000
2000
1000
0
-1000
**
*
Saline 1
CMF 50nmol
Saline 2
CMF 500nmol
Saline 3
CMF 5000nmol
F
Cardiac Output (RVU/min)
8000
6000
4000
2000
0
-2000
**
**
*
Saline 1
Apelin 10nmol
Saline 2
Apelin 50nmol
Saline 3
Apelin 150nmol

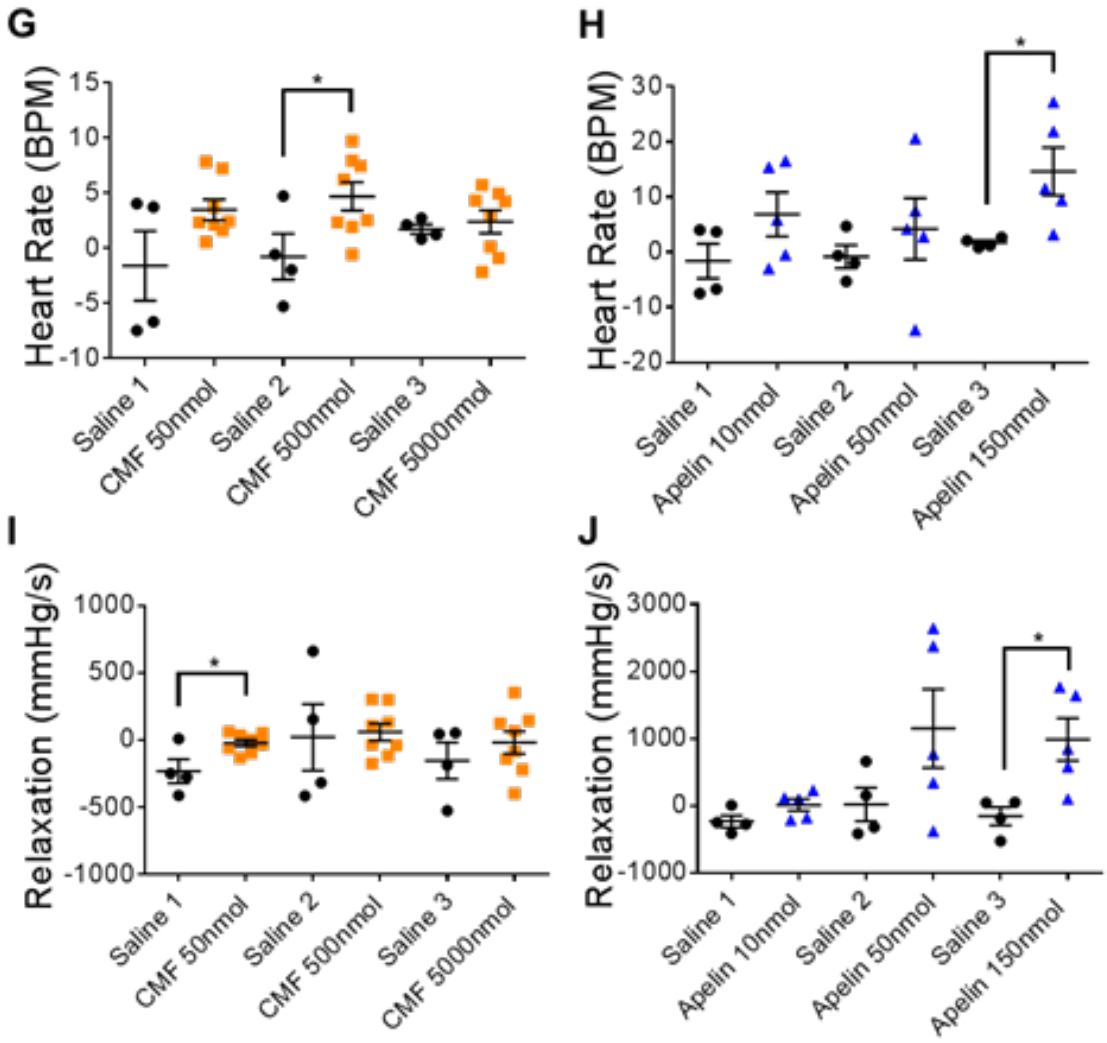

Figure 4.10: Cardiovascular responses to CMF-019 and [Pyr[1]]apelin-13 *in vivo* in the second acute study. Graphs showing changes in LVSP (A-B), stroke volume (C-D), cardiac output (E-F), heart rate (G-H) and relaxation (dp/dt_{MIN}) (I-J) for CMF-019 potassium salt (■, n=8, A,C,E,G) and [Pyr[1]]apelin-13 (apelin, ▲, n=5, B,D,F,H) compared to saline (●, n=4, A-H) when injected intravenously into anaesthetised male Sprague-Dawley rats. Each dose was compared by a Student's t-test to its corresponding saline control as doses were administered cumulatively and statistical significance was taken as 5%. *p<0.05, **p<0.01, ***p<0.001, ****p<0.0001

Again at 500nmol, CMF-019 a small elevation in heart rate of 5.46±2.32BPM (*p<0.05) was observed (Figure 4.10G). An increase in heart rate to [Pyr[1]]apelin-13 of 12.94±4.95BPM (*p<0.05) was also observed at 150nmol (Figure 4.10H). Unlike in the first study, some small lusitropic changes were observed (Figure 4.10I-J). CMF-019 led to a potential decrease in relaxation of 210±70mmHg/s (*p<0.05) at the lowest dose administered of 50mnol, whilst [Pyr[1]]apelin-13 led to a decrease of 1143±378mmHg/s (*p<0.05) at 150nmol . Finally, the changes in LVSP observed in this study to CMF-019 were different to those observed in the first study. Whereas, in the first study CMF-

019 caused small dose-dependent increases in LVSP (Figure 4.7A), here it decreased LVSP (Figure 4.10A) in concert with the arterial pressure. CMF-019 resulted in LVSP decreases of 1.88±0.57mmHg (**p<0.01) at 50nmol and 2.23±0.80mmHg (*p<0.05) at 500nmol. No significant change was observed at the highest dose of 5000nmol. [Pyr^{1}]apelin-13 also decreased LVSP (Figure 4.10B) and this was consistent with the first study (Figure 4.7B). [Pyr^{1}]apelin-13 led to decreases of 5.66±0.81mmHg (***p<0.001) at 10nmol, 11.02±1.70mmHg (***p<0.001) at 50nmol and 9.47±1.16mmHg (****p<0.0001) at 150nmol. Similarly, no adverse effects were observed at any of the doses administrated.

4.3.4.2 CMF-019 Does Not Desensitise the Apelin Receptor In Vivo

To study desensitisation at the apelin receptor *in vivo* a fourth dose of [Pyr^{1}]apelin-13 at 50nmol was administered to all of the treatment groups used in the study (Figure 4.11). In this figure the x-axis denotes whether the preceding three doses were saline or increasing cumulative doses of CMF-019 or [Pyr^{1}]apelin-13. Qualitatively, the responses to 50nmol [Pyr^{1}]apelin-13 were larger if the animal had previously received saline or CMF-019 than if they had received [Pyr1]apelin-13. This was only significant for the change in cardiac contractility where [Pyr^{1}]apelin-13 treated animals had a difference in response compared to saline treated animals of 544±81mmHg/s (***p<0.001). The responses to [Pyr^{1}]apelin-13 in CMF-019 treated animals compared to saline treated animals were not significantly different for any parameter.

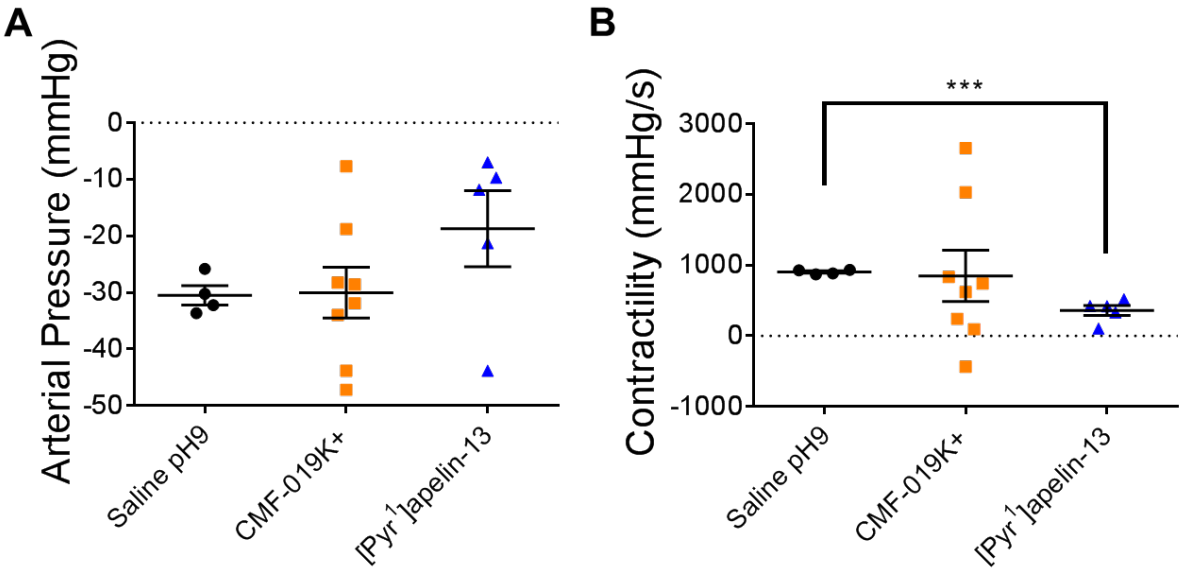

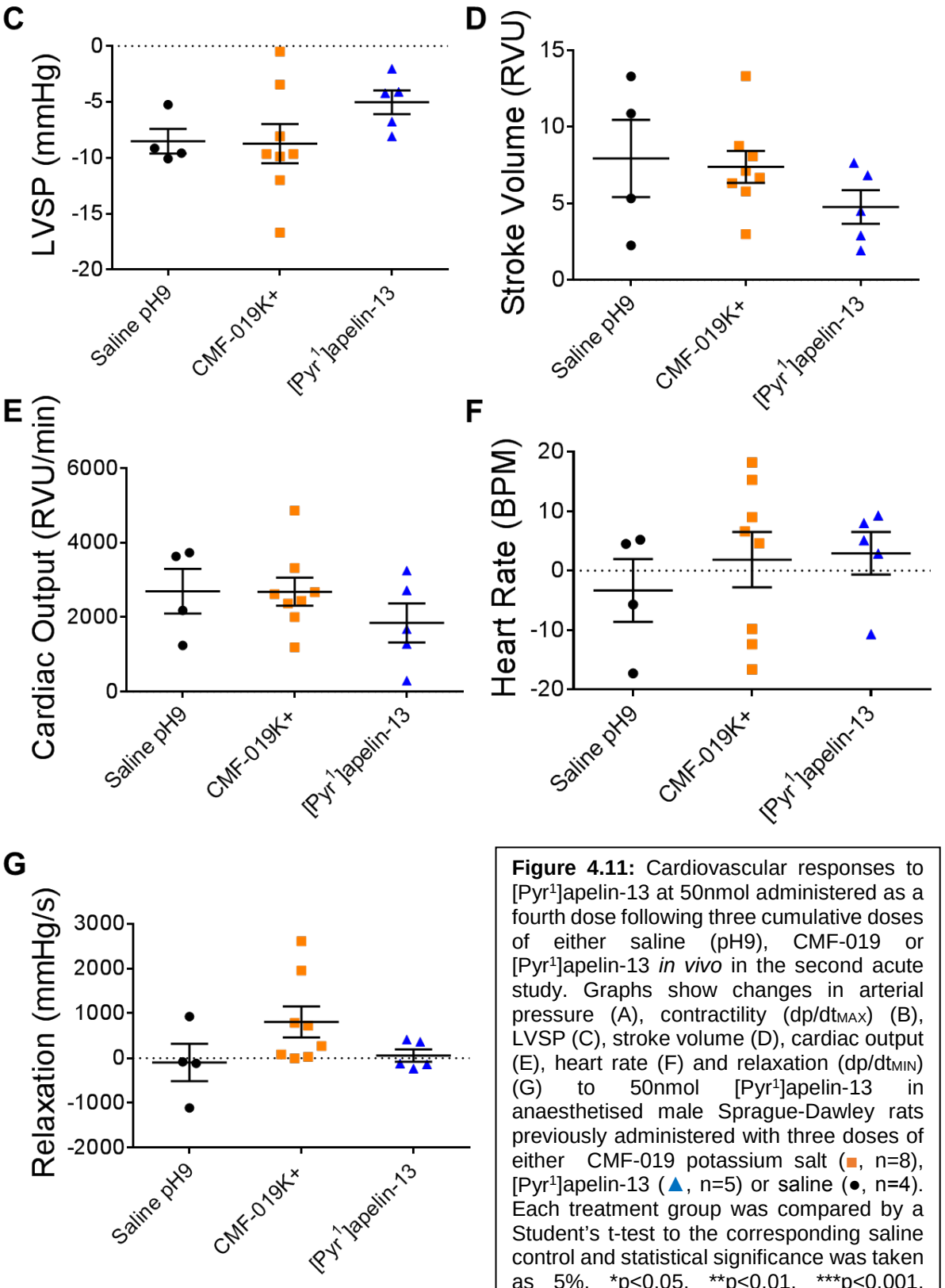

Figure 4.11: Cardiovascular responses to [Pyr[1]]apelin-13 at 50nmol administered as a fourth dose following three cumulative doses of either saline (pH9), CMF-019 or [Pyr[1]]apelin-13 *in vivo* in the second acute study. Graphs show changes in arterial pressure (A), contractility (dp/dt_{MAX}) (B), LVSP (C), stroke volume (D), cardiac output (E), heart rate (F) and relaxation (dp/dt_{MIN}) (G) to 50nmol [Pyr[1]]apelin-13 in anaesthetised male Sprague-Dawley rats previously administered with three doses of either CMF-019 potassium salt (■, n=8), [Pyr[1]]apelin-13 (▲, n=5) or saline (●, n=4). Each treatment group was compared by a Student's t-test to the corresponding saline control and statistical significance was taken as 5%. *p<0.05, **p<0.01, ***p<0.001, ****p<0.0001

4.4 Discussion

4.4.1 [Pyr^1]apelin-13 Produced Robust Cardiovascular Responses *In Vivo* Supporting the Apelin Receptor as a Suitable Therapeutic Target

Apelin has previously been reported to produce cardiovascular responses in rodents (Jia *et al*., 2006, Tatemoto *et al*., 2001, Ashley *et al*., 2005, Atluri *et al*., 2007, Berry *et al*., 2004). Therefore, to validate the *in vivo* assay developed, [Pyr^1]apelin-13, the most abundant cardiovascular isoform (Maguire *et al*., 2009), was tested. The example trace shown in Figure 4.4, clearly demonstrates that [Pyr^1]apelin-13 administered at the intermediate dose of 50nmol was capable of producing robust vasodilatation and cardiac inotropy as expected for apelin from these previous studies. Moreover, responses were sufficiently robust that they could be observed in real-time.

Having established that clear responses to [Pyr^1]apelin-13 were observable, it was important to assess the reproducibility of these responses. To do this data from across a number of studies where [Pyr^1]apelin-13 had been used as a positive control were compared. The different studies have been colour-coded in Figure 4.5 so that any trends could be more easily picked out. The data were assessed for normality using the D'Agostino-Pearson omnibus K^2 test. This is the recommended test for normality but requires n values of 8 or greater and so cannot be used for smaller data sets. By analysing this large data set of [Pyr^1]apelin-13 responses, it clearly demonstrated that the *in vivo* [Pyr^1]apelin-13 responses were normally distributed in every parameter that could be measured. In many *in vivo* studies sufficient n values cannot be obtained to calculate the D'Agostino-Pearson omnibus K^2 test as it is important to reduce animal use. Alternative tests, for example, the Shapiro-Wilks test may be used as this requires a minimum of 3 n values; however, this test is less robust and is not recommended. Instead, by demonstrating that collectively the responses to [Pyr^1]apelin-13 are normally distributed across all of the experiments performed, it seems justifiable to assume normality of the responses within individual experiments. As such, the Student's t-test, a parametric statistical calculation, has been used for all of the acute *in vivo* analysis as this is the most appropriate test to use for normally distributed data.

Overall, all of the animals administered the 50nmol or 400nmol dose of [Pyr^1]apelin-13 responded and there seem to be no obvious differences between the studies conducted over the two and a half year period. The responses observed were consistent with [Pyr^1]apelin-13 as a reported vasodilator and cardiac inotrope.

Crucially, in a study using invasive catheterisation in patients with PAH to assess responses to [Pyr^{1}]apelin-13, it was found that it primarily reduced total pulmonary vascular resistance and increased cardiac output (Brash *et al*., 2018), suggesting that the responses measured in our study in naïve normotensive male Sprague-Dawley rats are comparable to those one would expect in humans, even those with disease.

The clearest response observed in our study was a substantial reduction in arterial pressure, which was as much as 30mmHg with the 50nmol dose and 40mmHg with the 150nmol dose. Such a response is remarkable and demonstrates the potency of the apelin system, though it should be noted that such large responses have not been observed in humans. In the rats, the dilatation was sufficiently large that a drop in LVSP was observed, despite the inotropic effects of the compound. The most likely explanation for this is that the arterial dilatation led to a sufficient drop in afterload to reduce the pressure within the ventricular cavity. Simultaneously, the molecule acted as a positive inotrope, increasing the contractility of the LV, while enhancing stroke volume and cardiac output. The contractility showed a smaller response at 50nmol than at 150nmol where the responses were large but substantially more variable. A likely explanation for this comes from the fact that the dp/dt_{MAX} measurements are highly dependent on catheter location. In particular, with positive inotropes, it has been reported that the catheter can be pushed into the ventricular wall, giving an artificial elevation in the end-systolic pressure and an overestimate of the dp/dt_{MAX} (Wei *et al*., 2014). An example of such an artefact is shown below (Figure 4.12), in some cases these artefacts can be difficult to detect as the catheter movement can be gradual. In these studies, an attempt has been made to exclude such aberrant measurements by adjusting the catheter after the dose and demonstrating that a shift in location had occurred. Nevertheless, very large elevations or reductions in contractility should be interpreted cautiously.

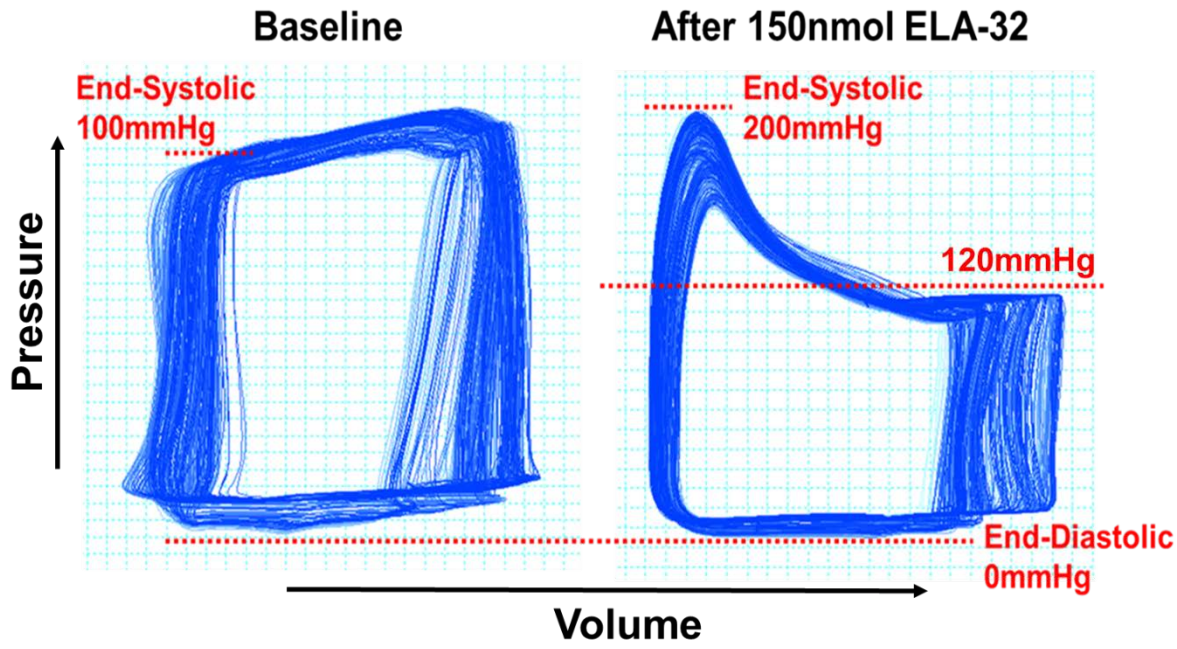

Figure 4.12: PV loops demonstrating artificial elevation of the end-systolic pressure due to catheter movement into the endocardial wall following a single 150nmol dose of ELA-32, a very powerful inotrope through the apelin receptor. Since cardiac contractility is calculated as the maximal change in pressure against time as shown in figure 4.1, such artefacts can lead to a dramatically overestimated Dp/Dt_{MAX} unless accounted for. In this case as the initial systolic pressure levels off before the peak artefact, the Dp/Dt_{MAX} would not actually be substantially perturbed, however, the Dp/Dt_{MIN}, a measure of lusitropy, would be overestimated.

A potential limitation of this *in vivo* study was the need to anaesthetise the animals with isoflurane which could have impacted responses. A possible manifestation of this could have been reduced or delayed homeostatic mechanisms and thus, enhanced responses relative to those that might be observed in a conscious animal. This could particularly have impacted vasodilatation and may have resulted in greater and more sustained drops in blood pressure than one would otherwise expect. However, this would not have been the case for the cardiac parameters, since isoflurane is a well characterised negative inotrope and is known to reduce cardiac contractility, stroke volume and output (Philbin and Lowenstein, 1975, Makela and Kapur, 1987, Lynch, 1990). Therefore, the cardiac responses measured were likely blunted compared to those in a conscious animal. It is arguable that alternative anaesthetics might have been preferable in this study because of the cardiac impact of isoflurane. However, other anaesthetics would also act as cardiac depressants and because many of them must be administered by injection, rather than inhalation as for isoflurane, it is harder to maintain a consistent level of anaesthesia. Instead isoflurane was considered the

best option and, in order to impact responses as little as possible, the animal was carefully monitored, by both heart and breathing rate, such that as light anaesthesia as possible could be maintained throughout the experiment.

One advantage of this cross-study comparison is that all of the rats used were outbred, suggesting that there should be genetic variation between batches. Many drugs are limited and fail in phase III clinical trials due to a lack of clinical efficacy. This is largely due to a lack of response in a subset or subsets of the population. Here, the number of 'responders' and 'non-responders' to [Pyr^{1}]apelin-13 were identified. It is remarkable that overall 93% of the animals tested with the 50nmol dose of [Pyr^{1}]apelin-13 responded. Moreover, of those that did not, there were clear reasons why they may not have responded, having previously received apelin mimetics that may have desensitised the receptor. Crucially, all of the animals that received either nothing or only saline (essentially naïve rats) before the [Pyr^{1}]apelin-13 dose responded. This 100% response rate is remarkably high and implies that the apelin system is efficacious across the population and would, therefore, be extremely suitable as a therapeutic target. A limitation of this study is that there is likely to be far less genetic variation in Sprague-Dawley populations, outbred or not, than is desirable for a cross-population study of responses. To better assess the consistency of apelin responses across rat populations, it would be interesting to perform similar experiments in different outbred rat strains. Such studies, while often not performed as they do not identify novel or controversial findings, would nonetheless be critical to confirming response within populations and have the potential to reduce phase III attrition by ensuring broad clinical efficacy from an early stage in the drug development process.

4.4.2 CMF-019 is a Cardiac Inotrope and Vasodilator *In Vivo*

In two separate *in vivo* studies conducted in normotensive male Sprague-Dawley rats, CMF-019 produced consistent cardiovascular responses compared to saline. In both cases an increase in contractility with concurrent increases in stroke volume and cardiac output were observed. Furthermore, in the second study in which a femoral artery catheter was employed, vasodilatation was observed. These responses are consistent with CMF-019 acting at the apelin receptor and the responses mimicked those observed with the endogenous agonist, [Pyr^{1}]apelin-13, a positive inotrope and vasodilator. It should be noted that the responses to CMF-019 were much smaller than those observed for [Pyr^{1}]apelin-13 and the highest dose of CMF-019 often did not

reach statistical significance. This suggests that either the maximal response to CMF-019 was achieved at the 500nmol dose or above this concentration no further drug was able to reach the receptor *in vivo*. The reasons as to why this might be are discussed later. Nevertheless, these studies critically showed that CMF-019 is active *in vivo* and that the activity observed in the *in vitro* screening assays translated effectively.

The use of the femoral artery catheter in the second study addressed a crucial question in the apelin signalling field, namely whether β-arrestin biased ligands are better able to induce vasodilatation. Such a result would imply that G protein biased ligands, such as CMF-019, would be less able to induce dilatation. This could limit their clinical efficacy, particularly as pulmonary dilatation is the main mechanism by which current PAH therapeutics function. The observation of enhanced dilatation in β-arrestin biased ligands has been reported on several occasions by the same group (El Messari *et al*., 2004, Iturrioz *et al*., 2010b, Ceraudo *et al*., 2014, Murza *et al*., 2015), however, it should be noted that the reported β-arrestin responses in these studies were modest. Their most recent publication argues for a correlation between β-arrestin signalling and propensity to induce hypotensive activity in Sprague-Dawley rats (Besserer-Offroy *et al*., 2018). A significant limitation is that the authors did not perform a similar correlation analysis against the G protein signalling pathway. From their data, a correlation looks likely and perhaps their observation is actually a correlation between *in vitro* efficacy through multiple pathways and hypotensive action *in vivo*. Indeed, they also falsely reported that MM07, a G protein biased cyclic peptide, was unable to induce vasodilatation. These studies from our laboratory, therefore, dispute their conclusions since we observed robust and sustained dilatation in humans with MM07 in forearm blood-flow and Aellig hand vein plethysmography experiments (Brame *et al*., 2015). Nonetheless, CMF-019 shows a much greater degree of bias than MM07 with very low potency in the β-arrestin assay *in vitro* and is a much keener test of whether G protein biased molecules can induce vasodilatation. The small but significant decrease in blood pressure of approximately 5mmHg with CMF-019 suggests that vasodilatation can occur independently of β-arrestin through alternative signalling pathways. While it could be argued that the smaller response to CMF-019 compared to [Pyr^{1}]apelin-13 (approximately 30mmHg decrease) is due to the bias of CMF-019, this seems unlikely and the responses in other cardiovascular parameters were also smaller for CMF-019.

4.4.3 CMF-019 Does Not Desensitise the Apelin Receptor *In Vivo*

To assess the ability of CMF-019 to internalise the apelin receptor *in vivo*, a protocol was devised whereby subsequent to the three cumulative doses of saline, CMF-019 or [Pyr^{1}]apelin-13 administered to test responses, a fourth dose of [Pyr^{1}]apelin-13 was administered at 50nmol to every animal regardless of the previous three doses. These fourth doses were compared to assess whether there was any desensitisation of the response as a consequence of the previous doses administered. Although this study was limited by the number of animals used and a high variance in the 50nmol [Pyr^{1}]apelin-13 responses, there is a clear trend across the parameters. There was very little difference in responses to 50nmol [Pyr^{1}]apelin-13 in any parameter when they had received either saline or CMF-019 for the first three doses. However, when they had received [Pyr^{1}]apelin-13, they displayed qualitatively reduced responses compared to the animals that had received saline in every parameter and this was statistically significant for contractility. A potential limitation of this study which should be considered is that the responses induced by CMF-019 compared to [Pyr^{1}]apelin-13 were smaller. This might suggest that had larger responses to CMF-019 been achievable *in vivo* then it would desensitise the receptor similarly to [Pyr^{1}]apelin-13. However, given there was no observable trend towards desensitisation, in contrast to [Pyr^{1}]apelin-13, overall the data suggest that CMF-019 did not desensitise the apelin receptor *in vivo* and that this corroborates the G protein bias observed *in vitro.*

4.4.4 CMF-019 *In Vivo vs In Vitro*

The responses to CMF-019 were much smaller than for [Pyr^{1}]apelin-13 *in vivo*, despite the fact that larger concentrations of CMF-019 were used. The reason for such a lower activity of CMF-019 is difficult to explain because CMF-019 displayed very similar binding affinity to [Pyr^{1}]apelin-13 at the apelin receptor in human and rat heart homogenates *in vitro*. A possible explanation is that CMF-019 is limited pharmacokinetically when administered *in vivo*. Prior to *in vivo* experimentation the predicted pharmacokinetic desirability of CMF-019 was considered computationally (Figure 4.13; data from Leen Kalash and Professor Robert Glen). CMF-019 displayed drug-like properties and a good physiochemical profile when compared to an oral drug library for Lipinski's rules (Figure 4.13A), Verber's rules (Figure 4.13B) and in a Principal Component Analysis (PCA) of 15 physiochemical descriptors (Figure 4.13C). CMF-019 had one Lipinski's Rule-of-Five violation (logP), although this was

ameliorated by the ionisation of the carboxylic acid at physiological pH, reducing the logD to a more acceptable range (logD=2.74 at pH7.4). Nevertheless, the solubility of the compound was not ideal and the potassium salt dissolved in pH9 saline was used in the *in vivo* studies to attain higher concentrations. Despite this, it is likely that the maximal solubility of CMF-019 was attained with the 500nmol dose, perhaps explaining why there was no greater response upon administration of the 5000nmol dose.

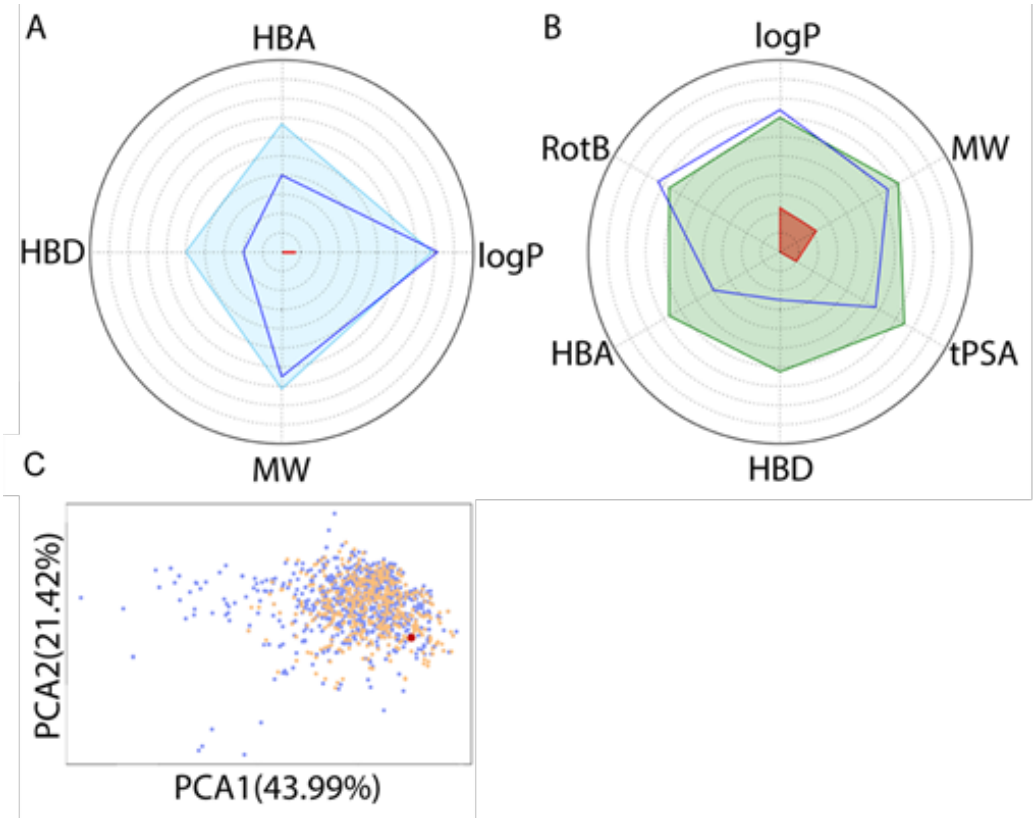

Figure 4.13: Assessment of drug-like properties of CMF-019 using FAF-Drugs3.
(A) The properties of CMF-019 (HBD; H-bond donors; HBA, H-bond acceptors; logP, octanol-water partition coefficient; MW, molecular weight) are shown as a dark blue line. A compound library of oral drugs was also assessed for these characteristics to illustrate the desirable physiochemical properties for a drug-like molecule according to Lipinski's rules (light blue line). The red area denotes where it was not possible to have a molecule with those properties, or where there was a lack of data in the library.
(B) An oral absorption estimation for CMF-019 (dark blue line) (HBD; H-bond donors; HBA, H-bond acceptors; RotB, rotatable bonds, logP, octanol-water partition coefficient; MW, molecular weight; tPSA, topological polar surface area). A compound library of oral drugs was also assessed for these characteristics to illustrate the desirable physiochemical properties for a drug-like molecule according to Verber's rules (dark green line). The red area denotes where it was not possible to have a molecule with those properties, or where there was a lack of data in the library.
(C) An oral property space obtained by applying a Principal Component Analysis (PCA) of 15 physicochemical descriptors of CMF-019 (shown as the red dot), compared to properties of oral drugs in current use, extracted as sublibraries from the databases, eDrugs (blue) and DrugBank (orange). Figure from Read *et al.* (2016).

Moreover, the plasma binding of the molecule was predicted to be in excess of 99% in favour of the bound form. This would likely substantially limit the responses that could be observed *in vivo* as the plasma would effectively act as a reservoir for the drug, limiting the amount that could perfuse into the tissue and engage the receptor target. Although a limitation for acute *in vivo* measurement, some plasma binding is generally considered beneficial for long-term therapeutics by acting as a mechanism for slow drug release. However, in this case with binding in excess of 99%, this is unlikely and it is probable that much of the drug remains in a bound and inaccessible form within the plasma.

To attempt to assess the stability of CMF-019 *in vivo*, following completion of the first study, blood samples were taken and the CMF-019 concentrations measured. A mean plasma concentration of ~25µM was detected. This blood was collected approximately ten minutes after the final dose of 5000nmol was administered; however, exact timings were not possible as blood could only be collected as part of the exsanguination protocol and regular blood sampling for pharmacokinetic analysis was not possible with our project licence. Approximating the rat blood volume as 20mL, one would expect a plasma concentration of 250µM immediately following this final injection of CMF-019. This would leave only 10% of the parent compound in the blood and since doses administered were cumulative, the concentration detected in the plasma was substantially lower than that administered over the course of the experiment. This suggests that CMF-019 is being rapidly metabolised or excreted and does not support it as a particularly stable compound *in vivo*, in contrast to the predicted stability from computational studies.

Despite these pharmacokinetic limitations, the very high concentrations of CMF-019 used in these experiments should have been sufficient to negate them as an issue. Taking the average plasma concentration of CMF-019 measured at the end of the first study of 25µM and the pK_i of CMF-019 in rat heart homogenate of 8.49, one can approximate the receptor occupancy at the rat heart as in excess of 99%. By taking the measured plasma concentration from the first study both solubility and excretion/metabolism have been removed as variables, suggesting that the maximal response to CMF-019 should have been achievable in both studies despite the pharmacokinetic issues. Therefore, this may explain why no increase in response was seen between the 5000nmol dose and the 500nmol dose of CMF-019 since maximal receptor occupancy had likely already been achieved.

4.5 Conclusions

The purpose of this study was to assess the *in vivo* activity of CMF-019. To do this an assay was developed and validated, during which it was demonstrated that cardiovascular responses to the endogenous molecule, [Pyr^{1}]apelin-13, are robust and highly reproducible. Such a finding supports the apelin system as a therapeutic target. Studying CMF-019, it was shown that it was active *in vivo*, demonstrating that *in vitro* binding and cell signalling efficacy were translatable to a whole-organism experimental set-up. Moreover, CMF-019 was shown to be both a positive inotrope and a vasodilator, mimicking all aspects of the [Pyr^{1}]apelin-13 response, despite reports that G protein biased ligands are limited to cardiac effects without vascular dilatation. Finally, it was shown that CMF-019 did not desensitise the apelin receptor *in vivo*. This corroborated the bias predicted from *in vitro* assays and again supports the translatability of these assays to a whole-organism system. Overall, this study supports CMF-019 as an efficacious and biased ligand both *in vitro* and *in vivo*.

5. CMF-019 and MM07 as Disease-Modifying Compounds for Pulmonary Arterial Hypertension *In Vitro* and *In Vivo*

5.1 Introduction

This chapter focuses on PAH, a disease in which both endogenous ligands of the apelin receptor, apelin (Goetze *et al*., 2006, Kim *et al*., 2013, Alastalo *et al*., 2011) and ELA (Yang *et al*., 2017b), have been shown to be downregulated. However, receptor expression is maintained (Andersen *et al*., 2009, Falcao-Pires *et al*., 2009) and crucially remains responsive to [Pyr^{1}]apelin-13 in human patients with PAH (Brash *et al*., 2018). This suggests that replacing the missing endogenous ligands could be a suitable therapeutic strategy for treating the disease. Indeed, it has been demonstrated in the MCT rat model of PAH that exogenous administration of both [Pyr^{1}]apelin-13 (Falcao-Pires *et al*., 2009), the most abundant form in the cardiovascular system (Maguire *et al*., 2009), and ELA-32 (Yang *et al*., 2017b) could prevent disease onset when given by IP injection daily for 21 days. However, both apelin and ELA have limited therapeutic potential being limited by half-life and route of administration. Furthermore, the apelin receptor is a GPCR and repeat stimulation by endogenous molecules will lead to β-arrestin recruitment and internalisation of the receptor, potentially blunting their therapeutic efficacy in the long-term. A preferable strategy is to utilise G protein biased ligands which would not induce receptor internalisation, such as, MM07 and CMF-019.

Having already established that both MM07 and CMF-019 are capable of inducing vasodilatation and cardiac inotropy *in vivo* mimicking the apelin response, an assay assessing prevention of apoptosis in human PAECs was used to study their disease-modifying potential. In the advanced stages of PAH, pathological remodelling of pulmonary vessels occurs including endothelial proliferation and the development of distinctive plexiform lesions which may in part be driven by imbalances in apelin signalling (Andersen *et al*., 2011, Yang *et al*., 2015a). However, in early disease it is thought that endothelial cell apoptosis, leading to vascular dysfunction may drive onset (Wilson *et al*., 1992, Rabinovitch, 2012) and that this is then followed by the hyperproliferation of a population of apoptosis-resistant endothelial cells (Sakao *et al*., 2005). Apelin has been suggested to mitigate this early apoptosis and promotes

survival of pulmonary vascular endothelial cells (Alastalo *et al*., 2011, Kim *et al*., 2013). This suggests that apelin not only benefits the heart and lungs in the disease situation to alleviate symptoms but also addresses the aetiology of the disease itself, something that current therapies do not do. Here the ability of the G protein biased apelin agonists, MM07 and CMF-019, to promote human PAEC survival in response to apoptotic stimulation with TNFα/CHX have been studied. TNFα usually prevents apoptosis of endothelial cells through activation of the NF-κB pathway, however, in conditions of global protein synthesis suppression, such as, with concurrent application of CHX, signalling through TNF-R1 dominates leading to JNK phosphorylation and apoptosis (Wajant *et al*., 2003).

Following assessment of disease-modification *in vitro*, the compounds were evaluated in the MCT rat model of PAH to establish whether they could prevent onset of PAH *in vivo*. This model has been used for decades (Kay *et al*., 1967) and causes PAH as a result of widespread pneumotoxicity (Wilson *et al*., 1989). The model has attracted criticism because it causes a complex multi-organ disease which ultimately results in PAH and RV failure and does not recapitulate all aspects of PAH, such as, the formation of plexiform lesions. However, the model recapitulates many other aspects of human disease, including changes in proximal bronchovascular structures (Colvin and Yeager, 2014). Furthermore, it remains the only animal model of PAH that has successfully translated a therapeutic from the laboratory to the clinic, this was Bosentan, the first endothelin receptor antagonist.

Other models of PAH in both the rat and mouse exist and these have been comprehensively reviewed (Colvin and Yeager, 2014). Studies in mice have often focussed on the genetics of the disease and several genetic models based around the BMPR2 receptor (bone morphogenetic protein receptor type 2), the most mutated gene in human PAH, have been developed (Long *et al*., 2015, West *et al*., 2004, Hong *et al*., 2008). In contrast, in rats where there has been less focus on genetic manipulation, other models have relied upon hypoxia with and without the VEGF receptor 2 inhibitor sugen-5416. Interestingly, hypoxia alone is sufficient to double mean pulmonary arterial pressure and cause structural changes in the pulmonary vasculature but the disease does not progress to RV failure (Taichman and Mandel, 2013), the ultimate cause of death in humans. However, when used in combination with sugen-5416, the disease progresses rapidly and severe PAH with RV failure develops (Taraseviciene-

Stewart *et al*., 2001, Toba *et al*., 2014, Christou *et al*., 2018, Shields *et al*., 2016). This model has also shown potential to develop plexiform lesions, a characteristic trait of human disease (Abe *et al*., 2010), although these only develop at a very late stage of the disease and most probably at a point where disease progression is irretrievable (Toba *et al*., 2014). It has also been suggested that other aspects of the sugen-5416/hypoxia model do not correlate well with human disease and certain aspects of the model may be reversible on return to normoxia (Colvin and Yeager, 2014). Furthermore, the severity of disease caused by sugen-5416/hypoxia raises a significant issue for animal welfare and disease progression can often be so severe that euthanasia is required prior to the end-point of the experiment. For this reason obtaining approval to perform such studies can represent a significant hurdle.

Taking all of the information into account, it was decided that the MCT model was preferable for our purposes, representing a model that recapitulates many aspects of the disease without causing excessive distress. Furthermore, both endogenous agonists of the apelin receptor, apelin and ELA, have prevented disease progression in this model (Falcao-Pires *et al*., 2009, Yang *et al*., 2017b), suggesting that other apelin agonists should similarly be efficacious. Most importantly, the MCT model is the only animal model of PAH that has seen a drug translated into the clinic and therefore, remains the only model that has demonstrated clinical relevance in humans.

This chapter demonstrates that both MM07 and CMF-019 are capable of preventing apoptosis in human PAECs *in vitro* and consequently, are able to protect against what is regarded as one of the key drivers of disease development. However, in the *in vivo* rat MCT model of PAH only MM07 was able to prevent disease progression.

5.2 Methods

5.2.1 Human PAEC Apoptosis Assay

The ability of [Pyr^{1}]apelin-13 (10 µM), MM07 (10µM) and CMF-019 (1-10µM) to rescue TNFα/CHX induced apoptosis of endothelial cells was compared to rhVEGF (10ng/mL) as described in the optimised protocol in Section 2.5. The average induction of apoptosis of the analysed experiments was 19.53±1.76%. Data were normally distributed using the D'Agostino-Pearson omnibus K^2 test and trends were compared using a matched ANOVA to account for variability observed in the basal amount of apoptotic induction observed between replicates. Statistical significance was taken as 5%.

5.2.2 Assessment of CMF-019 Administered Chronically in the Rat MCT Model of PAH

Male Sprague-Dawley rats (209±2g, n=35; Charles River Laboratories, Margate, UK) underwent a MCT prevention protocol as described in Section 2.7.1. CMF-019 (10mg/kg, n=18) or saline (equivalent volume by weight, n=17) were administered as a daily IP injection for 21 days. The MCT CMF-019 group was slightly but significantly heavier than the saline CMF-019 group at the start of the protocol (8.33±3.17, *$p<0.05$). The other groups were not significantly different in weight. The Fulton index, RVSP and LVSP were measured and analysis performed a two-tailed Student's t-test. Although n values were too small to use the recommended D'Agostino-Pearson omnibus K^2 test to test for normality, data were normally distributed using a Shapiro-Wilks test. Statistical significance was taken as 5%.

5.3 Results

5.3.1 Human PAEC Apoptosis Assay

5.3.1.1 Apelin Did Not Rescue Human PAEC Apoptosis Induced by TNFα/CHX

The ability of [Pyr^{1}]apelin-13 to prevent TNFα/CHX induced apoptosis in human PAECs was tested at 10μM (Figure 5.1). TNFα/CHX significantly increased the percentage of annexin^{+}/PI^{-} cells (20.53±1.67%, $^{\#\#\#\#}$p<0.0001) compared to the EBM-2 2% FBS control and rhVEGF was able to partially rescue this (12.20±2.01%, **p<0.01). However, 10μM [Pyr^{1}]apelin-13 provided no significant rescue (1.79±1.10%, ns).

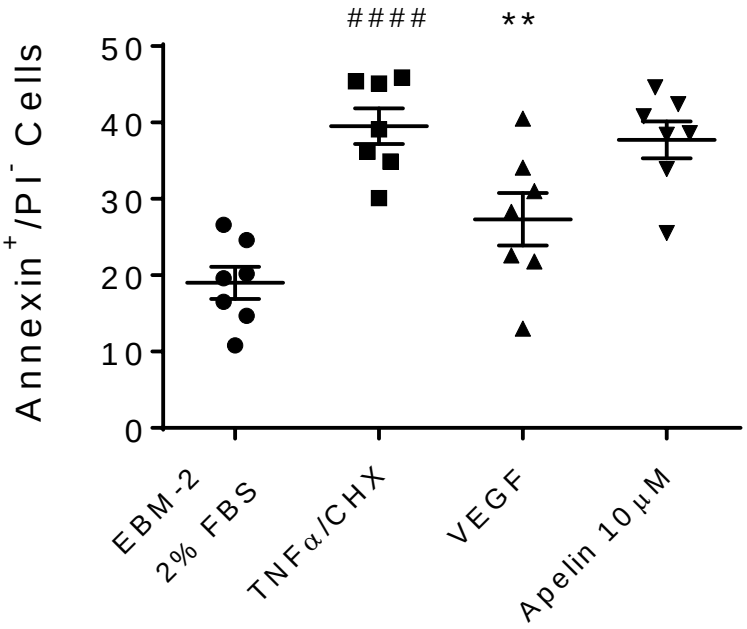

Figure 5.1: Dot plot of the percentage of annexin^{+}/PI^{-} stained human PAECs with mean±SEM data superimposed for 'control' (EBM-2 2%FBS), 'apoptotic' (TNFα/CHX) or cells pre-treated with rhVEGF (10ng/mL) or [Pyr^{1}]apelin-13 (10μM) prior to induction of apoptosis with TNFα/CHX. TNFα/CHX significantly increased the percentage of annexin^{+}/PI^{-} human PAECs and this could be rescued by 10ng/mL rhVEGF but not 10μM [Pyr^{1}]apelin-13. Each dot represents data from one experiment and data were collected from 3 cell lines. A matched ANOVA compared each treatment to TNFα/CHX and statistical significance was taken as 5%. *p<0.05, **p<0.01, ***p<0.001 and ****p<0.0001. #### indicates p<0.0001 compared to control (EBM-2 2% FBS).

5.3.1.2 [Pyr[1]]apelin-13 in Combination with a Protease Inhibitor Cocktail

A potential cause for apelin displaying no rescue of TNFα/CHX induced apoptosis in human PAECs could have been its short half-life and potential instability in media and FBS over the 18 hour incubation time. To attempt to mitigate this as a factor, a protease inhibitor cocktail (PIC) was added to the [Pyr[1]]apelin-13 treatment condition in one experiment. The results are shown in Figure 5.2 and it is clear that the PIC dramatically reduced the apoptotic induction.

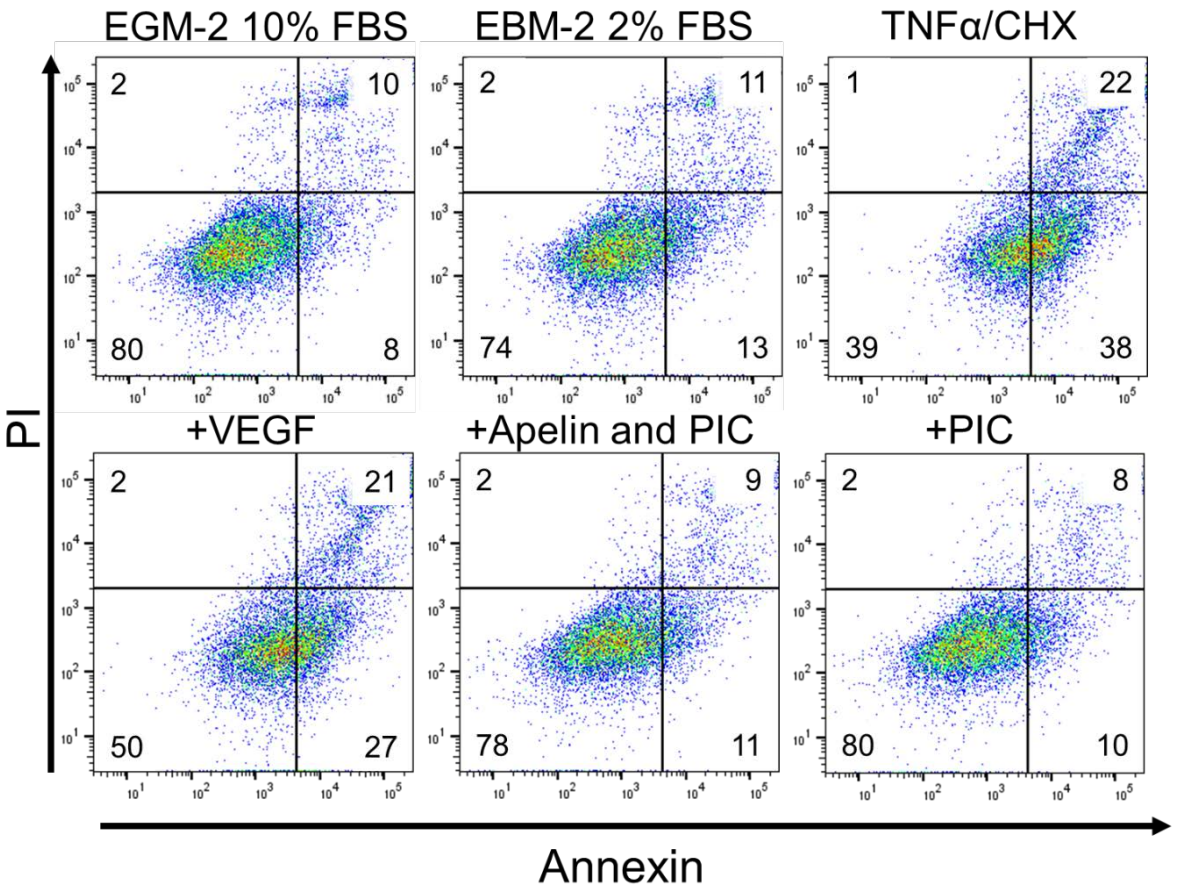

Figure 5.2: Dot plots of annexin staining vs PI staining in human PAECs when 'healthy' (EGM-2 10% FBS), 'control' (EBM-2 2% FBS), 'apoptotic' (TNFα/CHX) or pre-treated with rhVEGF (10ng/mL), [Pyr[1]]apelin-13 + a protease inhibitor cocktail (PIC) or PIC only prior to induction of apoptosis with TNFα/CHX. TNFα/CHX induced apoptosis compared to the EGM-2 10% FBS 'healthy' control and the EBM-2 2% FBS serum and GF starved control. This was partially rescued by rhVEGF and wholly prevented by both conditions using the PIC.

5.3.1.3 [Pyr[1]]apelin-13 Did Not Rescue Human PAEC Apoptosis Induced by Growth Factor and Serum Starvation

The ability of [Pyr[1]]apelin-13 to prevent GF and serum starvation induced apoptosis in human PAECs was tested at 10µM as a control (Figure 5.3). GF and serum starvation significantly increased the percentage of annexin$^+$/PI$^-$ cells (7.58±0.97%, $^{###}$p<0.001) compared to the EGM-2 10% FBS control and rhVEGF was able to completely rescue this (8.05±0.81%, ***p<0.001). However, 10µM [Pyr[1]]apelin-13 provided no significant rescue (0.01±1.32%, ns).

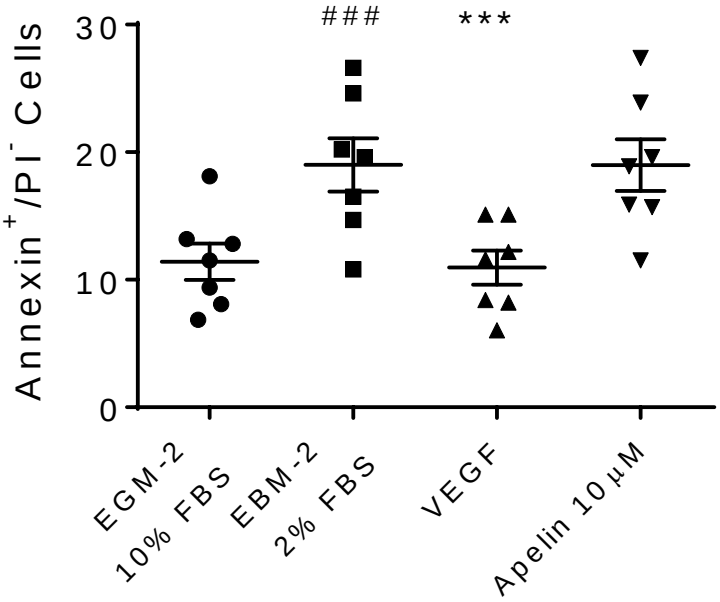

Figure 5.3: Dot plot of the percentage of annexin$^+$/PI$^-$ stained human PAECs with mean±SEM data superimposed when 'healthy' (EGM-2 10%FBS), 'control' (EBM-2 2% FBS) or treated with rhVEGF (10ng/mL) or [Pyr[1]]apelin-13 (10µM). GF and serum starvation (EBM-2 2% FBS) significantly increased the percentage of annexin$^+$/PI$^-$ human PAECs and this could be rescued by 10ng/mL rhVEGF but not 10µM [Pyr[1]]apelin-13. Each dot represents data from one experiment and data were collected from 3 cell lines. A matched ANOVA compared each treatment to the EBM-2 2% FBS condition and statistical significance was taken as 5%. *p<0.05, **p<0.01, ***p<0.001 and ****p<0.0001. ### indicates p<0.001 compared to the 'healthy' control (EGM-2 10% FBS).

5.3.1.4 MM07 and CMF-019 Rescued Human PAEC Apoptosis Induced by TNFα/CHX

The ability of MM07 and CMF-019 to prevent TNFα/CHX induced apoptosis in human PAECs were tested at 10μM and 1-10μM, respectively (Figure 5.4). TNFα/CHX significantly increased the percentage of annexin$^+$/PI$^-$ cells (19.54±1.76%, $^{\#\#\#\#}$p<0.0001) compared to the EBM-2 2% FBS control and rhVEGF was able to partially rescue this (11.59±1.85%, **p<0.01). As with MM07 at 10μM (4.45±0.89%, **p<0.01) and CMF-019 at 1μM (5.66±0.97%, **p<0.01). CMF-019 at 10μM displayed no significant rescue despite trending towards significance (4.38±1.48%, ns).

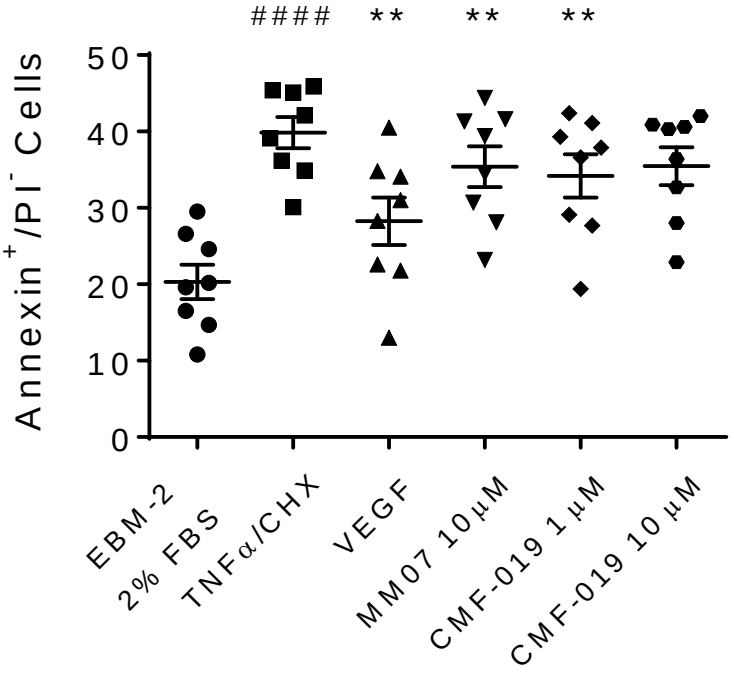

Figure 5.4: Dot plot of the raw percentage of annexin$^+$/PI$^-$ stained human PAECs with mean±SEM data superimposed when 'control' (EBM-2 2% FBS), 'apoptotic' (TNFα/CHX) or pre-treated with rhVEGF, MM07 (10μM) or CMF-019 (1-10μM) prior to induction of apoptosis with TNFα/CHX. TNFα/CHX significantly increased the percentage of annexin$^+$/PI$^-$ human PAECs and this could be rescued by 10ng/mL rhVEGF, MM07 at 10μM and CMF-019 at 1μM also displayed some rescue, however, CMF-019 at 10μM did not. Each dot represents data from one experiment and data were collected from 3 cell lines. A matched ANOVA compared each condition to TNFα/CHX and statistical significance was taken as 5%. *p<0.05, **p<0.01, ***p<0.001 and ****p<0.0001. #### indicates p<0.0001 compared to control (EBM-2 2% FBS). It should be noted that some of the control data points are the same as for the [Pyr^1]apelin-13 experiment in Section 5.3.1.1

5.3.1.5 MM07 and CMF-019 Did Not Rescue Human PAEC Apoptosis Induced by Growth Factor and Serum Starvation

The ability of MM07 and CMF-019 to prevent GF and serum starvation induced apoptosis in human PAECs was tested at 10µM and 1-10µM, respectively, as a control (Figure 5.5). GF and serum starvation significantly increased the percentage of annexin$^+$/PI$^-$ cells (9.33±1.94%, $^{\#\#}$p<0.01) compared to the EGM-2 10% FBS control and rhVEGF was able to completely rescue this (8.86±1.07%, ***p<0.001). However, MM07 at 10 µM (-1.09±0.97%, ns) and CMF-019 at 1 µM (1.04±0.86%, ns) and 10µM (-0.91±0.86%, ns) provided no significant rescue.

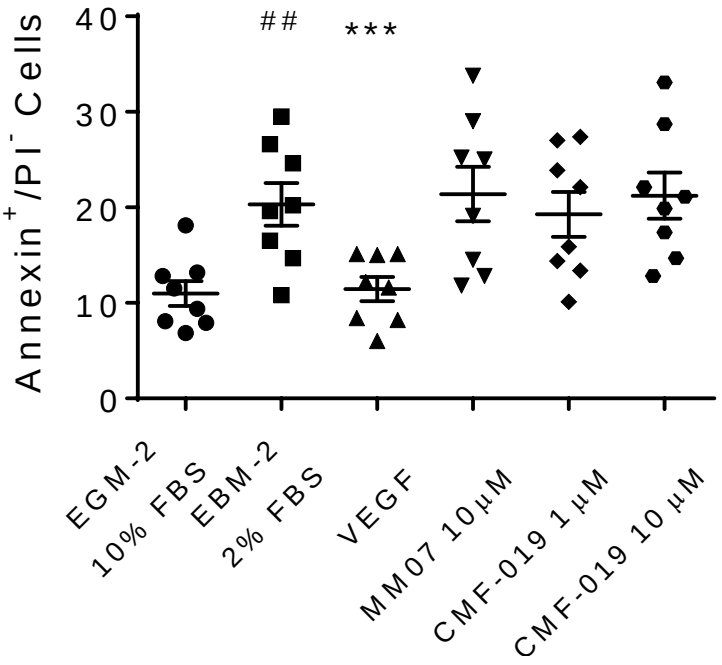

Figure 5.5: Dot plot of the percentage of annexin$^+$/PI$^-$ human PAECs with mean±SEM data superimposed when 'healthy' (EGM-2 10%FBS), 'control' (EBM-2 2%FBS) or treated with rhVEGF (10ng/mL), MM07 (10µM) or CMF-019 (1-10µM). GF and serum starvation (EBM-2 2% FBS) significantly increased the percentage of annexin$^+$/PI$^-$ human PAECs and this could be rescued by 10ng/mL rhVEGF. MM07 and CMF-019 did not rescue. Each dot represents data from one experiment and data were collected from 3 cell lines. A matched ANOVA compared each condition to the EBM-2 2% FBS condition and statistical significance was taken as 5%. *p<0.05, **p<0.01, ***p<0.001 and ****p<0.0001. ## indicates p<0.01 compared to the 'healthy' control (EGM-2 10% FBS). It should be noted that some of the control data points are the same as for the [Pyr^1]apelin-13 experiment in Section 5.3.1.3.

5.3.2 CMF-019 Did Not Prevent the Onset of PAH *In Vivo* in a Rat MCT Model

A single subcutaneous injection of 60mg/kg MCT (n=20) induced PAH in rats compared to an equivalent volume of saline (n=15) as illustrated in the saline treated control groups (Figure 5.6). Rats that received MCT demonstrated elevated RVSP (33.83±4.00mmHg, ****p<0.0001), reduced LVSP (-13.44±5.36mmHg, *p<0.05), increased RV hypertrophy (Fulton Index; 0.20±0.03, ****p<0.0001) and reduced body weights (-38.14±11.39g, **p<0.01).

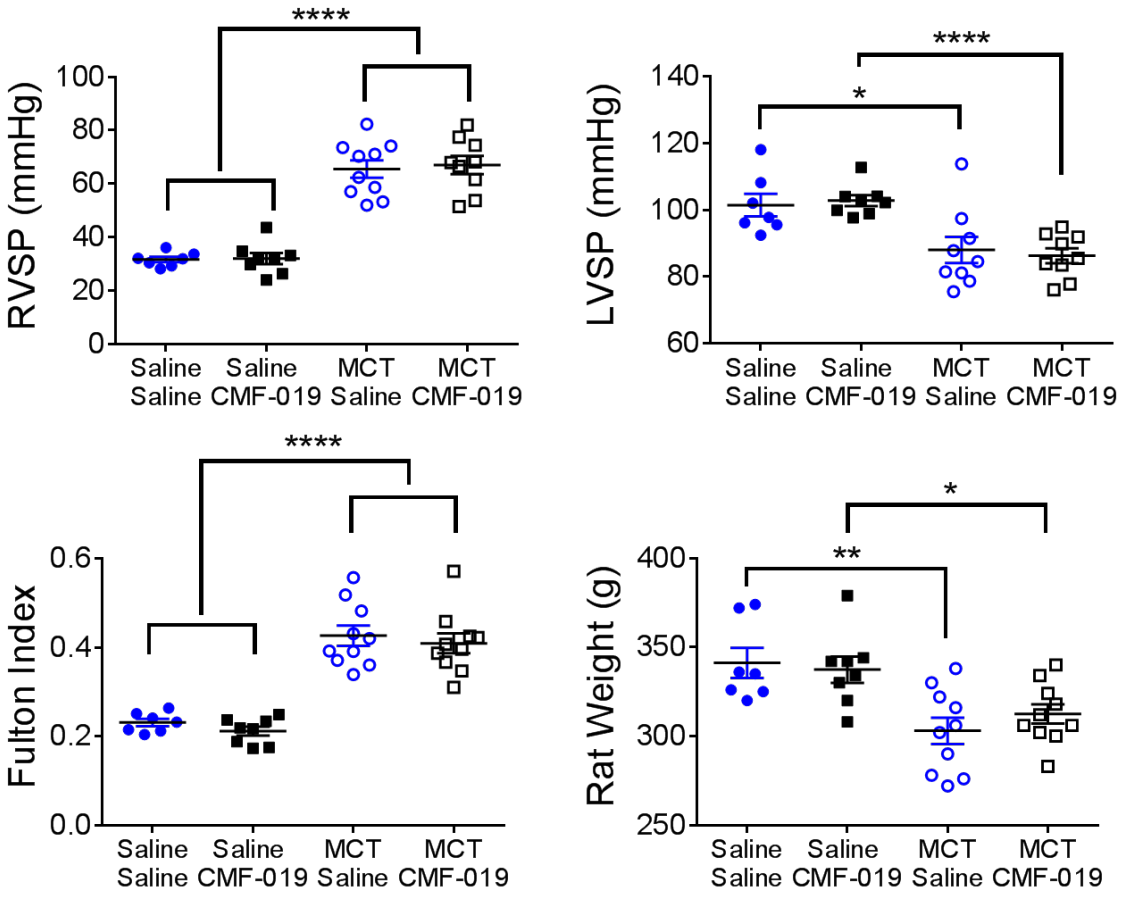

Figure 5.6: Terminal (day 21) measurements from a rat MCT-induced model of PAH assessing CMF-019 as a preventative therapeutic agent. Male Sprague-Dawley rats (n=35) received a subcutaneous injection of saline (n=15) or MCT (n=20) followed by 21 days of either daily IP injections of saline (n=17) or CMF-019 (n=18). The MCT animals displayed increased RVSPs and Fulton indices with reduced LVSPs and weights. There were no differences between saline and CMF-019 receiving MCT animals. Data were compared using a two-tailed Student's t-test and statistical significance was taken as 5%. *p<0.05, **p<0.01, ***p<0.001 and ****p<0.0001

CMF-019 administered daily by IP injection for 21 days at 10mg/kg showed no improvements compared to saline controls in preventing the onset of PAH in these MCT-treated animals. Compared to their corresponding saline CMF-019 treated controls, they also displayed elevated right ventricular systolic pressures (RVSP; 35.06±4.13mmHg, ****p<0.0001), reduced LVSP (-16.54±2.81mmHg, ****p<0.0001), increased RV hypertrophy (Fulton Index; 0.20±0.03, ****p<0.0001) and reduced body weights (-24.88±8.92g, *p<0.05).

5.4 Discussion

5.4.1 MM07 and CMF-019 are Disease-Modifying *In Vitro*

Current therapeutics for PAH, such as prostanoid infusions and endothelin antagonists, work by relieving pulmonary vasoconstriction to reduce pulmonary pressure and alleviate afterload on the RV. However, they do not benefit the heart itself to reduce remodelling and ultimately failure of the RV still leads to mortality. Moreover, they are only symptomatic and do not address the underlying cause of the pulmonary vasoconstriction and hypertension, the drivers of disease. Apelin is advantageous in both these regards. It acts as a vasodilator and an inotrope to provide benefit to the pulmonary vasculature and the heart. Furthermore, there is growing evidence that it may be able to alleviate disease progression by protecting the pulmonary vasculature, particularly by preventing endothelial damage in the early stages of the disease (Alastalo *et al*., 2011, Kim *et al*., 2013, Sakao *et al*., 2005). To this end, an apoptosis assay in human PAECs (Long *et al*., 2015) was employed (following optimisation and adaptation as detailed in Section 2.5) to assess the disease-modifying potential of apelin mimetics. This assay utilised TNFα/CHX to induce apoptosis in human PAECs which was subsequently measured by annexin V-FITC and PI staining detected by flow cytometry.

Initially, [Pyr^{1}]apelin-13 was used to assess whether rescue of apoptosis could be achieved with the endogenous agonist; however, none was observed either in the TNFα/CHX treated or the serum and GF starved control arm of the experiment. This could have been due to instability of the endogenous peptide during the 18 hour incubation time in media and FBS, the latter of which likely contains a number of proteases. To overcome this, a PIC was added to the apelin-treated wells. In both the apelin and PIC control wells, there was a substantial reduction in apoptosis. Such a result is unsurprising as inhibiting proteases within the experiment would effectively negate the effects of CHX by enhancing longevity of cellular peptides. Thus, without protein synthesis inhibition, TNFα functions to a greater extent through the antiapoptotic NF-κB pathway rather than promoting JNK phosphorylation and enhancing apoptosis. While this experiment did not establish whether apelin is capable of preventing TNFα/CHX induced apoptosis in human PAECs, it did act as an effective control for the experiment and confirm the necessity of protein synthesis inhibition by CHX for TNFα-induced apoptosis.

Alternatively, it is well known that media and serum contain a large number of plasma binding proteins and these might have acted as a reservoir, reducing the amount of free [Pyr^{1}]apelin-13 available to bind to the apelin receptor. To overcome this, cells were serum starved in 2% FBS prior to experimentation and a relatively high 10µM concentration of [Pyr^{1}]apelin-13 was used. It was decided not to serum starve with concentrations below 2% FBS as the aim was to induce apoptosis from a relatively healthy initial human PAEC population. This should better mimic early disease, where healthy human PAECs undergo apoptosis and also provide a larger window because healthy cells would be more prone to apoptotic stimuli, having not been conditioned previously. Given this, the concentrations of apelin were comparative to previous studies that have shown in 0.5% FBS serum starved PAECs apelin at 0.1µM promoted survival (Alastalo *et al*., 2011) and that 1µM was sufficient to lead to miRNA expression changes (Kim *et al*., 2013).

Even though [Pyr^{1}]apelin-13 was unable to rescue apoptosis induced by TNFα/CHX, MM07 and CMF-019 were nonetheless tested in the assay as they have greater predicted *in vitro* stability. Again similar concentrations to those with [Pyr^{1}]apelin-13 were used to overcome potential plasma protein binding. Both MM07 (10µM) and CMF-019 (1µM) displayed significant rescue, with CMF-019 at 10µM trending towards significance. The rescue of both compounds was approximately 50% of that observed for the positive control, rhVEGF, and supports a role for apelin agonists in preventing endothelial damage in healthy human PAECs when challenged with an apoptotic stimulus. The mechanism by which this occurs is not well characterised; however, both [Pyr^{1}]apelin-13 and ELA-32, endogenous agonists of the apelin receptor, promote ERK1/2 phosphorylation in human PAECs (Yang *et al*., 2017b), while some apelin isoforms have been shown to downregulate the JNK and p-38 pathways in osteoblasts (Tang *et al*., 2007) and neurons (Liu *et al*., 2018). These pathways both have known roles in apoptosis and are thought to be key ways that rhVEGF prevents apoptosis in endothelial cells induced by serum and GF starvation. Furthermore, there is evidence that apelin regulates myocyte enhancer factor 2 , which in turn activates miR-424/miR-503 and genes contributing to endothelial homeostasis. This axis may also be beneficial in PAH by acting on pulmonary arterial smooth muscle cells. Here it inhibits the expression of fibroblast growth factor 2 and its receptor, and thus exerts anti-proliferative effects, potentially preventing their over-proliferation and the subsequent

vessel muscularisation that contributes to elevated pulmonary pressures (Alastalo *et al*., 2011, Kim *et al*., 2013, Kim *et al*., 2015, Helenius *et al*., 2015). Finally, agents that activate apelin expression or act as downstream effectors of apelin signalling have demonstrated beneficial effects in PAH animal models (Kim *et al*., 2013, Nickel *et al*., 2015, Spiekerkoetter *et al*., 2013, Bertero *et al*., 2014).

Interestingly, neither MM07 nor CMF-019 rescued apoptosis induced by serum and GF starvation in the control arm of the experiment, although the positive control rhVEGF did. This suggests that rescue from serum and GF starvation is through a different mechanism to rescue from TNFα/CHX induced apoptosis. GF and serum starvation is something that has been widely observed in various endothelial cell lines (Gama Sosa *et al*., 2016, Gerber *et al*., 1998b, Karsan *et al*., 1997, Ueda *et al*., 2005, Date *et al*., 2005, Raymond *et al*., 2004) and the mechanisms for rescue with rhVEGF are thought to occur by both upregulation of the MAPK/ERK pathway alongside downregulation of JNK pathway (Gupta *et al*., 1999), leading to enhanced bcl-2 and decreased bax signalling (Gerber *et al*., 1998a, Ueda *et al*., 2005, Karsan *et al*., 1997). In contrast, TNFα/CHX stimulates apoptosis primarily through the TNF-R1 leading to induction of the JNK and p-38 MAPK pathways. As discussed earlier, both [Pyr^{1}]apelin-13 and ELA-32 have been shown to promote ERK1/2 phosphorylation in human PAECs (Yang *et al*., 2017b), while some apelin isoforms have been shown to downregulate the JNK and p-38 pathways in osteoblasts (Tang *et al*., 2007) and neurons (Liu *et al*., 2018). This suggests that the apelin mimetics might be promoting rescue through similar mechanisms to rhVEGF and does not explain why they do not promote rescue in response to serum and GF starvation. On balance there is greater evidence of apelin promoting ERK/MAPK signalling, especially in PAECs, and perhaps activation of this pathway was more efficacious in rescuing from JNK/p-38 mediated apoptosis induced by TNFα/CHX, rather than the more multi-factorial apoptotic mechanisms induced by serum and GF starvation.

Overall, it was considered appropriate to exclude experiments where there was limited or no induction of apoptosis by TNFα/CHX, such as with donors 4 and 5, since the mechanisms of apoptotic induction were different and would, therefore, impact upon the mechanisms of rescue. Both MM07 and CMF-019 rescued healthy endothelial cells from apoptosis in conditions induced by a severe stimulus using TNFα/CHX but not by

a weaker stimulus using GF and serum starvation, suggesting that they could be more beneficial as disease modifiers in early severe disease driving pathology.

It is arguable that such benefits in the context of early disease development may not be translatable to a therapeutic setting where the disease is already established. As such it would be interesting to assess whether CMF-019 and MM07 could have beneficial effects on HPAECs taken from patients with established disease. However, HPAECs from PAH patients are rare, difficult to obtain and since from pathological tissue likely reflect end-stage disease and not the progressive disease pathology. It is hoped that new methodologies, such as the use of blood outgrowth endothelial cells (Ormiston *et al*., 2015), might enable the production of stable cell lines from patients with established disease. Given these current limitations, it was decided to perform experiments on HPAEC lines from 'healthy' donors and therefore, assess early disease pathology as a proof-of-concept for the benefits of apelin agonism.

5.4.2 MM07 Prevents PAH Progression in an MCT Model

A MCT prevention study of PAH using MM07 (1mg/kg) injected IP for 21 days was performed by Peiran (Brian) Yang (Yang *et al*., 2018 *In Revision)*. This study showed that in addition to acting as a disease-modifier in human PAECs *in vitro*, MM07 could prevent the onset of PAH *in vivo*. MM07-injected rats were shown to have significantly lower RVSP in response to MCT exposure compared to those not treated with MM07, as well as less pronounced MCT-induced RV hypertrophy. Additionally, MM07 attenuated pulmonary vascular remodelling with reduced arteriolar muscularisation and wall thickening, mitigating a key driving feature in the pathogenesis of PAH (Rabinovitch, 2012, Morrell *et al*., 2016). This evidence of disease-modification *in vivo* strongly supports the observation that MM07 is capable of protecting human PAECs *in vitro*.

5.4.3 CMF-019 Did Not Prevent the Onset of PAH in an MCT Rat Model

Having established that CMF-019 could reduce TNFα/CHX induced apoptosis of disease relevant human PAECs *in vitro* and that such a result with MM07 translated to efficacy *in vivo* in an MCT prevention study of PAH, it was tested whether CMF-019 had similar therapeutic potential. The MCT rat model of PAH was chosen as a model that recapitulates many aspects of human disease without causing excessive distress to the animal. Furthermore, both endogenous agonists of the apelin receptor, apelin

and ELA, as well as the apelin mimetic, MM07, have demonstrated efficacy in the model (Falcao-Pires *et al*., 2009, Yang *et al*., 2017b). However, most importantly the MCT model is the only animal model of PAH that has enabled translation from the laboratory bench to the clinic and therefore, remains the only model that has demonstrated clinical relevance in humans.

In this study, MCT robustly induced PAH in male Sprague-Dawley rats; however, this was not prevented by CMF-019. CMF-019 displayed great promise in early *in vitro* studies demonstrating high binding affinity and efficacy at the apelin receptor, as well as disease-modifying potential in human PAECs. Furthermore, it showed activity *in vivo* and looked promising as a potential therapeutic, therefore, it is surprising that it was unsuccessful in preventing disease and there are a number of reasons why this might be.

One reason could have been the severity of disease observed in these animals. The average RVSP in the saline control MCT group was 65.44±3.23mmHg and PAH is defined when the pulmonary pressure exceeds 20mmHg. Therefore, these animals had dramatically elevated RVSPs and subsequent analysis of the Fulton index confirmed that they also had severely hypertrophied hearts. Furthermore, it was observed that the LVSPs were reduced in the MCT-treated animals suggesting that the hypertrophy of the RV was severe enough to compromise LV function. It is possible that the severe onset of the disease contributed to the lack of apparent efficacy of CMF-019.

Another potential issue with CMF-019 could have been the pharmacokinetics of the compound. It has already been discussed for the acute *in vivo* studies in Chapter 4 that doses of CMF-019 were limited by solubility. A potassium salt form of the compound was used and to overcome this and dissolved in pH9 saline. Following the first *in vivo* studies, plasma concentrations of CMF-019 were found to be substantially lower than the predicted concentrations following injection. This suggests that CMF-019 is not stable *in vivo*, despite computational studies suggesting it has a beneficial pharmacokinetic profile and may explain the limited responses observed acutely. Nevertheless, receptor occupancy calculations using the measured plasma concentrations of CMF-019 at the terminal end-point suggested that receptor occupancy would still be in excess of 99% even with this potential instability, yet responses to CMF-019 were smaller than those with [Pyr^{1}]apelin-13. These responses

should still have been sufficient to observe some benefit and it was hoped that potential issues might be overcome by regular daily dosing and the strong plasma binding of the molecule could have been beneficial in a long-term study. However, despite the maximal concentration attainable with CMF-019 (10mg/kg) being administered, there was insufficient target engagement to prevent PAH onset.

It is possible that high plasma protein binding restricted the amount reaching the receptor target and combined with a high clearance any free drug was rapidly metabolised. Equally, IP administration and low solubility could have resulted in the compound precipitating in the IP cavity. This might prevent the compound reaching the circulation and ultimately the target. These potential limiting factors, combined with the severity of disease in these animals, were the likely reasons that a beneficial therapeutic effect could not be observed. To better establish the reasons for the lack of efficacy of CMF-019 *in vivo*, a thorough pharmacokinetic analysis is required, such that newer molecules might be identified that do not possess the same limitations.

5.5 Conclusions

The purpose of this study was to assess the disease-modifying potential of MM07 and CMF-019 as G protein biased apelin agonists. It has previously been shown that both [Pyr^{1}]apelin-13 and ELA-32 can prevent disease progression in an MCT rat model of PAH. Moreover, there is growing evidence that the benefits of apelin may not only be due to haemodynamic alleviation of the disease but also through addressing disease aetiology within the pulmonary vasculature.

In this study, both MM07 and CMF-019 were effective in preventing apoptosis induced in healthy human PAECs *in vitro*, suggesting that they could be beneficial in preventing early disease onset in PAH. For MM07 this translated to an *in vivo* MCT prevention study of PAH where it displayed protection from RV hypertrophy and elevated RVSPs. Crucially, MM07-treated animals also showed improvements in pulmonary vascular remodelling, the driver of disease, with reduced pulmonary artery wall thickening and muscularisation. The beneficial effects seen with MM07 were not mimicked by CMF-019, despite similar results being obtained *in vitro*. The reason for this could have been instability or metabolic clearance of the small molecule when administered to a whole organism system and pharmacokinetic study of the molecule would be necessary to address this issue.

6. An Apelin Mimetic Peptide, MM202, Linked to an Anti-Serum Albumin Domain Antibody (AlbudAb™) is Efficacious *In Vitro* and *In Vivo*

6.1 Introduction

Previous chapters have focussed on identifying a biased small molecule apelin agonist to overcome the potential limitations of apelin and ELA as peptides in terms of bioavailability and half-life. An alternative approach is to utilise modified peptide mimetics which would have a selectivity advantage over small molecules by making use of highly specific protein-protein interactions. Appropriate modifications could be used to increase half-life and although unlikely to improve bioavailability, could vastly decrease the frequency of administration required, thus effectively negating this as a limitation. To date such approaches in the apelin signalling system have used unnatural amino acids, PEGylation and cyclisation, all of which have been discussed previously in Section 1.4.

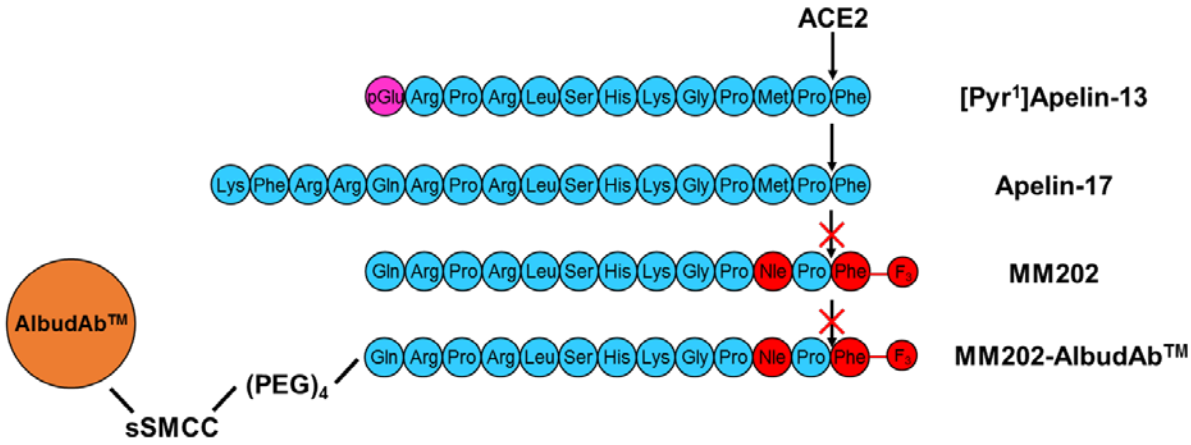

Figure 6.1: The structures of the endogenous peptides, [Pyr¹]apelin-13 and apelin-17, the analogue, MM202, and the MM202-AlbudAb™ construct. Substituted residues in MM202 are shown in red, pyroglutamate in pink and AlbudAb™ in orange. MM202 features a norleucine substituted for methionine to improve stability by reducing propensity for oxidation during subsequent reaction stages. Meanwhile, the tri-fluoro group attached to phenylalanine improves stability by reducing C-terminal cleavage by ACE2. In the AlbudAb™ construct, MM202 has first been linked to a PEG chain and then via a sulpho-SMCC (sulphosuccinimidyl 4-(N-maleimidomethyl)cyclohexane-1-carboxylate) linker to the AlbudAb™ moiety using maleimide chemistry.

In this study, a peptide mimetic, MM202, featuring unnatural amino acids has been generated and then linked chemically using sSMCC (sulphosuccinimidyl 4-(N-maleimidomethyl)cyclohexane-1-carboxylate) and maleimide chemistry via a $(PEG)_4$ linker to an AlbudAb™ construct (Figure 6.1). The purpose of the norleucine

substitution was to reduce the potential for oxidation of the methionine in the subsequent chemical manipulation of the molecule. The unnatural tri-fluoro phenylalanine amino acid and the $(PEG)_4$ linker were used to reduce proteolysis by protecting the peptide from peptidase degradation, especially ACE2 cleavage of the C-terminal phenylalanine. Meanwhile, the AlbudAb™ construct was to bind the molecule to HSA, therefore, retaining the molecule in the plasma and reducing renal clearance by preventing glomerular filtration.

The MM202-AlbudAb™ construct represents a novel approach to drug design. Although molecules have previously been conjugated to AlbudAb™ (Bao *et al*., 2013, O'Connor-Semmes *et al*., 2014, Goodall *et al*., 2015, Lin *et al*., 2015, Walker *et al*., 2010, Holt *et al*., 2008), these have been conjugated genetically and used endogenous molecules. An example of such a conjugation is the GLP-1 AlbudAb™ conjugate, GSK2374697, which has progressed to phase I clinical trials (Lin *et al*., 2015). The construct has demonstrated an improved half-life in humans of 6-10 days compared to ~5 minutes for the endogenous molecule and crucially demonstrated retention of GLP-1 receptor agonism (O'Connor-Semmes *et al*., 2014). Therefore, conjugation of endogenous molecules already presents a significant therapeutic advantage.

The study presented here demonstrates further improvements on the use of the AlbudAb™ platform. This is the first time that a molecule has been conjugated to AlbudAb™ chemically and the first time that a non-endogenous molecule featuring unnatural amino acids has been used. This process is possible because the AlbudAb™ has been modified such that it possesses only one cysteine residue at position 108, distant from the albumin binding domain. Using maleimide chemistry the thiol group on this cysteine could be linked to an sSMCC reagent with high efficiency (>95%). Subsequently, the sSMCC due to its possession of a thiol, as well as a maleimide group, could then be further combined with the MM202-$(PEG)_4$ construct using the same chemical reaction.

This proof-of-principle represents a great advance in the potential use of the AlbudAb™ platform by enabling conjugation of molecules that are not liable to proteolytic degradation, unlike previously used endogenous molecules, such as GLP-1. In this study, the MM202-AlbudAb™ conjugate has been pharmacologically characterised and crucially shown to retain ligand binding and *in vivo* activity.

6.2 Methods

6.2.1 Materials

MM202 was covalently bonded to AlbudAb™ using sSMCC (sulphosuccinimidyl 4-(N-maleimidomethyl)cyclohexane-1-carboxylate) and maleimide chemistry via a $(PEG)_4$ linker at the pyroglutamate on the N-terminus to retain binding at the apelin receptor as previously outlined in Patent WO 2012022703 (Holt *et al*., 2008). This strategy was selected based on extensive structure-activity relationship data that indicate that substitutions at the N-terminus of the ligand are well tolerated by the apelin receptor.

6.2.2 Competitive Radioligand Binding Assays

Competitive radioligand binding assays were performed in human LV homogenates (1.5mg/mL) using [Glp^{65},Nle^{75},Tyr^{77}][^{125}I]apelin-13 (0.1nmol/L) and increasing concentrations of [Pyr^{1}]apelin-13 (1pmol/L-5µmol/L), apelin-17 (1fmol/L-0.1µmol/L), MM202 (1fmol/L-0.1µmol/L) and MM202-AlbudAb™ (0.5pmol/L-1µmol/L) as previously described in Section 2.3. Binding in the presence of 2µmol/L of [Pyr^{1}]apelin-13 was considered to be non-specific.

6.2.3 Cell Signalling Assays

6.2.3.1 β-Arrestin Assay

[Pyr^{1}]apelin-13 (0.1pmol/L-1µmol/L), apelin-17 (1pmol/L-1µmol/L), MM202 (10fmol/L-3nmol/L) and MM202-AlbudAb™ (1pmol/L-0.1µmol/L) were screened for their ability to recruit β-arrestin to the apelin receptor in a CHO based cell assay as described in Section 2.4.1.

6.2.3.2 cAMP Assay

[Pyr^{1}]apelin-13 (1pmol/L-30nmol/L), apelin-17 (1pmol/L-30nmol/L), MM202 (1pmol/L-30nmol/L) and MM202-AlbudAb™ (10pmol/L-1nmol/L) were screened for their ability to reduce cAMP expression following forskolin stimulation in a CHO based cell assay as described in Section 2.4.2.

6.2.4 *In Vivo* LV and Femoral Artery Catheterisation for Measurement of Acute Cardiovascular Changes upon Administration of MM202-AlbudAb™

Male Sprague-Dawley rats (266±5g, n=27; Charles River Laboratories, Margate, UK) underwent jugular vein cannulation and LV and femoral artery catheterisation as described in Section 2.7.1. A first dose of either saline (0.9%, 0.5mL, Macopharma, n=12) or the MM202-AlbudAb™ conjugate (5nmol, 0.5mL) was administered to randomly chosen animals. Animals then received a second cumulative dose of [Pyr^{1}]apelin-13 (50nmol, 0.5mL). All doses were followed by a saline flush (0.9%, 0.1mL, Macopharma) to clear the cannula. In a preliminary study not using a femoral artery catheter, MM202 (n=2, 5, 50nmol, 0.5mL) was administered to see if responses were similar to the conjugated form.

6.2.5 A Time-Course in Heparinised Human Plasma *Ex Vivo* to Determine Compound Half-life

[Pyr^{1}]apelin-13, MM202 and MM202-AlbudAb™ (0.3 and 3nmol/L) were incubated in heparinised human plasma samples *ex vivo* (n=3) at 37ºC. 0.3nmol/L and 3nmol/L concentrations were chosen as they cross-reacted near the top of the linear portion of the [Pyr^{1}]apelin-13 standard curve (Figure 6.2). Heparinised blood was used as EDTA would likely have impacted on the half-lives measured by inhibiting proteases. Samples were snap-frozen at 30seconds, 5minutes, 15minutes, 1hour, 2hours and 24hours and subsequently run in an ELISA as detailed in Section 2.8. Cross-reactivity of all three peptides in the ELISA displayed parallelism over the same concentration range (Figure 6.2) and consequently plasma concentrations were calculated by interpolation from the [Pyr^{1}]apelin-13 standard curve. Plasma half-lives of the compounds were calculated by fitting the interpolated data to a single exponential curve (GraphPad Prism™).

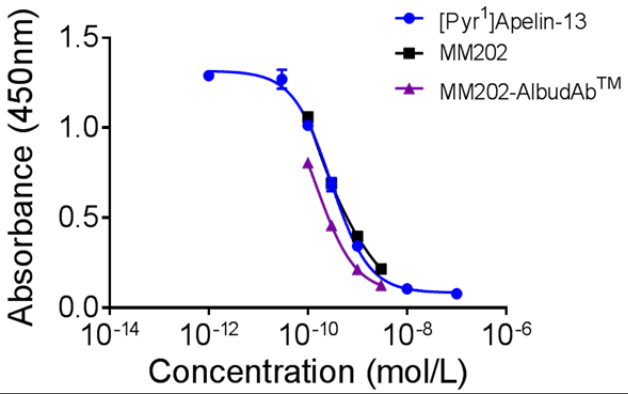

Figure 6.2: Concentration vs absorbance at 450nm for [Pyr^{1}]apelin-13, MM202 and MM202-AlbudAb™ in an ELISA. MM202 and MM202-AlbudAb™ cross-reacted and displayed parallelism over the same concentration range as the [Pyr^{1}]apelin-13 standard.

6.2.6 A Rat MCT Prevention Study of PAH Using MM202-AlbudAb™

Male Sprague-Dawley rats (213±2g, n=31; Charles River Laboratories, Margate, UK) underwent a MCT prevention protocol as described in Section 2.7.2. They received either IP injections of MM202-AlbudAb™ (1mg/kg, n=14) twice weekly or saline (equivalent volume by weight, n=17) daily for 21 days. The Fulton index, RVSP and LVSP were measured and analysis performed as described. Blood samples were collected in heparin-coated tubes during exsanguination following catheterisation.

6.2.6.1 Analysis of Plasma Samples by ELISA

Heparinised blood samples from each treatment group (n=6) were run in an ELISA as detailed in Section 2.8. Since cross-reactivity of MM202-AlbudAb™ occurred under the same concentration range as [Pyr^1]apelin-13 (Figure 6.2), plasma concentrations were calculated by interpolation from the [Pyr^1]apelin-13 standard curve.

6.2.7 Statistical Analysis

Binding experiments were performed in triplicate and K_i±SEM values calculated using the Cheng-Prusoff methodology. Cell based screening assays were performed in triplicate and presented as pD_2±SEM values. ELISAs were performed in duplicate and data are presented as mean±SEM. For the human plasma time-course, data were fitted to a single exponential curve to determine half-life and the 3nmol/L data compared using a two-tailed Student's t-test. For rat samples collected following chronic administration and *in vivo* analysis, data were compared using a two-tailed Student's t-test. Statistical significance was taken as 5%.

6.3 Results

6.3.1 Apelin-17 Displayed Similar Binding and Potency in Functional Assays to [Pyr^{1}]apelin-13

Apelin-17 bound to the native apelin receptor in human LV homogenates (pK_i=9.57±0.08) with approximately 7-fold greater binding affinity than [Pyr^{1}]apelin-13 (pK_i=8.82±0.05; Figure 6.3). In functional assays, whereas [Pyr^{1}]apelin-13 was approximately 10-fold more potent in the cAMP inhibition (pD_2=9.52±0.05) than β-arrestin (pD_2=8.53±0.03) signalling assay, apelin-17 was equipotent in both (pD_2=10.31±0.28 and 10.15±0.13, respectively; Figure 6.4).

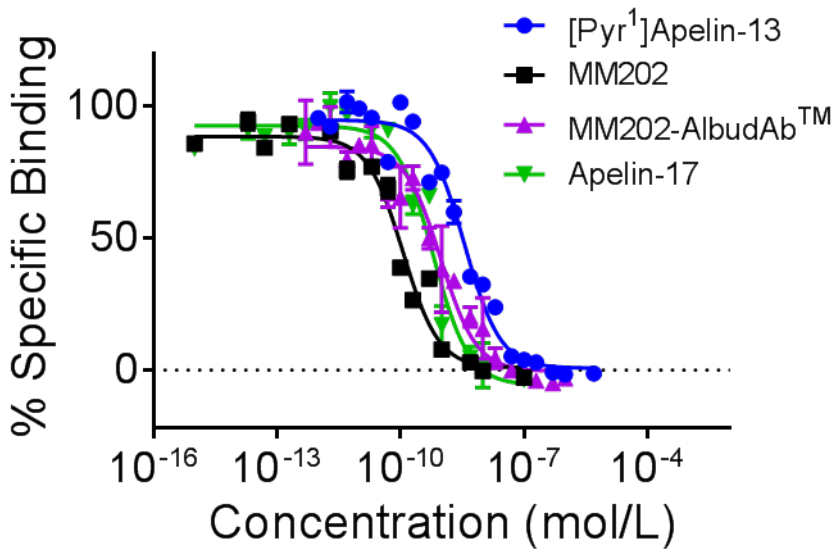

Figure 6.3: Competition radioligand binding of the endogenous peptides [Pyr^{1}]apelin-13 and apelin-17, as well as the synthetic peptide MM202 and its albudAb™ conjugate against [Glp65,Nle75,Tyr77][^{125}I]apelin-13 in human LV homogenates. All peptides competed with similar nanomolar affinities at the human apelin receptor.

6.3.2 MM202 and MM202-AlbudAb™ Bound with High Affinity Comparable to the Endogenous Agonist, [Pyr^{1}]apelin-13, at the Native Human Apelin Receptor

In competitive radioligand binding assays, MM202 bound to the native apelin receptor in human LV homogenates with high nanomolar affinity (pK_i=10.24±0.07). This was ten-fold greater than the endogenous peptide, [Pyr^{1}]apelin-13 (pK_i=8.82±0.05). Conjugating MM202 to AlbudAb™ slightly decreased the binding affinity of MM202 (pK_i=9.39±0.09; Figure 6.3).

6.3.3 MM202 and MM202-AlbudAb™ Displayed Functional Activity in Cell-Based Signalling Assays with Similar or Greater Potency than the Endogenous Agonist [Pyr¹]apelin-13

MM202 was able to recruit β-arrestin to the human apelin receptor in a CHO cell signalling assay (pD_2=10.71±0.58) with much greater potency than the endogenous agonist [Pyr¹]apelin-13 (pD_2=8.52±0.06; Figure 6.4A). It was also able to inhibit cAMP stimulated by forskolin (pD_2=9.96±0.14) with similar potency to [Pyr¹]apelin-13 (pD_2=9.70±0.08; Figure 6.4B). MM202, therefore, displayed considerable β-arrestin signalling bias. In both assays, the E_{MAX} values for MM202 were similar to [Pyr¹]apelin-13, suggesting it acts as a full agonist through both pathways. Conjugating AlbudAb™ to MM202 reduced potency in the β-arrestin assay (pD_2=9.26±0.03; Figure 6.4A) but to a lesser extent in the cAMP inhibition assay (pD_2=9.15±0.12; Figure 6,4B), leading to a reduction in the degree of biased signalling at the receptor. The conjugate also acted as a full agonist at the receptor.

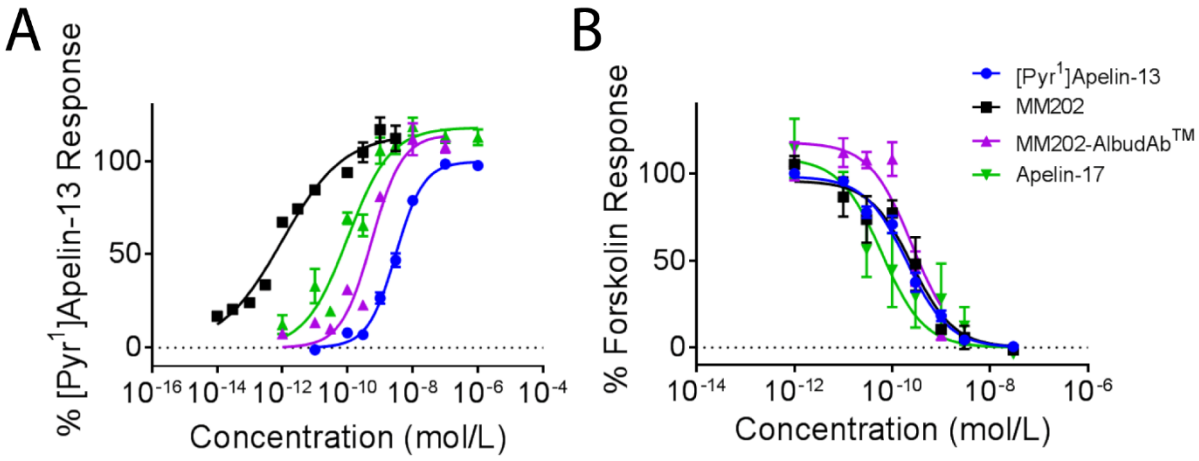

Figure 6.4: The functional activities of the endogenous peptides [Pyr¹]apelin-13 and apelin-17, as well as the synthetic peptide MM202 and its AlbudAb™ conjugate in human apelin receptor expressing CHO cell β-arrestin recruitment (A) and cAMP inhibition assays (B). In the β-arrestin assay the potencies generally corresponded to the rank order of the binding affinities, however, for cAMP inhibition they all displayed similar activity.

6.3.4 MM202-AlbudAb™ Produced Acute Cardiovascular Responses *In Vivo* in Normotensive Male Sprague-Dawley Rats

Bolus injections of the MM202-AlbudAb™ conjugate (5nmol, 0.5mL, n=15) through the jugular vein resulted in robust cardiovascular responses compared to saline (0.5mL, n=12) in normotensive male Sprague-Dawley rats (Figure 6.5). There was a small but significant difference in weight between the two groups with the treatment group 24.7±8.60g (**p<0.01) heavier than the saline group (data not shown). The LVSP was reduced by 6.61±1.46mmHg (***p<0.001) and the arterial pressure underwent a greater drop of 14.12±3.35mmHg (**p<0.01). The dp/dt_{MAX}, a measure of cardiac contractility, increased by 533±170mmHg/s (**p<0.01), meanwhile the dp/dt_{MIN} a measure of cardiac relaxation (where a negative value indicates greater relaxation) increased but by a smaller margin of 381±178mmHg (*p<0.05, data not shown). Additionally, the cardiac output increased by 1277±190RVU/min (****p<0.0001) and this was mirrored by an increase in stroke volume of 3.09±0.47RVU (****p<0.0001), as well as a small but significant increase in heart rate of 4.64±2.24BPM (*p<0.05).

These effects were very similar to those obtained with MM202 alone in a preliminary study at the same concentration (5nmol, 0.5mL, n=2). MM202 showed a dose-dependent cardiovascular action (Table 6.1) to elicit a reduction in LVSP and to increase cardiac output and increase contractility in a manner comparable to [Pyr[1]]apelin-13. Effects at the higher concentration of MM202 (50nmol, 0.5mL, n=2) were similar or greater than that obtained with the 400nmol bolus administration of [Pyr[1]]apelin-13 as previously reported in Section 4.3.2. The lower dose of MM202 (5nmol) was equivalent to the maximal attainable dose that could be administered of the MM202-AlbudAb™ conjugate.

Change in Cardiovascular Parameter	Dose 1 5nmol	Dose 2 50nmol
LVSP (mmHg)	-8.3	-30.76
dp/dt_{MAX} (mmHg/s)	693	4741
Cardiac Output (RVU/min)	2254	4900
Stroke Volume (RVU)	5.53	13.02
Heart Rate (BPM)	1.99	7.22

Table 6.1: Average changes in cardiovascular parameters from baseline values following bolus administration of MM202 (5-50nmol, n=2).

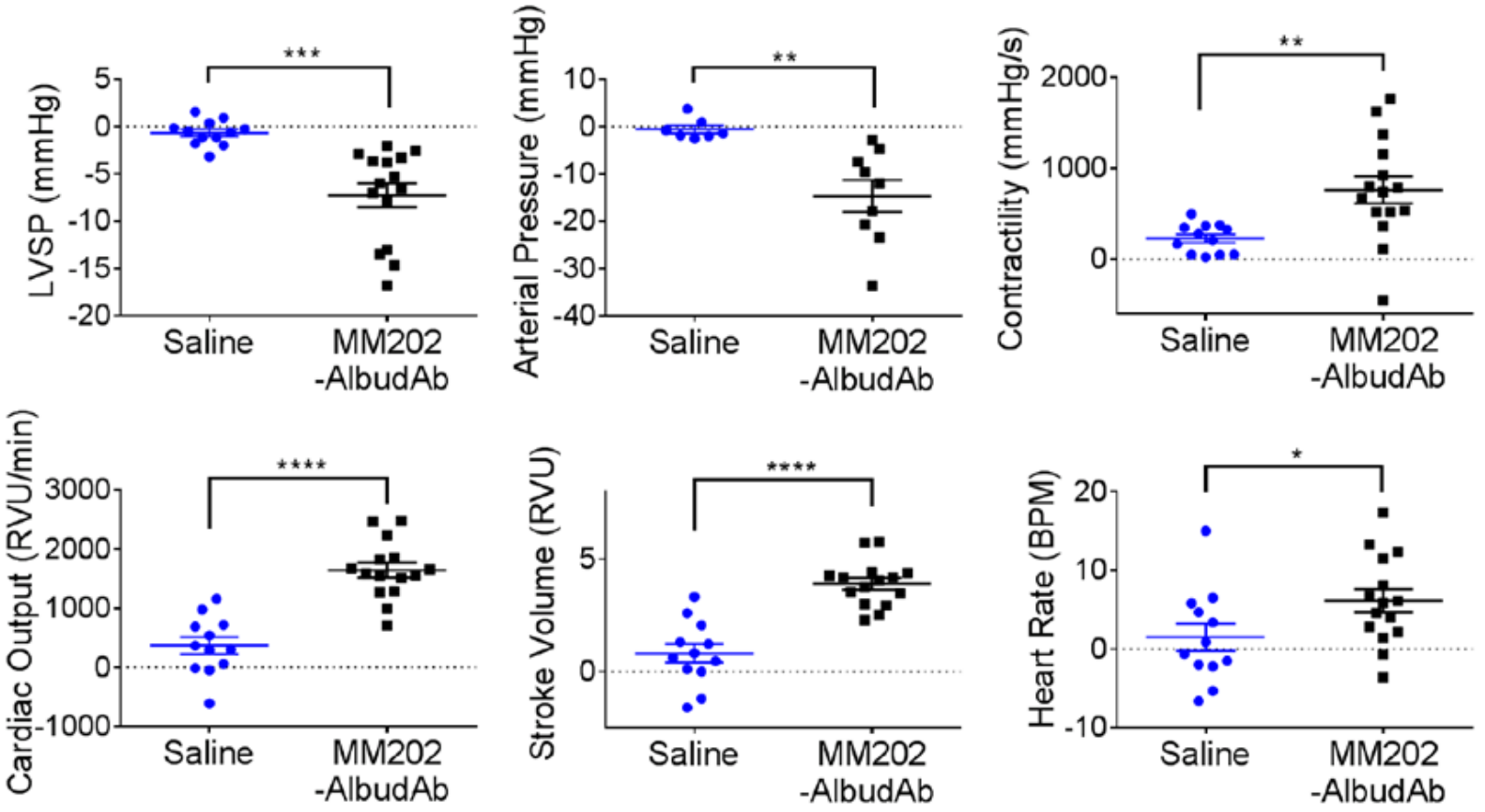

Figure 6.5: *In vivo* cardiovascular responses in normotensive male Sprague-Dawley rats to administration of either saline (n=12) or MM202-albudAb™ (5nmol, n=15). Compared to saline, MM202-albudAb™ reduced the LVSP (6.61±1.46mmHg, ****p<0.001) and the arterial pressure (14.12±3.35mmHg, **p<0.01), meanwhile, it increased the dp/dt_{MAX} (533±170mmHg/s, **p<0.01), the cardiac output (1277±190RVU/min, ****p<0.0001), the stroke volume (3.09±0.47RVU, ****p<0.0001) and the heart rate (4.64±2.24BPM, *p<0.05). Data were compared using a two-tailed Student's t-test and statistical significance was taken as 5%. *p<0.05, **p<0.01, ***p<0.001 and ****p<0.0001

A second dose of [Pyr^{1}]apelin-13 (50nmol, 0.5mL) was administered to all animals subsequently to the initial dose of either MM202-AlbudAb^{TM} or saline. All animals responded except the first two, one of which was then given a third dose of [Pyr^{1}]apelin-13 from a different batch to which it responded robustly. This second batch of [Pyr^{1}]apelin-13 was used for subsequent experiments and these first two excluded from the second dose analysis. The pattern of responses to [Pyr^{1}]apelin-13 was similar to that of the MM202-AlbudAb^{TM} conjugate and there were no significant differences between those that had received saline first or MM202-AlbudAb^{TM} (Figure 6.6). The LVSP was reduced by 12.89±2.21mmHg and 11.64±2.58mmHg and the arterial pressure by 24.75±1.47mmHg and 31.18±5.73mmHg in the saline and MM202-AlbudAb^{TM} groups, respectively. Similarly, the dp/dt_{MAX} was increased by 1660±210mHg/s and 890±434mmHg/s and the dp/dt_{MIN} by 658±499mmHg/s and 1553±494mmHg/s, respectively. Once again the cardiac output increased, 3143±707RVU/min and 2492±620RVU/min, with a concurrent stroke volume increase, 7.93±1.96RVU and 6.38±1.32RVU. The heart rate did not change in either the saline or MM202-AlbudAb^{TM} groups, 3.43±2.91BPM and 2.98±7.29BPM, respectively.

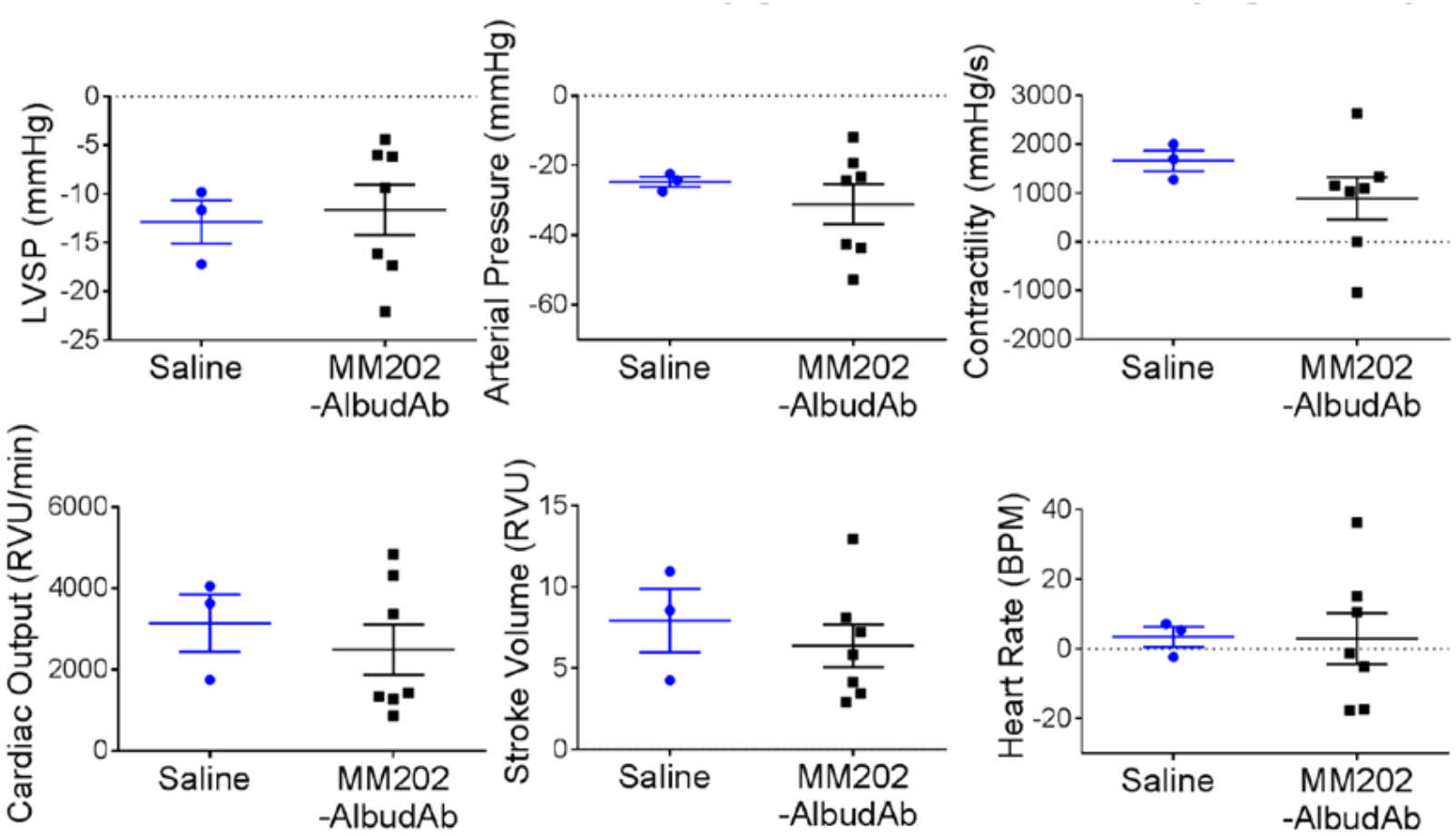

Figure 6.6: *In vivo* cardiovascular responses in normotensive male Sprague-Dawley rats to administration of [Pyr[1]]apelin-13 (50nmol, n=12) following a dose of either saline (n=3) or MM202-albudAb™ (5nmol, n=9). In two animals, the [Pyr[1]]apelin-13 dose had expired and these animals were excluded from analysis. No significant differences were observed in the cardiovascular responses to [Pyr[1]]apelin-13 between any of the parameters measured. Although this part of the study was underpowered due to the variability in Pyr[1]]apelin-13, it nonetheless suggests that MM202-albudAb™ did not robustly desensitise the apelin receptor *in vivo*. Data were compared using a two-tailed Student's t-test and statistical significance was taken as 5%. *p<0.05, **p<0.01, ***p<0.001 and ****p<0.0001

6.3.5 MM202-AlbudAb™ Displayed an Improved Plasma Half-life in Heparinised Human Plasma Samples *Ex Vivo*

MM202 demonstrated an extended plasma half-life *ex vivo* compared to the endogenous agonist, [Pyr¹]apelin-13 (3nmol/L: 23±6minutes, *p<0.05). MM202-AlbudAb™ demonstrated a further improvement over both [Pyr¹]apelin-13 (3nmol/L: 65±4minutes, ****p<0.0001) and also over MM202 (3nmol/L: 42±7minutes, **p<0.01) (Figure 6.7, Table 6.2).

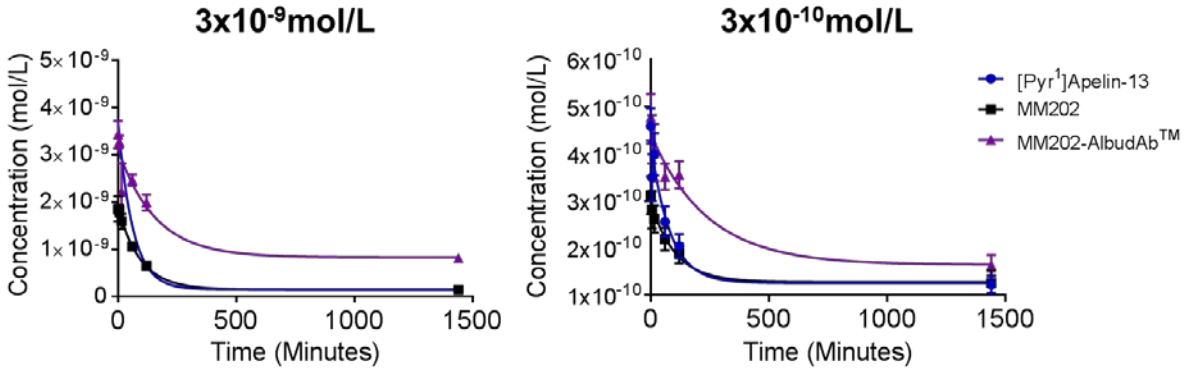

Figure 6.7: A time-course of concentrations of apelin-like cross-reactivity (mean±SEM) measured in plasma samples (n=3) when spiked with 3nmol/L or 0.3nmol/L of either [Pyr¹]apelin-13, MM202 or MM202-AlbudAb™. Data were fitted as a single exponential for each donor to calculate the half-life of each compound.

$t_{½}$ (Min)		[Pyr¹] Apelin-13	MM202	MM202-AlbudAb™
3x10⁻⁹mol/L	D1	39	67	112
	D2	46	56	113
	D3	45	77	102
	Mean ± SEM	**43±2**	**67±6**	**109±4**
3x10⁻¹⁰mol/L	D1	54	52	131
	D2	61	71	136
	D3	49	104	391
	Mean ± SEM	**55±4**	**76±15**	**219±86**

Table 6.2: The calculated plasma half-lives for [Pyr¹]apelin-13, MM202 or MM202-AlbudAb™ (n=3). MM202 had an improved plasma half-life compared to [Pyr¹]apelin-13 with MM202-AlbudAb™ demonstrating a further improvement.

6.3.6 Chronic Administration of MM202-AlbudAb™ Did Not Prevent Onset of PAH in a MCT Prevention Study *In Vivo*

Chronic IP injection of the MM202-AlbudAb™ conjugate (1mg/kg, n=14) twice weekly in male Sprague-Dawley rats was compared to saline controls (n=17) in a 21 day MCT study. At the end point of the study there was a small but significant difference in weight between control animals (n=13) receiving either saline or MM202-AlbudAb™ with the latter on average 32.52±13.83g (*p<0.05) heavier. Animals that received MCT (n=18) weighed significantly less than their corresponding controls with the saline group 38.14±11.39g (**p<0.01) and the treatment group 64.92±15.32g (**p<0.01) lighter. Additionally, these animals displayed RV hypertrophy with Fulton indices increased by 0.195±0.028 (****p<0.0001) and 0.233±0.036 (****p<0.0001), respectively. The RVSPs were increased by 33.83±3.99mmHg (****p<0.0001) and 31.30±3.13mmHg (****p<0.0001), with a reduction in the LVSP of 13.44±5.36mmHg (*p<0.05) and 23.58±5.81mmHg (**p<0.01), respectively. There was no significant difference between the saline and MM202-AlbudAb™ conjugate treated MCT groups in these three parameters (Figure 6.8).

6.3.6.1 Apelin-Like Reactivity was Detectable in Plasma from Rats Treated Chronically with MM202-AlbudAb™

Concentrations of apelin-like cross-reactivity were elevated in both saline control and MCT-treated groups when they had been administered MM202-AlbudAb™ (12.3±1.9nmol/L and 17.2±4.7nmol/L, respectively) compared to saline (5.9±0.6nmol/L, **p<0.01 and 6.6±1.1nmol/L, *p<0.05, respectively). The last MM202-AlbudAb™ dose administered to the animals was three days prior to catheterisation and blood collection. There was no significant difference in endogenous apelin levels between saline controls administered saline and animals that had received MCT and saline.

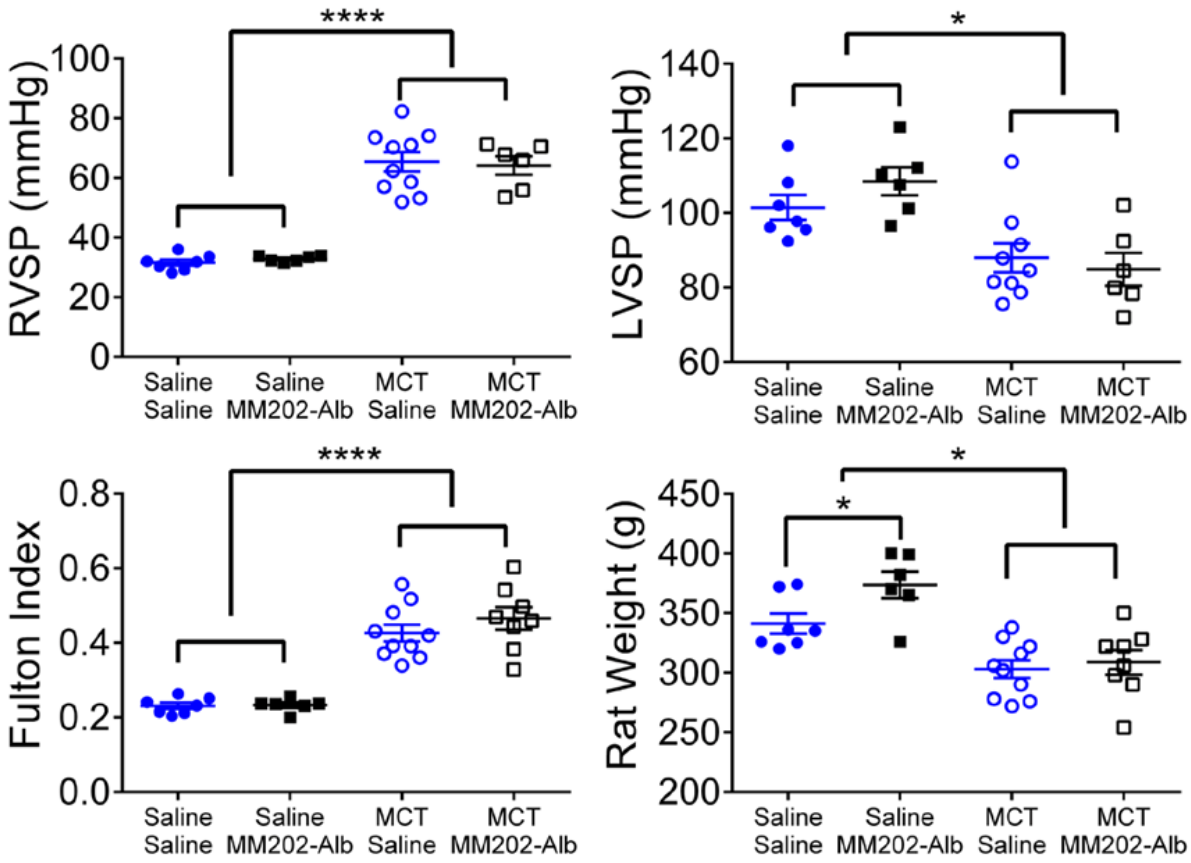

Figure 6.8: Terminal (day 21) measurements from an MCT-induced model of PAH assessing MM202-AlbudAb™ as a preventative therapeutic agent. Male Sprague-Dawley rats (n=31) received a subcutaneous injection of saline (n=13) or MCT (n=18) followed by 21 days of either daily IP injections of saline (n=17) or twice weekly MM202-albudAb™ (n=14). The MCT animals displayed increased RVSPs and Fulton indices with reduced LVSPs and weights. There were no differences between saline and MM202-albudAb™ receiving MCT animals. Data were compared using a two-tailed Student's t-test and statistical significance was taken as 5%. *p<0.05, **p<0.01, ***p<0.001 and ****p<0.0001

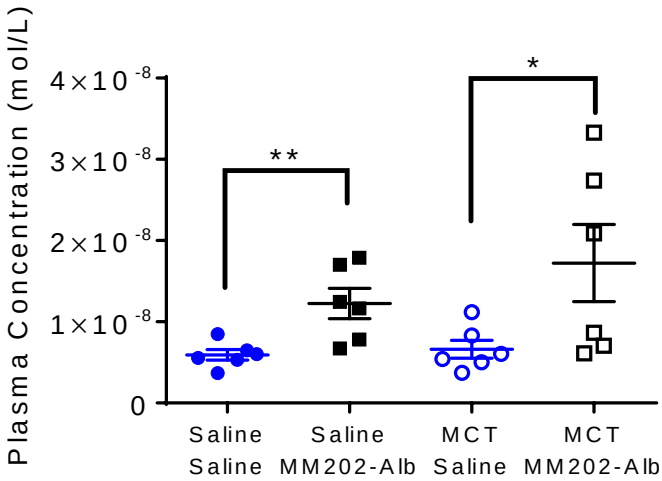

Figure 6.9: Plasma concentrations of apelin-like cross-reactivity measured in an ELISA from end-point plasma samples collected following chronic IP administration of MM202-AlbudAb™ in rats twice weekly for 21 days. Animals that received MM202-AlbudAb™ demonstrated significantly elevated concentrations of apelin-like cross-reactivity compared to saline controls. Data were compared using a two-tailed Student's t-test and statistical significance was taken as 5%. *p<0.05, **p<0.01, ***p<0.001 and ****p<0.0001

6.4 Discussion

6.4.1 Spacer and Apelin-17

Apelin-17 bound to the native human apelin receptor with slightly higher affinity than [Pyr^{1}]apelin-13. In functional assays, apelin-17 was similarly slightly more potent than [Pyr^{1}]apelin-13 but displayed a different signalling profile with some β-arrestin bias as has previously been suggested (El Messari *et al*., 2004). The fact that additional amino acids did not reduce binding affinity or functional activity in cell-based signalling assays, confirms tolerance to the addition of a spacer to apelin-13 at the N-terminus if required. Additionally, extensive homology modelling implies that the amino acids at the N-terminus added to the RPRL recognition sequence project beyond the receptor binding region into solvent and associate with the extracellular loop of the apelin receptor (collaborative work by Dr David Huggins and Professor Robert Glen). This suggests that an appropriate linker at the N-terminus should allow apelin binding while not causing interference by the conjugated antibody.

6.4.2 MM202 and MM202-AlbudAb^{TM} Bound to the Human Apelin Receptor and Showed Functional Activity

MM202 bound to the apelin receptor with high affinity and showed activity in cell-based functional assays. The high activity in the β-arrestin assay likely correlated with the higher binding affinity and is something that has been observed before, for instance with apelin-17. It is possible that the longer peptides, which have increased binding affinity, stabilise regions of the apelin-13 sequence within the binding pocket which increases β-arrestin signalling (Murza *et al*., 2015, Iturrioz *et al*., 2010b, El Messari *et al*., 2004, Ceraudo *et al*., 2014).

The addition of linker motifs to MM202 at the N-terminus and combining these with AlbudAb^{TM} did not result in a large loss in binding affinity at the apelin receptor. This suggests the linkers did not directly affect binding to the receptor but were able to provide sufficient mobility with reduced steric hindrance around the apelin binding pocket. In fact, although conjugating AlbudAb^{TM} to MM202 reduced the binding affinity to the receptor slightly, it led to a much greater decrease in β-arrestin signalling compared to cAMP signalling. In this case, it is probable that the steric bulk of the AlbudAb^{TM} molecule would partially restrict access of MM202 to the receptor, though this would largely be negated by the $(PEG)_4$ spacer and result in a small loss in affinity but a proportionally larger decrease in β-arrestin signalling. Fortuitously, reduced

signalling through the β-arrestin pathway is something that has been considered beneficial for apelin mimetics as has previously been discussed with MM07 and CMF-019 (Brame *et al*., 2015, Read *et al*., 2016).

6.4.3 Conjugating AlbudAb™ to Apelin Peptides Retained AlbudAb™ Activity at HSA

Experiments were performed using the Biacore T200 system (GE Healthcare Life Sciences, Little Chalfont, UK) by Total Scientific Ltd (Cambridge, UK) to determine the binding characteristic of AlbudAb™ (0.156-80nmol/L) and the MM202-AlbudAb™ conjugate (0.156-160nmol/L) to HSA. This involved HSA protein immobilised onto the Biacore CM5 chip and a multi-cycle kinetic binding study using increasing concentrations of both species. AlbudAb™ bound with high nanomolar affinity (pK_D=9.27, n=2) and conjugating MM202 to the AlbudAb™ molecule only very slightly reduced the binding affinity to HSA (pK_D=9.02, n=2). This demonstrates that the ability of the AlbudAb™ moiety to bind to HSA was retained and is consistent with previous AlbudAb™ conjugates.

6.4.4 MM202-AlbudAb™ was Active Acutely *In Vivo*

Injecting MM202-AlbudAb™ intravenously through the jugular vein resulted in robust cardiovascular responses as expected for an apelin agonist. The LVSP was reduced and this was likely due to a decrease in arterial pressure leading to a reduced afterload on the heart. At the same time the cardiac output increased in concert with the stroke volume and there was a small increase in heart rate, though this was probably not the driving factor in increasing cardiac output. Finally, the contractility of the heart (measured as change in maximal pressure over time, dp/dt_{MAX}) was also increased, as predicted for a positive inotrope. These cardiovascular changes have also been seen with [Pyr^1]apelin-13.

The fact that there was little difference in the [Pyr^1]apelin-13 responses following either treatment suggests that there was little desensitisation of the receptor by MM202-AlbudAb™. The responses to 5nmol MM202-AlbudAb™ were smaller than those to 50nmol [Pyr^1]apelin-13, this is not surprising as MM202-AlbudAb™ displayed similar activity in binding to the receptor and in functional assays. Doses higher than 5nmol could not be administered as the MM202-AlbudAb™ conjugate was limited by its solubility in saline. Moreover, one would expect that the high HSA binding of MM202-AlbudAb™ could limit the amount able to reach the cardiovascular tissues acutely, though this could have been balanced by protection from degradation. Importantly, the

magnitude of the effects of 5nmol MM202-AlbudAb™ were comparable to those obtained with 5nmol MM202 in a preliminary study, suggesting that the plasma protein bound AlbudAb™ conjugate is available for binding to the receptor. Only two animals were tested with MM202 alone as a control in order to preserve the supply of the compound for conjugation to AlbudAb™ such that enough might be available for the subsequent MCT study and to reduce unnecessary animal use. Indeed, it was clear from these two animals that responses to MM202 were robust and the use of more compound or animals was not required.

6.4.5 MM202-AlbudAb™ Displayed an Improved Plasma Half-life *Ex Vivo*

In a time-course experiment using human plasma samples spiked with 3nmol/L [Pyr[1]]apelin-13, MM202 or MM202-AlbudAb™ *ex vivo*, MM202-AlbudAb™ displayed a 2.5-fold improvement over [Pyr[1]]apelin-13 and a 1.6-fold improvement over MM202. This suggests that the peptide modifications in MM202 were sufficient to reduce proteolysis by plasma proteases. MM202-AlbudAb™ displayed such a further improvement in half-life over MM202 and likely reflects the PEG linker and AlbudAb™ moieties acting to sterically hinder plasma proteases. The extended plasma half-life observed with MM202-AlbudAb™ is consistent with observations of extended half-life in other AlbudAb™ constructs (Bao *et al*., 2013, O'Connor-Semmes *et al*., 2014, Goodall *et al*., 2015, Lin *et al*., 2015, Walker *et al*., 2010, Holt *et al*., 2008).

It is important to note that such a plasma half-life measured *in vitro* does not take into account renal filtration or metabolic clearance from the liver which are likely to be the largest contributors to peptide breakdown. As such, it is probable that MM202-AlbudAb™ is even more long-lived compared to either [Pyr[1]]apelin-13 or MM202 *in vivo*. Indeed, the half-life of 43minutes measured for [Pyr[1]]apelin-13 is exceptionally long for a peptide. Previously, its *in vivo* half-life in rats has been demonstrated to be only 2 minutes (Brame *et al*., 2015). An additional caveat is that endogenous apelin-like reactivity could not be distinguished from the exogenously administered compounds in the ELISA and so the half-lives of the compounds have likely been underestimated.

In order to calculate plasma half-lives, data were fitted to a single exponential curve and this provided a good fit to the data. For the experiments spiked with 3nmol/L, the C_0 values were as expected as the concentration was high enough to negate the effects of any endogenous apelin-like reactivity. For the 0.3nmol/L experiments, the C_0

values were closer to 0.5nmol/L and again this was as expected since endogenous apelin-like reactivity has previously been demonstrated to be around 0.3nmol/L in healthy heparinised human plasma (Yang *et al*., 2017b). Although the half-lives measured were similar using both concentrations as one would expect, the 0.3nmol/L was more variable and this probably reflects the fact that the drug concentrations were of the same order of magnitude as the endogenous apelin-like reactivity. For this reason these experiments were not analysed statistically but nonetheless are supportive of the conclusions drawn.

6.4.6 MM202-AlbudAb™ Did Not Prevent PAH when Administered Twice Weekly to MCT Treated Animals

Despite the efficacy of MM202-AlbudAb™ acutely and the extended plasma half-life it displayed, it was unable to prevent PAH in an MCT rat model when administered chronically by IP injection twice weekly at 1mg/kg for three weeks. The low dosing schedule was chosen due to the longer *ex vivo* plasma half-life and proposed improvements in metabolic stability and reduction in renal clearance.

Interestingly, the dose administered was sufficient that apelin-like reactivity could be detected in heparinised plasma samples collected during terminal exsanguination by ELISA. This may suggest that MM202-AlbudAb™ was sufficiently stable and long-lived *in vivo* that it could be detected. Performing calculations based upon the *in vitro* human plasma half-life of MM202-AlbudAb™, only 5fmol/L of MM202-AlbudAb™ would be expected to remain after three days. Nonetheless, it is possible that the IP cavity could have acted as a reservoir to enable release of the cumulative doses over an extended period of time. Moreover, it is notable that the basal levels of apelin-like reactivity in the rat saline controls were around 6nmol/L and approximately 20-fold greater than those occurring in humans (~0.3nmol/L; (Yang *et al*., 2017b). This suggests that apelin peptides are longer-lived in rat plasma and therefore, significantly higher levels of MM202-AlbudAb™ might well have been detectable in rat plasma 3 days subsequent to administration. Alternatively, MM202-AlbudAb™ might have resulted in upregulation of endogenous apelin levels. Such an effect has not been previously demonstrated at the plasma level following exogenous [Pyr^{1}]apelin-13 administration but has been demonstrated in specific tissues (Falcao-Pires *et al*., 2009). It is interesting that there was no decrease in endogenous apelin-like reactivity in plasma samples from MCT treated animal compared to saline controls given tissue-specific downregulation has been previously reported (Kim *et al*., 2013, Falcao-Pires *et al*., 2009).

Estimating the receptor occupancy at the measured plasma concentration in MM202-AlbudAb^{TM} treated animals (17nmol/L) suggests that it would be in excess of 99%. This implies that the reason for a lack of efficacy is more likely to be due to an inability of the molecule to access the target, something that could be the case if the serum albumin binding of MM202-AlbudAb^{TM} prevented it from being released from the blood. This might have been compounded by the severity of the disease response to MCT in this cohort of animals, which in addition to drastically elevated RVSPs (>60mmHg), displayed lowered LVSPs, due to the severe hypertrophying of the RV.

6.5 Conclusions

The aim of the study was to pharmacologically characterise a chemically conjugated apelin mimetic peptide containing unnatural amino acids linked to an AlbudAb™ molecule, in order to demonstrate retained activity of both constituent parts. Such a construct would represent a significant advance in use of the AlbudAb™ platform which has previously only used genetic conjugation of endogenous molecules, for example, the GLP-1 AlbudAb™ construct GSK2374697.

In this study, it has been demonstrated that MM202-AlbudAb™ retained a high nanomolar binding affinity to the human apelin receptor, as well as activity in *in vitro* cell screening assays. Meanwhile, the AlbudAb™ moiety also retained the ability to bind to HSA *in vitro* and displayed an improved plasma half-life over both its parent compound and the endogenous agonist. Finally, MM202-AlbudAb™ was active *in vivo* and demonstrated similar activity to both the endogenous molecule, [Pyr^{1}]apelin-13, and MM202. Crucially, such a study opens up the possibility that additional modified peptides could be used in concert with the AlbudAb™ platform by chemical rather than genetic conjugation, therefore, allowing for the use of proteolytically protected molecules. Hopefully, with such advances, other short peptide agonists can be adapted into more suitable therapeutics by avoiding both peptidases and renal filtration.

7. Concluding Remarks

The apelin system is an evolving transmitter system consisting of the class A G protein coupled apelin receptor (O'Dowd *et al*., 1993), its cognate ligand apelin (Tatemoto *et al*., 1998) and the recently discovered ELA (Chng *et al*., 2013, Pauli *et al*., 2014), a second endogenous agonist (Yang *et al*., 2017b). Apelin receptor agonists have been implicated as potential therapeutic agents for a number of diseases, especially cardiovascular and metabolic disorders (Yang *et al*., 2015a, Castan-Laurell *et al*., 2011, Castan-Laurell *et al*., 2012). Meanwhile, antagonists had shown potential in cancer (Yang *et al*., 2016, Harford-Wright *et al*., 2017). This study has focussed on the cardiovascular system where both apelin and ELA act through the receptor in the heart to increase the force of contraction (Maguire *et al*., 2009, Perjes *et al*., 2014, Szokodi *et al*., 2002, Yang *et al*., 2017b, Murza *et al*., 2016, Perjes *et al*., 2016, Atluri *et al*., 2007, Berry *et al*., 2004, Jia *et al*., 2006, Ashley *et al*., 2005, Japp *et al*., 2010, Japp *et al*., 2008) and in the vasculature to induce vasodilatation (Maguire *et al*., 2009, Brame *et al*., 2015, Tatemoto *et al*., 2001).

Targeting the apelin receptor with agonists in cardiovascular diseases, such as PAH, would be beneficial by effectively replacing the endogenous ligands which are downregulated. This hypothesis is supported by prevention studies in the MCT rat model of PAH, which show that exogenous administration of [Pyr^{1}]apelin-13 and ELA-32 significantly improves outcome (Falcao-Pires *et al*., 2009, Yang *et al*., 2017b). However, these small endogenous peptides are limited in their therapeutic potential as they lack bioavailability and are liable to metabolic and renal clearance.

To overcome these issues, this study attempted to identify a small molecule apelin agonist and simultaneously studied an apelin mimetic peptide containing unnatural amino acids conjugated to an AlbudAb^{TM} moiety. Both of these approaches have the potential to overcome the limitations of the endogenous peptides by improving longevity and, in the case of the small molecule, oral bioavailability. Furthermore, a small molecule apelin agonist would be invaluable to the field of research by providing a much needed experimental tool compound. In order to pharmacologically characterise these molecules, activity has been measured relative to the most abundant apelin isoform in the cardiovascular system, [Pyr^{1}]apelin-13 (Maguire *et al*., 2009), and PAH has been used as a model disease to evaluate therapeutic potential.

7.1 CMF-019, the First G Protein Biased Small Molecule Apelin Agonist

Despite the potential benefits of apelin agonists, few molecules that might find use as therapeutic agents have been identified. Moreover, with only expensive peptides available, research into the apelin system is limited. Readily available, easy to manufacture small molecule agonists and antagonists as experimental tool compounds could greatly progress this field of research. To this end, one of the primary aims of this study was to identify and pharmacologically characterise a small molecule apelin agonist for use as a tool compound in apelin research. Such a molecule could then be further evaluated for therapeutic potential subsequently.

As discussed in Section 1.4, previous small molecules at the apelin receptor have possessed significant limitations. In contrast, the molecule identified in this study, CMF-019, had a suitably low molecular weight (455Da) and very high nanomolar affinity for the apelin receptor. This high binding affinity was invariant between rodent species and man, supporting its use as an experimental tool compound across species. Such a finding ensures that development as a potential therapeutic agent would not be hindered by species variability, as has been the case for other molecules, such as, the urotensin-II receptor antagonist Palosuran.

The high binding affinity of CMF-019 translated into functional efficacy with similar levels of cAMP inhibition to [Pyr^{1}]apelin-13 observed in cells expressing the recombinant human apelin receptor. Interestingly, the molecule showed much lower activity in recruiting β-arrestin and in internalising the apelin receptor, suggesting that it was highly biased towards the G protein signalling pathway. Such bias could be very useful in an apelin therapeutic agent by enabling it to activate the beneficial G protein pathway without internalising the receptor and thereby maintaining response over time. Furthermore, it could simultaneously reduce activation of the β-arrestin stretch-mediated hypertrophic pathway (Scimia *et al*., 2012). A potential limitation of this study was that signalling through the $G_{\alpha q}$ pathway was not measured as a suitable assay could not be identified. It would be interesting to establish if the $G_{\alpha i}$ bias identified in this study is also seen with $G_{\alpha q}$ signalling. Arguably, the $G_{\alpha q}$ pathway is more therapeutically relevant and is thought to mediate some key aspects of the apelin

response, especially in cardiomyocytes (Yang *et al*., 2015a, Szokodi *et al*., 2002, Perjes *et al*., 2014).

Biased signalling displayed by a small molecule is an intriguing phenomenon and has not been widely studied to date. Such an observation is very revealing about signalling through the apelin receptor and supports the existing theory that longer agonists are better able to reach deeper regions of the apelin binding pocket to activate β-arrestin signalling motifs (El Messari *et al*., 2004). Following the recent crystal structure of the apelin receptor (Ma *et al*., 2017), it would be of great interest if CMF-019 could be crystallised within the binding pocket to better inform the design of future biased apelin ligands.

When assessed in normotensive male Sprague-Dawley rats *in vivo*, CMF-019 produced responses that were similar to the endogenous molecule, [Pyr^{1}]apelin-13, although smaller in magnitude. Both molecules acted as positive inotropes on the heart, increasing the dp/dt_{MAX}, a measure of cardiac contractility. At the same time the cardiac output was seen to increase and this was largely due to a corresponding increase in stroke volume. Finally, both molecules acted as vasodilators, decreasing the arterial pressure and in most cases causing a corresponding decrease in LVSP by reducing the afterload on the heart. The fact that CMF-019, a G protein biased agonist, could mirror all aspects of the [Pyr^{1}]apelin-13 response contrasts with observations by the Marsault group who have previously suggested that β-arrestin biased molecules exert greater hypotensive actions (El Messari *et al*., 2004, Iturrioz *et al*., 2010b, Ceraudo *et al*., 2014, Murza *et al*., 2015, Besserer-Offroy *et al*., 2018). Importantly, despite producing the same response profile to [Pyr^{1}]apelin-13, CMF-019 was much less effective at desensitising the apelin receptor *in vivo*, confirming that its *in vitro* bias was translatable.

Evaluating CMF-019 as a potential disease-modifying molecule in the prevention of PAH, it was found that it could demonstrate beneficial effects in an *in vitro* human PAEC apoptosis assay. This suggests that the advantages of apelin agonism extend beyond only haemodynamic alleviation and actually address the underlying aetiology of the disease itself. These results further support the stability of CMF-019 *in vitro* and suggest that it is a robust and useful experimental tool compound *in vitro*, as well as, for short-term acute *in vivo* study.

A potential drawback of CMF-019 was its high logD, which resulted in limited solubility and prevented high doses from being administered in *in vivo* studies. Furthermore, it was predicted to bind very strongly to plasma proteins and was probably pharmacokinetically unstable once *in vivo*, despite computational studies suggesting it demonstrates similar properties to currently available oral drugs. These pharmacokinetic limitations likely contributed to the molecule's lack of efficacy in preventing PAH in an MCT rat prevention study of the disease. Receptor occupancy calculations using the ~25μM concentration measured from plasma taken at the end-point of the first acute *in vivo* study, suggest that occupancy would still be in excess of 99% even though only approximately 10% of the drug remains in the system. However, if substantial amounts of the drug remained bound to plasma proteins and inaccessible to the receptor target then any free drug might be rapidly cleared. Additionally, in the chronic study the lack of solubility could have resulted in compound precipitation within the IP cavity, reducing the effective dose administered. Therefore, although the implication is that the molecule was not as effective *in vivo* as predicted *in vitro*, such a result is difficult to explain. Indeed, the molecule displayed such similar activity to the endogenous molecule *in vitro* and it seems more likely that the molecule's limitations are pharmacokinetic rather than pharmacodynamic.

Despite potential limitations of CMF-019 as a chronic *in vivo* drug treatment for PAH, it provides the most suitable scaffold upon which to explore new small molecule apelin agonists as a high affinity biased agonist. Interestingly, the scaffold of CMF-019 consisting of a heterocycle with two attached hydrophobic groups, appears to be very similar to four recent compound series identified in patents from Amgen (Chen *et al*., 2017b), Bristol-Myers Squibb (Myers *et al*., 2017), RTI International (Narayanan *et al*., 2016) and Sanford-Burnham (Pinkerton and Smith, 2015) (Figure 3.13), suggesting a remarkably convergent evolution of apelin small molecules. Indeed, molecular docking of these compounds in the apelin binding pocket supports clear similarities in their binding motifs (Figure 3.14). Despite this, it is unknown whether these compounds will also display bias in a similar manner to CMF-019. One suspects that such experiments will be forthcoming following this study.

One of the primary aims of this study was to identify a small molecule apelin agonist for use as an experimental tool compound and as a potential therapeutic lead compound. This aim has been met and illustrates the success of the project. Indeed,

the identification of CMF-019 represents a great advance in the development of small molecule apelin agonists for use as experimental tool compounds. This is confirmed by the fact that it is already widely commercially available and methods to improve the synthesis of the molecule have been attempted (Trifonov *et al*., 2018). The high binding affinity displayed for a small molecule combined with biased signalling, make it very interesting for further study. Moreover, it has shown activity *in vitro* in modifying disease and when administered acutely *in vivo*. One expects that soon it will be used widely for *in vitro* study in the apelin field. It could also form the basis for the development of newer small molecule G protein biased apelin agonists for use in chronic *in vivo* studies.

7.2 MM202-AlbudAb™, a Proof-of-Principle Study of a Chemically Conjugated Unnatural Peptide to an AlbudAb™ Moiety

The development of new apelin agonists has largely been driven by a desire to move away from the endogenous peptides, apelin and ELA, which are not orally bioavailable, metabolically stable or massive enough to escape glomerula filtration. While the identification of CMF-019 as a small molecule can overcome many of these issues, an alternative approach is to utilise a modified peptide. Previous studies have developed modified apelin peptides with improved metabolic properties either through PEGylation (Jia *et al*., 2012), cyclisation (Brame *et al*., 2015, Hamada *et al*., 2008, Macaluso and Glen, 2010, Murza *et al*., 2017, Golosov *et al*., 2013) or the incorporation of unnatural amino acids (Wang *et al*., 2013b, Murza *et al*., 2015, Juhl *et al*., 2016). Similarly, previous studies in other transmitter systems have utilised endogenous molecules conjugated genetically to the ~81KDa AlbudAb™ moiety to provide protection from renal filtration (Bao *et al*., 2013, O'Connor-Semmes *et al*., 2014, Goodall *et al*., 2015, Lin *et al*., 2015, Holt *et al*., 2008, Walker *et al*., 2010). The most successful of these, a GLP-1 AlbudAb™ conjugate, has progressed to phase I clinical trials where it demonstrated improved plasma half-life and retained GLP-1 activity (Lin *et al*., 2015, O'Connor-Semmes *et al*., 2014). However, this approach using endogenous molecules and genetic conjugation does not offer any protection from proteolytic cleavage.

This study aims to act as a proof-of-principle by combining the two approaches for the first time. The resulting molecule would consist of a modified apelin mimetic peptide containing unnatural amino acids chemically conjugated to an AlbudAb™ moiety. The unnatural amino acids would protect it from proteolytic degradation, meanwhile the AlbudAb™ moiety would retain it in the plasma and allow it to avoid renal filtration. To do this, MM202, an apelin mimetic peptide, where the C-terminal phenylalanine has been tri-fluorinated to protect it from cleavage by ACE2, was linked via a $(PEG)_4$ linker to AlbudAb™ using an sSMCC reagent and maleimide chemistry.

The resulting MM202-AlbudAb™ molecule was assessed for binding to the native human apelin receptor and cell signalling *in vitro*. It retained activity and showed similar activities to the original MM202 molecule and [Pyr^1]apelin-13. Furthermore, the AlbudAb™ moiety retained the ability to bind to HSA. Given that the MM202 peptide is ~15KDa and the AlbudAb™ moiety is ~81KDa, the fact that the individual active parts

of the combined construct retained such high activity is remarkable; one would have anticipated that steric hindrance would have had a greater impact. It is testament to the careful consideration of the structure-activity data available and use of appropriately sized linkers that two large peptides could be conjugated together so successfully, greatly supporting chemical conjugation as an effective method to generate a peptide-AlbudAb^{TM} construct.

The study went on to show that MM202-AlbudAb^{TM} was active *in vivo* when administered acutely and that it produced responses consistent for an apelin mimetic. Moreover, these responses were similar to those obtained with MM202 administered alone in a preliminary experiment, suggesting the molecule possessed similar activity to the parent compound in support of the *in vitro* data. Finally, the construct was tested in an MCT prevention study of PAH, however, no benefits were observed and it is most likely that the dose and frequency of administration were too low to attain a therapeutic effect.

It is interesting that the construct displayed an enhanced plasma half-life when incubated *ex vivo* in heparinised human plasma. Although had it been possible on the project licence, it would have been useful to obtain *in vivo* pharmacokinetic data. Nonetheless, it was possible to detect elevated apelin-like reactivity following chronic IP administration twice weekly for three weeks in rat plasma, perhaps supporting the construct's stability *in vivo*. Without detailed pharmacokinetic data on the compound it is difficult to assess how much was reaching the target and, therefore, how appropriate the dosing schedule was. Moreover, the fact that it displayed similar activity *in vivo* to the parent molecule either suggests it is engaging the receptor target successfully or the construct is breaking down and releasing MM202 to bind the receptor. From the *in vitro* plasma time-course, the fact that MM202-AlbudAb^{TM} had such a longer half-life does not support this scenario but it is difficult to know for certain without accurate pharmacokinetic data on metabolism and clearance.

Overall this proof-of-principle study of an unnatural peptide mimetic of apelin, MM202, combined with an AlbudAb^{TM} moiety by chemical conjugation demonstrates the utility and potential of the approach. The conjugation was successful and produced a construct in which both the AlbudAb^{TM} and apelin agonist retained full activity relative to their respective targets when tested alone. This is the first time that such an approach has been attempted and its success opens up the possibility that it could be

more widely applicable to other transmitter systems where the endogenous agonist is also a short-lived peptide.

7.3 Conclusions

The studies presented here represent a significant advance in the discovery and development of synthetic agonists at the apelin receptor through a range of multidisciplinary methods. Such molecules are necessary for the progression of the apelin system as a therapeutic target since both of the endogenous agonists, apelin and ELA, are limited by oral bioavailability, half-life and excretion. A proteolytically protected peptide could avoid metabolism and, if combined with a suitable antibody to sufficiently extend half-life, could reduce the frequency of administration required such that a lack of oral bioavailability is no longer a concern. An additional constraint is that the endogenous apelin agonists lead to rapid desensitisation of the apelin receptor and would thus, be expected to produce only transient benefits in preventing disease progression. In contrast, a G protein biased small molecule apelin agonist would have great potential to overcome all of the issues of the endogenous molecules by providing an orally bioavailable drug that could avoid excretion and not desensitise the receptor, therefore, providing a long-term treatment for chronic disease.

Previous studies have utilised peptide modification to improve plasma stability and affinity through a range of methods, including PEGylation, cyclisation and the addition of unnatural amino acids. Here an alternative and novel approach was used. By combining a modified peptide agonist containing unnatural amino acids conjugated chemically to AlbudAb^{TM}, it has been demonstrated that activity of both parts of the molecule could be retained and the molecule displayed activity *in vivo*. This is the first time that a non-endogenous peptide has been conjugated chemically to an AlbudAb^{TM} and presents a novel approach to drug design.

Initial studies to identify small molecules at the apelin receptor have been limited and although some successes have been reported, they have often had significant issues. Perhaps, the greatest advance demonstrated in this study has been the discovery and identification of CMF-019 as a G protein biased small molecule apelin agonist. This molecule will be very useful in future studies as an experimental tool compound, exemplified by the fact it is already available commercially and newer syntheses are being researched. CMF-019 has great potential as a starting point for the development of newer biased small molecule therapeutics at the apelin receptor with improved pharmacokinetic profiles. Such molecules could overcome all of the issues posed by

the short-lived endogenous peptides, apelin and ELA, as therapeutic agents and provide drugs with oral bioavailability, long half-lives and no desensitisation of the receptor; thereby, providing effective and easily manufactured treatments for chronic life-long diseases.

References

Abe, K., Toba, M., Alzoubi, A., Ito, M., Fagan, K. A., Cool, C. D., Voelkel, N. F., McMurtry, I. F. and Oka, M. (2010). *Formation of plexiform lesions in experimental severe pulmonary arterial hypertension.* Circulation. **121(25)**:2747-54.

Akcilar, R., Turgut, S., Caner, V., Akcilar, A., Ayada, C., Elmas, L. and Ozcan, T. O. (2015). *The effects of apelin treatment on a rat model of type 2 diabetes.* Adv Med Sci. **60(1)**:94-100.

Alastalo, T. P., Li, M., Perez Vde, J., Pham, D., Sawada, H., Wang, J. K., Koskenvuo, M., Wang, L., Freeman, B. A., Chang, H. Y. and Rabinovitch, M. (2011). *Disruption of PPARgamma/beta-catenin-mediated regulation of apelin impairs BMP-induced mouse and human pulmonary arterial EC survival*. J Clin Invest. **121(9)**:3735-46.

Andersen, C. U., Hilberg, O., Mellemkjaer, S., Nielsen-Kudsk, J. E. and Simonsen, U. (2011). *Apelin and pulmonary hypertension*. Pulm Circ. **1(3)**:334-46.

Andersen, C. U., Markvardsen, L. H., Hilberg, O. and Simonsen, U. (2009). *Pulmonary apelin levels and effects in rats with hypoxic pulmonary hypertension.* Respir Med. **103(11)**:1663-71.

Anecchino, C., Fanizza, C., Marino, V. and Romero, M. (2015). *Drug outcome survey to evaluate anti-TNF treatment in rheumatoid arthritis: an Italian observational study (the DOSE study).* Clin Exp Rheumatol. **33(6)**:779-87.

Ashley, E. A., Powers, J., Chen, M., Kundu, R., Finsterbach, T., Caffarelli, A., Deng, A., Eichhorn, J., Mahajan, R., Agrawal, R., Greve, J., Robbins, R., Patterson, A. J., Bernstein, D. and Quertermous, T. (2005). *The endogenous peptide apelin potently improves cardiac contractility and reduces cardiac loading in vivo*. Cardiovasc Res. **65(1)**:73-82.

Atluri, P., Morine, K. J., Liao, G. P., Panlilio, C. M., Berry, M. F., Hsu, V. M., Hiesinger, W., Cohen, J. E. and Joseph Woo, Y. (2007). *Ischemic heart failure enhances endogenous myocardial apelin and APJ receptor expression.* Cell Mol Biol Lett. **12(1)**:127-38.

Attane, C., Foussal, C., Le Gonidec, S., Benani, A., Daviaud, D., Wanecq, E., Guzman-Ruiz, R., Dray, C., Bezaire, V., Rancoule, C., Kuba, K., Ruiz-Gayo, M., Levade, T., Penninger, J., Burcelin, R., Penicaud, L., Valet, P. and Castan-Laurell, I. (2012). *Apelin treatment increases complete Fatty Acid oxidation, mitochondrial oxidative capacity, and biogenesis in muscle of insulin-resistant mice.* Diabetes. **61(2)**:310-20.

Bao, W., Holt, L. J., Prince, R. D., Jones, G. X., Aravindhan, K., Szapacs, M., Barbour, A. M., Jolivette, L. J., Lepore, J. J., Willette, R. N., DeAngelis, E. and Jucker, B. M. (2013). *Novel fusion of GLP-1 with a domain antibody to serum albumin prolongs protection against myocardial ischemia/reperfusion injury in the rat.* Cardiovasc Diabetol. **12**:148.

Barnes, G. D., Alam, S., Carter, G., Pedersen, C. M., Lee, K. M., Hubbard, T. J., Veitch, S., Jeong, H., White, A., Cruden, N. L., Huson, L., Japp, A. G. and Newby, D. E. (2013). *Sustained cardiovascular actions of APJ agonism during renin-angiotensin system activation and in patients with heart failure.* Circ Heart Fail. **6(3)**:482-91.

Berry, M. F., Pirolli, T. J., Jayasankar, V., Burdick, J., Morine, K. J., Gardner, T. J. and Woo, Y. J. (2004). *Apelin has in vivo inotropic effects on normal and failing hearts.* Circulation. **110(11)**:187-93.

Bertero, T., Lu, Y., Annis, S., Hale, A., Bhat, B., Saggar, R., Wallace, W. D., Ross, D. J., Vargas, S. O., Graham, B. B., Kumar, R., Black, S. M., Fratz, S., Fineman, J. R., West, J. D., Haley, K. J., Waxman, A. B., Chau, B. N., Cottrill, K. A. and Chan, S. Y. (2014). *Systems-level regulation of microRNA networks by miR-130/301 promotes pulmonary hypertension.* J Clin Invest. **124(8)**:3514-28.

Besserer-Offroy, E., Berube, P., Cote, J., Murza, A., Longpre, J. M., Dumaine, R., Lesur, O., Auger-Messier, M., Leduc, R., Marsault, E. and Sarret, P. (2018). *The hypotensive effect of activated apelin receptor is correlated with beta-arrestin recruitment.* Pharmacol Res. **131**:7-16.

Black, J. W. and Leff, P. (1983). *Operational models of pharmacological agonism.* Proc R Soc Lond B Biol Sci. **220(1219)**:141-62.

Blanc, M., David, F., Abrami, L., Migliozzi, D., Armand, F., Burgi, J. and van der Goot, F. G. (2015). *SwissPalm: Protein palmitoylation database.* F1000Res. **4**:261.

Boal, F., Roumegoux, J., Alfarano, C., Timotin, A., Calise, D., Anesia, R., Drougard, A., Knauf, C., Lagente, C., Roncalli, J., Desmoulin, F., Tronchere, H., Valet, P., Parini, A. and Kunduzova, O. (2015). *Apelin regulates FoxO3 translocation to mediate cardioprotective responses to myocardial injury and obesity.* Sci Rep. **5**:16104.

Brame, A. L., Maguire, J. J., Yang, P., Dyson, A., Torella, R., Cheriyan, J., Singer, M., Glen, R. C., Wilkinson, I. B. and Davenport, A. P. (2015). *Design, characterization, and first-in-human study of the vascular actions of a novel biased apelin receptor agonist.* Hypertension. **65(4)**:834-40

Brash, L., Barnes, G. D., Brewis, M. J., Church, A. C., Gibbs, S. J., Howard, L., Jayasekera, G., Johnson, M. K., McGlinchey, N., Onorato, J., Simpson, J., Stirrat, C., Thomson, S., Watson, G., Wilkins, M. R., Xu, C., Welsh, D. J., Newby, D. E. and Peacock, A. J. (2018). *Short-term hemodynamic effects of apelin in patients with pulmonary arterial hypertension.* JACC Basic Transl Sci. **3(2)**:176-186.

Butcher, A. J., Prihandoko, R., Kong, K. C., McWilliams, P., Edwards, J. M., Bottrill, A., Mistry, S. and Tobin, A. B. (2011). *Differential G-protein-coupled receptor phosphorylation provides evidence for a signaling bar code.* J Biol Chem. **286(13)**:11506-18.

Castan-Laurell, I., Dray, C., Attane, C., Duparc, T., Knauf, C. and Valet, P. (2011). *Apelin, diabetes, and obesity.* Endocrine. **40(1)**:1-9.

Castan-Laurell, I., Dray, C., Knauf, C., Kunduzova, O. and Valet, P. (2012). *Apelin, a promising target for type 2 diabetes treatment?* Trends Endocrinol Metab. **23(5)**:234-41.

Cayabyab, M., Hinuma, S., Farzan, M., Choe, H., Fukusumi, S., Kitada, C., Nishizawa, N., Hosoya, M., Nishimura, O., Messele, T., Pollakis, G., Goudsmit, J., Fujino, M. and Sodroski, J. (2000). *Apelin, the natural ligand of the orphan seven-transmembrane receptor APJ, inhibits human immunodeficiency virus type 1 entry.* J Virol. **74(24)**:11972-6.

Ceraudo, E., Galanth, C., Carpentier, E., Banegas-Font, I., Schonegge, A. M., Alvear-Perez, R., Iturrioz, X., Bouvier, M. and Llorens-Cortes, C. (2014). *Biased signaling favoring gi over beta-arrestin promoted by an apelin fragment lacking the C-terminal phenylalanine.* J Biol Chem. **289(35)**:24599-610.

Chandrasekaran, B., Dar, O. and McDonagh, T. (2008). *The role of apelin in cardiovascular function and heart failure.* Eur J Heart Fail. **10(8)**:725-32.

Charo, D. N., Ho, M., Fajardo, G., Kawana, M., Kundu, R. K., Sheikh, A. Y., Finsterbach, T. P., Leeper, N. J., Ernst, K. V., Chen, M. M., Ho, Y. D., Chun, H. J., Bernstein, D., Ashley, E. A. and Quertermous, T. (2009). *Endogenous regulation of cardiovascular function by apelin-APJ.* Am J Physiol Heart Circ Physiol. **297(5)**:1904-13.

Chen, H., Wan, D., Wang, L., Peng, A., Xiao, H., Petersen, R. B., Liu, C., Zheng, L. and Huang, K. (2015). *Apelin protects against acute renal injury by inhibiting TGF-beta1.* Biochim Biophys Acta. **1852(7)**:1278-87.

Chen, H., Wang, L., Wang, W., Cheng, C., Zhang, Y., Zhou, Y., Wang, C., Miao, X., Wang, J., Li, J., Zheng, L. and Huang, K. (2017a). *Elabela and an elabela fragment protect against AKI.* J Am Soc Nephrol. **28(9)**:2694-2707.

Chen, M. M., Ashley, E. A., Deng, D. X., Tsalenko, A., Deng, A., Tabibiazar, R., Ben-Dor, A., Fenster, B., Yang, E., King, J. Y., Fowler, M., Robbins, R., Johnson, F. L., Bruhn, L., McDonagh, T., Dargie, H., Yakhini, Z., Tsao, P. S. and Quertermous, T. (2003). *Novel role for the potent endogenous inotrope apelin in human cardiac dysfunction.* Circulation. **12**:1432-9.

Chen, N., Chen, X., Chen, Y., Cheng, A. C., Connors, R. V., Deignan, J., Dransfield, P. J., Du, X., Fu, Z. and Heath, J. A. (2017b). *Triazole agonists of the APJ receptor.* Google Patents. **WO2016187308A1**

Chen, X., Bai, B., Tian, Y., Du, H. and Chen, J. (2014). *Identification of serine 348 on the apelin receptor as a novel regulatory phosphorylation site in apelin-13-induced G protein-independent biased signalling.* J Biol Chem. **289(45)**:31173-87.

Cheng, Y. and Prusoff, W. H. (1973). *Relationship between the inhibition constant (K1) and the concentration of inhibitor which causes 50 per cent inhibition (I50) of an enzymatic reaction.* Biochem Pharmacol. **22(23)**:3099-108.

Chng, S. C., Ho, L., Tian, J. and Reversade, B. (2013). *Elabela: a hormone essential for heart development signals via the apelin receptor.* Dev Cell. **27(6)**:672-80.

Choe, H., Farzan, M., Konkel, M., Martin, K., Sun, Y., Marcon, L., Cayabyab, M., Berman, M., Dorf, M. E., Gerard, N., Gerard, C. and Sodroski, J. (1998). *The orphan seven-transmembrane receptor APJ supports the entry of primary T-cell-line-tropic and dualtropic human immunodeficiency virus type 1.* J Virol. **72(7)**:6113-8.

Chong, K. S., Gardner, R. S., Morton, J. J., Ashley, E. A. and McDonagh, T. A. (2006). *Plasma concentrations of the novel peptide apelin are decreased in patients with chronic heart failure.* Eur J Heart Fail. **8(4)**:355-60.

Christou, H., Hudalla, H., Michael, Z., Filatava, E. J., Li, J., Zhu, M., Possomato-Vieira, J. S., Dias-Junior, C., Kourembanas, S. and Khalil, R. A. (2018). *Impaired pulmonary arterial vasoconstriction and nitric oxide-mediated relaxation underlie severe pulmonary hypertension in the sugen-hypoxia rat model.* J Pharmacol Exp Ther. **364(2)**:258-274.

Chun, H. J., Ali, Z. A., Kojima, Y., Kundu, R. K., Sheikh, A. Y., Agrawal, R., Zheng, L., Leeper, N. J., Pearl, N. E., Patterson, A. J., Anderson, J. P., Tsao, P. S., Lenardo, M. J., Ashley, E. A. and Quertermous, T. (2008). *Apelin signaling antagonizes Ang II effects in mouse models of atherosclerosis.* J Clin Invest. **118(10)**:3343-54.

Colvin, K. L. and Yeager, M. E. (2014). *Animal models of pulmonary hypertension: Matching disease mechanisms to aetiology of the human disease.* J Pulm Respir Med. **4(4)**:198

Cordeaux, Y., Briddon, S. J., Megson, A. E., McDonnell, J., Dickenson, J. M. and Hill, S. J. (2000). *Influence of receptor number on functional responses elicited by agonists acting at the human adenosine A(1) receptor: evidence for signaling pathway-dependent changes in agonist potency and relative intrinsic activity.* Mol Pharmacol. **58(5)**:1075-84.

Dan, N., Setua, S., Kashyap, V. K., Khan, S., Jaggi, M., Yallapu, M. M. and Chauhan, S. C. (2018). *Antibody-drug conjugates for cancer therapy: Chemistry to clinical implications.* Pharmaceuticals (Basel). **11(2)**:32

Date, T., Taniguchi, I., Inada, K., Matsuo, S., Miyanaga, S., Yamane, T., Abe, Y., Sugimoto, K. and Mochizuki, S. (2005). *Nicorandil inhibits serum starvation-induced apoptosis in vascular endothelial cells.* J Cardiovasc Pharmacol. **46(6)**:721-6.

De Mota, N., Lenkei, Z. and Llorens-Cortes, C. (2000). *Cloning, pharmacological characterization and brain distribution of the rat apelin receptor.* Neuroendocrinology. **72(6)**:400-7.

Deshwar, A. R., Chng, S. C., Ho, L., Reversade, B. and Scott, I. C. (2016). *The apelin receptor enhances Nodal/TGFbeta signaling to ensure proper cardiac development.* Elife. **5**:e13758

DeWire, S. M., Yamashita, D. S., Rominger, D. H., Liu, G., Cowan, C. L., Graczyk, T. M., Chen, X. T., Pitis, P. M., Gotchev, D., Yuan, C., Koblish, M., Lark, M. W. and Violin, J. D. (2013). *A G protein-biased ligand at the mu-opioid receptor is potently analgesic with reduced gastrointestinal and respiratory dysfunction compared with morphine.* J Pharmacol Exp Ther. **344(3)**:708-17.

Dray, C., Knauf, C., Daviaud, D., Waget, A., Boucher, J., Buleon, M., Cani, P. D., Attane, C., Guigne, C., Carpene, C., Burcelin, R., Castan-Laurell, I. and Valet, P. (2008). *Apelin stimulates glucose utilization in normal and obese insulin-resistant mice.* Cell Metab. **8(5)**:437-45.

Edinger, A. L., Hoffman, T. L., Sharron, M., Lee, B., Yi, Y., Choe, W., Kolson, D. L., Mitrovic, B., Zhou, Y., Faulds, D., Collman, R. G., Hesselgesser, J., Horuk, R. and Doms, R. W. (1998). *An orphan seven-transmembrane domain receptor expressed widely in the brain functions as a coreceptor for human immunodeficiency virus type 1 and simian immunodeficiency virus.* J Virol. **72(10)**:7934-40.

El Messari, S., Iturrioz, X., Fassot, C., De Mota, N., Roesch, D. and Llorens-Cortes, C. (2004). *Functional dissociation of apelin receptor signaling and endocytosis: implications for the effects of apelin on arterial blood pressure.* J Neurochem. **90(6)**:1290-301.

Evans, N. A., Groarke, D. A., Warrack, J., Greenwood, C. J., Dodgson, K., Milligan, G. and Wilson, S. (2001). *Visualizing differences in ligand-induced beta-arrestin-GFP interactions and trafficking between three recently characterized G protein-coupled receptors.* J Neurochem. **77(2)**:476-85.

Falcao-Pires, I., Goncalves, N., Henriques-Coelho, T., Moreira-Goncalves, D., Roncon-Albuquerque, R., Jr. and Leite-Moreira, A. F. (2009). *Apelin decreases myocardial injury and improves right ventricular function in monocrotaline-induced pulmonary hypertension.* Am J Physiol Heart Circ Physiol. **296(6)**:2007-14.

Fan, X., Zhou, N., Zhang, X., Mukhtar, M., Lu, Z., Fang, J., DuBois, G. C. and Pomerantz, R. J. (2003). *Structural and functional study of the apelin-13 peptide, an endogenous ligand of the HIV-1 coreceptor, APJ.* Biochemistry. **42(34)**:10163-8.

Fan, X. F., Xue, F., Zhang, Y. Q., Xing, X. P., Liu, H., Mao, S. Z., Kong, X. X., Gao, Y. Q., Liu, S. F. and Gong, Y. S. (2015a). *The apelin-APJ axis is an endogenous counterinjury mechanism in experimental acute lung injury.* Chest. **147(4)**: 969-78.

Fan, Y., Zhang, Y., Li, X., Zheng, H., Song, Y., Zhang, N., Shen, C., Fan, X., Ren, F., Shen, J., Ren, G. and Yang, J. (2015b). *Treatment with metformin and a dipeptidyl peptidase-4 inhibitor elevates apelin levels in patients with type 2 diabetes mellitus.* Drug Des Devel Ther. **9**:4679-83.

Felker, G. M., Butler, J., Collins, S. P., Cotter, G., Davison, B. A., Ezekowitz, J. A., Filippatos, G., Levy, P. D., Metra, M., Ponikowski, P., Soergel, D. G., Teerlink, J. R., Violin, J. D., Voors, A. A. and Pang, P. S. (2015). *Heart failure therapeutics on the basis of a biased ligand of the angiotensin-2 type 1 receptor. Rationale and design of the BLAST-AHF study (Biased Ligand of the Angiotensin Receptor Study in Acute Heart Failure).* JACC Heart Fail. **3(3)**:193-201.

Flahault, A., Couvineau, P., Alvear-Perez, R., Iturrioz, X. and Llorens-Cortes, C. (2017). *Role of the vasopressin/apelin balance and potential use of metabolically stable apelin analogs in water metabolism disorders.* Front Endocrinol (Lausanne). **8**:120.

Foldes, G., Horkay, F., Szokodi, I., Vuolteenaho, O., Ilves, M., Lindstedt, K. A., Mayranpaa, M., Sarman, B., Seres, L., Skoumal, R., Lako-Futo, Z., deChatel, R., Ruskoaho, H. and Toth, M. (2003). *Circulating and cardiac levels of apelin, the novel ligand of the orphan receptor APJ, in patients with heart failure*. Biochem Biophys Res Commun. **308(3)**:480-5.

Francia, P., Salvati, A., Balla, C., De Paolis, P., Pagannone, E., Borro, M., Gentile, G., Simmaco, M., De Biase, L. and Volpe, M. (2007). *Cardiac resynchronization therapy increases plasma levels of the endogenous inotrope apelin.* Eur J Heart Fail. **9(3)**:306-9.

Freyer, L., Hsu, C. W., Nowotschin, S., Pauli, A., Ishida, J., Kuba, K., Fukamizu, A., Schier, A. F., Hoodless, P. A., Dickinson, M. E. and Hadjantonakis, A. K. (2017). *Loss of apela peptide in mice causes low penetrance embryonic lethality and defects in early mesodermal derivatives.* Cell Rep. **20(9)**:2116-2130.

Fulton, R. M., Hutchinson, E. C. and Jones, A. M. (1952). *Ventricular weight in cardiac hypertrophy.* Br Heart J. **14(3)**:413-20.

Galandrin, S., Oligny-Longpre, G. and Bouvier, M. (2007). *The evasive nature of drug efficacy: implications for drug discovery.* Trends Pharmacol Sci. **28(8)**:423-30.

Gama Sosa, M. A., De Gasperi, R., Hof, P. R. and Elder, G. A. (2016). *Fibroblast growth factor rescues brain endothelial cells lacking presenilin 1 from apoptotic cell death following serum starvation.* Sci Rep. **6**:30267.

Gerber, H. P., Dixit, V. and Ferrara, N. (1998a). *Vascular endothelial growth factor induces expression of the antiapoptotic proteins Bcl-2 and A1 in vascular endothelial cells.* J Biol Chem. **273(21)**:13313-6.

Gerber, H. P., McMurtrey, A., Kowalski, J., Yan, M., Keyt, B. A., Dixit, V. and Ferrara, N. (1998b). *Vascular endothelial growth factor regulates endothelial cell survival through the phosphatidylinositol 3'-kinase/Akt signal transduction pathway. Requirement for Flk-1/KDR activation.* J Biol Chem. **273(46)**:30336-43.

Gerbier, R., Leroux, V., Couvineau, P., Alvear-Perez, R., Maigret, B., Llorens-Cortes, C. and Iturrioz, X. (2015). *New structural insights into the apelin receptor: identification of key residues for apelin binding.* Faseb J. **29(1)**:314-22.

Goetze, J. P., Rehfeld, J. F., Carlsen, J., Videbaek, R., Andersen, C. B., Boesgaard, S. and Friis-Hansen, L. (2006). *Apelin: a new plasma marker of cardiopulmonary disease.* Regul Pept. **133(1-3)**:134-8.

Golosov, A., Grosche, P., Hu, Q. Y., Imase, H., Parker, D. T., Yasoshima, K., Zecri, F. and Zhao, H. (2013). *Synthetic apelin mimetics for the treatment of heart failure.* Google Patents. **WO2013111110A3**

Goodall, L. J., Ovecka, M., Rycroft, D., Friel, S. L., Sanderson, A., Mistry, P., Davies, M. L. and Stoop, A. A. (2015). *Pharmacokinetic and pharmacodynamic characterisation of an anti-mouse TNF receptor 1 domain antibody formatted for in vivo half-life extension.* PLoS One. **10(9)**:e0137065.

Gourdy, P., Cazals, L., Thalamas, C., Sommet, A., Calvas, F., Galitzky, M., Vinel, C., Dray, C., Hanaire, H., Castan-Laurell, I. and Valet, P. (2018). *Apelin administration improves insulin sensitivity in overweight men during hyperinsulinaemic-euglycaemic clamp.* Diabetes Obes Metab. **20(1)**:157-164.

Gupta, K., Kshirsagar, S., Li, W., Gui, L., Ramakrishnan, S., Gupta, P., Law, P. Y. and Hebbel, R. P. (1999). *VEGF prevents apoptosis of human microvascular endothelial cells via opposing effects on MAPK/ERK and SAPK/JNK signalling.* Exp Cell Res. **247(2)**:495-504.

Habata, Y., Fujii, R., Hosoya, M., Fukusumi, S., Kawamata, Y., Hinuma, S., Kitada, C., Nishizawa, N., Murosaki, S., Kurokawa, T., Onda, H., Tatemoto, K. and Fujino, M. (1999). *Apelin, the natural ligand of the orphan receptor APJ, is abundantly secreted in the colostrum.* Biochim Biophys Acta. **1452(1)**:25-35.

Hachtel, S., Wohlfart, P., Weston, J., Müller, M., Defossa, E., Mertsch, K., Weng, J., Binnie, R. A., Abdul-Latif, F. and Bock, W. J. (2014). *Benzoimidazole-carboxylic acid amide derivatives as APJ receptor modulators.* Google Patents. **WO2014044738A1**

Hamada, J., Baasanjav, A., Ono, N., Murata, K., Kako, K., Ishida, J. and Fukamizu, A. (2015). *Possible involvement of downregulation of the apelin-APJ system in doxorubicin-induced cardiotoxicity.* Am J Physiol Heart Circ Physiol. **308(8)**:931-41.

Hamada, J., Kimura, J., Ishida, J., Kohda, T., Morishita, S., Ichihara, S. and Fukamizu, A. (2008). *Evaluation of novel cyclic analogues of apelin.* Int J Mol Med. **22(4)**:547-52.

Han, S., Englander, E. W., Gomez, G. A., Rastellini, C., Quertermous, T., Kundu, R. K. and Greeley, G. H., Jr. (2015). *Pancreatic islet APJ deletion reduces islet density and glucose tolerance in mice.* Endocrinology. **156(7)**:2451-60.

Harford-Wright, E., Andre-Gregoire, G., Jacobs, K. A., Treps, L., Le Gonidec, S., Leclair, H. M., Gonzalez-Diest, S., Roux, Q., Guillonneau, F., Loussouarn, D., Oliver, L., Vallette, F. M., Foufelle, F., Valet, P., Davenport, A. P., Glen, R. C., Bidere, N. and Gavard, J. (2017). *Pharmacological targeting of apelin impairs glioblastoma growth.* Brain. **140(11)**:2939-2954.

Hassan, A. S., Hou, J., Wei, W. and Hoodless, P. A. (2010). *Expression of two novel transcripts in the mouse definitive endoderm.* Gene Expr Patterns. **10(2-3)**:127-34.

Helenius, M. H., Vattulainen, S., Orcholski, M., Aho, J., Komulainen, A., Taimen, P., Wang, L., de Jesus Perez, V. A., Koskenvuo, J. W. and Alastalo, T. P. (2015). *Suppression of endothelial CD39/ENTPD1 is associated with pulmonary vascular remodeling in pulmonary arterial hypertension.* Am J Physiol Lung Cell Mol Physiol. **308(10)**:1046-57.

Helker, C. S., Schuermann, A., Pollmann, C., Chng, S. C., Kiefer, F., Reversade, B. and Herzog, W. (2015). *The hormonal peptide elabela guides angioblasts to the midline during vasculogenesis.* Elife. **4**:06726

Ho, L., Tan, S. Y., Wee, S., Wu, Y., Tan, S. J., Ramakrishna, N. B., Chng, S. C., Nama, S., Szczerbinska, I., Chan, Y. S., Avery, S., Tsuneyoshi, N., Ng, H. H., Gunaratne, J., Dunn, N. R. and Reversade, B. (2015). *Elabela is an endogenous growth factor that sustains hESC self-renewal via the PI3K/AKT pathway.* Cell Stem Cell. **17(4)**:435-47.

Ho, L., van Dijk, M., Chye, S. T. J., Messerschmidt, D. M., Chng, S. C., Ong, S., Yi, L. K., Boussata, S., Goh, G. H., Afink, G. B., Lim, C. Y., Dunn, N. R., Solter, D., Knowles, B. B. and Reversade, B. (2017). *Elabela deficiency promotes preeclampsia and cardiovascular malformations in mice.* Science. **357(6352)**:707-713.

Holt, L. J., Basran, A., Jones, K., Chorlton, J., Jespers, L. S., Brewis, N. D. and Tomlinson, I. M. (2008). *Anti-serum albumin domain antibodies for extending the half-lives of short lived drugs.* Protein Eng Des Sel. **21(5)**:283-8.

Hong, K. H., Lee, Y. J., Lee, E., Park, S. O., Han, C., Beppu, H., Li, E., Raizada, M. K., Bloch, K. D. and Oh, S. P. (2008). *Genetic ablation of the BMPR2 gene in pulmonary endothelium is sufficient to predispose to pulmonary arterial hypertension.* Circulation. **118(7)**:722-30.

Hosoya, M., Kawamata, Y., Fukusumi, S., Fujii, R., Habata, Y., Hinuma, S., Kitada, C., Honda, S., Kurokawa, T., Onda, H., Nishimura, O. and Fujino, M. (2000). *Molecular and functional characteristics of APJ. Tissue distribution of mRNA and interaction with the endogenous ligand apelin*. J Biol Chem. **275(28)**:21061-7.

Huang, S., Chen, L., Lu, L. and Li, L. (2016). *The apelin-APJ axis: A novel potential therapeutic target for organ fibrosis.* Clin Chim Acta. **456**:81-8.

Hus-Citharel, A., Bodineau, L., Frugiere, A., Joubert, F., Bouby, N. and Llorens-Cortes, C. (2014). *Apelin counteracts vasopressin-induced water reabsorption via cross talk between apelin and vasopressin receptor signaling pathways in the rat collecting duct.* Endocrinology. **155(11)**:4483-93.

Ishida, J., Hashimoto, T., Hashimoto, Y., Nishiwaki, S., Iguchi, T., Harada, S., Sugaya, T., Matsuzaki, H., Yamamoto, R., Shiota, N., Okunishi, H., Kihara, M., Umemura, S., Sugiyama, F., Yagami, K., Kasuya, Y., Mochizuki, N. and Fukamizu, A. (2004). *Regulatory roles for APJ, a seven-transmembrane receptor related to angiotensin-type 1 receptor in blood pressure in vivo.* J Biol Chem. **279(25)**:26274-9.

Iturrioz, X., Alvear-Perez, R., De Mota, N., Franchet, C., Guillier, F., Leroux, V., Dabire, H., Le Jouan, M., Chabane, H., Gerbier, R., Bonnet, D., Berdeaux, A., Maigret, B., Galzi, J. L., Hibert, M. and Llorens-Cortes, C. (2010a). *Identification and pharmacological properties of E339-3D6, the first nonpeptidic apelin receptor agonist.* Faseb J. **24(5)**:1506-17.

Iturrioz, X., Gerbier, R., Leroux, V., Alvear-Perez, R., Maigret, B. and Llorens-Cortes, C. (2010b). *By interacting with the C-terminal Phe of apelin, Phe255 and Trp259 in helix VI of the apelin receptor are critical for internalization.* J Biol Chem. **285(42)**:32627-37.

Iwanaga, Y., Kihara, Y., Takenaka, H. and Kita, T. (2006). *Down-regulation of cardiac apelin system in hypertrophied and failing hearts: Possible role of angiotensin II-angiotensin type 1 receptor system.* J Mol Cell Cardiol. **41(5)**:798-806.

Japp, A. G., Cruden, N. L., Amer, D. A., Li, V. K., Goudie, E. B., Johnston, N. R., Sharma, S., Neilson, I., Webb, D. J., Megson, I. L., Flapan, A. D. and Newby, D. E. (2008). *Vascular effects of apelin in vivo in man.* J Am Coll Cardiol. **52(11)**:908-13.

Japp, A. G., Cruden, N. L., Barnes, G., van Gemeren, N., Mathews, J., Adamson, J., Johnston, N. R., Denvir, M. A., Megson, I. L., Flapan, A. D. and Newby, D. E. (2010). *Acute cardiovascular effects of apelin in humans: potential role in patients with chronic heart failure.* Circulation. **121(16)**:1818-27.

Jia, Y. X., Pan, C. S., Zhang, J., Geng, B., Zhao, J., Gerns, H., Yang, J., Chang, J. K., Tang, C. S. and Qi, Y. F. (2006). *Apelin protects myocardial injury induced by isoproterenol in rats.* Regul Pept. **133(1-3)**:147-54.

Jia, Z. Q., Hou, L., Leger, A., Wu, I., Kudej, A. B., Stefano, J., Jiang, C., Pan, C. Q. and Akita, G. Y. (2012). *Cardiovascular effects of a PEGylated apelin.* Peptides. **38(1)**:181-8.

Jones, G., Willett, P. and Glen, R. C. (1995). *Molecular recognition of receptor sites using a genetic algorithm with a description of desolvation.* J Mol Biol. **245(1)**:43-53.

Jones, G., Willett, P., Glen, R. C., Leach, A. R. and Taylor, R. (1997). *Development and validation of a genetic algorithm for flexible docking.* J Mol Biol, **267(3)**:727-48.

Juhl, C., Els-Heindl, S., Schonauer, R., Redlich, G., Haaf, E., Wunder, F., Riedl, B., Burkhardt, N., Beck-Sickinger, A. G. and Bierer, D. (2016). *Development of potent and metabolically stable APJ ligands with high therapeutic potential.* ChemMedChem. **11(21)**:2378-2384

Kang, Y., Kim, J., Anderson, J. P., Wu, J., Gleim, S. R., Kundu, R. K., McLean, D. L., Kim, J. D., Park, H., Jin, S. W., Hwa, J., Quertermous, T. and Chun, H. J. (2013). *Apelin-APJ signaling is a critical regulator of endothelial MEF2 activation in cardiovascular development.* Circ Res. **113(1)**:22-31.

Karsan, A., Yee, E., Poirier, G. G., Zhou, P., Craig, R. and Harlan, J. M. (1997). *Fibroblast growth factor-2 inhibits endothelial cell apoptosis by Bcl-2-dependent and independent mechanisms.* Am J Pathol. **151(6)**:1775-84.

Katugampola, S. D., Maguire, J. J., Matthewson, S. R. and Davenport, A. P. (2001). *[(125)I]-(Pyr(1))Apelin-13 is a novel radioligand for localizing the APJ orphan receptor in human and rat tissues with evidence for a vasoconstrictor role in man.* Br J Pharmacol. **132(6)**:1255-60.

Kay, J. M., Harris, P. and Heath, D. (1967). *Pulmonary hypertension produced in rats by ingestion of Crotalaria spectabilis seeds.* Thorax. **22(2)**:176-9.

Kenakin, T. (1995). *Agonist-receptor efficacy. II. Agonist trafficking of receptor signals.* Trends Pharmacol Sci. **16(7)**:232-8.

Kenakin, T., Watson, C., Muniz-Medina, V., Christopoulos, A. and Novick, S. (2012). *A simple method for quantifying functional selectivity and agonist bias.* ACS Chem Neurosci. **3(3)**:193-203.

Khan, P., Maloney, P. R., Hedrick, M., Gosalia, P., Milewski, M., Li, L., Roth, G. P., Sergienko, E., Suyama, E., Sugarman, E., Nguyen, K., Mehta, A., Vasile, S., Su, Y., Shi, S., Stonich, D., Nguyen, H., Zeng, F. Y., Novo, A. M., Vicchiarelli, M., Diwan, J., Chung, T. D. Y., Pinkerton, A. B. and Smith, L. H. (2010). *Functional agonists of the apelin (APJ) receptor.* Probe Reports from the NIH Molecular Libraries Program. **PMID:22834038**

Kidoya, H., Naito, H., Muramatsu, F., Yamakawa, D., Jia, W., Ikawa, M., Sonobe, T., Tsuchimochi, H., Shirai, M., Adams, R. H., Fukamizu, A. and Takakura, N. (2015). *APJ regulates parallel alignment of arteries and veins in the skin.* Dev Cell. **33(3)**:247-59.

Kidoya, H., Ueno, M., Yamada, Y., Mochizuki, N., Nakata, M., Yano, T., Fujii, R. and Takakura, N. (2008). *Spatial and temporal role of the apelin/APJ system in the caliber size regulation of blood vessels during angiogenesis.* Embo j. **27(3)**:522-34.

Kim, J., Hwangbo, C., Hu, X., Kang, Y., Papangeli, I., Mehrotra, D., Park, H., Ju, H., McLean, D. L., Comhair, S. A., Erzurum, S. C. and Chun, H. J. (2015). *Restoration of impaired endothelial myocyte enhancer factor 2 function rescues pulmonary arterial hypertension.* Circulation. **131(2)**:190-9.

Kim, J., Kang, Y., Kojima, Y., Lighthouse, J. K., Hu, X., Aldred, M. A., McLean, D. L., Park, H., Comhair, S. A., Greif, D. M., Erzurum, S. C. and Chun, H. J. (2013). *An endothelial apelin-FGF link mediated by miR-424 and miR-503 is disrupted in pulmonary arterial hypertension.* Nat Med. **19(1)**:74-82.

Kim, S. K., Li, Y., Park, C., Abrol, R. and Goddard, W. A., 3rd (2010). *Prediction of the three-dimensional structure for the rat urotensin II receptor, and comparison of the antagonist binding sites and binding selectivity between human and rat receptors from atomistic simulations.* ChemMedChem. **5(9)**:1594-608.

Klein Herenbrink, C., Sykes, D. A., Donthamsetti, P., Canals, M., Coudrat, T., Shonberg, J., Scammells, P. J., Capuano, B., Sexton, P. M., Charlton, S. J., Javitch, J. A., Christopoulos, A. and Lane, J. R. (2016). *The role of kinetic context in apparent biased agonism at GPCRs.* Nat Commun. **7**:10842.

Kleinz, M. J. and Davenport, A. P. (2005). *Emerging roles of apelin in biology and medicine.* Pharmacol Ther. **107(2)**:198-211.

Kocer, D., Karakukcu, C., Ozturk, F., Eroglu, E. and Kocyigit, I. (2016). *Evaluation of fibrosis markers: Apelin and transforming growth factor-beta1 in autosomal dominant polycystic kidney disease patients.* Ther Apher Dial. **20(5)**:517-522.

Koguchi, W., Kobayashi, N., Takeshima, H., Ishikawa, M., Sugiyama, F. and Ishimitsu, T. (2012). *Cardioprotective effect of apelin-13 on cardiac performance and remodeling in end-stage heart failure.* Circ J. **76(1)**:137-44.

Koitabashi, N., Danner, T., Zaiman, A. L., Pinto, Y. M., Rowell, J., Mankowski, J., Zhang, D., Nakamura, T., Takimoto, E. and Kass, D. A. (2011). *Pivotal role of cardiomyocyte TGF-beta signaling in the murine pathological response to sustained pressure overload.* J Clin Invest. **121(6)**:2301-12.

Kuba, K., Zhang, L., Imai, Y., Arab, S., Chen, M., Maekawa, Y., Leschnik, M., Leibbrandt, A., Markovic, M., Schwaighofer, J., Beetz, N., Musialek, R., Neely, G. G., Komnenovic, V., Kolm, U., Metzler, B., Ricci, R., Hara, H., Meixner, A., Nghiem, M., Chen, X., Dawood, F., Wong, K. M., Sarao, R., Cukerman, E., Kimura, A., Hein, L., Thalhammer, J., Liu, P. P. and Penninger, J. M. (2007). *Impaired heart contractility in apelin gene-deficient mice associated with aging and pressure overload.* Circ Res. **101(4)**:32-42.

Kuzuya, M. and Kinsella, J. L. (1994). *Induction of endothelial cell differentiation in vitro by fibroblast-derived soluble factors.* Exp Cell Res. **215(2)**:310-8.

Lagorce, D., Sperandio, O., Baell, J. B., Miteva, M. A. and Villoutreix, B. O. (2015). *FAF-Drugs3: a web server for compound property calculation and chemical library design.* Nucleic Acids Res. **43**:200-7.

Lanctot, P. M., Leclerc, P. C., Escher, E., Leduc, R. and Guillemette, G. (1999). *Role of N-glycosylation in the expression and functional properties of human AT1 receptor.* Biochemistry. **38(27)**:8621-7.

Lane, J. R., May, L. T., Parton, R. G., Sexton, P. M. and Christopoulos, A. (2017). *A kinetic view of GPCR allostery and biased agonism.* Nat Chem Biol. **13(9)**:929-937.

Langelaan, D. N., Reddy, T., Banks, A. W., Dellaire, G., Dupre, D. J. and Rainey, J. K. (2013). *Structural features of the apelin receptor N-terminal tail and first transmembrane segment implicated in ligand binding and receptor trafficking.* Biochim Biophys Acta. **1828(6)**:1471-83.

Lawson, E. C., Luci, D. K., Ghosh, S., Kinney, W. A., Reynolds, C. H., Qi, J., Smith, C. E., Wang, Y., Minor, L. K., Haertlein, B. J., Parry, T. J., Damiano, B. P. and Maryanoff, B. E. (2009). *Nonpeptide urotensin-II receptor antagonists: A new ligand class based on piperazino-phthalimide and piperazino-isoindolinone subunits.* J Med Chem. **52(23)**:7432-45.

Le Gonidec, S., Chaves-Almagro, C., Bai, Y., Kang, H. J., Smith, A., Wanecq, E., Huang, X. P., Prats, H., Knibiehler, B., Roth, B. L., Barak, L. S., Caron, M. G., Valet, P., Audigier, Y. and Masri, B. (2017). *Protamine is an antagonist of apelin receptor, and its activity is reversed by heparin.* Faseb J. **31(6)**:2507-2519.

Leask, A. and Abraham, D. J. (2004). *TGF-beta signaling and the fibrotic response.* Faseb J. **18(7)**:816-27.

Lee, D. K., Ferguson, S. S., George, S. R. and O'Dowd, B. F. (2010). *The fate of the internalized apelin receptor is determined by different isoforms of apelin mediating differential interaction with beta-arrestin.* Biochem Biophys Res Commun. **395(2)**:185-9.

Lee, D. K., Saldivia, V. R., Nguyen, T., Cheng, R., George, S. R. and O'Dowd, B. F. (2005). *Modification of the terminal residue of apelin-13 antagonizes its hypotensive action.* Endocrinology. **146(1)**:231-6.

Li, L., Yang, G., Li, Q., Tang, Y., Yang, M., Yang, H. and Li, K. (2006). *Changes and relations of circulating visfatin, apelin, and resistin levels in normal, impaired glucose tolerance, and type 2 diabetic subjects.* Exp Clin Endocrinol Diabetes. **114(10)**:544-8.

Li, L., Zeng, H. and Chen, J. X. (2012). *Apelin-13 increases myocardial progenitor cells and improves repair postmyocardial infarction.* Am J Physiol Heart Circ Physiol. **303(5)**:605-18.

Li, L., Zeng, H., Hou, X., He, X. and Chen, J. X. (2013). *Myocardial injection of apelin-overexpressing bone marrow cells improves cardiac repair via upregulation of Sirt3 after myocardial infarction.* PLoS One. **8(9)**:e71041.

Li, M., Gou, H., Tripathi, B. K., Huang, J., Jiang, S., Dubois, W., Waybright, T., Lei, M., Shi, J. and Zhou, M. (2015). *An apela RNA-containing negative feedback loop regulates p53-mediated apoptosis in embryonic stem cells.* Cell Stem Cell. **16(6)**:669-83.

Lin, J., Hodge, R. J., O'Connor-Semmes, R. L. and Nunez, D. J. (2015). *GSK2374697, a long duration glucagon-like peptide-1 (GLP-1) receptor agonist, reduces postprandial circulating endogenous total GLP-1 and peptide YY in healthy subjects.* Diabetes Obes Metab. **17(10)**:1007-10.

Liu, D. R., Hu, W. and Chen, G. Z. (2018). *Apelin-12 exerts neuroprotective effect against ischemia-reperfusion injury by inhibiting JNK and P38MAPK signaling pathway in mouse.* Eur Rev Med Pharmacol Sci. **22(12)**:3888-3895.

Long, L., Ormiston, M. L., Yang, X., Southwood, M., Graf, S., Machado, R. D., Mueller, M., Kinzel, B., Yung, L. M., Wilkinson, J. M., Moore, S. D., Drake, K. M., Aldred, M. A., Yu, P. B., Upton, P. D. and Morrell, N. W. (2015). *Selective enhancement of endothelial BMPR-II with BMP9 reverses pulmonary arterial hypertension.* Nat Med. **21(7)**:777-85.

Luttrell, L. M., Maudsley, S. and Bohn, L. M. (2015). *Fulfilling the promise of "biased" G protein-coupled receptor agonism.* Mol Pharmacol. **88(3)**:579-88.

Lynch, C., 3rd (1990). *Differential depression of myocardial contractility by volatile anesthetics in vitro: Comparison with uncouplers of excitation-contraction coupling*. J Cardiovasc Pharmacol. **15(4)**:655-65.

Ma, W. Y., Yu, T. Y., Wei, J. N., Hung, C. S., Lin, M. S., Liao, Y. J., Pei, D., Su, C. C., Lu, K. C., Liu, P. H., Lin, C. H., Chuang, L. M., Kao, H. L., Lin, J. W., Chuang, Y. J. and Li, H. Y. (2014). *Plasma apelin: A novel biomarker for predicting diabetes*. Clin Chim Acta. **435**:18-23.

Ma, Y., Yue, Y., Zhang, Q., Zhou, Q., Song, Y., Shen, Y., Li, X., Ma, X., Li, C., Hanson, M. A., Han, G. W., Sickmier, E. A., Swaminath, G., Zhao, S., Stevens, R. C., Hu, L. A., Zhong, W., Zhang, M. and Xu, F. (2017). *Structural basis for apelin control of the human apelin receptor.* Structure. **25(6)**:858-866

Macaluso, N. J. and Glen, R. C. (2010). *Exploring the 'RPRL' motif of apelin-13 through molecular simulation and biological evaluation of cyclic peptide analogues.* ChemMedChem. **5(8)**:1247-53.

Macaluso, N. J., Pitkin, S. L., Maguire, J. J., Davenport, A. P. and Glen, R. C. (2011). *Discovery of a competitive apelin receptor (APJ) antagonist.* ChemMedChem. **6(6)**:1017-23.

Maguire, J. J., Kleinz, M. J., Pitkin, S. L. and Davenport, A. P. (2009*). [Pyr1]apelin-13 identified as the predominant apelin isoform in the human heart: Vasoactive mechanisms and inotropic action in disease.* Hypertension. **54(3)**:598-604.

Makela, V. H. and Kapur, P. A. (1987). *Amrinone blunts cardiac depression caused by enflurane or isoflurane anesthesia in the dog.* Anesth Analg. **66(3)**:215-21.

Maloney, P. R., Khan, P., Hedrick, M., Gosalia, P., Milewski, M., Li, L., Roth, G. P., Sergienko, E., Suyama, E., Sugarman, E., Nguyen, K., Mehta, A., Vasile, S., Su, Y., Stonich, D., Nguyen, H., Zeng, F. Y., Novo, A. M., Vicchiarelli, M., Diwan, J., Chung, T. D., Smith, L. H. and Pinkerton, A. B. (2012). *Discovery of 4-oxo-6-((pyrimidin-2-ylthio)methyl)-4H-pyran-3-yl 4-nitrobenzoate (ML221) as a functional antagonist of the apelin (APJ) receptor.* Bioorg Med Chem Lett. **22(21)**:6656-60.

Manglik, A., Lin, H., Aryal, D. K., McCorvy, J. D., Dengler, D., Corder, G., Levit, A., Kling, R. C., Bernat, V., Hubner, H., Huang, X. P., Sassano, M. F., Giguere, P. M., Lober, S., Da, D., Scherrer, G., Kobilka, B. K., Gmeiner, P., Roth, B. L. and Shoichet, B. K. (2016). *Structure-based discovery of opioid analgesics with reduced side effects.* Nature. **537(7619)**:185-190

Margathe, J. F., Iturrioz, X., Alvear-Perez, R., Marsol, C., Riche, S., Chabane, H., Tounsi, N., Kuhry, M., Heissler, D., Hibert, M., Llorens-Cortes, C. and Bonnet, D. (2014). *Structure-activity relationship studies toward the discovery of selective apelin receptor agonists.* J Med Chem. **57(7)**:2908-19.

Masri, B., Lahlou, H., Mazarguil, H., Knibiehler, B. and Audigier, Y. (2002). *Apelin (65-77) activates extracellular signal-regulated kinases via a PTX-sensitive G protein.* Biochem Biophys Res Commun. **290(1)**:539-45.

McKeown, S. C., Zecri, F. J., Fortier, E., Taggart, A., Sviridenko, L., Adams, C. M., McAllister, K. H. and Pin, S. S. (2014). *The design and implementation of a generic lipopeptide scanning platform to enable the identification of 'locally acting' agonists for the apelin receptor.* Bioorg Med Chem Lett. **24(20)**:4871-5.

Medhurst, A. D., Jennings, C. A., Robbins, M. J., Davis, R. P., Ellis, C., Winborn, K. Y., Lawrie, K. W., Hervieu, G., Riley, G., Bolaky, J. E., Herrity, N. C., Murdock, P. and Darker, J. G. (2003). *Pharmacological and immunohistochemical characterization of the APJ receptor and its endogenous ligand apelin.* J Neurochem. **84(5)**:1162-72.

Morrell, N. W., Bloch, D. B., ten Dijke, P., Goumans, M. J., Hata, A., Smith, J., Yu, P. B. and Bloch, K. D. (2016). *Targeting BMP signalling in cardiovascular disease and anaemia.* Nat Rev Cardiol. **13(2)**:106-20.

Murtha, L. A., Schuliga, M. J., Mabotuwana, N. S., Hardy, S. A., Waters, D. W., Burgess, J. K., Knight, D. A. and Boyle, A. J. (2017). *The processes and mechanisms of cardiac and pulmonary fibrosis.* Front Physiol. **8**:777.

Murza, A., Besserer-Offroy, E., Cote, J., Berube, P., Longpre, J. M., Dumaine, R., Lesur, O., Auger-Messier, M., Leduc, R., Sarret, P. and Marsault, E. (2015). *C-Terminal modifications of apelin-13 significantly change ligand binding, receptor signaling, and hypotensive action.* J Med Chem. **58(5)**:2431-40.

Murza, A., Parent, A., Besserer-Offroy, E., Tremblay, H., Karadereye, F., Beaudet, N., Leduc, R., Sarret, P. and Marsault, E. (2012). *Elucidation of the structure-activity relationships of apelin: Influence of unnatural amino acids on binding, signaling, and plasma stability.* ChemMedChem. **7(2)**:318-25.

Murza, A., Sainsily, X., Coquerel, D., Cote, J., Marx, P., Besserer-Offroy, E., Longpre, J. M., Laine, J., Reversade, B., Salvail, D., Leduc, R., Dumaine, R., Lesur, O., Auger-Messier, M., Sarret, P. and Marsault, E. (2016). *Discovery and structure-activity relationship of a bioactive fragment of elabela that modulates vascular and cardiac functions.* J Med Chem. **59(7)**:2962-72.

Murza, A., Sainsily, X., Cote, J., Bruneau-Cossette, L., Besserer-Offroy, E., Longpre, J. M., Leduc, R., Dumaine, R., Lesur, O., Auger-Messier, M., Sarret, P. and Marsault, E. (2017). *Structure-activity relationship of novel macrocyclic biased apelin receptor agonists.* Org Biomol Chem. **15(2)**:449-458.

Myers, M. C., Lawrence, R. M., Bilder, D. M., Meng, W., Pi, Z., Brigance, R. P. and Finlay, H. 2017. *Heteroarylhydroxypyrimidinones as agonists of the APJ receptor.* Google Patents. **WO2017106396A1**

Nagpal, V., Rai, R., Place, A. T., Murphy, S. B., Verma, S. K., Ghosh, A. K. and Vaughan, D. E. (2016). *MiR-125b is critical for fibroblast-to-myofibroblast transition and cardiac fibrosis.* Circulation. **133(3)**:291-301.

Narayanan, S., Maitra, R., Deschamps, J. R., Bortoff, K., Thomas, J. B., Zhang, Y., Warner, K., Vasukuttan, V., Decker, A. and Runyon, S. P. (2016). *Discovery of a novel small molecule agonist scaffold for the APJ receptor.* Bioorg Med Chem. **24(16)**:3758-70.

Nasman, J., Kukkonen, J. P., Ammoun, S. and Akerman, K. E. (2001). *Role of G-protein availability in differential signaling by alpha 2-adrenoceptors.* Biochem Pharmacol. **62(7)**:913-22.

Nickel, N. P., Spiekerkoetter, E., Gu, M., Li, C. G., Li, H., Kaschwich, M., Diebold, I., Hennigs, J. K., Kim, K. Y., Miyagawa, K., Wang, L., Cao, A., Sa, S., Jiang, X., Stockstill, R. W., Nicolls, M. R., Zamanian, R. T., Bland, R. D. and Rabinovitch, M. (2015). *Elafin reverses pulmonary hypertension via caveolin-1-dependent bone morphogenetic protein signaling.* Am J Respir Crit Care Med. **191(11)**:1273-86.

Nobles, K. N., Xiao, K., Ahn, S., Shukla, A. K., Lam, C. M., Rajagopal, S., Strachan, R. T., Huang, T. Y., Bressler, E. A., Hara, M. R., Shenoy, S. K., Gygi, S. P. and Lefkowitz, R. J. (2011). *Distinct phosphorylation sites on the beta(2)-adrenergic receptor establish a barcode that encodes differential functions of beta-arrestin.* Sci Signal. **4(185)**:ra51.

Nowell, P. C. (1962). *The minute chromosome (Phl) in chronic granulocytic leukemia*. Blut. **8**:65-6.

O'Connor-Semmes, R. L., Lin, J., Hodge, R. J., Andrews, S., Chism, J., Choudhury, A. and Nunez, D. J. (2014). *GSK2374697, a novel albumin-binding domain antibody (AlbudAb), extends systemic exposure of exendin-4: First study in humans-PK/PD and safety.* Clin Pharmacol Ther. **96(6)**:704-12.

O'Dowd, B. F., Heiber, M., Chan, A., Heng, H. H., Tsui, L. C., Kennedy, J. L., Shi, X., Petronis, A., George, S. R. and Nguyen, T. (1993). *A human gene that shows identity with the gene encoding the angiotensin receptor is located on chromosome 11.* Gene. **136(1-2)**:355-60.

Ormiston, M. L., Toshner, M. R., Kiskin, F. N., Huang, C. J., Groves, E., Morrell, N. W. and Rana, A. A. (2015). *Generation and culture of blood outgrowth endothelial cells from human peripheral blood*. J Vis Exp. **106**:e53384.

Pacher, P., Nagayama, T., Mukhopadhyay, P., Batkai, S. and Kass, D. A. (2008). *Measurement of cardiac function using pressure-volume conductance catheter technique in mice and rats.* Nat Protoc. **3(9)**:1422-34.

Pang, H., Han, B., Yu, T. and Zong, Z. (2014). *Effect of apelin on the cardiac hemodynamics in hypertensive rats with heart failure.* Int J Mol Med. **34(3)**:756-64.

Pang, P. S., Butler, J., Collins, S. P., Cotter, G., Davison, B. A., Ezekowitz, J. A., Filippatos, G., Levy, P. D., Metra, M., Ponikowski, P., Teerlink, J. R., Voors, A. A., Bharucha, D., Goin, K., Soergel, D. G. and Felker, G. M. (2017). *Biased ligand of the angiotensin II type 1 receptor in patients with acute heart failure: a randomized, double-blind, placebo-controlled, phase IIB, dose ranging trial (BLAST-AHF)*. Eur Heart J. **38(30)**:2364-2373.

Patel, S. J., Sanjana, N. E., Kishton, R. J., Eidizadeh, A., Vodnala, S. K., Cam, M., Gartner, J. J., Jia, L., Steinberg, S. M., Yamamoto, T. N., Merchant, A. S., Mehta, G. U., Chichura, A., Shalem, O., Tran, E., Eil, R., Sukumar, M., Guijarro, E. P., Day, C. P., Robbins, P., Feldman, S., Merlino, G., Zhang, F. and Restifo, N. P. (2017) *Identification of essential genes for cancer immunotherapy.* Nature. **548(7669)**:537-542.

Pauli, A., Norris, M. L., Valen, E., Chew, G. L., Gagnon, J. A., Zimmerman, S., Mitchell, A., Ma, J., Dubrulle, J., Reyon, D., Tsai, S. Q., Joung, J. K., Saghatelian, A. and Schier, A. F. (2014). *Toddler: an embryonic signal that promotes cell movement via apelin receptors.* Science. **343(6172)**:1248636.

Perjes, A., Kilpio, T., Ulvila, J., Magga, J., Alakoski, T., Szabo, Z., Vainio, L., Halmetoja, E., Vuolteenaho, O., Petaja-Repo, U., Szokodi, I. and Kerkela, R. (2016). *Characterization of apela, a novel endogenous ligand of apelin receptor, in the adult heart.* Basic Res Cardiol, **111(1)**:2.

Perjes, A., Skoumal, R., Tenhunen, O., Konyi, A., Simon, M., Horvath, I. G., Kerkela, R., Ruskoaho, H. and Szokodi, I. (2014). *Apelin increases cardiac contractility via protein kinase C-epsilon and extracellular signal-regulated kinase-dependent mechanisms.* PLoS One. **4**:e93473.

Philbin, D. M. and Lowenstein, E. (1975). *Hemodynamic consequences of the combination of isoflurane anesthesia (1 MAC) and beta-adrenergic blockade in the dog*. Anesthesiology. **42(5)**:567-73.

Pinkerton, A. B. and Smith, L. H. (2015). *Agonists of the apelin receptor and methods of use thereof.* Google Patents. **WO2015184011A2**.

Pisarenko, O., Shulzhenko, V., Studneva, I., Pelogeykina, Y., Timoshin, A., Anesia, R., Valet, P., Parini, A. and Kunduzova, O. (2015a). *Structural apelin analogues: mitochondrial ROS inhibition and cardiometabolic protection in myocardial ischaemia reperfusion injury.* Br J Pharmacol. **172(12)**:2933-45.

Pisarenko, O. I., Shulzhenko, V. S., Studneva, I. M., Serebryakova, L. I., Pelogeykina, Y. A. and Veselova, O. M. (2015b). *Signaling pathways of a structural analogue of apelin-12 involved in myocardial protection against ischemia/reperfusion injury.* Peptides. **73**:67-76.

Pitkin, S. L., Maguire, J. J., Bonner, T. I. and Davenport, A. P. (2010). *International Union of Basic and Clinical Pharmacology. LXXIV. Apelin receptor nomenclature, distribution, pharmacology, and function.* Pharmacol Rev. **62(3)**:331-42.

Principe, A., Melgar-Lesmes, P., Fernandez-Varo, G., del Arbol, L. R., Ros, J., Morales-Ruiz, M., Bernardi, M., Arroyo, V. and Jimenez, W. (2008). *The hepatic apelin system: A new therapeutic target for liver disease.* Hepatology. **48(4)**:1193-201.

Puffer, B. A., Sharron, M., Coughlan, C. M., Baribaud, F., McManus, C. M., Lee, B., David, J., Price, K., Horuk, R., Tsang, M. and Doms, R. W. (2000). *Expression and coreceptor function of APJ for primate immunodeficiency viruses.* Virology. **276(2)**:435-44.

Qanbar, R. and Bouvier, M. (2003). *Role of palmitoylation/depalmitoylation reactions in G-protein-coupled receptor function.* Pharmacol Ther. **97(1)**:1-33.

Rabinovitch, M. (2012). *Molecular pathogenesis of pulmonary arterial hypertension.* J Clin Invest. **122(12)**:4306-13.

Rajagopal, S., Ahn, S., Rominger, D. H., Gowen-MacDonald, W., Lam, C. M., Dewire, S. M., Violin, J. D. and Lefkowitz, R. J. (2011). *Quantifying ligand bias at seven-transmembrane receptors.* Mol Pharmacol. **80(3)**:367-77.

Raymond, M. A., Desormeaux, A., Laplante, P., Vigneault, N., Filep, J. G., Landry, K., Pshezhetsky, A. V. and Hebert, M. J. (2004). *Apoptosis of endothelial cells triggers a caspase-dependent anti-apoptotic paracrine loop active on VSMC.* Faseb J. **18(6)**:705-7.

Read, C., Fitzpatrick, C. M., Yang, P., Kuc, R. E., Maguire, J. J., Glen, R. C., Foster, R. E. and Davenport, A. P. (2016). *Cardiac action of the first G protein biased small molecule apelin agonist.* Biochem Pharmacol.**166**:63-72

Reichenbach, V., Ros, J., Fernandez-Varo, G., Casals, G., Melgar-Lesmes, P., Campos, T., Makriyannis, A., Morales-Ruiz, M. and Jimenez, W. (2012). *Prevention of fibrosis progression in CCl4-treated rats: Role of the hepatic endocannabinoid and apelin systems.* J Pharmacol Exp Ther. **340(3)**:629-37.

Ren, J., Wen, L., Gao, X., Jin, C., Xue, Y. and Yao, X. (2008). *CSS-Palm 2.0: An updated software for palmitoylation sites prediction.* Protein Eng Des Sel. **21(11)**:639-44.

Ringstrom, C., Nitert, M. D., Bennet, H., Fex, M., Valet, P., Rehfeld, J. F., Friis-Hansen, L. and Wierup, N. (2010). *Apelin is a novel islet peptide.* Regul Pept. **162(1-3)**:44-51.

Roberts, E. M., Newson, M. J., Pope, G. R., Landgraf, R., Lolait, S. J. and O'Carroll, A. M. (2009). *Abnormal fluid homeostasis in apelin receptor knockout mice.* J Endocrinol. **202(3)**:453-62.

Rowley, J. D. (1973). *Letter: A new consistent chromosomal abnormality in chronic myelogenous leukaemia identified by quinacrine fluorescence and Giemsa staining.* Nature. **243(5405)**:290-3.

Sakao, S., Taraseviciene-Stewart, L., Lee, J. D., Wood, K., Cool, C. D. and Voelkel, N. F. (2005). *Initial apoptosis is followed by increased proliferation of apoptosis-resistant endothelial cells.* Faseb J. **19(9)**:1178-80.

Sato, T., Sato, C., Kadowaki, A., Watanabe, H., Ho, L., Ishida, J., Yamaguchi, T., Kimura, A., Fukamizu, A., Penninger, J. M., Reversade, B., Ito, H., Imai, Y. and Kuba, K. (2017). *Elabela-APJ axis protects from pressure overload heart failure and angiotensin II-induced cardiac damage*. Cardiovasc Res. **113(7)**:760-769.

Savage, D. G. and Antman, K. H. (2002). *Imatinib mesylate: A new oral targeted therapy.* N Engl J Med. **346(9)**:683-93.

Schreiber, C. A., Holditch, S. J., Generous, A. and Ikeda, Y. (2016). *Sustained elabela gene therapy in high salt-induced hypertensive rats.* Curr Gene Ther. **16(5)**:349-360

Scimia, M. C., Hurtado, C., Ray, S., Metzler, S., Wei, K., Wang, J., Woods, C. E., Purcell, N. H., Catalucci, D., Akasaka, T., Bueno, O. F., Vlasuk, G. P., Kaliman, P., Bodmer, R., Smith, L. H., Ashley, E., Mercola, M., Brown, J. H. and Ruiz-Lozano, P. (2012). *APJ acts as a dual receptor in cardiac hypertrophy.* Nature. **7411**:394-8.

Scott, I. C., Masri, B., D'Amico, L. A., Jin, S. W., Jungblut, B., Wehman, A. M., Baier, H., Audigier, Y. and Stainier, D. Y. (2007). *The g protein coupled receptor agtrl1b regulates early development of myocardial progenitors.* Dev Cell. **12(3)**:403-13.

Serpooshan, V., Sivanesan, S., Huang, X., Mahmoudi, M., Malkovskiy, A. V., Zhao, M., Inayathullah, M., Wagh, D., Zhang, X. J., Metzler, S., Bernstein, D., Wu, J. C., Ruiz-Lozano, P. and Rajadas, J. (2015). *[Pyr1]-Apelin-13 delivery via nano-liposomal encapsulation attenuates pressure overload-induced cardiac dysfunction.* Biomaterials **37**:289-98.

Sharma, B., Ho, L., Ford, G. H., Chen, H. I., Goldstone, A. B., Woo, Y. J., Quertermous, T., Reversade, B. and Red-Horse, K. (2017). *Alternative progenitor cells compensate to rebuild the coronary vasculature in elabela- and APJ-deficient hearts.* Dev Cell. **42(6)**:655-666.

Shields, K. J., Verdelis, K., Passineau, M. J., Faight, E. M., Zourelias, L., Wu, C., Chong, R. and Benza, R. L. (2016). *Three-dimensional micro computed tomography analysis of the lung vasculature and differential adipose proteomics in the sugen/hypoxia rat model of pulmonary arterial hypertension.* Pulm Circ. **6(4)**:586-596.

Shin, K., Pandey, A., Liu, X. Q., Anini, Y. and Rainey, J. K. (2013). *Preferential apelin-13 production by the proprotein convertase PCSK3 is implicated in obesity.* FEBS Open Bio. **3**:328-33.

Smith, N. J., Bennett, K. A. and Milligan, G. (2011). *When simple agonism is not enough: Emerging modalities of GPCR ligands.* Mol Cell Endocrinol. **331(2)**:241-7.

Soriguer, F., Garrido-Sanchez, L., Garcia-Serrano, S., Garcia-Almeida, J. M., Garcia-Arnes, J., Tinahones, F. J. and Garcia-Fuentes, E. (2009). *Apelin levels are increased in morbidly obese subjects with type 2 diabetes mellitus.* Obes Surg. **19(11)**:1574-80.

Soto, A. G., Smith, T. H., Chen, B., Bhattacharya, S., Cordova, I. C., Kenakin, T., Vaidehi, N. and Trejo, J. (2015). *N-linked glycosylation of protease-activated receptor-1 at extracellular loop 2 regulates G-protein signaling bias.* Proc Natl Acad Sci USA. **112(27)**:3600-8.

Spiekerkoetter, E., Tian, X., Cai, J., Hopper, R. K., Sudheendra, D., Li, C. G., El-Bizri, N., Sawada, H., Haghighat, R., Chan, R., Haghighat, L., de Jesus Perez, V., Wang, L., Reddy, S., Zhao, M., Bernstein, D., Solow-Cordero, D. E., Beachy, P. A., Wandless, T. J., Ten Dijke, P. and Rabinovitch, M. (2013). *FK506 activates BMPR2, rescues endothelial dysfunction, and reverses pulmonary hypertension.* J Clin Invest. **123(8)**:3600-13.

Szokodi, I., Tavi, P., Foldes, G., Voutilainen-Myllyla, S., Ilves, M., Tokola, H., Pikkarainen, S., Piuhola, J., Rysa, J., Toth, M. and Ruskoaho, H. (2002). *Apelin, the novel endogenous ligand of the orphan receptor APJ, regulates cardiac contractility.* Circ Res. **91(5)**:434-40.

Taheri, S., Murphy, K., Cohen, M., Sujkovic, E., Kennedy, A., Dhillo, W., Dakin, C., Sajedi, A., Ghatei, M. and Bloom, S. (2002). *The effects of centrally administered apelin-13 on food intake, water intake and pituitary hormone release in rats.* Biochem Biophys Res Commun. **291(5)**:1208-12.

Taichman, D. B. and Mandel, J. (2013). *Epidemiology of pulmonary arterial hypertension.* Clin Chest Med. **34(4)**:619-37.

Tang, S. Y., Xie, H., Yuan, L. Q., Luo, X. H., Huang, J., Cui, R. R., Zhou, H. D., Wu, X. P. and Liao, E. Y. (2007). *Apelin stimulates proliferation and suppresses apoptosis of mouse osteoblastic cell line MC3T3-E1 via JNK and PI3-K/Akt signaling pathways.* Peptides. **28(3)**:708-18.

Taraseviciene-Stewart, L., Kasahara, Y., Alger, L., Hirth, P., Mc Mahon, G., Waltenberger, J., Voelkel, N. F. and Tuder, R. M. (2001). *Inhibition of the VEGF receptor 2 combined with chronic hypoxia causes cell death-dependent pulmonary endothelial cell proliferation and severe pulmonary hypertension.* Faseb J. **15(2)**:427-38.

Tatemoto, K., Hosoya, M., Habata, Y., Fujii, R., Kakegawa, T., Zou, M. X., Kawamata, Y., Fukusumi, S., Hinuma, S., Kitada, C., Kurokawa, T., Onda, H. and Fujino, M. (1998). *Isolation and characterization of a novel endogenous peptide ligand for the human APJ receptor.* Biochem Biophys Res Commun. **251(2)**:471-6.

Tatemoto, K., Takayama, K., Zou, M. X., Kumaki, I., Zhang, W., Kumano, K. and Fujimiya, M. (2001). *The novel peptide apelin lowers blood pressure via a nitric oxide-dependent mechanism.* Regul Pept. **99(2-3)**:87-92.

Than, A., He, H. L., Chua, S. H., Xu, D., Sun, L., Leow, M. K. and Chen, P. (2015). *Apelin enhances brown adipogenesis and browning of white adipocytes.* J Biol Chem. **290(23)**:14679-91.

Thenappan, T., Ormiston, M. L., Ryan, J. J. and Archer, S. L. (2018). *Pulmonary arterial hypertension: Pathogenesis and clinical management.* BMJ. **360**:5492.

Toba, M., Alzoubi, A., O'Neill, K. D., Gairhe, S., Matsumoto, Y., Oshima, K., Abe, K., Oka, M. and McMurtry, I. F. (2014). *Temporal hemodynamic and histological progression in sugen5416/hypoxia/normoxia-exposed pulmonary arterial hypertensive rats.* Am J Physiol Heart Circ Physiol. **306(2)**:243-50.

Tobin, A. B., Butcher, A. J. and Kong, K. C. (2008). *Location, location, location...site-specific GPCR phosphorylation offers a mechanism for cell-type-specific signalling.* Trends Pharmacol Sci. **29(8)**:413-20.

Trifonov, L., Afri, M., Palczewski, K., Korshin, E. E. and Gruzman, A. (2018). *An expedient synthesis of CMF-019: (S)-5-Methyl-3-{1-(pentan-3-yl)-2-(thiophen-2-ylmethyl)-1H-benzo[d]imidazole-5-ca rboxamido}hexanoic acid, a potent apelin receptor (APJ) agonist.* Med Chem. **EPub**: PMID:29651942

Turecek, P. L., Bossard, M. J., Schoetens, F. and Ivens, I. A. (2016). *PEGylation of biopharmaceuticals: A review of chemistry and nonclinical safety information of approved drugs.* J Pharm Sci. **105(2)**:460-75.

Ueda, Y., Nakagawa, T., Kubota, T., Ido, K. and Sato, K. (2005). *Glioma cells under hypoxic conditions block the brain microvascular endothelial cell death induced by serum starvation.* J Neurochem. **95(1)**:99-110.

Urban, J. D., Clarke, W. P., von Zastrow, M., Nichols, D. E., Kobilka, B., Weinstein, H., Javitch, J. A., Roth, B. L., Christopoulos, A., Sexton, P. M., Miller, K. J., Spedding, M. and Mailman, R. B. (2007). *Functional selectivity and classical concepts of quantitative pharmacology.* J Pharmacol Exp Ther. **320(1)**:1-13.

Vaidehi, N. and Kenakin, T. (2010). *The role of conformational ensembles of seven transmembrane receptors in functional selectivity.* Curr Opin Pharmacol. **10(6)**:775-81.

Van Coillie, E., Proost, P., Van Aelst, I., Struyf, S., Polfliet, M., De Meester, I., Harvey, D. J., Van Damme, J. and Opdenakker, G. (1998). *Functional comparison of two human monocyte chemotactic protein-2 isoforms, role of the amino-terminal pyroglutamic acid and processing by CD26/dipeptidyl peptidase IV.* Biochemistry. **37(36)**:12672-80.

van der Westhuizen, E. T., Breton, B., Christopoulos, A. and Bouvier, M. (2014). *Quantification of ligand bias for clinically relevant beta2-adrenergic receptor ligands: implications for drug taxonomy.* Mol Pharmacol. **85(3)**:492-509.

Varani, J., Dame, M. K., Taylor, C. G., Sarma, V., Merino, R., Kunkel, R. G., Nunez, G. and Dixit, V. M. (1995). *Age-dependent injury in human umbilical vein endothelial cells: Relationship to apoptosis and correlation with a lack of A20 expression.* Lab Invest. **73(6)**:851-8.

Vickers, C., Hales, P., Kaushik, V., Dick, L., Gavin, J., Tang, J., Godbout, K., Parsons, T., Baronas, E., Hsieh, F., Acton, S., Patane, M., Nichols, A. and Tummino, P. (2002). *Hydrolysis of biological peptides by human angiotensin-converting enzyme-related carboxypeptidase.* J Biol Chem. **277(17)**:14838-43.

Viscusi, E. R., Webster, L., Kuss, M., Daniels, S., Bolognese, J. A., Zuckerman, S., Soergel, D. G., Subach, R. A., Cook, E. and Skobieranda, F. (2016). *A randomized, phase 2 study investigating TRV130, a biased ligand of the mu-opioid receptor, for the intravenous treatment of acute pain.* Pain. **157(1)**:264-72.

Visser, Y. P., Walther, F. J., Laghmani el, H., Laarse, A. and Wagenaar, G. T. (2010). *Apelin attenuates hyperoxic lung and heart injury in neonatal rats.* Am J Respir Crit Care Med. **182(10)**:1239-50.

Wajant, H., Pfizenmaier, K. and Scheurich, P. (2003). *Tumor necrosis factor signalling.* Cell Death Differ. **10(1)**:45-65.

Wakabayashi, H., Hasegawa, M., Nishioka, Y., Minami, Y., Nishioka, K. and Sudo, A. (2013). *Clinical outcome in patients with rheumatoid arthritis switched to tocilizumab after etanercept or infliximab failure.* Clin Rheumatol. **32(2)**:253-9.

Walker, A., Dunlevy, G., Rycroft, D., Topley, P., Holt, L. J., Herbert, T., Davies, M., Cook, F., Holmes, S., Jespers, L. and Herring, C. (2010). *Anti-serum albumin domain antibodies in the development of highly potent, efficacious and long-acting interferon.* Protein Eng Des Sel. **23(4)**:271-8.

Wang, L. Y., Diao, Z. L., Zhang, D. L., Zheng, J. F., Zhang, Q. D., Ding, J. X. and Liu, W. H. (2014). *The regulatory peptide apelin: A novel inhibitor of renal interstitial fibrosis.* Amino Acids. **46(12)**:2693-704.

Wang, M., Gupta, R. C., Rastogi, S., Kohli, S., Sabbah, M. S., Zhang, K., Mohyi, P., Hogie, M., Fischer, Y. and Sabbah, H. N. (2013a). *Effects of acute intravenous infusion of apelin on left ventricular function in dogs with advanced heart failure.* J Card Fail. **19(7)**:509-16.

Wang, W., McKinnie, S. M., Patel, V. B., Haddad, G., Wang, Z., Zhabyeyev, P., Das, S. K., Basu, R., McLean, B., Kandalam, V., Penninger, J. M., Kassiri, Z., Vederas, J. C., Murray, A. G. and Oudit, G. Y. (2013b). *Loss of apelin exacerbates myocardial infarction adverse remodeling and ischemia-reperfusion injury: Therapeutic potential of synthetic apelin analogues.* J Am Heart Assoc. **2(4)**:e000249.

Wang, Z., Yu, D., Wang, M., Wang, Q., Kouznetsova, J., Yang, R., Qian, K., Wu, W., Shuldiner, A., Sztalryd, C., Zou, M., Zheng, W. and Gong, D. W. (2015). *Elabela-apelin receptor signaling pathway is functional in mammalian systems.* Sci Rep. **5**:8170.

Wei, A. E., Maslov, M. Y., Pezone, M. J., Edelman, E. R. and Lovich, M. A. (2014). *Use of pressure-volume conductance catheters in real-time cardiovascular experimentation.* Heart Lung Circ. **23(11)**:1059-69.

West, J., Fagan, K., Steudel, W., Fouty, B., Lane, K., Harral, J., Hoedt-Miller, M., Tada, Y., Ozimek, J., Tuder, R. and Rodman, D. M. (2004). *Pulmonary hypertension in transgenic mice expressing a dominant-negative BMPRII gene in smooth muscle.* Circ Res. **94(8)**:1109-14.

Wilson, D. W., Segall, H. J., Pan, L. C. and Dunston, S. K. (1989). *Progressive inflammatory and structural changes in the pulmonary vasculature of monocrotaline-treated rats.* Microvasc Res. **38(1)**:57-80.

Wilson, D. W., Segall, H. J., Pan, L. C., Lame, M. W., Estep, J. E. and Morin, D. (1992). *Mechanisms and pathology of monocrotaline pulmonary toxicity.* Crit Rev Toxicol. **22(5-6)**:307-25.

Wisler, J. W., DeWire, S. M., Whalen, E. J., Violin, J. D., Drake, M. T., Ahn, S., Shenoy, S. K. and Lefkowitz, R. J. (2007). *A unique mechanism of beta-blocker action: Carvedilol stimulates beta-arrestin signalling.* Proc Natl Acad Sci USA. **104(42)**:16657-62.

Xie, F., Lv, D. and Chen, L. (2014). *Elabela: A novel hormone in cardiac development acting as a new endogenous ligand for the APJ receptor.* Acta Biochim Biophys Sin (Shanghai). **46(7)**:620-2.

Yang, P., Kuc, R. E., Brame, A. L., Dyson, A., Singer, M., Glen, R. C., Cheriyan, J., Wilkinson, I. B., Davenport, A. P. and Maguire, J. J. (2017a). *[Pyr1]apelin-13(1-12) is a biologically active ACE2 metabolite of the endogenous cardiovascular peptide [Pyr1]apelin-13.* Front Neurosci. **11**:92.

Yang, P., Maguire, J. J. and Davenport, A. P. (2015a). *Apelin, elabela/toddler, and biased agonists as novel therapeutic agents in the cardiovascular system.* Trends Pharmacol Sci. **36(9)**:560-7.

Yang, P., Read, C., Kuc, R. E., Buonincontri, G., Southwood, M., Torella, R., Upton, P. D., Crosby, A., Sawiak, S. J., Carpenter, T. A., Glen, R. C., Morrell, N. W., Maguire, J. J. and Davenport, A. P. (2017b). *Elabela/toddler is an endogenous agonist of the apelin APJ receptor in the adult cardiovascular system, and exogenous administration of the peptide compensates for the downregulation of its expression in pulmonary arterial hypertension.* Circulation. **135(12)**:1160-1173.

Yang, S., Li, H., Tang, L., Ge, G., Ma, J., Qiao, Z., Liu, H. and Fang, W. (2015b). *Apelin-13 protects the heart against ischemia-reperfusion injury through the RISK-GSK-3beta-mPTP pathway.* Arch Med Sci. **11(5)**:1065-73.

Yang, Y., Lv, S. Y., Ye, W. and Zhang, L. (2016). *Apelin/APJ system and cancer.* Clin Chim Acta. **457**:112-6.

Zhang, L., Takara, K., Yamakawa, D., Kidoya, H. and Takakura, N. (2016). *Apelin as a marker for monitoring the tumour vessel normalisation window during antiangiogenic therapy.* Cancer Sci. **107(1)**:36-44.

Zhang, Y., Maitra, R., Harris, D. L., Dhungana, S., Snyder, R. and Runyon, S. P. (2014). *Identifying structural determinants of potency for analogs of apelin-13: Integration of C-terminal truncation with structure-activity.* Bioorg Med Chem. **22(11)**:2992-7.

Zhang, Y. J., Dragic, T., Cao, Y., Kostrikis, L., Kwon, D. S., Littman, D. R., KewalRamani, V. N. and Moore, J. P. (1998). *Use of coreceptors other than CCR5 by non-syncytium-inducing adult and pediatric isolates of human immunodeficiency virus type 1 is rare in vitro*. J Virol. **72(11)**:9337-44.

Zhou, N., Fan, X., Mukhtar, M., Fang, J., Patel, C. A., DuBois, G. C. and Pomerantz, R. J. (2003a). *Cell-cell fusion and internalization of the CNS-based, HIV-1 co-receptor, APJ*. Virology. **307(1)**:22-36.

Zhou, N., Fang, J., Acheampong, E., Mukhtar, M. and Pomerantz, R. J. (2003b). *Binding of ALX40-4C to APJ, a CNS-based receptor, inhibits its utilization as a co-receptor by HIV-1.* Virology. **312(1)**:196-203.

Zhu, X., Gilbert, S., Birnbaumer, M. and Birnbaumer, L. (1994). *Dual signaling potential is common among Gs-coupled receptors and dependent on receptor density.* Mol Pharmacol. **46(3)**:460-9.

Zou, M. X., Liu, H. Y., Haraguchi, Y., Soda, Y., Tatemoto, K. and Hoshino, H. (2000). *Apelin peptides block the entry of human immunodeficiency virus (HIV).* FEBS Lett. **473(1)**:15-8.